# CARBON AND WATER RELATIONS IN *PINUS TAEDA*: BRIDGING THE GAP ACROSS PLANT PHYSIOLOGY, GENOMICS, AND GLOBAL CLIMATE CHANGE

by

Catarina Fernandes Moura

Department of Biology
Duke University

Date:_____

Approved:

_____
Robert B. Jackson, Supervisor

_____
Gabriel G. Katul

_____
Michael L. Lavine

_____
Zhen-Ming Pei

_____
John Willis

Dissertation submitted in partial fulfillment of
the requirements for the degree of Doctor
of Philosophy in the Department of
Biology in the Graduate School
of Duke University

2008

ABSTRACT

# CARBON AND WATER RELATIONS IN *PINUS TAEDA*: BRIDGING THE GAP ACROSS PLANT PHYSIOLOGY, GENOMICS, AND GLOBAL CLIMATE CHANGE

by

Catarina Fernandes Moura

Department of Biology
Duke University

Date:_____

Approved:

_____
Robert B. Jackson, Supervisor

_____
Gabriel G. Katul

_____
Michael L. Lavine

_____
Zhen-Ming Pei

_____
John Willis

An abstract of a dissertation submitted in partial fulfillment of the requirements for the degree of Doctor of Philosophy in the Department of Biology in the Graduate School of Duke University

2008

## Abstract

Plants respond to changes in their local environment and, at the same time, influence the environment at a global scale. The molecular and physiological mechanisms regulating this interaction are not completely understood and this limits our capacity to predict the response of vegetation to future environmental changes. This dissertation combined tools from genomics, physiology, and ecology to examine the response of plants to environmental change. Specifically, it focused on processes affecting carbon and water exchange in forest trees because (1) trees are long-lived species that might face repeated environmental challenges; (2) relatively little information exists about the genes and the molecular mechanisms regulating structural and physiological traits in adult, long-lived woody plants; and (3) forest trees exchange a significant amount of carbon and water with the atmosphere and are therefore major players in the global carbon and water cycles.

Water flux through forests depends both on environmental conditions (e.g., soil moisture) and on the hydraulic architecture of individual trees. Resistance to xylem cavitation is an important hydraulic trait that is often associated with drought tolerance but potentially at the cost of reduced carbon uptake. The second chapter of this dissertation evaluated the variation in resistance to xylem cavitation, hydraulic conductivity, wood anatomy traits, and leaf gas exchange across 14 co-occurring temperate tree species including both angiosperms and gymnosperms. The relationship

between vulnerability to cavitation ($\Psi_{50}$) and hydraulic conductivity within specific organs (i.e. stems and roots) was not significant when considering the phylogenetic association between species. However, even after phylogenetic correction, photosynthetic carbon uptake (A) was positively correlated with both stem and root $\Psi_{50}$, and stomatal conductance ($g_s$) was strongly correlated with root $\Psi_{50}$. These results suggest that there is a trade-off between vulnerability to cavitation and water transport capacity at the whole-plant level, and that this functional relationship reflects an adaptive response to the environment.

Forests are an important component of the global carbon cycle that can be directly impacted by a rise in atmospheric $CO_2$ concentration.. The third chapter of this dissertation investigated the effects of long-term exposure to elevated $CO_2$ on the gene expression of mature, field-grown loblolly pine trees. Using cDNA microarrays, I compared the expression of 1784 pine transcripts in trees growing under ambient and those under elevated $CO_2$ at monthly intervals throughout a growing season. Overall, more genes were upregulated than downregulated by elevated $CO_2$, although the total number of genes differentially expressed varied throughout the season. The pattern of increasing number of differentially expressed genes until the peak of the growing season (July and August) followed by a decrease in that number, matched the seasonal trend of tree growth and photosynthetic response to elevated $CO_2$ in this species. The seasonal trend also reflected the interaction among multiple abiotic factors intrinsic to field

conditions and emphasized the relevance of evaluating the role of genes in their natural environment. Genes consistently upregulated by elevated $CO_2$ were functionally associated with environmental sensing, cellular signaling, and carbon metabolism, in particular the degradation of carbohydrates through respiration. An increase in carbohydrates degradation is particularly relevant in the context of carbon balance of forest trees because of the potential for enhanced leaf and tree respiration leading to a reduced sink capacity for $CO_2$.

Loblolly pine produces several flushes of needles throughout the year each with an average lifespan of 19 months. Each year, two age classes of needles contribute to the annual carbon sequestration of the loblolly pine forest. To address the impact of leaf age on the effects of elevated $CO_2$ in carbon metabolism regulation, I compared the gene expression profiles from trees under ambient and elevated $CO_2$ conditions in two needle cohorts: one-year-old and current-year. Differential expression under elevated $CO_2$ was seven times more frequent in current-year than in one-year-old needles. Despite differences in magnitude, many of the patterns within specific groups of genes were similar across age classes. For instance, there was a trend for downregulation of genes involved in the light-reactions of photosynthesis and those in photorespiration in both age classes, while genes associated with dark respiration were largely upregulated by elevated $CO_2$ in both cases. The difference between the two cohorts was particularly evident in the group of genes related to energy production (ATP synthesis) and the

group associated with carbon partitioning (sucrose and starch metabolism). Because sucrose and starch metabolism categories included many genes known to be important regulators of gene expression and plant physiological processes, this suggests that this stage of carbon metabolism might be an important control point in age-dependent foliar responses to elevated $CO_2$.

This dissertation examined both structural and physiological components of plant water and carbon relations (Chapter 2) across different biological scales of organization (whole-plant level in Chapter 2; gene-level response to ecosystem-level changes in Chapters 3 and 4) and reflecting adjustments at distinct temporal scales (life-span of the organism vs. evolutionary selection of traits). An integrative approach was used to advance our understanding of how plants acclimate and adapt to their environment, and to provide a mechanistic framework for predictive models of plant response to environmental change.

***À minha mãe,***
*Por ter aberto portas e desbravado o caminho*
***À minha avó,***
*Pelo apoio incondicional durante o percurso*
***À minha irmã,***
*Por ser a luz do farol no nevoeiro mais escuro*

# Table of Contents

## List of Tables

## List of Figures

## List of Abbreviations

A (Chapter 2) — Photosynthetic rate

A (Chapters 3 and 4) — Ambient $CO_2$

$A_{net}$ — Net photosynthetic rate

$A_{sat}$ — Light-saturated photosynthesis

cDNA — Complementary deoxyribonucleic acid

C — Carbon

$CO_2$ — Carbon dioxide

DNA — Deoxyribonucleic acid

E — Elevated $CO_2$

EST — Expressed sequence tag

FACE — Free Air $CO_2$ Enrichment

G6P — Glucose-6-phosphate

$g_s$ — Stomatal conductance

$J_{max}$ — Maximum photosynthetic electron rate

$K_H$ — Hydraulic conductivity

$K_L$ — Leaf specific conductivity

$K_S$ — Specific conductivity

mRNA — messenger ribonucleic acid

N — Nitrogen

PET — Photosynthetic electron transport

PCR — Polymerase chain reaction

PS — Photosystem (I or II)

qPCR — Quantitative PCR

rbcS — Ribulose 1,5-bisphosphate carboxylase/oxidase small subunit

RNA — Ribonucleic acid

RT-PCR — Reverse-transcription PCR

Rubisco — Ribulose 1,5-bisphosphate carboxylase/oxidase

RuBP — Ribulose 1,5-bisphosphate

SuSy — Sucrose synthase

TCA — Tricarboxylic (Citric) Acid Cycle

$V_c$ — Carboxylation capacity of rubisco

$V_{c,max}$ — Maximum carboxylation capacity of rubisco

$V_o$ — Oxidation capacity of rubisco

$\Psi_{50}$ — Xylem tension at 50% reduction in hydraulic conductivity

## Acknowledgements

Many years ago, when I crossed the Atlantic Ocean, I was diving into a myriad of simultaneous and previously inexperienced adventures: living, for the first time, outside of my country and out of the comfort of the growing-up nest; speaking this new language every day while seldom using my mother-tongue; facing daily, and learning about, a different social and academic culture; and finally, embarking in a doctoral program at Duke shortly after completing my undergraduate degree at home. I realize now, and must therefore acknowledge it, that I was probably quite eager for a challenge! This adventure and the resulting thesis would not have been the same if it weren't for the contribution of many relatives, friends and colleagues, more than might be named in these pages but that are not forgotten in my mind.

I would like to thank my advisor, Robert Jackson, for providing a welcoming and diverse lab environment where I felt comfortable starting my PhD, and for opening the doors that allowed me to pursue ambitious and independent research. I am especially grateful for the many times that Rob encouraged me to present my results and ideas at national and international meetings where I was able to interact with scientists from across the globe and a wide research spectrum – an experience that was determinant for my progress during graduate school and that I will carry and cherish throughout the future. During these years, Rob also shared his thoughts on how to strive for an efficient

way of working, and I thank him for helping me realize the importance of saying *no* and the concept of *good enough* –tools perhaps not easy to learn, but surely valuable for life.

I would not have come to the Jackson lab nor to Duke if it weren't for the initial suggestion and encouragement of my *Portuguese advisor* (as she is known around here), Helena Freitas. Although our research paths diverged substantially and my initial plans for field work in Portugal did not materialize, Helena never ceased to provide her unconditional moral support and to show her enthusiasm for my achievements (be them small or large!). Despite my heart-felt embarrassment, I am deeply grateful for the times when she advertised my accomplishments to the whole lab, for repeatedly telling me to never doubt my capacities, and for welcoming me back home with open arms.

I am fortunate to have interacted with, and counted on the support of, my committee members Gaby Katul, Michael Lavine, Zhen-Ming Pei, and Steven Vogel. I am convinced that I had one of the most research-wise diverse committees in the department, but amazingly I still managed to develop my dissertation project away from their core expertise. In spite of it, my committee members were always kind with their time and willing to share ideas. A special thank-you is due to Steven for his eagerness to design and build field tools, to Michael for the many times he listened patiently to my questions about statistics, and to Gaby for listening to almost anything and for sharing his enthusiasm about coffee and science. I also thank Dr. Richard White, who briefly served in my committee and shared both a smile and good ideas, and John

Willis who joined the committee for a last minute replacement, and nevertheless provided helpful comments about my thesis and a contagious energy.

Although they were not in my committee, I was incredibly lucky to have two unofficial mentors and close friends who have helped me throughout this journey with their support, discussions about science and academia, and feedback on my professional progress and personal life. For this and much more, I am forever indebted to Chantal Reid and Esteban Jobággy. Mercí, Chantal; Gracias, Esteban!

I am thankful to all collaborators, field companions, and lab assistants that contributed towards my research accomplishments. I thank Hafiz Maherali and Conceição Caldeira (Xixão) for their hard-work towards the manuscript included in chapter 2 of this dissertation, and Cynthia Willson for kindly sharing part of her dissertation data with us. The Grene lab at Virginia Tech taught me the fundamentals of microarray experiments and hosted me during many consecutive weeks of intense molecular work. I could not have explored the genomic world without them. I also thank Andrew McElrone for his participation and enthusiasm about the microarrays research project. Rob Addington, Rae Banks, Rachel Cohen, Will Cook, and Tracey Croker gave valuable field, lab, and image analysis assistance. Profs. Helena Freitas and Cristina Nabais kindly hosted and offered me office space in the Center for Functional Ecology while I was writing my thesis and visiting Portugal. Laurie Anderson, Christy

Henzler, Rebecca McCulley, Chantal Reid, Ariana Sutton-Grier, and Eileen Thorsos provided crucial comments and editing help during the last stages of my dissertation.

Throughout the years, I have interacted with many students and post-docs in the Jackson lab and I want to thank all of them who shared their time, thoughts, and willingness to help. I was truly blessed to always count on the friendly reception of students, post-docs, and faculty in the Plant Ecology group and the Department of Botany at the University of Coimbra during my visits back home. I must also thank the Cunningham lab for the daily interactions on the second floor, for their advice, and for adopting me into their lab and their social events. My path throughout the Ph.D. would certainly not have been the same without their personal and academic imprint!

I am deeply grateful to Anne Lacey, Jim Tunney, and Susan Gerbeth-Jones who provided administrative, accounting, and computer support and were therefore instrumental to the completion of this Ph.D. None of this work could have been done without funding, and I must acknowledge two main sources of financial support: (1) Doctoral fellowship PRAXIS XXI/BD/21668/99 from the Portuguese Foundation for Science and Technology (FCT) and (2) Overseas doctoral fellowship from the Foundation Calouste Gulbenkian (Portugal). Additional funds from Research and Teaching Assistantships, and the awards listed in the Biography section, were also greatly appreciated.

My graduate school experience was enriched by many good friends among my fellow students. Christy, Maria Pia, Alberto, Mario, and Mike were my immediate — and forever remembered —"family" at Duke, but I leave with good memories from many other friends. In particular, Chris, Patrícia, Marta, Vanessa, João, João Pedro, Constanze, Steven, Kathleen, Rebecca, Cristina, Jen, and John made my stay in Durham a rewarding and memorable experience. Although from faraway, my friends in Portugal were crucial in maintaining my spirits high throughout these years. I am especially grateful for the friendship and continuous affection of Susana (my *Su*), Isabel, Cândida, Joana Damasceno, Joana Patrício and Joana Paredes. I could not have faced the struggle of finishing up without the support of recent but not less dedicated friends: Susana Rodriguez and Kiki (Portugal); Melissa ("nerd-camp" and California); Kristin, Mariana, Julie, Michelle and Valerie (Durham). I do not have enough words to thank you all, but I have a special thank-you for two of you: Christy and John – muito obrigada por tudo!

I would not have reached this far if it weren't for my family's support and dedication while I was growing up. I thank my parents, grandparents, and aunts for their love and for accompanying me through life, and wish they had suffered less with my prolonged absence during graduate school. I thank everyone for doing their best, and my dad for reading my soul.

My final thought and my immense gratitude go to my siblings, Inês and Ricardo, for being the best gifts I could ever wish for.

xx

## Preface

Humans' footprint is now evident in each corner of the globe and our species has become a major evolutionary force on Earth (Vitousek 1997, Palumbi 2001). In the last 250 years alone, human activities have caused an unprecedented rate of accumulation of carbon dioxide in the atmosphere. The global atmospheric concentration of this greenhouse gas now largely exceeds its natural range over the last 650,000 years (180 to 300ppm; IPCC 2007). Because greenhouse gases play a crucial role in global climate and temperature regulation, their rate of accumulation in the atmosphere can have profound repercussions on Earth's ecosystems and living species. Earth's biota faces now a major challenge since many species might not have time to adapt to such rapid changes in global climate. We should use the best tools possible to advance knowledge and contribute novel information towards improved predictive models of the response of species to future climate scenarios. Stronger and more mechanism-based models should pave the way to judicious choices about strategies that can help slow down the rate, and mitigate the impact, of the current trend of global climate change. It was with this large framework in mind that I developed the research presented in this dissertation. Although modest comparatively to the overarching theme aforementioned, I hope this doctoral dissertation can contribute towards making our science relevant to the decisions that we face today but that will impact many generations to come.

# Chapter 1: Introduction

## 1.1 Context for the dissertation

Plants have successfully colonized vast areas of the globe and a diverse array of environmental conditions. The distribution of plant species is determined by the interplay of genetic constrains and the environmental context in which they are expressed (Figure 1). The phenotypic traits observed at the organism level (e.g., carbon and hydraulic traits) are the result of the interaction between genes and the environment across different levels of biological organization (individual vs. population) and temporal scales (life-time vs. evolutionary; Figure 1).

Water ($H_2O$) and carbon dioxide ($CO_2$) are two crucial environmental resources required for plant growth and survival, and together they provide the necessary chemical elements (C, H, O) for living tissues across the biosphere. Global water and carbon fluxes are intimately connected at the plant level where carbon uptake (from the atmosphere) and water loss (to the atmosphere) occur simultaneously through stomatal pores in leaves. Among plant communities, forest trees play a major role in the global carbon and water cycles because they exchange large quantities of both water and $CO_2$ with the atmosphere (Schlesinger 1997). In addition, wood, the major component and main sink of carbon in trees, is also the conductive tissue of water from the soil to the atmosphere.

Wood anatomy is an important determinant of the hydraulic architecture of trees determining both the efficiency and the safety of water transport. Traditionally, the term efficiency has described the capacity to maximize the amount of water transported through the system (hydraulic conductivity), while safety referred to the capacity of avoiding a rupture of the water column (a process known as cavitation; Zimmermann 1983). Resistance to cavitation is a plant hydraulic trait that often correlates with variation in soil moisture availability, a relationship that is adaptive across a broad range of species (Maherali, Pockman and Jackson 2004). Adaptive traits can emerge from selection over evolutionary time-scales that span many generations of a population; however, plants still face environmental challenges during the life-time of one generation and this is especially the case in long-lived species such as trees.

Atmospheric $CO_2$ concentration has been rising at an unprecedented rate since the Industrial Revolution and now largely exceeds its natural range over the last 650,000 years (180 to 300ppm; IPCC 2007). This is creating a disturbance in the global carbon cycle and altering the environment of current forest species. Moreover, a climate scenario with the double of today's $CO_2$ concentrations is projected to occur by the end of the century (IPCC 2007). Since this scenario will likely happen within the life-span of most tree species these are expected to respond via changes in gene expression leading to phenotypic plasticity and, eventually, acclimation to the new environment conditions.

The mechanisms by which trees interact with, and respond to changes in, the surrounding environment are far from being elucidated and pose a problem for predictive models of vegetation response to global climate change. In particular, we have a remarkably poor understanding of the contribution of molecular processes that underlie structural and physiological traits of individual trees and may ultimately affect ecosystem function. Molecular processes such as the control of gene expression are fundamental to physiological responses and the acclimation of trees to new environments, and provide the raw material for long-term selection of adaptive traits.

In this dissertation, I combine methodologies from different research fields to provide a more integrative and mechanistic view of the processes regulating the response of forest trees to environmental changes. In particular, I examine the role of gene regulation (Chapters 3 and 4) and trade-offs among whole-plant traits (Chapter 2) in the response of trees to environmental changes such as the availability of water and carbon dioxide, two environmental resources crucial for plant photosynthesis and forest productivity.

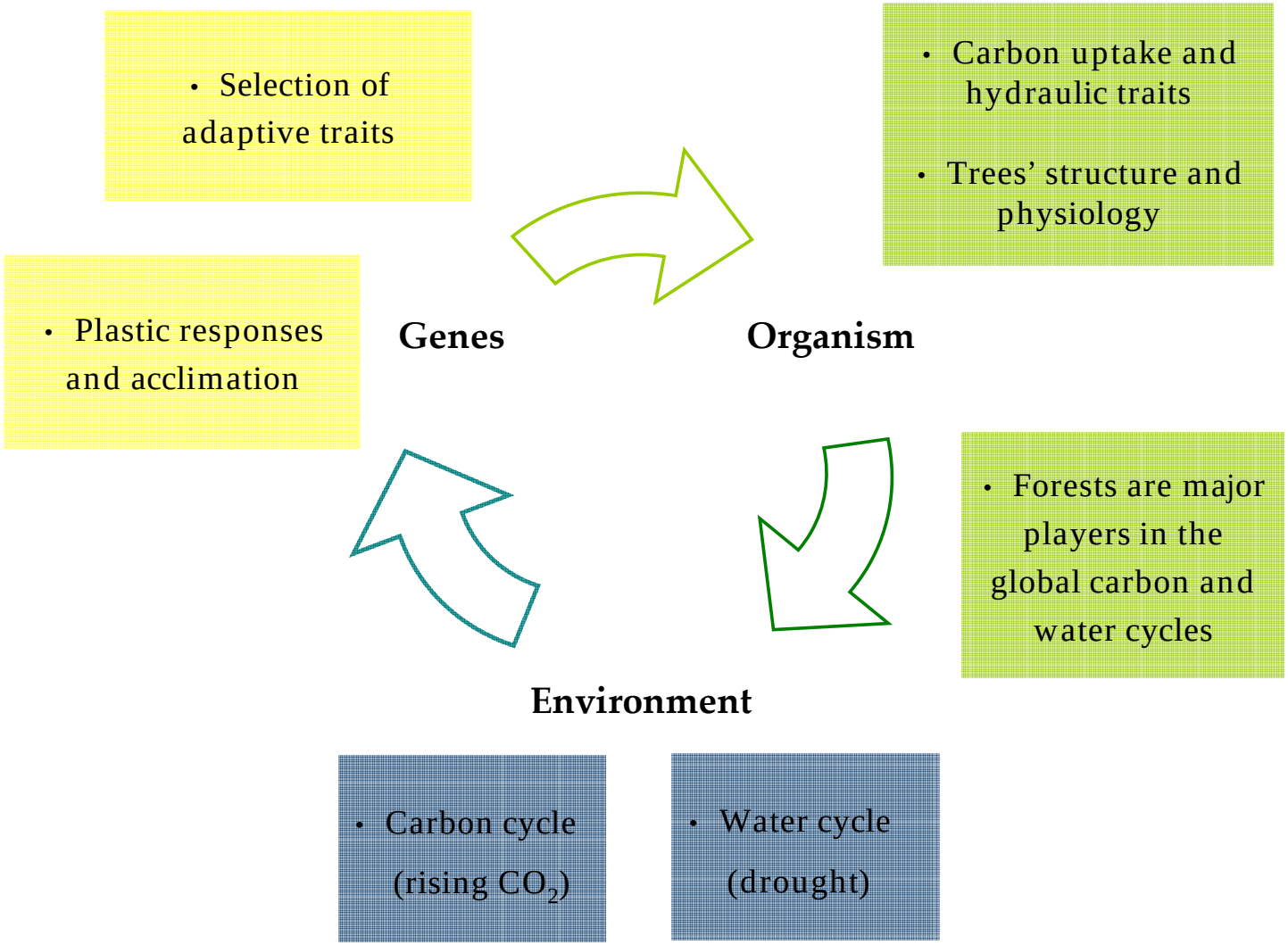


Figure 1.1 – Conceptual diagram representing the overall theme of this dissertation

## 1.2 Brief background on genomic tools

Although each chapter provides its own methods section, I include here a brief contextualizing section for the methods used in Chapters 3 and 4 because these are still relative new applications in ecological settings.

### *Transcriptome, Microarrays, and Ecological Genomics*

According to the Central Dogma of Molecular Biology, genetic information encoded in DNA is expressed through messenger RNA (mRNA) molecules, also known as gene transcripts, and later translated into proteins. However, not every gene is expressed in all cells at every time and condition. Selective expression contributes to the differentiation of tissues and developmental stages and allows relatively specific responses to different environmental stimuli or stresses. The mRNA levels found in a given tissue, developmental stage, or environmental condition, can therefore provide important clues about the function of the genes encoding them. The collection of all gene transcripts in a cell or organisms is called the *Transcriptome* (in analogy to *Genome*). Accordingly, high-throughput techniques looking at large-scale numbers of transcripts are referred to as *Transcriptomics*, although they are often included in the general concept of *Genomic technologies*. Microarrays are an example of such tools (Schena et al. 1995) and one that has become particularly important for gene discovery and plant functional genomics (Somerville and Somerville 1999; Wu et al. 2001; Jackson et al. 2002).

Microarrays consist of a solid substrate (often a glass slide) where hundreds or thousands of DNA sequences are physically attached (Schena et al. 1995). Their working

principle relies on the property of base-pairing that allows two complementary strands of nucleic acids (DNA or RNA) to hybridize. Following this principle, and in the case of spotted two-color microarrays specifically, two independent samples of RNA - or the corresponding complementary DNA (cDNA) – are each labeled with a unique fluorescent dye, and subsequently combined hybridization to a single microarray slide. This process is commonly described as *competitive hybridization*[1] alluding to the "competition" between the RNA/cDNA sequences (targets) in each sample for the same complementary sequencing attached to the slide (probe). In theory, the sample containing more transcripts (and consequently, more dye molecules) corresponding to a given cDNA sequence should hybridize to a further extent to the complementary sequence on the microarray and emit a stronger fluorescent signal in that spot. The difference in dye intensities reflects therefore the relative expression change between the two samples, i.e., whether genes are equally expressed in, or differentially expressed between, both conditions (samples). If one sample contains more transcripts of a specific gene, we say that the gene is upregulated in that condition. Likewise, it there are fewer transcripts, than the gene is said to be downregulated.

[1] Note however that competition is not an accurate description since one of the pre-requisites of this technique is that the probe sequence must be sufficiently abundant to allow complete hybridization of the corresponding target sequences. Therefore there is not a limiting "resource" to compete for (Benfey, P., pers. comm.).

Microarrays have been used in a wide variety of organisms (although most frequently in the so-called "model organisms", of which humans, fruit flies, and the plant *Arabidopsis*, are some examples) as a tool to answer an even wider range of questions. Their recent application to non-model organisms and field experiments has contributed to the emergence of a new field called Ecological Genomics. This new area of research aims to combine a more realistic, natural context for the interpretation of genes studied under controlled, laboratory conditions as well as a more detailed and mechanistic explanation for broader-scale questions in Ecology.

## 1.3 Outline of the dissertation

The unifying goal of this dissertation is to investigate the processes underlying the response of forest trees to changes in the availability of carbon and water in the environment. It includes a combination of approaches exploring both structural and physiological components of plant water and carbon relations (Chapter 2) across different biological scales of organization (whole-plant level in Chapter 2; gene-level response to ecosystem-level changes in Chapters 3 and 4) and reflecting adjustments at distinct temporal scales (life-span of the organism vs. evolutionary selection of traits; Figure 1)

In Chapter 2, I evaluate the variation in vulnerability to xylem cavitation across 16 different temperate forest tree species that include angiosperms and gymnosperms (such as loblolly pine) as well as three different wood anatomy types (ring-porous, diffuse-

porous, and non-porous). In summary, this chapter investigates the potential adaptive significance of resistance to cavitation while determining possible trade-offs with other carbon and water exchange physiological traits.[2]

In Chapter 3, I examine the effects of elevated $CO_2$, a major cause of global climate change, on gene expression patterns in loblolly pine trees. This chapter summarizes the results of the first transcriptome-scale study of effects of elevated $CO_2$ on mature, field-grown forest trees. It examines the effects of elevated $CO_2$ across a large number of genes and provides information on the seasonal variation of these effects.

In Chapter 4, I explore in more detail the effects of elevated $CO_2$ on gene-level regulation of carbon metabolism affecting carbon assimilation, partitioning, and oxidation. Additionally, I compare the gene expression response to elevated $CO_2$ across two foliage age classes: one-year-old and current-year needles. This chapter evolves from the data and concepts examined in Chapter 3 but focuses on larger-scale implications involving the carbon sequestration potential of the pine trees in the forest ecosystem.

In Chapter 5, I conclude with a brief analysis of the work included in this dissertation, and some thoughts about its overall significance.

---

[2] This chapter reflects a collaborative effort with a previous post-doctoral associate in the Jackson lab, Hafiz Maherali (now at University of Guelph, Canada), and includes data collected by other researchers. The manuscript was published as Maherali H.*, **Moura C.F.***, Caldeira M.C., Willson C.J. and Jackson R.B. 2005. Functional coordination between leaf gas exchange and vulnerability to xylem cavitation in temperate forest trees. *Plant Cell and Environment*, 29: 571-583 (* these authors contributed equally to this work).

# Chapter 2: Trade-offs between vulnerability to xylem cavitation and leaf gas exchange in temperate forest trees

## 2.1 Introduction

Water supply to leaves depends on maintaining an intact water column in the xylem from roots to shoots. Because this hydraulic pathway is under increasing tension during transpiration, it is vulnerable to cavitation through air seeding, which occurs when air bubbles are aspirated into water filled conduits (Zimmermann 1983, Tyree and Sperry 1989). Each time cavitation occurs, the resulting vapor filled conduit no longer carries water, causing a decrease in xylem hydraulic conductivity (Tyree and Ewers 1991). The vulnerability of plants to xylem cavitation is often correlated with variation in moisture availability, and recent evidence indicates that this relationship is adaptive across a broad range of taxonomic groups (Maherali, Pockman and Jackson 2004).

Our understanding of how vulnerability of xylem to cavitation is associated with other plant functional traits that control carbon and water balance, however, is still incomplete. For example, resistance to water-stress induced cavitation via air seeding in a large majority of angiosperms depends on the surface tension of the meniscus in each pore of the pit membrane connecting adjacent conduits (Jarbeau, Ewers and Davis 1995). Increased resistance to cavitation should therefore be accompanied by decreased pore hydraulic conductivity, and ultimately, stem hydraulic conductivity (Zimmermann 1983; Sperry and Hacke 2004). Nevertheless, evidence for a trade-off between stem cavitation resistance and xylem water transport across species is inconsistent (e.g.

Maherali et al. 2004). The direct link between sustained water transport and leaf transpiration also suggests that there should be functional coordination between vulnerability to xylem cavitation and the regulation of stomatal conductance (Sperry and Pockman 1993; Sparks and Black 1999; Brodribb et al. 2003). In addition, the observation that tissue construction costs are associated with vulnerability to xylem cavitation across species (Hacke et al. 2001a) suggests that xylem cavitation could be associated with traits that affect plant carbon uptake. Although there is evidence of functional coordination between hydraulic conductivity and gas exchange (Hubbard et al. 2001; Meinzer 2002), few studies have explicitly considered the link between cavitation resistance and suites of leaf physiological traits that control $CO_2$ and $H_2O$ fluxes.

Many insights about the functional significance of xylem cavitation across species have been derived from studies on stems (Tyree and Ewers 1991; Pockman and Sperry 2000; Maherali et al. 2004). Yet root xylem properties generally differ from stems and may be more tightly linked to the control of whole plant water transport (Jackson, Sperry and Dawson 2000). For example, roots typically have wider xylem conduits, and in consequence, higher segment hydraulic conductivity per unit cross sectional area than stems (e.g., McElrone et al. 2004). In addition, roots are generally more vulnerable to xylem cavitation than stems, suggesting that they may be the weakest link along the soil to leaf water transport pathway (Kavanagh et al. 1999; Martínez-Villalta et al. 2002; McElrone et al. 2004). Therefore, incorporating information on the hydraulic properties

of roots in addition to that of stems in comparative studies may help identify adaptive relationships between xylem function and other physiological traits.

We examined the relationship between resistance to xylem cavitation and other physiological traits using a group of diverse, co-occurring tree species commonly found in the temperate forest of eastern North America. We determined (1) if there was a trade-off between vulnerability to xylem cavitation and xylem water transport traits, (2) whether vulnerability to xylem cavitation was correlated with traits associated with leaf carbon and water vapor fluxes and (3) if the strength of these relationships differed between stems and roots. Because a significant proportion of species at our Duke Forest study site were from the genus *Quercus*, we also took the opportunity to examine functional associations within this clade by adding additional oak species from a nearby temperate sand hill savanna ecosystem. To determine the influence of shared ancestry on the strength of trait relationships and to account for the statistical non-independence of species, we calculated correlations with and without phylogenetic information (e.g. Maherali et al. 2004).

## 2.2 Materials and methods

### *Study site and plant material*

Our study was conducted in the Durham Division of Duke Forest, located near Durham, North Carolina (36º 01' N, 78º 59' W, elevation 150 m). The climate is warm temperate, with a mean annual temperature of 15ºC and average monthly maxima and minima of 26ºC (July) and -2.3ºC (January), respectively (1971-2000 record). The mean annual precipitation is 1220 mm with approximately half this amount (627 mm) received during the growing season (April-September; Southeastern Regional Climate Center, http://cirrus.dnr.state.sc.us). The site was an 80-100 year-old second-growth mixed hardwood – conifer forest upon well drained loamy soils with a predominantly flat topography. We sampled 14 common canopy and sub-canopy tree species from nine seed plant families and a variety of wood types (Table 1). Stems from two additional temperate oak species were sampled from a site typical of the sandhills ecosystem in the southeastern USA located in the U.S. Army's Fort Bragg Military Base (35° 10' 17"N, 79° 22' 56"W). This site is characterized by deep (~4 m) sandy soils and experiences similar weather conditions to the Duke Forest site. The site is managed as a long-leaf pine savanna with periodic burning every 3 years that maintains a *Pinus palustris* canopy with various oak species in the subcanopy, of which *Q. laevis* and *Q. stellata* are the most abundant.

### *Leaf gas exchange*

To facilitate access for gas exchange measurements and to ensure that all samples experienced similar light environments, we sampled saplings or young trees ranging from 2-4 m tall that occurred in canopy gaps created by natural disturbance or near clearings associated with forest roads. We measured photosynthetic $CO_2$ assimilation ($A$) and stomatal conductance ($g_s$) to water vapour with an open gas-exchange system (LI-6400, Li-Cor Inc., Lincoln, NE, USA) on 2-3 sun-exposed leaves of 9-12 individuals of each species during July 2000, after leaves had expanded fully. To ensure that leaf gas exchange values reflected the maximum capacities of leaves, we attempted to make measurements under non-limiting conditions. Therefore, individuals were sampled before midday (930 and 1200 hours EST). Incident irradiance was maintained at saturating levels (1800 μmol $m^{-2}$ $s^{-1}$) by red-blue light-emitting diodes and a Peltier cooling module maintained leaf temperature between 25-30ºC. Although the relative humidity was not controlled directly, vapour pressure deficit (VPD) varied between 1.5-2.0 kPa and approximated ambient conditions. To calculate $g_s$, we used a boundary layer conductance of 1.42 mol $m^{-2}$ $s^{-1}$, which was calculated on the basis of leaf area and fan speed using the energy balance algorithms of the LI-6400. Following enclosure in the leaf cuvette, leaves reached steady-state values (e.g., when the coefficients of variation of $CO_2$ and $H_2O$ within the chamber were < 0.25%) within 5 minutes. To assess the trade-off between $CO_2$ uptake and water loss, we calculated instantaneous water-use efficiency (WUE) as $A/g_s$. Gas exchange was expressed on a one-sided leaf area basis for all species.

Angiosperm leaves were larger than cuvette, so the default area of 6 $cm^2$ was used for all calculations. For *Pinus taeda,* we measured the widest diameter of each needle in the cuvette, and calculated projected leaf area as the product of the length of the cuvette (3 cm) and the aggregate diameter of all needles. *Juniperus virginiana* leaf samples were excised after gas exchange measurements and projected leaf area were made with a LI-3100A leaf area meter (Li-Cor, Inc.).

Following gas exchange measurements, shoot water potential (Ψ) was measured with a pressure chamber (Plant Moisture Status Instrument Company, Corvallis, OR, USA). In addition, individual leaves used for gas exchange were excised and placed in plastic bags containing moist paper towels. For angiosperms, individual leaf size was subsequently measured with the LI-3100A. For *Pinus taeda*, individual fascicles were separated to allow needles to lay flat on the conveyer belt of the LI-3100A, facilitating projected area measurement. These leaves were dried to constant mass in a forced convection oven at 65°C for 48 h and weighed. Specific leaf area (SLA) was calculated by dividing leaf size by leaf mass. Leaves were subsequently ground to a powder using a Crescent Wig-L-Bug (Crescent Dental, Lyons, IL, USA). Powder samples were assessed for %C and %N content using a CE Instruments NC 2100 elemental analyzer (ThermoQuest Italia, Milan, Italy). Integrated WUE was determined on six of these powdered samples per species by measuring carbon isotope discrimination ($\delta^{13}C$; Farquhar *et al*. 1989) with a Finnigan MAT Delta Plus XL continuous flow mass spectrometer (Finnigan MAT GmbH, Bremen, Germany).

### *Vulnerability to xylem cavitation*

We measured the vulnerability of xylem to cavitation on stem and root segments of 5-7 of the same individuals of each species previously sampled for gas exchange. We collected 0.5-1.0 m-long sun-exposed shoots and 30-70 cm-long roots from 20-50 cm soil depths during August and September of 2001 (stems) and 2003 (roots). Stem and root samples were typically 2-5 years old, as determined by growth ring counts of cross sections. To minimize dehydration, all tissue was immediately placed in plastic bags containing wet paper towels. In the laboratory, all stem samples were re-cut under water to a length of 14 cm, and the cut ends trimmed with a razor blade. Root samples were re-cut to longer lengths (between 24 and 59 cm) to minimize refilling of cavitated vessels during measurements, particularly for *Quercus*. Although we have no information on vessel length distributions for our species, previous studies in diffuse porous angiosperms indicated that average vessel lengths for similar aged tissue was < 4 cm. Average vessel length is typically longer in ring porous species (e.g., ~13 cm in *Vitis vinifera*) suggesting that at least some vessels were open in *Quercus*.

Hydraulic conductivity ($K_H$) was measured as described by Sperry, Donnelly and Tyree (1988) in an air-conditioned laboratory (20°C). Segments were cleared of air-emboli by perfusing them at high pressure with a filtered (0.2 µm) solution of distilled water for 15-20 minutes at 100 kPa. A hydrostatic pressure of 1.5 – 2 kPa was used to measure volume flow rate ($Q$, kg/s), which was calculated by collecting efflux continuously with a vial placed on a 0.0001 g balance connected to a computer (e.g.

Hacke et al. 2000). Hydraulic conductivity ($K_H$; kg m $MPa^{-1}$ $s^{-1}$) was expressed as the volume flow rate divided by the pressure gradient [$Q/(dP/dx)$]. Specific conductivity ($K_S$; kg $m^{-1}$ $MPa^{-1}$ $s^{-1}$) was calculated by dividing $K_H$ by cross-sectional xylem area of the segment. Leaf specific conductivity ($K_L$; kg $m^{-1}$ $MPa^{-1}$ $s^{-1}$) was calculated by dividing $K_H$ by the leaf area distal to the measured segment. Leaf area distal to the measured stem segment was measured on fresh tissue using a LI-3100A leaf area meter (Li-Cor, Inc.).

Vulnerability to drought-induced xylem cavitation was measured as the reduction in hydraulic conductivity of a stem or root segment as a function of decreasing xylem tension (a vulnerability curve, Sperry et al. 1988). For stem segments of all species and root segments of *Juniperus virginiana*, vulnerability curves were constructed with the centrifuge technique (Pockman, Sperry and O'Leary 1995; Alder et al. 1997). Segments were spun on an axis for 5 min in a custom designed rotor (Alder et al.et al. 1997) at a specific rotational velocity to produce xylem tensions ranging from -0.5 to -10 MPa in 0.5 - 2 MPa increments. $K_H$ was measured on each stem following each successive spin in the centrifuge. Preliminary experiments indicated that for many species (especially ring-porous *Quercus*), an initial spin at 1 MPa produced large (70-90%) losses in $K_H$. As a result, it was possible that flushing stems prior to constructing vulnerability curves refilled non-functional conduits (termed cavitation fatigue, Hacke et al. 2001b) or that this initial exposure to low negative pressures caused open vessels to cavitate. Regardless of the mechanism operating, all stems were spun at low speed (-0.5 MPa) after flushing to allow functional conduits to remain filled while embolizing non-

functional conduits (i.e., Hacke, Sperry and Pittermann 2000) and to prevent open vessels from contributing to measurements of xylem vulnerability to cavitation. In addition, only water transport measurements made after this initial spin were used in calculations to prevent non-functional conduits and open vessels from contributing to estimates of $K_H$, $K_S$ and $K_L$.

Although the use of pure water as a perfusing solution can underestimate $K_H$ because of hydrogels in the pit membrane (Zwieniecki, Melcher and Holbrook 2001), we used a solution of pure water, rather than a solution of KCl for our measurements. The effect of KCl on $K_H$ varies considerably across angiosperms (Boyce et al. 2004), and even among individuals of a single species (Zwieniecki et al. 2001). This variable effect may be associated with differences in the ionic concentrations of xylem sap across individuals and species. To utilize KCl effectively therefore, we would have had to determine an appropriate molar concentration that is representative of the xylem sap of each species. As a result, the use of a constant KCl solution may not correct the bias in our interspecific comparisons that is associated with using pure water. We note that KCl and pure water solutions have produced similar vulnerability curves in other angiosperm species (Davis et al. 2002). In addition previous studies have detected trade-offs between vulnerability to cavitation and hydraulic conductivity despite using non-KCl solutions (e.g. Sperry and Pockman 1993; Hacke et al. 2000; Martinez-Vilalta et al. 2002).

The large size of conduits in roots (McElrone et al. 2004) prevented us from constructing vulnerability curves with the centrifuge method because attaching samples

to the hydrostatic measuring apparatus refilled embolized conduits. Therefore, vulnerability curves for roots were constructed using the air-injection method (Cochard et al. 1992, Sperry and Saliendra 1994) in which xylem cavitation was induced by successively increasing positive air pressures on a segment inside a double-ended pressure chamber. Previous studies indicate that the centrifuge and air-injection methods yield very similar vulnerability curves (Pockman et al. 1995). Each root segment was notched (0.5 - 1 mm deep) with a razor blade to provide an entry point for air, the bark at the proximal ends removed and then inserted into a pressure chamber with both ends protruding. The root ends were connected to the hydraulic measurement apparatus and $K_H$ was measured as described previously. The pressure inside the chamber was then raised to 0.5 MPa and maintained at that pressure for 15 min. After pressurization, the segment was allowed to equilibrate for 10 min. at low pressure (0.1 MPa) followed by 5 more min. at 0 MPa and hydraulic conductivity was measured again. This process was repeated at progressively higher pressures in 0.5-1.0 MPa increments to generate a vulnerability curve for each segment. To maintain consistency with vulnerability curves constructed with the centrifuge method, $K_H$ after pressurization at 0.5 MPa was taken as the reference value.

Percent loss in conductivity (PLC) following each spin in the centrifuge or pressurization of the chamber was calculated as $PLC=100*[(K_{max}-K_H)/K_{max}]$, where $K_H$ is the hydraulic conductivity of the segment measured after each chamber pressurization and $K_{max}$ is the hydraulic conductivity after the initial 0.5 MPa spin or pressurization.

Vulnerability curves were fit with an exponential sigmoid equation (Pammenter and Vander Willigen 1998):

$$PLC = \frac{100}{\left[1 + \exp(a(\Psi - b))\right]} \quad (1)$$

where $\Psi$ is the negative of the injection pressure, $a$ is a measure of the degree that conductivity responds to injection pressure or tension (curve slope) and $b$ represents the $\Psi$ at which a 50% loss in conductivity occurs ($\Psi_{50}$ or curve displacement along the x-axis). Coefficients $a$ and $b$ were estimated using the non-linear regression procedure in Systat 8.0 (SPSS, Evanston, IL, USA).

### *Xylem conduit measurements*

Xylem conduit diameter was measured on stem segments used for hydraulic measurements. Stem cross sections (20-µm thick) were made with a sliding microtome (American Optical Co., Buffalo, NY, USA) and stained with toluidine blue. Cross-sections were viewed with a light microscope interfaced with a Nikon CoolPix 950 digital camera (Nikon Inc., Melville, NY, USA). Captured images were downloaded onto a computer for image-analysis using NIH Image 1.58 (U.S. National Institutes of Health; http://rsb.info.nih.gov/nih-image/). We measured radial strips of cells on sectors spaced at 90° intervals in the outermost portion (2 – 5 growth rings) of each cross section. Up to 300 conduits were measured for each stem segment. Hydraulic diameter ($D_h$) of lumens was calculated as $D_h = 2xy/[x+y]$ for tracheids and $D_h = (2x^2y^2/[x+y])^{1/2}$ for vessels, where $x$ and $y$ are the short and long sides of the conduit, respectively (Lewis and Boose 1995).

To determine functional significance of conduit size distribution within each segment, we calculated the hydraulically-weighted mean diameter ($D_{h\text{-}w}$) for each segment as $\Sigma D_h^5/\Sigma D_h^4$ (Pockman and Sperry 2000).

### *Statistical and Phylogenetic analyses*

Because our primary interest was in examining which traits are functionally integrated with xylem vulnerability to cavitation, correlations were examined with root and stem $\Psi_{50}$ as the anchor traits (i.e. Schwilk and Ackerly 2001). A limitation of solely using cross-species comparisons to determine functional integration of physiological traits is that these correlations may be biased by the similarity of closely-related species (Felsenstein 1985, Harvey and Pagel 1991). This shared evolutionary history prevents individual species from being statistically independent data points (Harvey and Pagel 1991). To account for shared evolutionary history, we calculated phylogenetically independent contrasts (PICs, Felsenstein 1985), which are determined for each speciation event in the phylogeny (e.g., as the difference in trait values between sister taxa along each branch; Felsenstein 1985, Garland et al. 1992). This method identifies adaptive relationships because the strength and sign of the contrast correlation indicates whether evolutionary shifts in a trait are associated with changes in another trait or ecological variable (Pagel 1993, Ackerly and Reich 1999).

A fully bifurcated phylogenetic tree (Figure 1) incorporating taxa sampled at our study site was derived from published sources, using methods and assumptions described in Maherali et al. (2004). Relationships between traits were evaluated using

traditional cross-species correlations and correlations among PICs. Pearson correlations for the cross-species analysis were calculated using SPSS 10.0 (R; SPSS, Evanston IL, USA). PICs and Pearson correlations among PICs were calculated using the Phenotypic Diversity Analysis Programs (PDAP; http://www.biology.ucr.edu/people/faculty/Garland/PDAP.html; Garland et al. 1999; Garland and Ives 2000) from within the Mesquite system for phylogenetic computing (Maddison and Maddison 2004). All data were log-transformed prior to analyses. Because trees from various sources were combined to produce our phylogeny, it was impossible to incorporate into our analysis information on phylogenetic branch lengths, which indicate the number of evolutionary changes along each ancestor-descendant pathway (Harvey and Pagel 1991). In the absence of such information, we assumed that branch lengths are equal to calculate PIC correlations, a conservative assumption that minimizes type I error rate (Ackerly 2000). We note that because our study species were sampled non-randomly and disjunctly across seed plant families, ancestral reconstructions based on parsimony are likely to be biased, and this bias will influence the strength and statistical significance of PIC correlations. However, this limitation must be balanced against inflated Type I error rates of non-phylogenetically corrected cross-species correlations (Garland et al. 1992, Ackerly 2000). To be conservative and to facilitate interpretation, we present both standard and PIC correlations.

## 2.3 Results

The vulnerability of roots and stems to xylem cavitation varied widely across species (Figures 2 and 3). The most resistant species in the community, *Juniperus virginiana*, reached 50% stem cavitation ($\Psi_{50}$) at a water potential that was nearly 8-fold more negative than that of the most vulnerable species, *Quercus falcata*. In general, stems of *Quercus* were more vulnerable to cavitation than other species. Even the *Quercus* species occurring on well-drained sandy soils at the Fort Bragg site were more vulnerable to cavitation than most of the non-*Quercus* Duke Forest species. With the exception of *Cercis canadensis*, *Quercus* species also had roots that were the most vulnerable to cavitation. Roots were more vulnerable to xylem cavitation than stems in all species (Figures 2 and 3). In addition, the specific conductivity of roots was on average 5.6-times higher than that of stems (Paired t-test, $P < 0.01$, Table 2).

Based on rank order, species with low stem $\Psi_{50}$ also had low root $\Psi_{50}$ (Figure 4). However, we observed that differences between stem and root $\Psi_{50}$ increased as overall vulnerability to xylem cavitation decreased. For example, species with vulnerable xylem, such as those in *Quercus* and *Nyssa sylvatica* had similar stem and root $\Psi_{50}$, whereas species with resistant xylem, such as *Cornus florida* and *J. virginiana* had stems with much more negative stem $\Psi_{50}$ than root $\Psi_{50}$ (Figure 4).

In the cross-species analysis, stem $\Psi_{50}$ increased significantly with specific conductivity ($K_S$; Figure 5A, $P < 0.001$) and with mean hydraulically weighted conduit diameter ($D_{h\text{-}w}$; Figure 5C, $P < 0.001$), but was only marginally associated with leaf

specific conductivity ($K_L$; Figure 5B, $P = 0.06$). However, the phylogenetically independent contrast (PIC, Table 3) correlation for each of these relationships was not statistically significant (Figure 5A-C, insets). The absence of an evolutionary correlation across taxa is consistent with the observation that data points among more closely related species tended to be clustered on all three plots of the relationship between hydraulic efficiency and $\Psi_{50}$ (Figure 5A-C). In addition, there was no relationship between root $\Psi_{50}$ and root $K_S$ for both cross-species and phylogenetically independent contrast correlations (Table 3). Within *Quercus*, $\Psi_{50}$ increased significantly with increasing $K_L$ (Figure 6B, $P = 0.05$) but was not associated with either $K_S$ (Figure 6A) or $D_{h\text{-}w}$ (Figure 6C). Although significant PIC correlations suggested that there were evolutionary correlations between $\Psi_{50}$ and $K_S$ (Figure 6A, inset, $P = 0.05$) and $\Psi_{50}$ and $K_L$ (Figure 6B, inset, $P = 0.01$), these relationships were driven by a single contrast between *Q. laevis* and *Q. falcata*, and may therefore not be biologically meaningful within the genus.

There were important associations between $\Psi_{50}$ and leaf level traits, particularly for roots. In the cross species analysis, both photosynthetic rate ($A$) and stomatal conductance ($g_s$) increased with increasing stem $\Psi_{50}$ (Figure 7A, B; $P = 0.02$ and 0.10, respectively), but there was only an association between $A$ stem $\Psi_{50}$ ($P = 0.04$; Figure 7A inset) and no relationship between $g_s$ and stem $\Psi_{50}$ in the PIC analysis (Figure 7B inset). Both the cross species and PIC correlations for these relationships were sensitive to the inclusion of conifers in the analysis. For example, when only angiosperms were

included, $A$ was weakly correlated with stem $\Psi_{50}$ (R = -0.47, $P$ = 0.15; PIC = -0.18, $P$ = 0.30). In contrast, $A$ and $g_s$ increased strongly with increasing root $\Psi_{50}$ in both the cross species ($P < 0.001$; Figure 7C, inset) and PIC analyses ($P < 0.01$; Figure 7D, inset). These relationships were also strong within the angiosperms (for $A$ vs. root $\Psi_{50}$: R = 0.82, $P$ = 0.002, PIC = -0.79, $P$ = 0.002; for $g_s$ vs. root $\Psi_{50}$: R = -0.64 , $P$ = 0.04, PIC = -0.58 , $P$ = 0.03].

Instantaneous water-use efficiency, calculated as $A/g_s$, was not correlated with $\Psi_{50}$ in either stems or roots. In addition, $A$ and $g_s$ were not associated with measures of hydraulic conductivity ($K_S$ and $K_L$) in stems (data not shown, $R \leq 0.35$, $P \geq 0.25$). Leaf size was not associated with stem $\Psi_{50}$, but was positively correlated with root $\Psi_{50}$ ($P < 0.01$, Table 3), a relationship that was robust to phylogenetic correction ($P$ = 0.01; Table 3), but was weaker when conifers were removed from the analysis (R = -0.31, $P$ = 0.35, PIC = -0.23, $P$ = 0.25). Other leaf traits of functional significance such as integrated water-use efficiency (measured as carbon isotope discrimination [$\delta^{13}C$]), leaf nitrogen or specific leaf area were either marginally associated (e.g. $\delta^{13}C$) or not associated with stem or root $\Psi_{50}$ (Table 3).

## 2.4 Discussion

### *Vulnerability to xylem cavitation and water transport*

Studies within single communities have provided evidence that there is a cross-species correlation, and thus a trade-off, between vulnerability to xylem cavitation and xylem transport capacity (Pockman and Sperry 2000; Martínez-Vilalta et al. 2002). On the surface, our results are consistent with these previous studies. We found considerable interspecific variation in how vulnerable stems and roots were to xylem cavitation for a group of co-occurring woody species (Table 2). There were also large differences across species in the efficiency of xylem transport, as measured by specific conductivity ($K_S$) and leaf specific conductivity ($K_L$). However, even though all three measures of hydraulic efficiency ($K_S$, $K_L$ and mean $D_{h\text{-}w}$) increased with $\Psi_{50}$ across 14 co-occurring species, there was no relationship between these parameters when phylogenetic information was included (Figure 5A-C, insets). These results are consistent with a broader analysis of stems of 167 woody plant species across a variety of biomes (Maherali et al. 2004). Similarly, there was no relationship between the vulnerability of roots to cavitation and root $K_S$ for these species for both cross-species and phylogenetically independent contrast correlations (Table 3). We conclude, therefore, that there was weak evidence for a trade-off between$\Psi_{50}$ and the efficiency of xylem transport within stems or roots for the species in this temperate forest community.

Resistance to water stress induced cavitation via air seeding in a large majority of angiosperms depends on the surface tension of the meniscus in each of the pores of the

pit membrane that connects adjacent conduits (Tyree and Sperry 1989). As a result, increases in resistance to cavitation must be accompanied by presumably costly decreases in pore hydraulic conductivity (Sperry and Hacke 2004). The absence of a correlation between $\Psi_{50}$ and xylem transport efficiency, despite a tradeoff between air seeding pressure and pit conductivity, may be associated with differences in other xylem traits across our broad taxonomic sample (Figure 1). For example, increased vessel length and diameter both increase hydraulic conductivity, and may compensate for hydraulic limitations in the pit membrane (Comstock and Sperry 2000; Sperry and Hacke 2004).

Since the ability to detect trade-offs between vulnerability to cavitation and xylem water transport capacity may be confounded by large differences in xylem vessel length and diameter across taxa, comparative studies with closely related species with similar xylem anatomy may yield insights on the evolution of this physiological trade-off. However, our comparisons of $\Psi_{50}$ and water transport capacity within a single genus, *Quercus*, were equivocal. Of the three indices of hydraulic efficiency, only $K_L$ was correlated with vulnerability to cavitation in the cross-species analysis (Figure 6). However, the statistical significance of this correlation was driven by the presence of a single species, *Q. laevis*. Similarly, the significant phylogenetically independent contrast correlations between hydraulic conductivity (both $K_S$ and $K_L$) and $\Psi_{50}$ were driven by a single contrast between *Q. laevis* and *Q. falcata*. The sensitivity of these relationships to a

single data point suggests that there may not be an evolutionary trade-off between $\Psi_{50}$ and xylem water transport capacity in *Quercus* stems.

Roots were more vulnerable to xylem cavitation than stems (Figures 2, 3 and 4), a result that is consistent with previous studies (Kavanagh et al. 1999; Jackson et al. 2000; Martínez-Vilalta et al. 2002; McElrone et al. 2004). Interestingly, the magnitude of the difference between stem $\Psi_{50}$ and root $\Psi_{50}$ appeared to be correlated with overall vulnerability to xylem cavitation. For example, species that were relatively vulnerable to cavitation, such as *Quercus*, had stem $\Psi_{50}$ and root $\Psi_{50}$ values that differed only modestly (an average of 25%), whereas resistant species such as *Oxydendrum arboreum* and *Cornus florida* had stem xylem that was more than twice as resistant to cavitation than root xylem. These differences may be species specific or reflect some level of acclimation by roots of all species to the relatively high soil moisture levels at the Duke Forest site (H. Maherali, personal observation). For example, it is possible that vulnerability to cavitation in roots is more closely calibrated to the less negative water potentials they experience relative to stems. Although there is some evidence that cavitation resistance in roots is phenotypically plastic (as reviewed in Sperry et al. 2002), little is known about the degree to which phenotypic plasticity influences vulnerability to cavitation in roots versus stems.

Root $K_S$ was higher than stem $K_S$ in all species (Table 3), a result that has been reported in other studies (e.g. Kavanagh et al. 1999; Martínez-Vilalta et al. 2002; McElrone et al. 2004). Higher $K_S$ in roots also suggests that conduit diameter was greater

in roots than in stems. Like differences in $\Psi_{50}$, systematically larger vessels in roots relative to stems may be associated with less negative water potentials present in the root zone. If roots experience limited cavitation, the maintenance of high $K_S$ would decrease the overall hydraulic resistance of the root system and suggests that root tissue may be specialized for water uptake and transport. It is also possible that roots are more specialized for water transport than stems because biomechanical stresses on xylem for canopy support and wind resistance would be less severe in roots than stems (McElrone et al. 2004).

### *Vulnerability to xylem cavitation and leaf traits*

Our results reveal a strong association between leaf gas exchange and the vulnerability of xylem to cavitation. For example, we observed that photosynthetic rate ($A$) and stomatal conductance ($g_s$) both increased with increasing $\Psi_{50}$ (Figure 7A-D). Previous studies have identified roots as the most limiting component of the hydraulic pathway (as reviewed in Meinzer 2002; Sperry et al. 2002). Our results are consistent with this hypothesis; relationships between gas exchange and $\Psi_{50}$ were stronger for roots than for stems, suggesting that vulnerability of roots to cavitation places the largest constraint on leaf $CO_2$ and $H_2O$ fluxes. Moreover, the correlation between root $\Psi_{50}$ and $A$ or $g_s$ was quite robust even with the inclusion of phylogenetic information, suggesting that the functional relationship among these traits is adaptive.

The observation that root $\Psi_{50}$ increased with increasing maximum $g_s$ is consistent with a more general trade-off between vulnerability to cavitation and water transport

capacity (Figure 7D). Since the magnitude of $g_s$ depends on the hydraulic conductivity of the entire soil – leaf pathway (Sperry and Pockman 1993; Nardini and Salleo 2000; Hubbard et al. 2001; Meinzer 2002), our results suggest that the conducting efficiency versus xylem safety trade-off can be manifested at the level of the whole plant, rather than just within specific organs. A relationship between root $\Psi_{50}$ and maximum $g_s$ is also consistent with the expectation of functional coordination between vulnerability to xylem cavitation and the regulation of stomatal conductance across species. For example, species with less negative $\Psi_{50}$ might behave as cavitation avoiders through tight regulation of stomatal opening, whereas those species with more negative $\Psi_{50}$ could behave as cavitation resisters with relatively weak stomatal regulation (Sparks and Black 1999; Martínez-Vilalta, Sala and Pinol 2004). If stomata act to maintain a constant leaf water potential through hydraulic regulation, stomatal sensitivity to vapour pressure deficit must be positively correlated with the magnitude of maximum $g_s$ (Oren et al. 1999). Our results are consistent with this model because species in Duke Forest with high $g_s$, and therefore high stomatal sensitivity to water deficits, also have xylem that is more vulnerable to cavitation.

The correlation between photosynthetic rate and the vulnerability of roots to xylem cavitation may be an indirect effect of coordination between $g_s$ and $\Psi_{50}$, rather than the direct influence of root hydraulic traits on photosynthetic capacity. Several lines of evidence support this conclusion. First, photosynthesis and stomatal conductance are generally correlated, both within populations and across species, suggesting that

photosynthetic capacity is determined by stomatal limits to $CO_2$ diffusion (Wong, Cowan and Farquhar 1979). In addition, we observed no relationship between vulnerability to cavitation and other traits associated with carbon uptake, such as N content and specific leaf area (Table 3). Finally, although there was a weak association between root $\Psi_{50}$ and integrated water-use efficiency (as measured by $\delta^{13}C$), variation in carbon isotope discrimination was correlated with $g_s$ and not $A$ (data not shown).

Unlike previous studies (as reviewed in Mienzer 2002), we did not observe a significant correlation between $K_L$ and leaf gas exchange. It is possible that the relationship between $K_L$ and leaf gas exchange was confounded by variation in leaf water potential across species (Table 2). For example, leaf water potential in some oaks (*Q. nigra, Q. phellos*, and *Q. falcata*) was negative enough to exceed the point at which 50% of stem hydraulic conductivity would be lost (Figure 2). As a result, stomatal closure might have occurred in these species, reducing gas exchange from its maximum. However, we note that *Quercus* species generally had higher gas exchange than other species (Figure 7A-D), despite operating at water potentials that were closer to the hydraulic safety margin. An alternate explanation is that the stem segments we measured accounted for much less resistance to the hydraulic pathway than that provided by xylem in the petioles and leaf veins, as has been suggested in other studies of deciduous trees (e.g., Brodribb, Holbrook and Gutiérrez 2002; Sack et al. 2003). Our observation that $K_L$, unlike other hydraulic traits, did not vary greatly across species (Figure 5B) provides support for the latter explanation.

## 2.5 Conclusions

Our findings add to the recent body of evidence documenting an important role for roots in controlling plant water transport (Jackson et al. 2000; Sperry et al. 2002). In particular, we identified a strong link between the vulnerability of root xylem to cavitation and leaf gas exchange. As a result, physiological integration between these different organs may represent a trade-off between vulnerability to xylem cavitation and water transport at the whole plant level and may ultimately reflect correlated evolution between root and leaf traits. Moreover, the relationship between root vulnerability to cavitation and leaf $CO_2$ and $H_20$ fluxes represents a functional link between two major physiological strategies associated with plant performance (Westoby et al. 2002; Ackerly 2004). Further studies of links between hydraulic function and other major axes of plant performance (e.g., leaf life span, seed size, plant architecture) will increase our understanding of how organisms adapt to their environment and provide a framework for predicting ecological responses to environmental change.

Table 2.1 – Species names, family, wood type (RP, ring-porous; sRP, semi-ring porous; DP, diffuse porous; NP, non-porous) and location for the 16 tree species from the Piedmont (Duke Forest) and Sandhills (Fort Bragg) of North Carolina used in this study. All angiosperms are winter deciduous and all conifers are evergreen. The phylogenetic relationship among species is contained in Figure 1.

| Species | Family | Wood type | Location |
|---|---|---|---|
| **Angiosperms** | | | |
| *Acer rubrum* L. | Aceraceae | DP | Duke Forest |
| *Cornus florida* L. | Cornaceae | DP | Duke Forest |
| *Oxydendrum arboreum* (L.) DC | Ericaceae | DP | Duke Forest |
| *Quercus alba* L. | Fagaceae | RP | Duke Forest |
| *Quercus falcata* Michaux | Fagaceae | RP | Duke Forest |
| *Quercus laevis* Walter | Fagaceae | RP | Fort Bragg |
| *Quercus nigra* L. | Fagaceae | RP | Duke Forest |
| *Quercus phellos* L. | Fagaceae | RP | Duke Forest |
| *Quercus rubra* L. | Fagaceae | RP | Duke Forest |
| *Quercus stellata* Wang. | Fagaceae | RP | Fort Bragg |
| *Cercis canadensis* L. | Fabaceae | sRP | Duke Forest |
| *Liquidambar styraciflua* L. | Hamamelidaceae | DP | Duke Forest |
| *Nyssa sylvatica* Marshall | Nyssaceae | DP | Duke Forest |
| **Conifers** | | | |
| *Juniperus virginiana* L. | Cupressaceae | NP | Duke Forest |
| *Pinus taeda* L. | Pinaceae | NP | Duke Forest |
| *Pinus echinata* Miller | Pinaceae | NP | Duke Forest |

Table 2.2 – Leaf water potential (MPa) during gas exchange measurements, and stem KS (kg m-1 MPa-1 s-1), stem KL (kg m-1 MPa-1 s-1) and root KS (kg m-1 MPa-1 s-1) for each species in the study.

| **Species** | **Water potential (± 1 SE)** | **Stem *K*S** | **Stem *K*L (× $10^{-4}$)** | **Root *K*S** |
|---|---|---|---|---|
| **Angiosperms** | | | | |
| *A. rubrum* | -1.30 ± 0.11 | 0.55 ± 0.09 | 1.20 ± 0.21 | 0.90 ± 0.23 |
| *C. florida* | -0.81 ± 0.07 | 0.15 ± 0.02 | 0.22 ± 0.02 | 1.62 ± 0.52 |
| *O. arboreum* | -1.24 ± 0.11 | 0.32 ± 0.06 | 0.56 ± 0.11 | 1.48 ± 0.66 |
| *Q. alba* | -1.14 ± 0.19 | 1.37 ± 0.18 | 2.02 ± 0.25 | 15.4 ± 5.98 |
| *Q. falcata* | -1.92 ± 0.07 | 1.49 ± 0.58 | 2.78 ± 0.79 | 4.82 ± 1.86 |
| *Q. laevis* | -- | 0.49 ± 0.27 | 0.84 ± 0.12 | -- |
| *Q. nigra* | -1.54 ± 0.26 | 1.19 ± 0.20 | 2.56 ± 0.48 | 2.66 ± 0.89 |
| *Q. phellos* | -1.97 ± 0.16 | 1.35 ± 0.36 | 2.44 ± 0.58 | 11.1 ± 8.23 |
| *Q. rubra* | -1.30 ± 0.09 | 1.33 ± 0.30 | 2.26 ± 0.47 | 2.42 ± 0.82 |
| *Q. stellata* | -- | 0.81 ± 0.25 | 1.83 ± 0.49 | -- |
| *C. canadensis* | -1.41 ± 0.09 | 0.25 ± 0.07 | 0.38 ± 0.11 | 3.23 ± 0.87 |
| *L. styraciflua* | -1.17 ± 0.10 | 0.70 ± 0.11 | 1.45 ± 0.29 | 2.07 ± 0.94 |
| *N. sylvatica* | -1.01 ± 0.09 | 0.18 ± 0.02 | 0.29 ± 0.04 | 2.14 ± 0.62 |
| **Conifers** | | | | |
| *J. virginiana* | -1.10 ± 0.07 | 0.25 ± 0.04 | 1.38 ± 0.15 | 1.69 ± 1.21 |
| *P. taeda* | -1.57 ± 0.04 | 0.32 ± 0.02 | 0.99 ± 0.15 | 3.82 ± 1.17 |
| *P. echinata* | -- | 0.26 ± 0.04 | 2.12 ± 0.43 | 0.91 ± 0.32 |

No water potential data were collected for *Q. laevis*, *Q. stellata* and *P. echinata*. No root data were collected for *Q. laevis* and *Q. stellata*.

Table 2.3 – Magnitude and statistical significance of Pearson correlations on cross-species and phylogenetically independent contrast (PIC) datasets comprising 14 co-occurring tree species in Duke Forest, Durham, NC.

| Trait or contrast | Cross-species | | PIC | |
|---|---|---|---|---|
| | Stem $\psi_{50}$ | Root $\psi_{50}$ | Stem $\psi_{50}$ | Root $\psi_{50}$ |
| Root $\psi_{50}$ | 0.83**** | -- | 0.62** | -- |
| Root $K_S$ | -- | -0.43 | -- | -0.02 |
| Stem $K_S$ | -0.77**** | -- | -0.43 | -- |
| Stem $K_L$ | -0.52* | -- | -0.30 | -- |
| Stem $D_{h\text{-}w}$ | -0.80**** | -- | -0.45 | -- |
| $A_L/A_S$ | -0.36 | -0.41 | -0.09 | -0.17 |
| $A$ | -0.65** | -0.90**** | -0.51** | -0.92**** |
| $g_s$ | -0.47* | -0.80**** | -0.11 | -0.70*** |
| $\delta^{13}C$ | -0.31 | -0.52* | 0.002 | -0.32 |
| %N | -0.35 | -0.33 | 0.06 | 0.10 |
| Leaf size | -0.48 | -0.72*** | -0.17 | -0.62** |
| SLA | -0.16 | -0.44 | 0.04 | -0.43 |

*$P \leq 0.10$, **$P < 0.05$, ***$P < 0.01$, ****$P < 0.001$

Negative xylem tension data were converted to positive values for $\log_{10}$ transformation. Therefore, the sign of the correlation coefficients are negative, even though they describe positive correlations.

$K_S$, specific conductivity; $K_L$, leaf specific conductivity; $D_{h\text{-}w}$, hydraulically weighted mean conduit diameter; $A_L/A_S$, leaf: xylem area ratio; $A$, photosynthetic rate; $g_s$, stomatal conductance; SLA, specific leaf area.

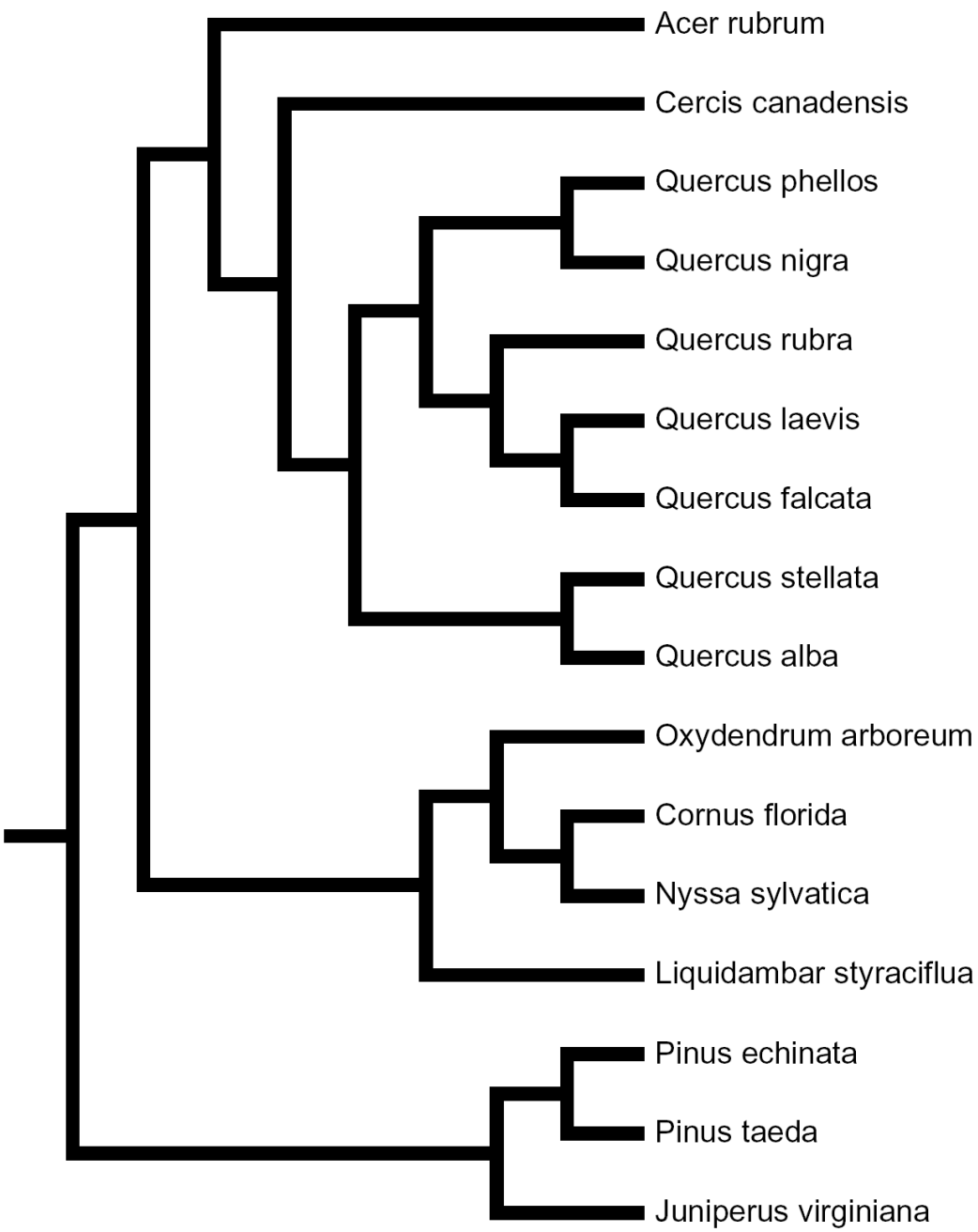


Figure 2.1 – A phylogenetic tree showing the relationship among the species used in this study.

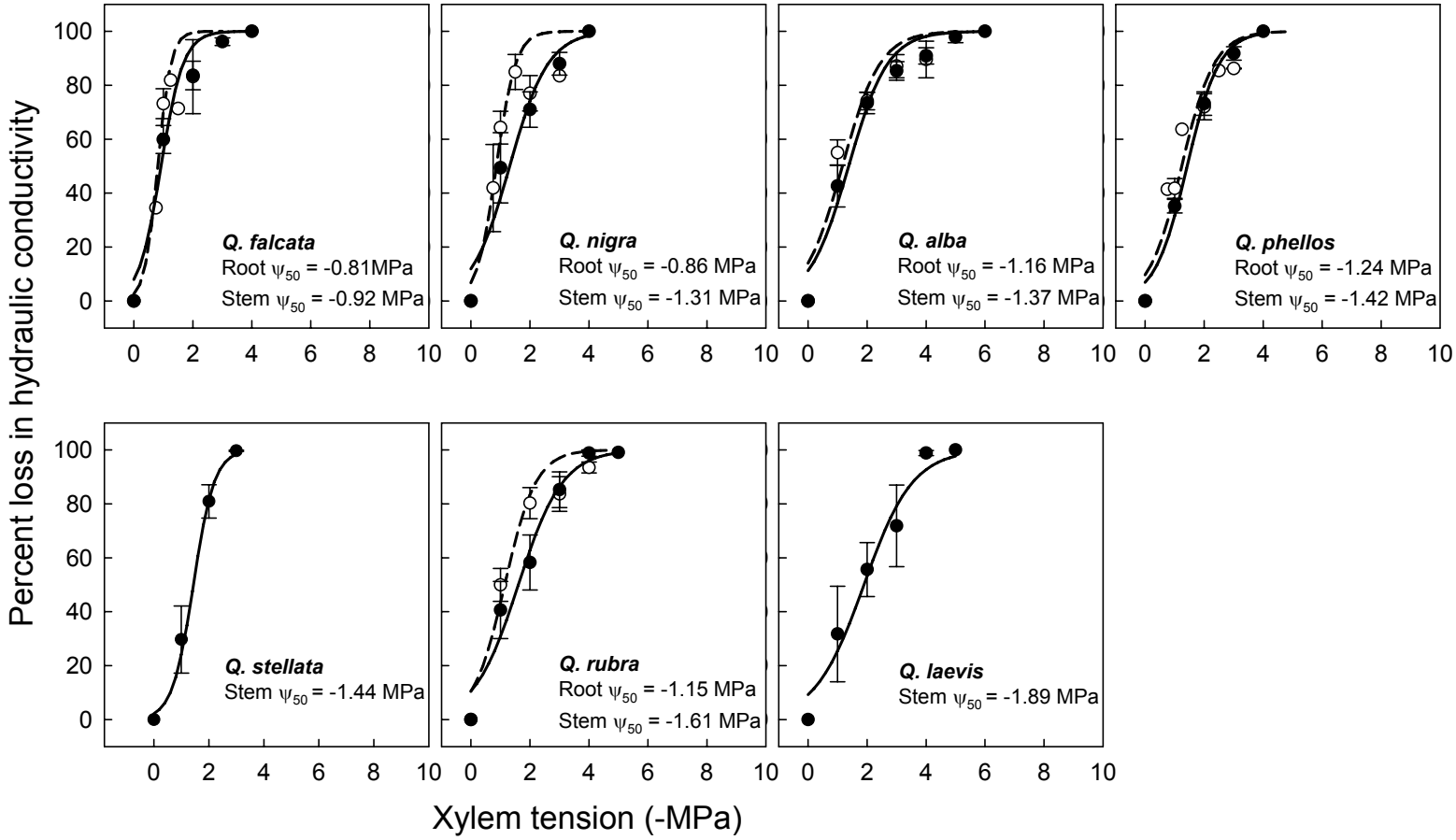


Figure 2.2 – Curves of the vulnerability of xylem to cavitation for stems (filled circles and solid lines) and roots (empty circles and dashed lines) in seven oak species from Duke Forest and Fort Bragg, North Carolina. Although means (±1 SE) are presented, curves were fit using all data. The xylem tension causing 50% loss in hydraulic conductivity ($\Psi_{50}$) for each species is shown in the legend.

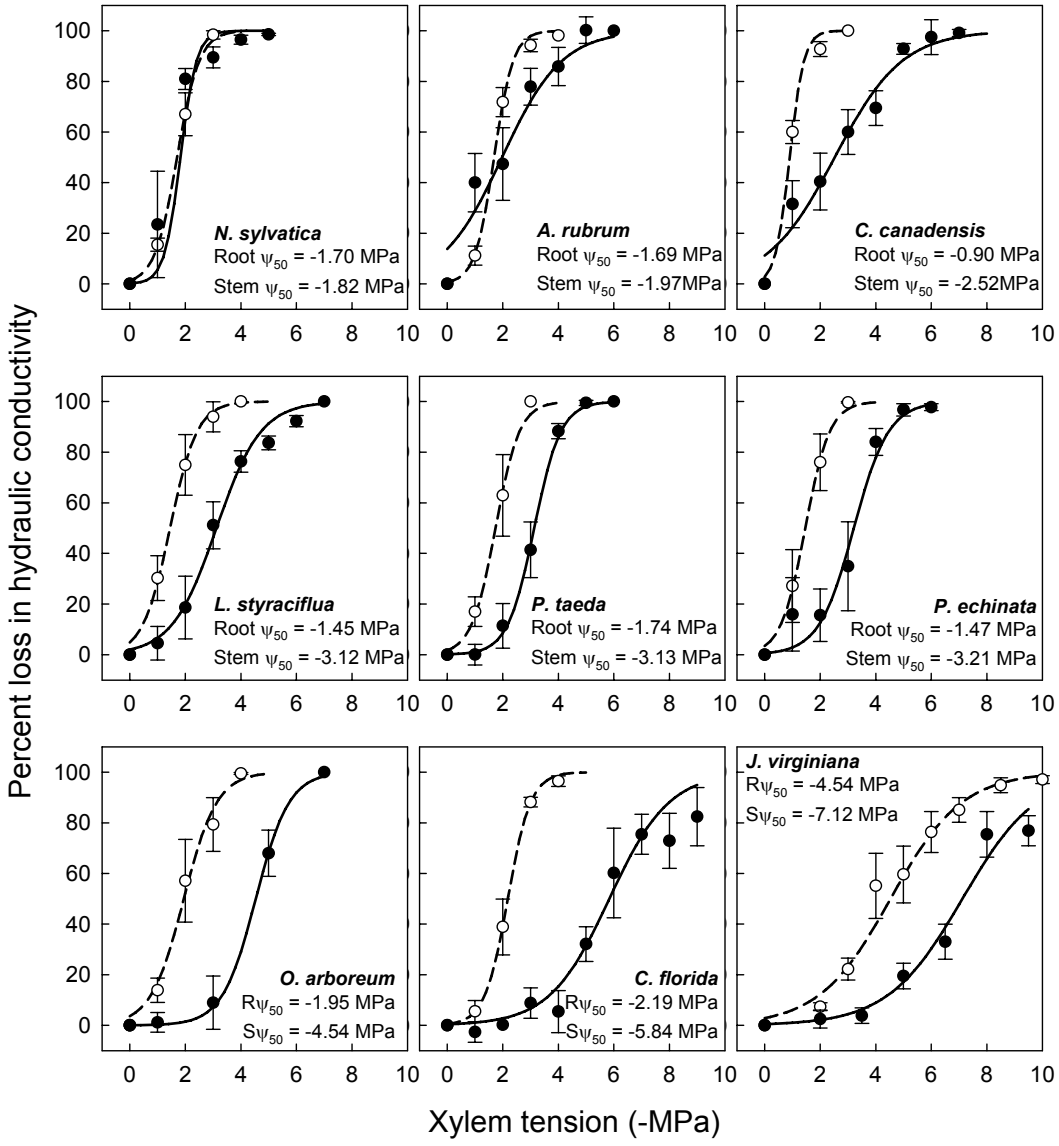


Figure 2.2 – Curves of the vulnerability of xylem to cavitation for stems (filled circles and solid lines) and roots (empty circles and dashed lines) in nine deciduous and conifer species from Duke Forest, NC. Although means (±1 SE) are presented, curves were fit using all data. The xylem tension causing 50% loss in hydraulic conductivity ($\Psi_{50}$) for each species in shown at the bottom of each panel.

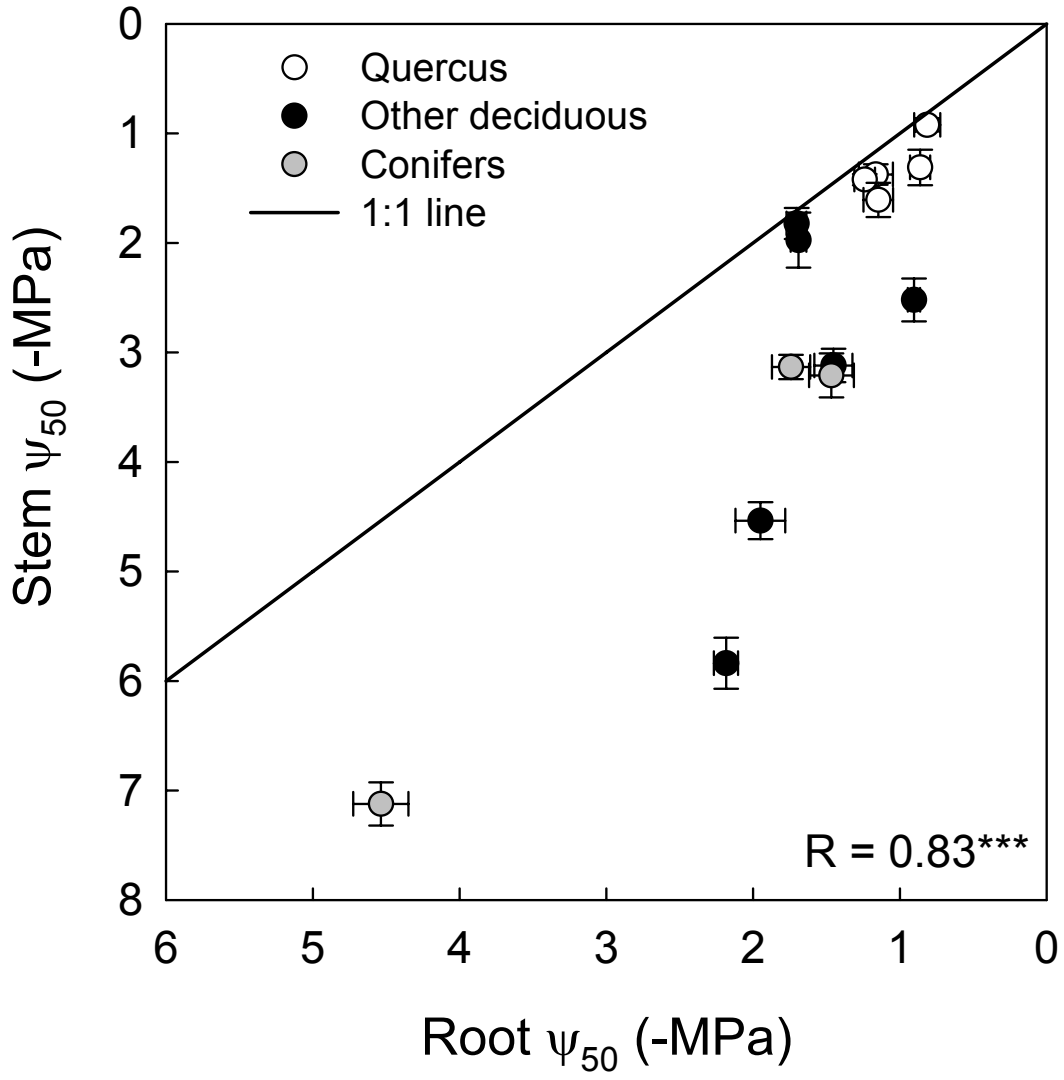


Figure 2.3 – The xylem tension causing 50% loss in hydraulic conductivity ($\Psi_{50}$) for stems plotted against the same parameter for roots for 14 co-occurring species in Duke Forest. Correlation coefficients for cross species and for phylogenetically independent contrast comparisons are listed in Table 2.

Figure 2.4 (next page) – Specific conductivity ($K_S$; A), leaf specific conductivity ($K_L$; B), and hydraulically weighted conduit diameter (Dh-w; C) expressed as functions of xylem tension causing 50% loss in hydraulic conductivity ($\Psi_{50}$) for stems of 14 co-occurring tree species from Duke Forest. Note that negative xylem tension data were converted to positive values for $\log_{10}$ transformation. Therefore, the sign of the correlation coefficients are negative, even though they describe positive correlations. Plots of phylogenetically independent contrasts for each pair of traits and the corresponding correlation coefficients (PIC) are shown in the insets. †$P \leq 0.10$, ***$P < 0.001$

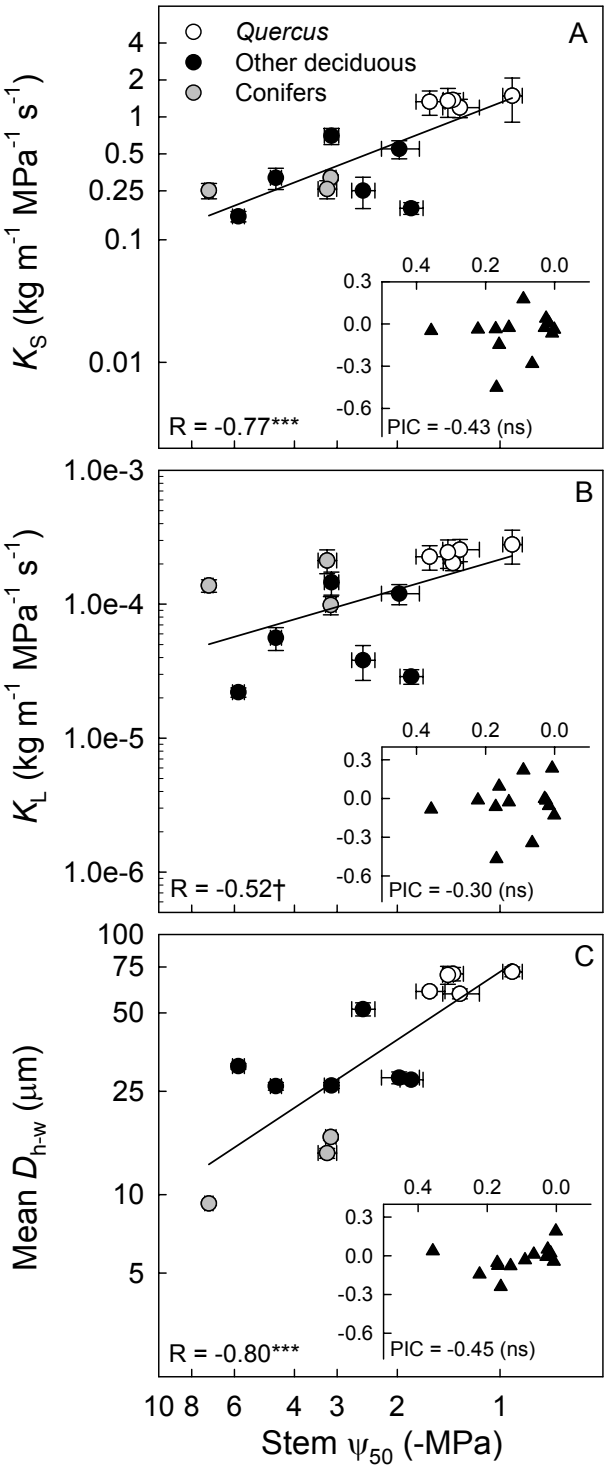
Quercus
Other deciduous
Conifers
A
B
C
$K_S$ (kg m$^{-1}$ MPa$^{-1}$ s$^{-1}$)
$K_L$ (kg m$^{-1}$ MPa$^{-1}$ s$^{-1}$)
Mean $D_{h\text{-}w}$ (μm)
Stem $\psi_{50}$ (-MPa)
R = -0.77***
PIC = -0.43 (ns)
R = -0.52†
PIC = -0.30 (ns)
R = -0.80***
PIC = -0.45 (ns)

Figure 2.5 (next page) – Specific conductivity ($K_S$; A), leaf specific conductivity ($K_L$; B), and hydraulically weighted conduit diameter (Dh-w; C) expressed as functions of xylem tension at 50% cavitation ($\Psi_{50}$) for stems of seven Quercus species. Note that negative xylem tension data were converted to positive values for $\log_{10}$ transformation. Therefore, the sign of the correlation coefficients are negative, even though they describe positive correlations. Plots of phylogenetically independent contrasts for each pair of traits and the corresponding correlation coefficients (PIC) are shown in the insets. The statistically significant relationship (B) is driven by a single species (Q. laevis). *$P \leq 0.05$

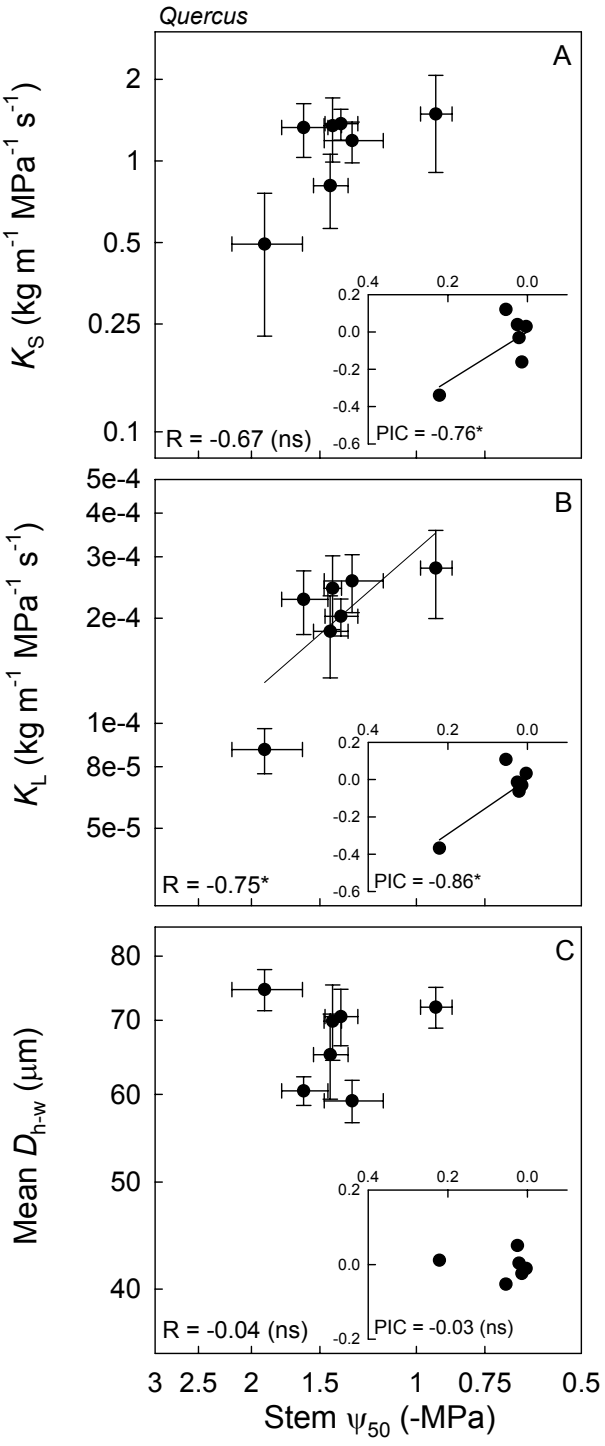
Quercus
A
B
C
$K_S$ (kg m$^{-1}$ MPa$^{-1}$ s$^{-1}$)
$K_L$ (kg m$^{-1}$ MPa$^{-1}$ s$^{-1}$)
Mean $D_{h\text{-}w}$ (μm)
R = -0.67 (ns)
PIC = -0.76*
R = -0.75*
PIC = -0.86*
R = -0.04 (ns)
PIC = -0.03 (ns)
Stem $\psi_{50}$ (-MPa)

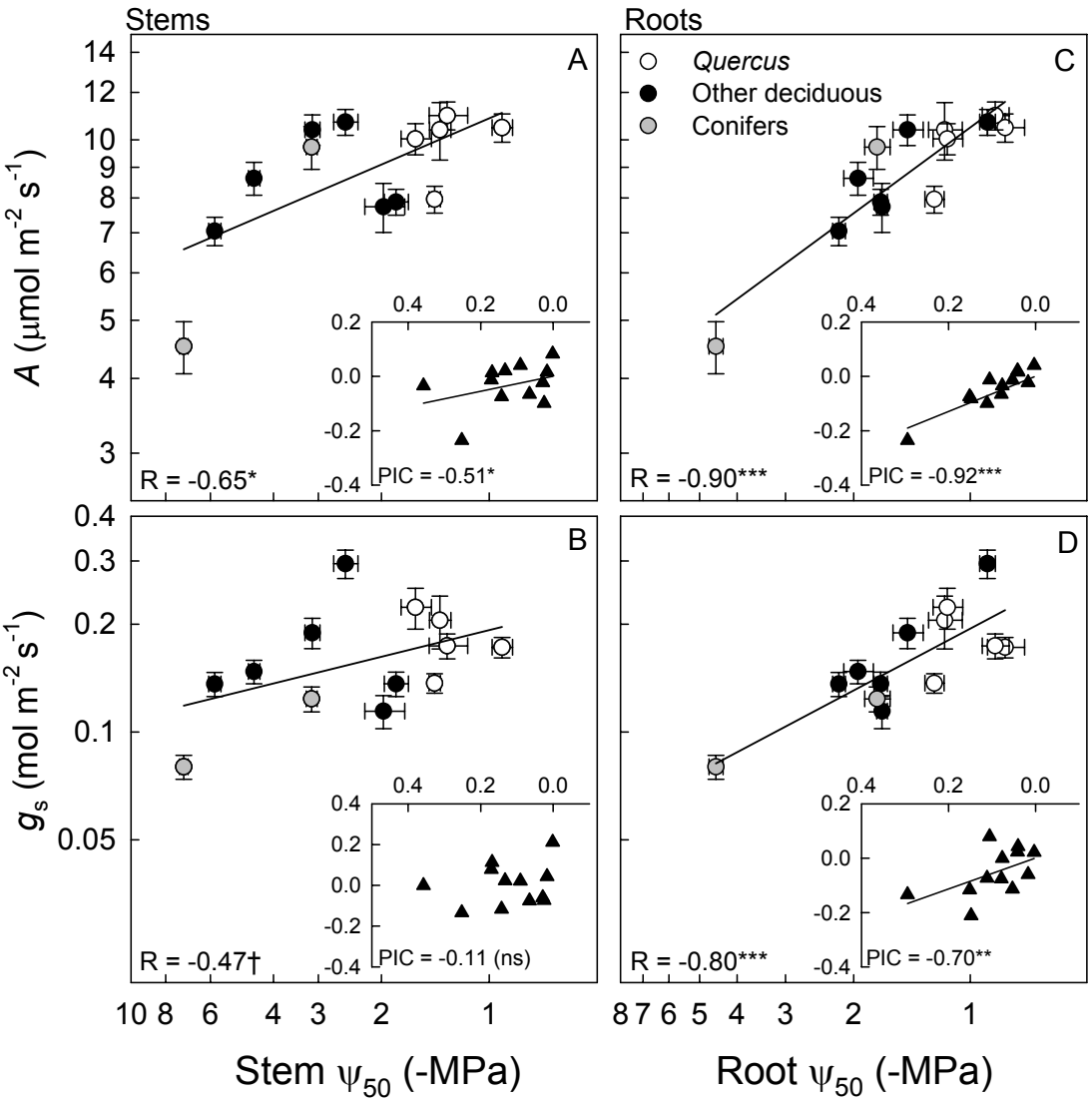


Figure 2.6 – Photosynthetic rate (A), stomatal conductance (gs), and leaf size expressed as functions of stem (A, B) and root (C, D) xylem tension at 50% cavitation ($\Psi_{50}$) for 13 co-occurring tree species in Duke Forest. Note that negative xylem tension data were converted to positive values for log transformation. Therefore, the sign of the correlation coefficients are negative, even though they describe positive correlations. Plots of phylogenetically independent contrasts for each pair of traits and the corresponding correlation coefficients (PIC) are shown in the insets. †P ≤ 0.10, *P < 0.05, **P < 0.01, ***P < 0.001.

# Chapter 3: Effects of elevated $CO_2$ on the gene expression of field-grown, mature loblolly pine trees

## 3.1 Introduction

Atmospheric carbon dioxide (CO2) has been rising dramatically since the Industrial Revolution (~35% to date) and is estimated to double its current concentration by the end of the century (IPCC 2007). Such a rapid rate of increase is unprecedented in human history and has not been experienced by current terrestrial ecosystems (Schlesinger 1997, Körner 2006). How terrestrial vegetation and ecosystems will respond to the projected increases in atmospheric $CO_2$ has been a central question in ecological research of recent decades (e.g., reviewed in Eamus and Jarvis 1989, Woodward et al. 1991, Amthor 1995, Saxe et al. 1998, Norby et al. 1999, Ward and Strain 1999, Norby et al. 2005, and Körner 2006). However, the bulk of this research has focused primarily on plant responses at the leaf to ecosystem scales with very few contributions of molecular and genetic studies, which limits our ability to provide mechanism-based predictions of an ecosystem's function under future climate scenarios of high $CO_2$.

Reducing uncertainty in predictions of the response of terrestrial ecosystems to elevated $CO_2$ is particularly important for policy decisions concerning global climate change mitigation (IPCC 2007). In this context, understanding the response of forests to elevated $CO_2$ is crucial because of the large carbon sequestration and storage potential of tree species in these ecosystems. Trees are long-lived, sessile organisms that must cope with environmental changes by developing local strategies of acclimation or adaptation.

Environmental change associated with the doubling of atmospheric $CO_2$ that is projected to occur within the lifespan of many trees is likely to trigger molecular mechanisms that underlie the process of acclimation and might control potential adaptive plant traits (IPCC 2007; Ward and Kelly 2004). Regulation of gene expression is one of the primary molecular mechanisms involved in such changes and is the foundation for physiological and morphological modifications that will modulate individual, community, and potentially ecosystem responses to rising atmospheric $CO_2$.

Changes in gene expression to increasing atmospheric $CO_2$ will most likely occur across many different metabolic pathways. Characterizing the response of trees to environmental change by looking at only a small number of genes is therefore problematic because important metabolic interactions and regulatory points can be overlooked. Advances in high-throughput sequencing and other genomic tools, such as microarrays, make it possible to monitor thousands of gene sequences simultaneously (Schena et al. 1995). Microarrays are a powerful tool to evaluate gene expression at these large, genomic scales and have become one of the most important experimental approaches for discovering gene function (Somerville and Somerville 1999). Besides their role in gene discovery, microarrays can also be important for the understanding of adaptation and evolution of plants in natural systems (Lev-Yadun and Sederoff 2000). Despite their potential to reveal aspects of the genome responsible for adaptive traits in nature and to uncover the role of genes in an ecological context, microarray applications

to field studies and ecosystem experiments are still scarce, particularly for mature long-lived trees (Jackson et al. 2002, Nösberger and Long 2006).

Large-scale field experiments using Free-Air-$CO_2$-Enrichment (FACE) technology allow researchers to manipulate atmospheric $CO_2$ levels in realistic, and otherwise undisturbed, ecosystems experiencing natural variation in a full suite of abiotic (e.g., drought) and biotic (e.g., herbivory) factors (Hendrey et al. 1999, Miglietta et al. 2001). The combination of FACE experiments and genomic-scale analysis of gene expression therefore provides a unique opportunity to achieve a comprehensive and mechanistic understanding of the response of forests to global climate change. With this goal in mind, we used cDNA microarrays to generate the first genomic-scale expression profile of a coniferous forest exposed to different levels of atmospheric $CO_2$. Our main objective was to investigate the effects of elevated $CO_2$ on broad gene expression patterns of mature, field-grown loblolly pine (*Pinus taeda*) trees. More specifically, we aimed to answer the following questions: (1) What are the differences in gene expression between trees grown under elevated and ambient $CO_2$? (2) How do these differences vary throughout the season? and (3) What are the most strongly affected genes and their corresponding functional categories?

## 3.2 Materials and Methods

### *Study site and plant material*

The Duke Forest FACE (Free Air $CO_2$ Enrichment) site is located in the Blackwood Division of Duke Forest in Chapel Hill, North Carolina (35° 58' N, 79° 5' W). The soils at this site are nutrient-poor, acidic hapludalfs, typical of uplands in the southeastern U.S. Mean annual temperature and mean annual precipitation are 15.5° C and 1154 mm, respectively, and the frost-free season usually ranges from late March to mid-October. In 1983, an even-aged loblolly pine (*Pinus taeda*) plot was planted in a half-sib design after clear-cutting and burning the site. The FACE experiment, fully established in 1996, consists of six 30-m diameter plots (rings) surrounded by an array of vertical air-releasing vent pipes that extend from the floor to the top of the forest canopy. In three plots, designated as *elevated* (or treatment) rings, air is enriched with 200 ppm of $CO_2$ above the ambient atmospheric concentration, while the other three *ambient* (or control) rings, are operated in identical form but without the injection of additional $CO_2$. For a detailed description of the site see Hendrey et al. (1999).

Our study took place during the 6$^{th}$ year of fumigation (2002) when $CO_2$ enrichment was still being provided continuously for 24 h per day except when air temperature was below 5° C for more than 1 h (Hendrey et al. 1999). At this stage, pine trees were ~18 m tall and comprised 90% of the basal area of the forest stand (McCarthy et al. 2006). Sampling was done once a month from March through September between 1000 and 1200 EST on mostly sunny days. Environmental conditions during this growing season

included a severe drought (see table 1 in Crous and Ellsworth 2004 for average precipitation records). A subset of environmental data continuously monitored at the site (soil moisture, photosynthetic active radiation, precipitation, temperature) and spanning our sampling period is included in Appendix A.

Personnel lifts for canopy access (UL48, Upright, Charlotte, NC) were used to sample needles from sun-exposed branches at the top of three individual pine trees in each of the six experimental rings. In March only, sampling was limited to four rings due to technical problems with the canopy lifts. Needles were harvested from the most recent fully-expanded flush present on each sampling date: one-year-old needles were sampled until June and current-year needles were sampled from July to September. Needles were frozen in liquid nitrogen immediately upon removal from the original branches to stop any metabolic activity. All frozen samples were subsequently transported to a -80º C freezer in the laboratory where they were stored until further analysis.

### *Microarrays*

For easier interpretation of the methods described below, the steps involved in a two-color spotted microarray experiment are summarized in the flow diagram in Figure 1.

*Probe selection, preparation and printing*

Approximately 2,000 cDNA clones (microarray probes) were selected from five existing pine cDNA libraries at North Carolina State University: NXNV (xylem normal wood

vertical), NXCI (xylem compression wood inclined), NXSI (xylem side-wood inclined), ST (shoot-tip), and PC (pollen cone; Heath et al. 2002, Watkinson et al. 2003). These cDNA clones (hereafter referred to as transcripts or genes) were assigned according to each transcript's putative annotation to 20 functional categories modified from the MIPS (Munich Information Center for Protein Sequences) classification. The categories defined in this study range in size from 4 to 472 genes and are not mutually exclusive (i.e., the same gene may belong to more than one category; Appendix B).

Probes selected from the cDNA libraries were amplified and cleaned following the procedures in Stasolla et al. (2003) and were spotted onto poly-lysine microscope glass slides (arrays) at the Duke University Microarray facility. Each microarray included at least four replicates of each pine transcript, several external controls, and blank spots, randomly placed on the slide for a total of 9216 spots. A set of non-plant genes - to avoid cross-hybridization with pine clones - were used as external positive controls (human genes SP1, SP2, SP3). These were spiked at known concentrations and used for quality control and image normalization. Blank spots were used as negative controls to confirm that there were no technical artifacts such as hybridization in the absence of cDNA probes.

*Target preparation: RNA isolation and hybridization*

Each individual sample or biological replicate used for target preparation consisted of needles pooled from three trees within each single ring at FACE. Total RNA was isolated from the pooled sample using an adaptation of Chang et al.'s (1993) method as

described by Watkinson et al. (2003). In summary, each sample of recently ground pine needles was added to pre-warmed cetyl-trimethyl-ammonium bromide (CTAB) extraction buffer and the solution was further homogenized with a polytron tissue homogenizer at full speed for 1 min and then kept at 65º C for 20min. After centrifugation (9,000 *g* for 10 min at 4º C), the supernatant was transferred to a new tube with one-fifth volume of 5% (w/v) CTAB and heated to 65° C for 10 min. An equal volume of chloroform:isoamyl alcohol (24:1 [v/v]) was added, and the sample was centrifuged as before. The supernatant was re-extracted with an equal volume of chloroform:isoamyl alcohol (24:1 [v/v]) and centrifuged again. This last supernatant was transferred to a new tube with one-half volume of 10M LiCl and left to precipitate overnight at -20º C. The resulting RNA pellet was rinsed with 80% ethanol, dried, and re-suspended in a solution of Nuclease-free-water (NFW) and 0.1 mM EDTA. The concentration and purity of total RNA extracted were checked with a UV spectrophotometer (determined using 260 nm and the 260/280 nm ratio, respectively) and its integrity checked by 1% agarose gel electrophoresis.

Two paired samples (one elevated, or E, and one ambient, or A) were contrasted on each array. Ten μg of total RNA (*target*) from each sample were reverse-transcribed to cDNA and labeled with a different fluorescent dye (Cy3 or Cy5, Amersham Pharmacia, Piscataway, NJ). A known quantity of cDNA from each external control gene was added to each sample before labeling. Each pair of samples was loaded to a microarray slide and left to hybridize overnight following the protocol of Stasolla et al. (2003). Reciprocal

labeling was carried out for each comparison to avoid bias due to differential incorporation of each dye. Therefore, two microarray slides (technical replicates) were used for each comparison of elevated and ambient $CO_2$ samples (three paired biological replicates) for a total of six microarray slides per sampling date. A total of 40 microarrays were used in this experiment.

*Slide scanning and image processing*

Following hybridization and post-hybridization cleaning, slides were readily scanned using a ScanArray 5000 (Perkin Elmer, Boston). Each slide was scanned at two different wavelengths (~543 nm and ~633 nm for Cy3 and Cy5, respectively) generating two 16-bit TIFF images for each slide. The Cy5 channel was always scanned first since this dye is known to be more susceptible to photodegradation than Cy3. Control genes were used to calibrate the scanner laser and photomultiplier properties to maintain consistency across different slides. Raw intensity and local background values for each spot in the arrays were collected using Quantarray software (Perkin-Elmer, Boston). Spots with background higher than local intensity (due to fluorescence noise or scratches) or very low intensity due to printing problems were flagged as unacceptable and removed from further analysis. Spots associated with 275 clones that showed irregularities during PCR amplification were also excluded from the analysis at this point. A maximum of 8068 spots, including blanks, controls, and replicates of 1784 individual pine transcripts, were used for each of the 40 microarray slides scanned.

### *Data extraction and statistical analysis*

For each sampling date, the intensity values for all valid spots on the arrays were used as input data in a two-step mixed linear model (Wolfinger et al. 2001, Jin et al. 2001). The first step removes general effects associated with the use of different slides (microarrays), dyes, and spot location, while the second step estimates the interaction between individual genes and experimental treatments. For the first step, we used the following model:

$$y_{\text{gijkmn}} = \mu + T_i + M_j + D_k + P_m + MP_{jm} + \varepsilon_{\text{gijkmn}},$$

where $y_{gijkmn}$ is the logarithmic transformed intensity corresponding to gene *g*, treatment *i*, array *j*, dye *k*, printing pin *m*, and spot *n*, while $\mu$ is the overall mean. Factors in this model are $T_i$ (Treatment: **E**levated or **A**mbient), $M_j$ (Microarray: one of six), $D_k$ (Dye: Cy3 or Cy5), $P_m$ (Printing pin: one of four), and $(MP)_{jm}$ (the interaction between microarrays and pins). Mj and MPjm were treated as random effects while the other terms were treated as fixed. The residuals from the first step, $\varepsilon_{gijkmn}$, were used as input data for the second step, the following gene model:

$$\varepsilon_{gijkmn} = G_g + GT_{gi} + GM_{ij} + GD_{gk} + GS(M)_{gjn} + r_{gijkn},$$

where $G_g$ is the mean of all residuals for gene *g*. The interaction terms between gene and treatment (GTgi) and between gene and dye (GDgk) are fixed effects, and the interaction terms between gene and microarray (GMij) and gene and spot [GS(M)gjn] are random effects. The spot effect was added because each gene was represented by more than one spot in each array. To determine the significance of the treatment effect on the

expression levels of each gene, we tested the following hypotheses using a t-test for each pairwise comparison:

H0: $GT_{gA} = GT_{gE}$ (No differential expression of gene *g* between $CO_2$ treatments)

$H_a$: $GT_{gA} \neq GT_{gE}$ (Gene *g* is differentially expressed between $CO_2$ treatments)

The difference $GT_{gA} - GT_{gE}$, expressed as $\log_2(E/A)_g$, is the estimated relative change in expression of gene *g* between treatments E and A. Therefore our null hypothesis, $H_0$, is equivalent to $\log_2(E/A)_g = 0$, i.e., $E/A_g=1$.

For each of the 1784 pine genes on the arrays, we obtained a mean fold-change representing the average of, at least, 24 replicated spots (four or more spots per slide, with six slides) and an associated p-value (gene-level, *P*). For easier interpretation, we report changes in gene expression in the original linear scale but maintain a symmetric relationship around 1 (no differential expression). For that purpose, we report E/A values for upregulated genes (E/A > 1) and -A/E values for downregulated genes (0 < E/A < 1; for instance, a gene with a relative expression, E/A, of -½, we report as being downregulated -2-fold). Percentage change between elevated and ambient conditions was calculated accordingly. The gene-level significance threshold ($\alpha = 0.05$) was used to determine the total number of genes differentially expressed in each sampling date.

To identify individual genes with a particularly relevant response to the $CO_2$ treatment, we used a more conservative statistical approach based on a false-discovery-rate (FDR) of 0.05 (Benjamini and Hochberg 1995; as described in the GeneSpring software manual, Agilent Technologies). Sampling throughout a growing season

included the intrinsic variation in field environmental conditions and needle developmental stages. Therefore we considered good candidate genes for a $CO_2$-specific response only those that were differentially expressed by elevated $CO_2$ at the experiment-wide (FDR < 0.05) at two or more sampling dates.

## 3.3 Results

### *Effects of elevated $CO_2$ on broad-scale gene expression patterns*

Fourteen percent of 12,327 pairwise comparisons (~1784 genes replicated through seven months) were statistically different between elevated and ambient $CO_2$ (gene-level $P \leq 0.05$; Figure 2, Table 1). Among those genes differentially expressed (1685), four times more genes were upregulated in elevated $CO_2$ than were downregulated (Figure 2, Table 1; 1350 genes upregulated (E/A > 1) compared with 335 downregulated (E/A < 1)). The magnitude of differential expression (E/A when $P \leq 0.05$) for each gene ranged from -6.7-fold to 6.1-fold across the season, although 95% of these differences were within the interval ±2-fold (Figure 2).

### *Seasonality of elevated $CO_2$ effects*

There was strong seasonal variation in the distribution of changes in gene expression between elevated and ambient $CO_2$, with maximum differences occurring in mid-summer. The lowest number of differentially expressed genes occurred at the beginning of the growing season (32 in March and 50 in April). In contrast, changes peaked in August, with 850 differentially expressed genes, and decreased again at the end of the season (165 in September; Table 1). The same trend was observed in the distribution of total upregulated genes and a similar distribution (peaking in July instead) described the total number of downregulated genes (Figure 3; Table 1). Likewise, a strong seasonal variation was noticeable across most functional gene categories (Figure 4).

### *Effects of elevated $CO_2$ on functional categories*

The highest number of total differentially expressed genes was found in *Carbon metabolism* (432), followed by the categories *Environment* (287) and *Cell membranes* (252). These categories showed also the highest number of genes upregulated and downregulated (Table 2). When taking into account the initial gene number in each category, *Photorespiration* showed the highest percentage of differential expression (18.4%), followed by the categories *Nucleus* (17.9%) and *Trafficking* (16.7%). *Photorespiration* was also the category with the highest percentage of downregulated genes (6.1%), while *Nucleus* and *Trafficking* had the largest percentage of upregulated genes (14.3% and 13%, respectively). Overall, upregulation was 2 to 12 times more frequent than downregulation across all categories (Table 2).

### *Effects of elevated $CO_2$ on individual genes*

To identify genes with a particularly relevant response to elevated $CO_2$, we chose a conservative approach and considered only genes whose expression was statistically different between $CO_2$ conditions at the experiment-wide level (multiple-comparison adjustment at each sampling date; FDR $\leq$ 0.05) at least at two different sampling dates (each date including the analysis of six microarrays for three pairs of biological replicates). Among the ten transcripts that matched the selection criterion (Table 3), six showed a remarkably consistent behavior throughout most of the growing season (Figure 5, Table 3) and therefore represent our best estimate of candidate genes with a direct role in the response (and potential acclimation) of loblolly pine trees to elevated

$CO_2$. These genes coded for an alanine aminotransferase (“Alanine”, NXLV082_B07), a citrate synthase (“Citrate”, NXCI_163_C01), a cytosolic glucose-6-phosphate isomerase (“Glucose-6P”, NXCI_165_A01), a small GTP-binding protein (“sGTP protein”, NXCI_123_D05), and two small heat-shock proteins (“sHSP1” and “sHSP2”, NXLV108_A02 and NXLV123_E04, respectively; Figure 5).

The genes coding for the enzymes alanine aminotransferase (amino acid metabolism and carbon respiratory pathway), glucose-6-phosphate isomerase (glycolysis and hexose conversion), and citrate synthase (citric acid cycle) were consistently upregulated throughout the peak of the growing season (April through August) and showed no response to $CO_2$ in either March or September (Figure 5). Besides a very consistent individual behavior during most of the season, these genes also showed a remarkably similar pattern of expression as a group, both in the direction of the $CO_2$ effect (increased expression) and the magnitude of change (E/A; Figure 5), which is a strong sign of gene co-regulation.

The small GTP binding-protein-coding gene was upregulated through most of the season with the exception of March and August (Figure 5), suggesting increased cellular trafficking and signaling transduction levels in trees under elevated $CO_2$. Elevated $CO_2$ also increased expression levels of two genes coding for sHSP, potentially reflecting increased stress response in trees under high $CO_2$. Both genes were upregulated in April ($P \leq 0.05$), July, and August (P and FDR $\leq 0.05$), while the first transcript was also

upregulated in September and the second was upregulated in March and June as well (Figure 5).

Among the four other genes, one coding for a transcription factor and related to signal transduction ("HD-Zip"; NXLV_038_F09) was upregulated in the peak of the summer (June through August). Two others associated with carbon metabolism were also upregulated by elevated $CO_2$ in a few months: transcript NXCI_151_G07 ("UDP-glucose ") coding for a UDP-glucose glucosyltransferase - an enzyme involved in sucrose metabolism and synthesis of cell wall polymers - was upregulated in April and July (FDR < 0.05); gene ST22D05 ("Hydroxypyruvate") coding for hydroxypyruvate reductase (involved in photorespiration) was upregulated from June to August, but also showed a highly significant downregulation by elevated $CO_2$ at the end of the season (Figure 5). Likewise, transcript NXLV107_B07 ("Unknown") was significantly downregulated in August, but upregulated in July by 2-fold (the largest change in relative expression among the ten selected genes, Figure 5).

## 3.4 Discussion

The effects of elevated $CO_2$ on forest ecosystems have been well documented from leaf to ecosystem scales. The molecular drivers underlying such responses are however largely unknown. In this study, we compared the expression profile of 1784 genes from mature loblolly pine trees growing in the field under contrasting atmospheric $CO_2$ levels. At the Duke Forest FACE site, trees exposed to elevated $CO_2$ showed a general pattern of increased gene expression with a particular incidence in transcripts broadly associated with (1) environmental and cellular signal integration and (2) metabolism of carbohydrates. Differences in the total number of differentially expressed genes, both across the whole dataset and within functional categories, exhibited marked seasonal patterns. Seasonality was also apparent in the behavior of individual genes, in particular in the magnitude of differential expression between ambient and elevated $CO_2$.

### *Effects of elevated $CO_2$ on broad patterns of gene expression*

This study quantified, for the first time, the contribution of genome-scale molecular regulation to the response of loblolly pine trees to increased atmospheric $CO_2$. Fourteen percent of all genes included in the cDNA microarrays across all dates were differentially expressed between elevated and ambient $CO_2$ concentrations (Table 1). Most differentially expressed genes were upregulated by elevated $CO_2$ (80% compared to 20% downregulated; Figure 2; Table 1), which suggests that under the prevailing environmental conditions an increase in $CO_2$ has a predominantly stimulatory effect on gene activity in pine trees.

Most changes in gene expression were rather subtle in intensity with only a small proportion (5%) showing differences larger than two-fold in each direction (Figure 2). Relative expression ratios of two-fold and higher (an arbitrary, non-statistical threshold adopted in many microarray studies to identify genes as differentially expressed between two conditions) are often associated with acute, short-term treatments in controlled laboratory conditions that may not accurately represent the response observed in field conditions. The potential for such discrepancy was clearly illustrated in a pilot study comparing gene expression profiles of *Arabidopsis thaliana* plants exposed to elevated $CO_2$ in the field with the profiles of those growing under ambient $CO_2$ both in the field and in the laboratory (Miyazaki et al. 2004). The final outcome revealed more differences in gene expression between the plants growing in the laboratory and those in the field (both at ambient $CO_2$) than among plants grown under contrasting $CO_2$ concentrations in the field.

Our study examined the consequences of long-term exposure of pine trees to a rather subtle increase in the treatment variable (atmospheric $CO_2$ concentration); the low fold-change differences in gene expression might therefore reflect the chronic type of treatment and potentially some degree of acclimation already in place. This observation is in agreement with the few published reports of long-term effects of $CO_2$ on the transcriptome of other plant species growing in FACE experiments (aspen, Gupta et al. 2005; poplar, Taylor et al. 2005; soybean, Ainsworth et al. 2006). The difference between the large fold-changes observed in some studies and the range observed in studies

looking at long-term treatments applied in natural settings highlights the necessity of evaluating realistic treatments that are within ecological and physiological meaningful ranges.

### *Seasonality of elevated $CO_2$ effects*

Effects of elevated $CO_2$ in the loblolly pine system were highly influenced by seasonality with the highest number of differentially expressed genes occurring in mid-summer and fewer differences found both at the beginning and end of the growing season (Figure 3, Table 1). This pattern follows closely the seasonal trends observed in photosynthetic rate differences between elevated and ambient $CO_2$ conditions in loblolly pine trees growing both in Open-Top-Chambers (Lewis et al. 1996, Tissue et al. 1996, Tissue et al. 1997) and at the Duke Forest FACE site (Ellsworth 1999, Myers et al. 1999). This variation is also in accordance with periods of slow (beginning and end of the season) and rapid (mid-season) growth of loblolly pine trees (Myers et al. 1999) which suggests that upregulation of gene expression under elevated $CO_2$ supported an increase in metabolic activity required for carbon uptake and plant growth. Nevertheless, seasonality patterns were seen across most categories, suggesting that the interaction of climate and/or developmental factors with $CO_2$ affected the majority of metabolic functions (Figure 4).

*Interaction of $CO_2$ and leaf development*

Similarly to the data for the whole growing season, more genes were upregulated than downregulated by elevated $CO_2$ within most individual months (Figure 3, Table 1). July,

with roughly equal number of downregulated and upregulated genes was an exception to this trend (Figure 3, Table 1), perhaps reflecting the concurrent change in the cohort of needles being sampled. While from March through June we sampled one-year-old needles, in July we sampled the first flush of the year which by then contained fully expanded needles. Current-year and one-year-old needles of pine trees at this site showed differences in $CO_2$-induced effects on gas exchange and rubisco activity in certain years during the on-going FACE experiment (Rogers and Ellsworth 2002, Crous and Ellsworth 2004) which suggests that they might also respond differently at the gene expression level. However, the general gene expression patterns in July might also be exacerbated by effects of elevated $CO_2$ on needle development (elaborated further in the next paragraph).

Elevated $CO_2$ can accelerate plant phenology including needle development rates in pine trees (e.g., Tissue et al. 1996). It is possible that at the time of our July sampling, needles under ambient $CO_2$ had not reached their maximal expansion in contrast to those under elevated $CO_2$. If that were the case, one would expect that some metabolic processes (e.g., related to needle growth) still taking place in ambient $CO_2$ would have already ceased (or diminished their activity) under elevated $CO_2$. A partial or full reduction of these metabolic processes in elevated $CO_2$ could therefore have been detected as downregulation at the gene expression level. Interestingly, but perhaps not surprisingly, *Plant growth regulation* was the functional category with the highest ratio of downregulation to upregulation in July (27 genes, or 18%, downregulated vs. 8 genes

(5%) upregulated; data not shown). An interaction between leaf phenology and high $CO_2$ was also evident in transcriptome studies of poplar and soybean, with both cases reporting a large number of gene expression differences associated with developmental effects alone (Taylor et al. 2005 and Ainsworth et al. 2006). Our interpretation for the July data and the results from the poplar and soybean studies strongly emphasize a need for multiple sampling times during leaf maturation. In other words, leaf age alone might not be sufficient to determine which samples to compare between ambient and elevated $CO_2$, since leaves of the same age might be in different developmental stages thereby affecting our inferences about the direct effects of $CO_2$ on gene expression.

*Interaction of $CO_2$ and drought*

Gene expression patterns in August were particularly striking due to the disproportionately large number of differentially expressed genes in comparison to other months. One possible explanation for the large differences between elevated and ambient $CO_2$ in August is an interaction between $CO_2$ treatment and the severe drought occurring in the summer of 2002. Although the drought was felt throughout most of the growing season and monthly precipitation values were similar for July and August, our sampling in August took place after a relatively long dry-spell when soil moisture values were particularly low (0.14 % vol; Appendix A). On the other hand, a large number of the genes included in these microarrays are known to be responsive to drought stress and many of the upregulated transcripts in elevated $CO_2$ in August correspond to genes and proteins involved in acclimation to water stress and drought

tolerance mechanisms (e.g., sHSP, late embryogenesis-abundant proteins, aquaporins; Appendix B; Watkinson et al. 2003). It is plausible then, that the large-scale induction of such genes would confer higher metabolic flexibility and/or improved stress-response capacity in trees growing under elevated $CO_2$, allowing these to cope better with drought conditions when compared to trees growing under current atmospheric $CO_2$ levels. To clarify further the molecular mechanisms operating in field-grown tree species facing concurrent conditions of drought and elevated $CO_2$ it would be necessary to measure independent, rather than relative differences in, gene expression levels (e.g., by qRT-PCR techniques) in individual biological samples from ambient and elevated $CO_2$ spanning both wet and dry conditions. In our study, it would be especially interesting to determine whether the relative upregulation of gene expression (E/A) in high $CO_2$ at that time was a result of (1) an induction effect of elevated $CO_2$ during drought (considering the expression levels in a wet year as the "control"), or instead, (2) a repression effect of drought in ambient conditions (with gene expression levels in elevated $CO_2$ remaining largely unchanged across water supply conditions).

### *Effects of elevated $CO_2$ on functional categories and individual genes*

Elevated $CO_2$ affected the expression levels of genes across a diverse range of functional categories, but was mostly seen in categories of genes that respond to and integrate environmental and cellular signals (*Environment*, *Cell membranes*, *Nucleus,* and *Trafficking*) and in those related to carbon utilization (*Carbon metabolism*, *Photorespiration*). This tendency was observed in the total number of genes affected within each category

(Table 2), but also corroborated by the individual genes that were identified as particularly responsive to $CO_2$ (Table 3).

*Environmental and cellular signaling genes are upregulated under elevated $CO_2$*

The upregulation of a transcript coding for a small membrane GTP-binding protein (sGTP protein) in five of the sampled months (April through July, and September) suggests higher levels of signal transduction activity under elevated $CO_2$ during most of the season (Figure 5). Small GTP-binding proteins interact with cell receptors that recognize diverse internal or external signals (e.g., environmental stimuli) and participate in a cascade of metabolic interactions that often leads to regulation of gene expression through the activation of transcription factors (Takai, Sasaki and Marozaki 2001). Although not necessarily involved in the same signaling pathway, the presence and upregulation of a transcription factor encoding gene (NXLV_038_F09) among the ten transcripts selected as highly significant also points to higher levels of signal transduction and regulatory activity under elevated $CO_2$.

An increased response to environmental stimuli is also corroborated by the upregulation of the two small heat-shock protein transcripts (sHSP1 and sHSP2; Figure 5, Table 3). Small heat shock proteins act as molecular chaperones (helping in protein folding and preventing incorrect aggregation) mainly upon induction by environmental stress. They are thought to protect cells from stress damage and confer increased tolerance to several abiotic factors such as heat and drought stresses (Vierling 1991; Sun, Van Montagu and Verbruggen 2002). The consistent upregulation of the two transcripts

under elevated $CO_2$ may therefore reflect higher stress tolerance in trees growing under elevated $CO_2$ as well as an improvement of the trees' capacity to cope with drought relative to trees in ambient $CO_2$ (Watkinson et al. 2003)

*Carbon metabolism genes are upregulated under elevated $CO_2$*

The genes coding for enzymes directly involved in (citrate synthase and glucose-6-phosphate isomerase) or closely related to (alanine aminotransferase) the respiratory pathway were consistently upregulated under elevated $CO_2$ conditions (April to August), a pattern that strongly suggests an increase in cellular respiration of carbohydrates under elevated $CO_2$. Indeed, a higher availability of carbon substrates from the continued stimulation of photosynthetic rates under elevated $CO_2$ (Myers et al. 1999, Crous and Ellsworth 2004, Clint et al. 2004) could keep fueling central carbon metabolism as well as pathways dependent on energy or carbon skeletons resulting from respiration (e.g., biosynthesis of amino acids). This is an important topic that deserves further study since alterations of carbon metabolism at the leaf and tree level can have important implications for the ecosystem carbon balance and the role of forests as either sources or sinks in the global carbon cycle.

The increase in expression levels of the alanine aminotransferase is particularly exciting in the context of nitrogen cycling in this loblolly pine ecosystem. While inorganic nitrogen (nitrate and ammonium) is a more common source of nitrogen for root uptake, plants can directly obtain organic nitrogen as long as there are free amino acids in the soil. Alanine aminotransferase catalyzes the reversible reaction between

pyruvate (carbon substrate for respiration) and alanine (an amino acid). Coincidently, alanine is the most common free amino acid (25% of total pool) in the soils at the Duke Forest FACE site, and lobolly pine roots are capable of direct uptake of this amino acid in the field (Hofmockel 2007). Although there was not a significant difference in potential uptake rates of alanine between elevated and ambient $CO_2$ grown pine trees at FACE (Hofmockel 2007), the upregulation of an alanine aminotransferase gene in our study suggests that trees under high $CO_2$ might have higher rates of alanine assimilation. Perhaps a higher enzyme turnover or efficiency under elevated $CO_2$ could lead to improved assimilation or recycling rates of nitrogen in these trees without higher uptake rates of alanine (or other nitrogen sources) from the soil, if the former proved to be metabolically more economical than the latter. Gene expression analysis performed in parallel with measurements of amino acid and protein levels, and enzyme activity assays would be required to test the suggested hypothesis.

The similarity in expression patterns between the three genes mentioned above indicates a potential co-regulation of these transcripts and may reveal another important link between carbon and nitrogen metabolisms. Carbon and nitrogen pathways strongly interact with each other from molecular (Stitt and Krapp 1999, Palenchar et al. 2004) to ecosystem levels (Luo, Hui and Zhang 2006; Reich, Hungate and Luo 2006). Although most studies concentrate on the effect of nitrogen availability on carbon uptake, carbon availability also influences nitrogen uptake and assimilation. The results of our study suggest that an increase in carbon substrates may lead either to

increased nitrogen assimilation from alternative sources or to more efficient recycling rates within the plant under elevated $CO_2$.

The upregulation, twice in the season, of a transcript coding for UDP-glucose glucosyltransferase (sucrose metabolism) also suggests higher levels of carbon metabolism and increased use of sucrose under elevated $CO_2$. Interestingly, this gene and the other three involved in the respiratory pathway (Alanine, Citrate, and Glucose-6P) were all significantly upregulated at the experiment-wide level (FDR < 0.05) in both April and July, strongly supporting the idea of an increase in carbohydrate export and respiration at this time. This could be a result of a higher sink demand for carbohydrates reflecting the emergence of new flushes of needles during those months (first flush of the year in April and second flush in July, approximately; pers. obs.).

A clone coding for hydroxypyruvate reductase was downregulated in September, towards the end of the growing season. Hydroxypyruvate reductase catalyzes the reduction of hydroxypyruvate to glycerate in the peroxysomes of plants as part of photorespiration. Downregulation of the hydroxypyruvate reductase gene may be associated with a decline in photorespiratory rates which is in agreement with expectations of lower photorespiration under high $CO_2$ conditions due to inhibition of the oxygenation capacity of rubisco. The fact that this difference was only observed in September could be explained by the lower temperatures relative to mid-summer and the expectation that negative effects of rising $CO_2$ on photorespiration are counterbalanced by higher temperatures (Ehleringer et al. 1991).

Microarrays are functional genomics tools with a crucial role in gene discovery and assignment of gene function. The large amount of data generated from these studies makes it possible to search for novel candidate genes along with the analysis of the behavior of already annotated genes. Among the genes highlighted here, the transcript NXLV107_B07 has currently no annotated function in genomic databases but shows a significant and relative large response (in comparison with the other genes) to elevated $CO_2$, which could indicate an association with ecologically-relevant traits.

## 3.5 Conclusions

This study examined transcriptome-scale molecular processes underlying the response of loblolly pine trees to atmospheric $CO_2$ levels predicted to occur around 2050 (IPCC 2007). We highlighted genes and metabolic functional categories that might be particularly affected by elevated $CO_2$ in the atmosphere and analyzed how changes varied throughout the season. Our results provide novel hypotheses and source material for further research regarding the acclimation of natural ecosystems to future global change scenarios, while also pointing out potential interaction factors, both biotic (e.g., leaf development) and abiotic (e.g., drought), that need to be carefully considered in the design of future experiments. However, in spite of seasonal and developmental variation throughout the season, we identified six genes that showed a consistent and significant upregulation by elevated $CO_2$. Furthermore, variation in environmental factors can add insightful information about the potential for synergistic (or other) effects from different stress factors on the same transcriptome – a research area with many unanswered questions. Finally, the large dataset obtained here should both prove useful to researchers in diverse fields, from biochemistry to molecular biology and ecology, and help promote the emerging field of Evolutionary and Ecological Genomics.

Table 3.1 – Total number of genes (N) analyzed per month and number of genes upregulated and downregulated by elevated $CO_2$ ($P \leq 0.05$) within each month. For upregulated (E/A > 1), downregulated (E/A <1), and total differentially expressed genes (sum of upregulated and downregulated), we indicate both the absolute number (N) and the corresponding percentage (%) values for each month.

| **Month** | **Genes** | **Upregulated** | | **Downregulated** | | **Differentially expressed** | |
|---|---|---|---|---|---|---|---|
| | N | N | % | N | % | N | % |
| MARCH | 1750 | 20 | 1.1 | 12 | 0.7 | 32 | 1.8 |
| APRIL | 1720 | 34 | 2.0 | 16 | 0.9 | 50 | 2.9 |
| MAY | 1775 | 44 | 2.5 | 9 | 0.5 | 53 | 3.0 |
| JUNE | 1772 | 147 | 8.3 | 31 | 1.7 | 178 | 10.0 |
| JULY | 1755 | 176 | 10.0 | 181 | 10.3 | 357 | 20.3 |
| AUGUST | 1771 | 805 | 45.5 | 45 | 2.5 | 850 | 48.0 |
| SEPTEMBER | 1784 | 124 | 7.0 | 41 | 2.3 | 165 | 9.2 |
| **WHOLE-SEASON** | **12 327** | **1 350** | **10.9** | **335** | **2.7** | **1 685** | **13.7** |

Table 3.2 – Total number of genes analyzed and number of genes differentially expressed (both up- and downregulated) within each category. Differentially expressed genes are reported both as absolute number and as percentages from the total analyzed.

| Functional categories | Total genes analyzed | | Differentially expressed genes (whole-season) | | | |
|---|---|---|---|---|---|---|
| | Each month | Whole-season | Up | Down | Total | Percentage |
| CARBON METABOLISM | 472 | 3273 | 354 | 78 | 432 | 13.2 |
| ENVIRONMENT | 282 | 1957 | 233 | 54 | 287 | 14.7 |
| CELL MEMBRANES | 304 | 2112 | 204 | 48 | 252 | 11.9 |
| SIGNAL TRANSDUCTION | 212 | 1468 | 152 | 28 | 180 | 12.3 |
| PLANT GROWTH REGULATION | 152 | 1064 | 132 | 34 | 166 | 15.6 |
| GENE EXPRESSION | 155 | 1073 | 134 | 31 | 165 | 15.4 |
| NITROGEN AND SULFUR METABOLISM | 170 | 1183 | 128 | 25 | 153 | 12.9 |
| PHENYLPROPANOID PATHWAY | 135 | 944 | 100 | 18 | 118 | 12.5 |
| UNASSIGNED | 120 | 833 | 95 | 22 | 117 | 14.0 |
| CHLOROPLAST ASSOCIATED | 96 | 669 | 84 | 23 | 107 | 16.0 |
| CELL WALL RELATED | 54 | 372 | 48 | 10 | 58 | 15.6 |
| MITOCHONDRION | 50 | 347 | 36 | 15 | 51 | 14.7 |
| PHOTORESPIRATION | 22 | 147 | 18 | 9 | 27 | 18.4 |
| TRAFFICKING | 20 | 138 | 18 | 5 | 23 | 16.7 |
| OSMOLYTES | 15 | 105 | 12 | 1 | 13 | 12.4 |
| CELL STRUCTURE AND DIFFERENTIATION | 12 | 84 | 6 | 2 | 8 | 9.5 |
| METALS | 10 | 70 | 6 | 1 | 7 | 10.0 |
| PHOSPHATE ASSOCIATED | 7 | 49 | 6 | 1 | 7 | 14.3 |
| PROTEASES | 8 | 56 | 5 | 2 | 7 | 12.5 |
| NUCLEUS | 4 | 28 | 4 | 1 | 5 | 17.9 |

Table 3.3 – List of individual genes selected for being differentially expressed between elevated and ambient $CO_2$ conditions at the significance level FDR < 0.05 in two or more different months. Clone ID, putative annotation, and functional categories with which they are associated are presented. The last column refers to the labels used to identify the same genes in Figure 5.

| Clone | Annotation | Functional categories | Figure 5 |
|---|---|---|---|
| NXLV082_B07 | Alanine aminotransferase | Nitrogen and sulfur metabolism (amino acids) | Alanine |
| NXCI_163_C01 | Citrate synthase | Carbon metabolism (TCA cycle) | Citrate |
| NXCI_165_A01 | Glucose-6-phosphate isomerase (cytosolic) | Carbon metabolism (glycolysis/gluconeogenesis)<br>Cell wall related | Glucose-6P |
| NXCI_151_G07 | UDP-glucose glucosyltransferase | Carbon metabolism (sucrose)<br>Cell wall related | UDP-glucose |
| ST22D05 | Hydroxypyruvate reductase | Nitrogen and sulfur metabolism (amino acids)<br>Photorespiration | Hydroxy-pyruvate |
| NXCI_123_D05 | Membrane-bound small GTP-binding-like protein | Cell membranes (membrane proteins)<br>Trafficking | sGTP protein |
| NXLV_038_F09 | HD-Zip transcription factor | Signal transduction (transcription factors) | Transcription factor |
| NXLV108_A02 | Low-molecular-weight heat shock protein | Environment (abiotic – heat)<br>Gene expression (post-translational processing) | sHSP1 |
| NXLV123_E04 | Small heat shock protein | Environment (abiotic – heat)<br>Gene expression (post-translational processing) | sHSP2 |
| NXLV107_B07 | Unknown protein | Unassigned | Unknown |

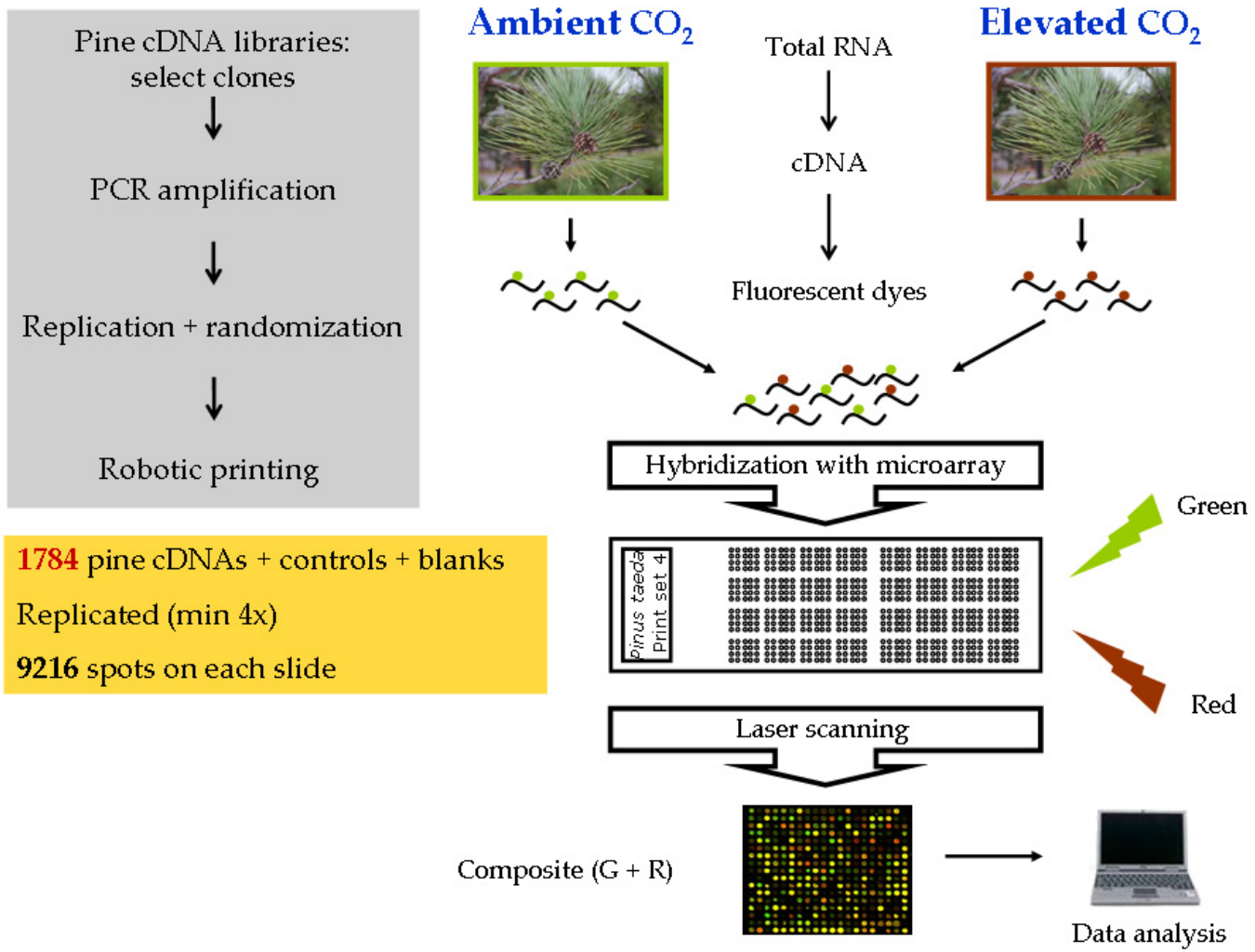


Figure 3.1 – Flow diagram of microarray experiment

Figure 3.2 (next page) – Volcano plot of relative change in gene expression levels between elevated and ambient $CO_2$ conditions (x-axis) and the corresponding statistical significance for each gene (y-axis: negative $\log_{10}$-transformed P-value at gene-level). Each point on the graph represents a different gene and month (plot contains all data pooled from seven months). At the center of the x-axis, a ratio E/A=1 indicates no differential expression between the two $CO_2$ concentrations; genes to the right of 1 on the x-axis have higher expression levels under elevated $CO_2$ relative to ambient, while genes to the left of 1 have lower expression values under elevated $CO_2$ compared to ambient (note that the numbers to the left are equal to (-A/E) to maintain symmetry; e.g., a value of -2 corresponds to a ratio E/A = ½). The horizontal dashed line indicates a gene-level $P = 0.05$ and genes above that line are considered statistically differentially expressed between elevated and ambient $CO_2$ conditions (up-regulated to the right (black circles); down-regulated to the left (dark gray circles)).

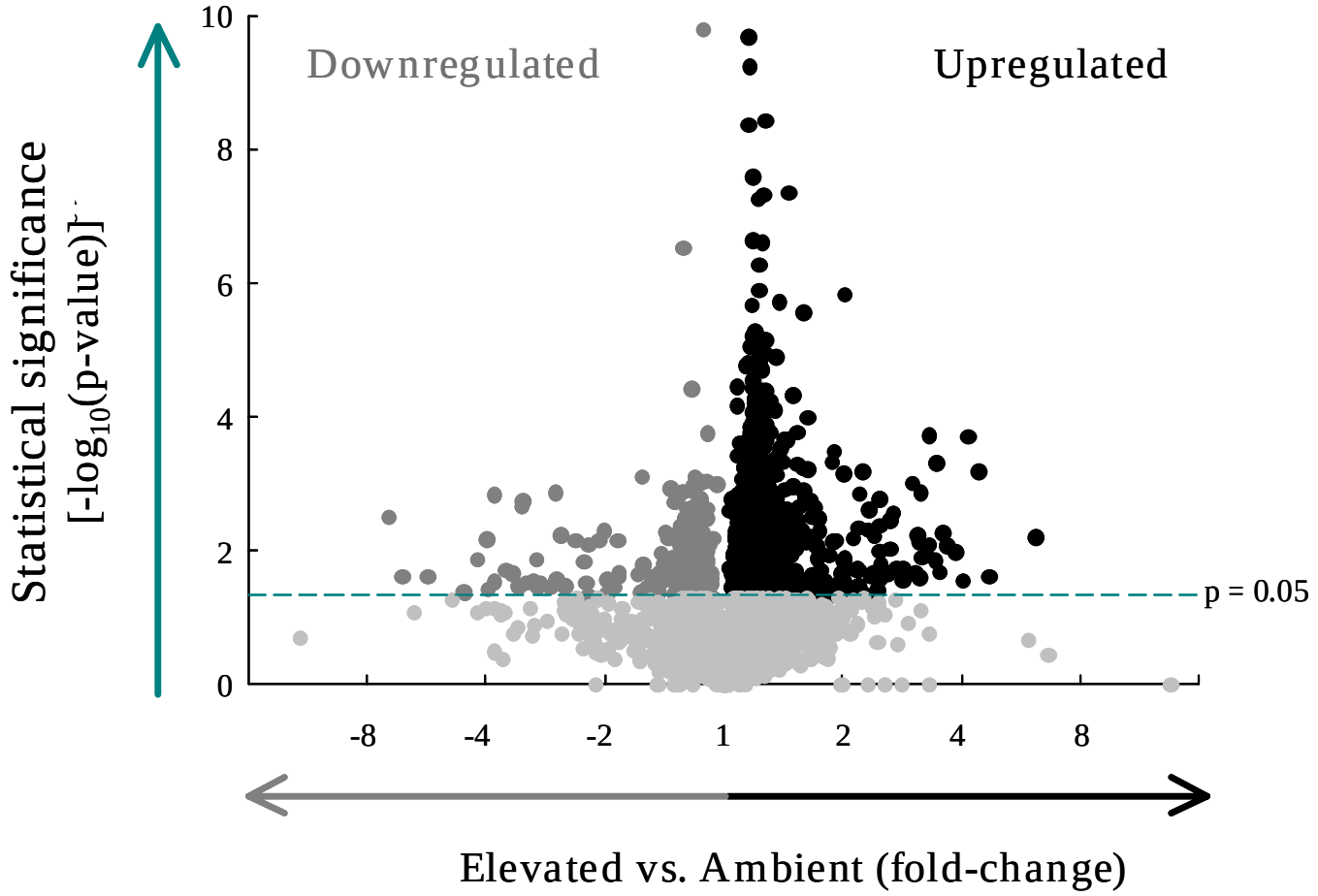
Downregulated
Upregulated
Statistical significance
[-log10(p-value)]
10
8
6
4
2
0
p = 0.05
-8
-4
-2
1
2
4
8
Elevated vs. Ambient (fold-change)

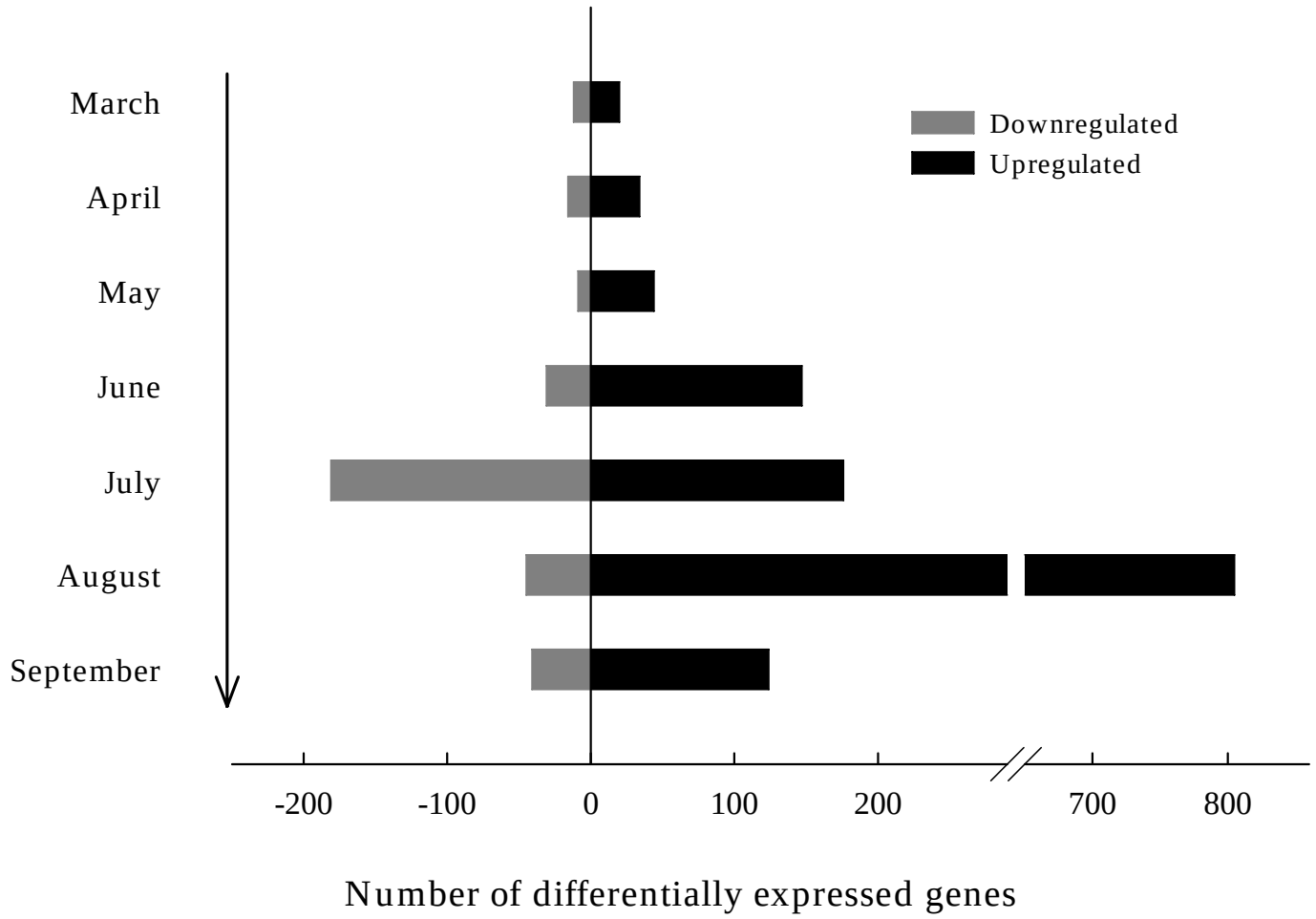


Figure 3.3 – Total number of differentially expressed genes per month of sampling (March, at the top, through September, at the bottom). Upregulated genes are shown on the positive x-axis (black bars) while downregulated are shown on the negative x-axis (gray bars).

Figure 3.4 (next 4 pages) – Seasonal distribution of total number of genes differentially expressed within functional categories. Each plot represents a different functional category ordered by decreasing number of clones per category: (a) Carbon metabolism, (b) Cell membranes, (c) Environment, (d) Signal transduction, (e) Nitrogen and sulfur metabolism, (f) Gene expression, (g) Plant growth regulation, (h) Phenylpropanoid pathway, (i) Unassigned function, (j) Chloroplast associated, (k) Cell wall related, (l) Mitochondrion, (m) Photorespiration, (n) Trafficking, (o) Osmolytes, (p) Cell structure and differentiation, (q) Metals, (r) Proteases, (s) Phosphate associated, (t) Nucleus.

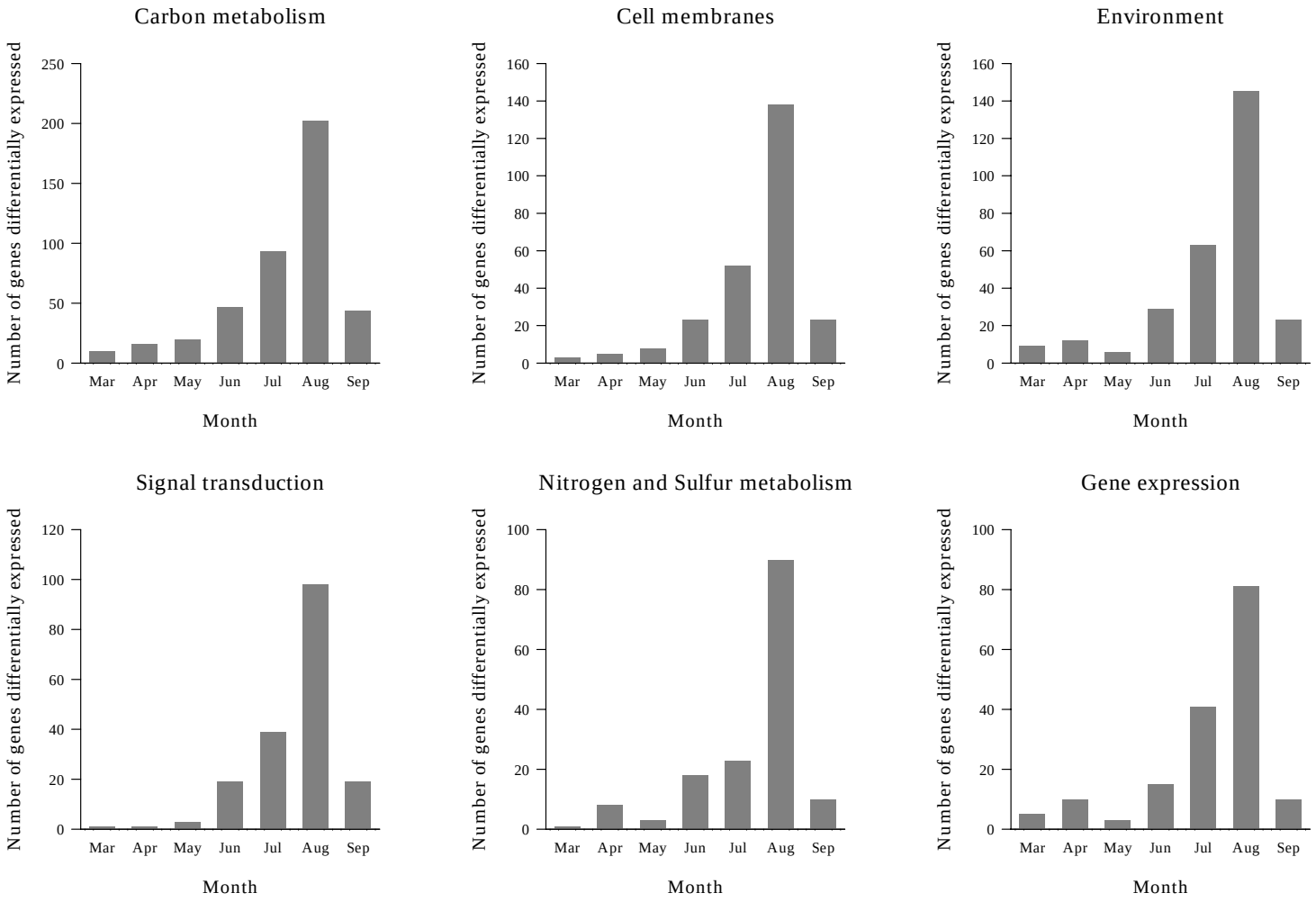
Carbon metabolism
Number of genes differentially expressed
0
50
100
150
200
250
Mar
Apr
May
Jun
Jul
Aug
Sep
Month
Cell membranes
Number of genes differentially expressed
0
20
40
60
80
100
120
140
160
Mar
Apr
May
Jun
Jul
Aug
Sep
Month
Environment
Number of genes differentially expressed
0
20
40
60
80
100
120
140
160
Mar
Apr
May
Jun
Jul
Aug
Sep
Month
Signal transduction
Number of genes differentially expressed
0
20
40
60
80
100
120
Mar
Apr
May
Jun
Jul
Aug
Sep
Month
Nitrogen and Sulfur metabolism
Number of genes differentially expressed
0
20
40
60
80
100
Mar
Apr
May
Jun
Jul
Aug
Sep
Month
Gene expression
Number of genes differentially expressed
0
20
40
60
80
100
Mar
Apr
May
Jun
Jul
Aug
Sep
Month

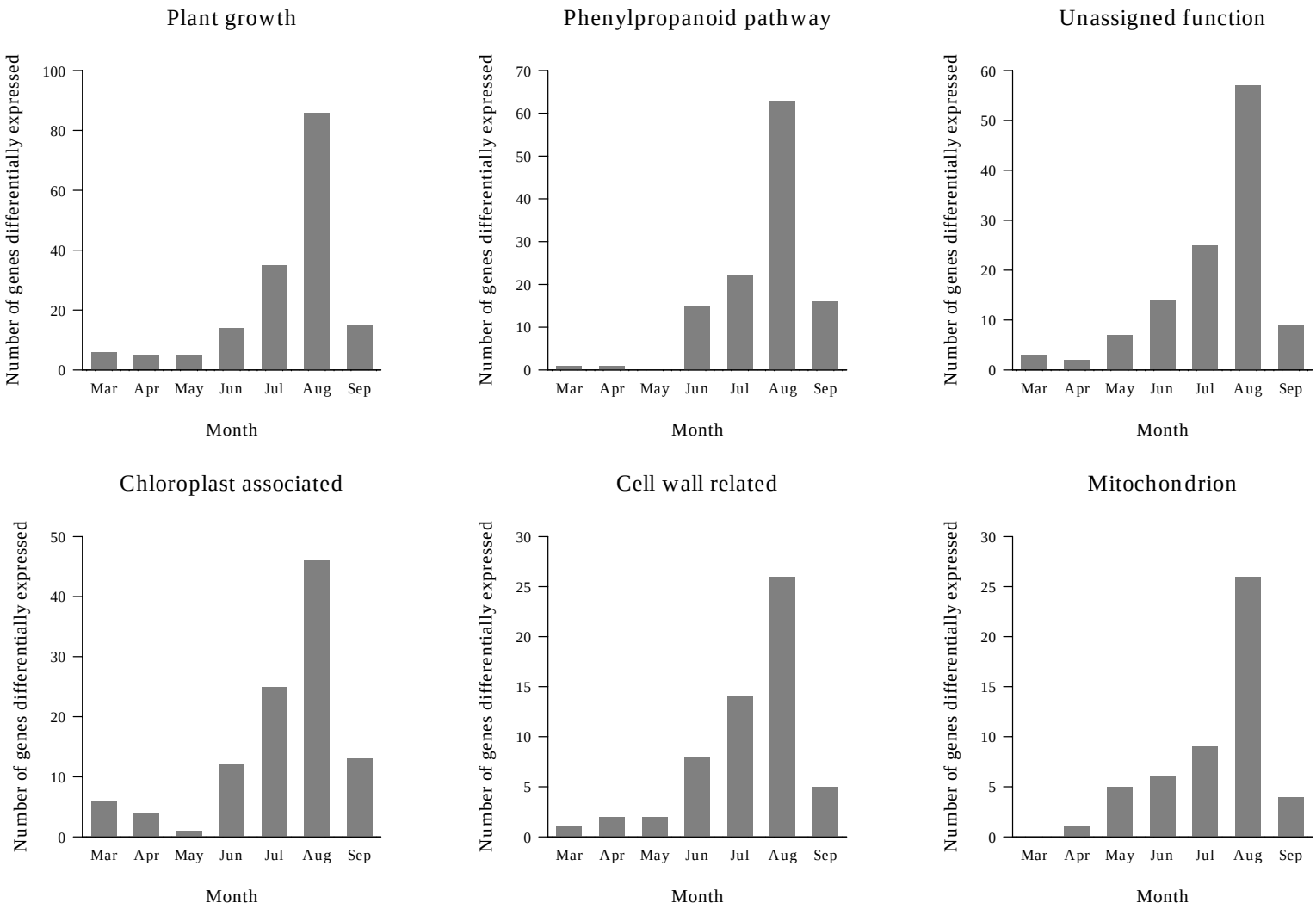
Plant growth
Number of genes differentially expressed
0
20
40
60
80
100
Mar Apr May Jun Jul Aug Sep
Month
Phenylpropanoid pathway
Number of genes differentially expressed
0
10
20
30
40
50
60
70
Mar Apr May Jun Jul Aug Sep
Month
Unassigned function
Number of genes differentially expressed
0
10
20
30
40
50
60
Mar Apr May Jun Jul Aug Sep
Month
Chloroplast associated
Number of genes differentially expressed
0
10
20
30
40
50
Mar Apr May Jun Jul Aug Sep
Month
Cell wall related
Number of genes differentially expressed
0
5
10
15
20
25
30
Mar Apr May Jun Jul Aug Sep
Month
Mitochondrion
Number of genes differentially expressed
0
5
10
15
20
25
30
Mar Apr May Jun Jul Aug Sep
Month

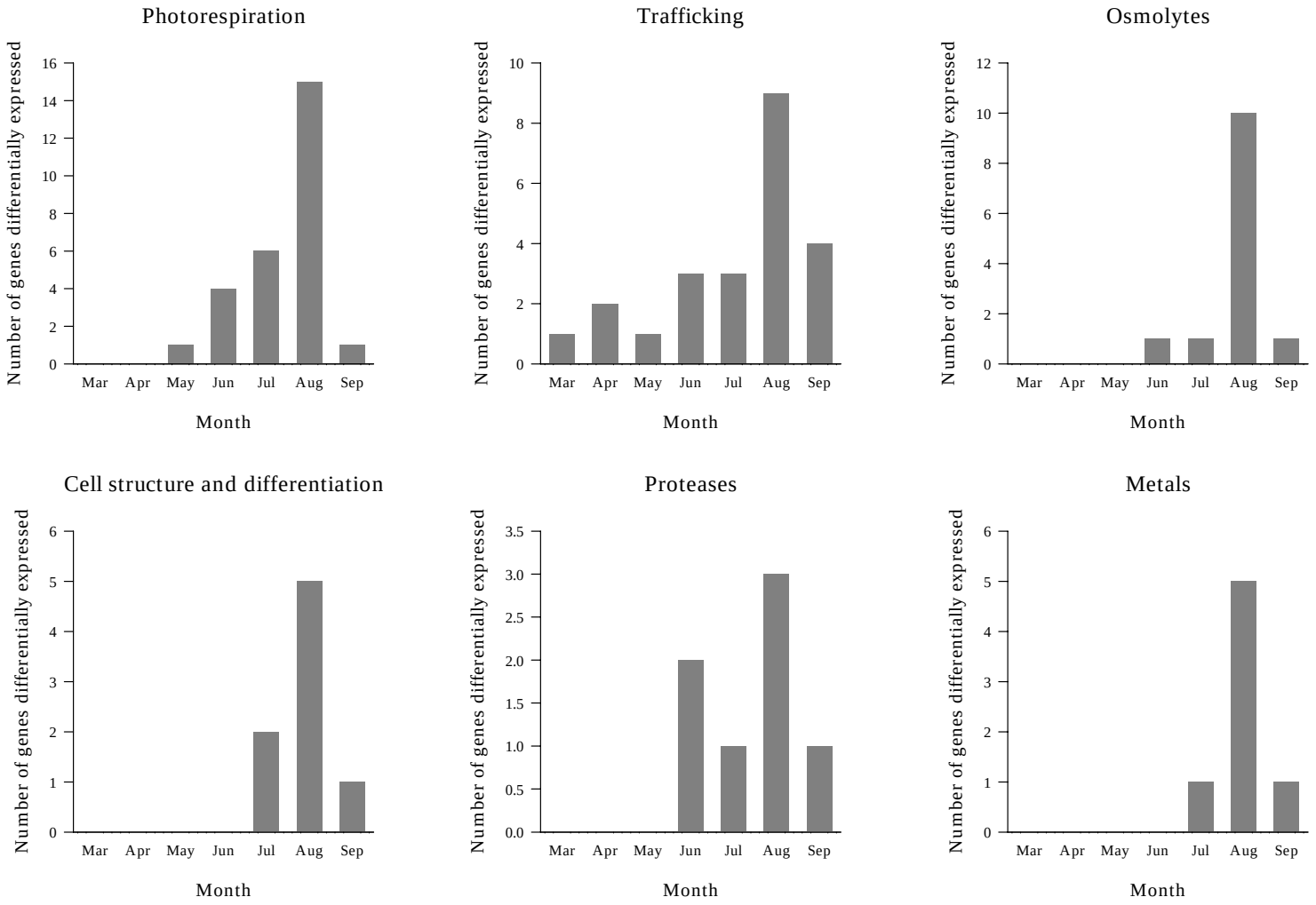
Photorespiration
Number of genes differentially expressed
0
2
4
6
8
10
12
14
16
Mar Apr May Jun Jul Aug Sep
Month
Trafficking
Number of genes differentially expressed
0
2
4
6
8
10
Mar Apr May Jun Jul Aug Sep
Month
Osmolytes
Number of genes differentially expressed
0
2
4
6
8
10
12
Mar Apr May Jun Jul Aug Sep
Month
Cell structure and differentiation
Number of genes differentially expressed
0
1
2
3
4
5
6
Mar Apr May Jun Jul Aug Sep
Month
Proteases
Number of genes differentially expressed
0.0
0.5
1.0
1.5
2.0
2.5
3.0
3.5
Mar Apr May Jun Jul Aug Sep
Month
Metals
Number of genes differentially expressed
0
1
2
3
4
5
6
Mar Apr May Jun Jul Aug Sep
Month

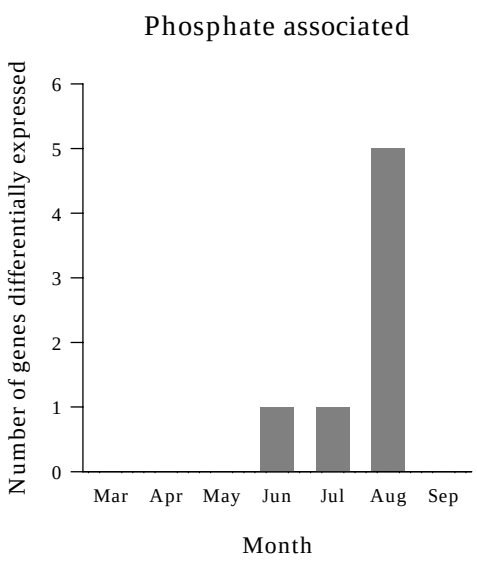
Phosphate associated
Number of genes differentially expressed
0
1
2
3
4
5
6
Mar
Apr
May
Jun
Jul
Aug
Sep
Month

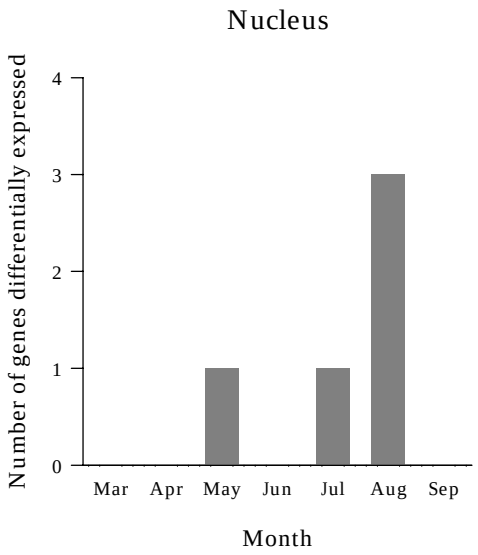
Nucleus
Number of genes differentially expressed
0
1
2
3
4
Mar
Apr
May
Jun
Jul
Aug
Sep
Month

Figure 3.5 (next page) – Relative expression levels between elevated and ambient $CO_2$ conditions of ten selected genes showing highly statistically significant differential expression (FDR ≤ 0.05) in two or more months of sampling. Abbreviated gene labels (corresponding to notation in the results section) are depicted on the x-axis and percentage of fold-change on the y-axis.

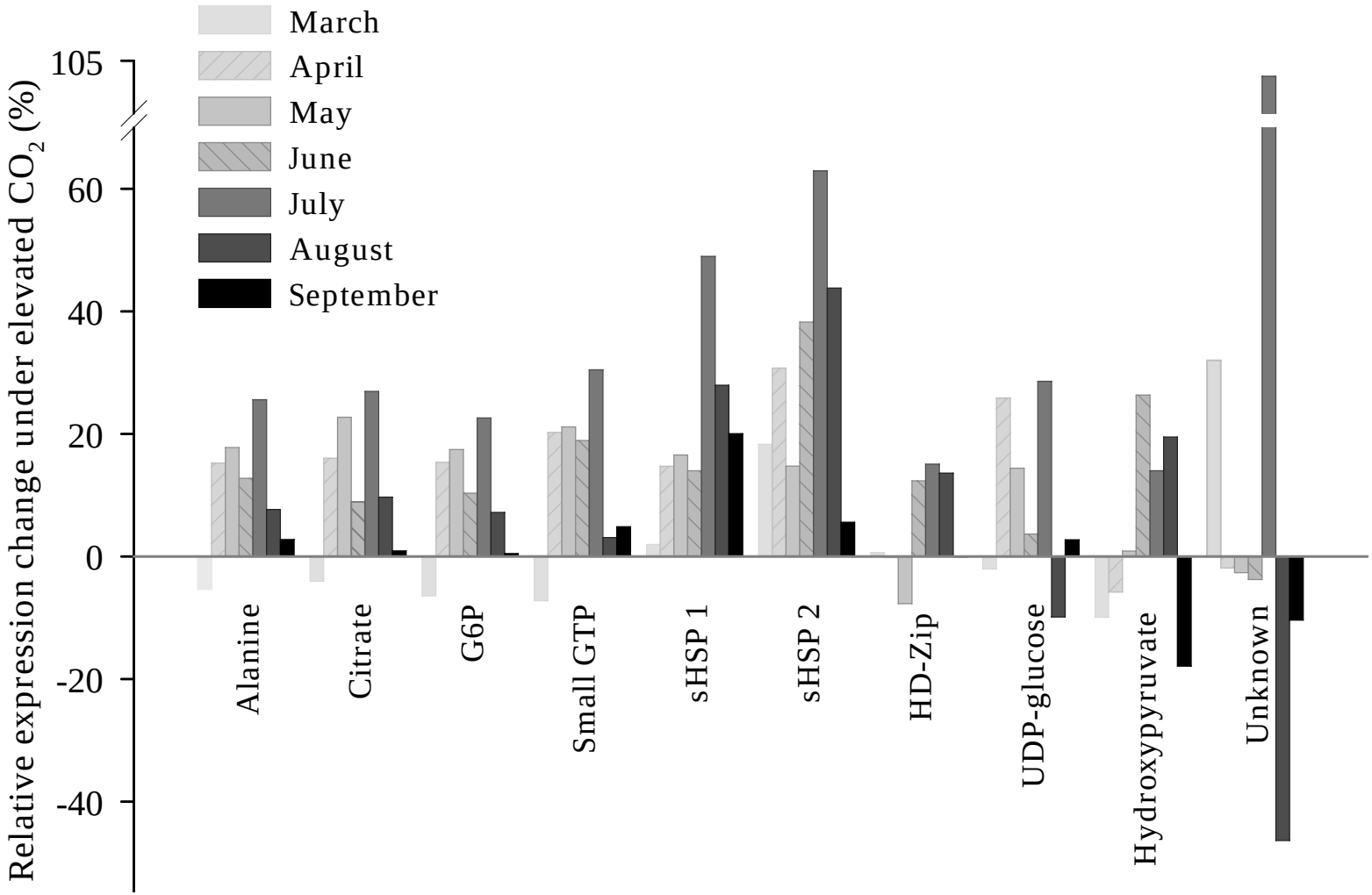
March
April
May
June
July
August
September
Relative expression change under elevated $CO_2$ (%)
105
60
40
20
0
-20
-40
Alanine
Citrate
G6P
Small GTP
sHSP 1
sHSP 2
HD-Zip
UDP-glucose
Hydroxypyruvate
Unknown

# Chapter 4: Regulation of carbon metabolism in two needle cohorts of loblolly pine trees exposed to elevated $CO_2$

## 4.1 Introduction

Terrestrial plant communities hold almost as much carbon globally (500 PgC) as the atmosphere (780Pg) and are currently strong sinks for atmospheric carbon dioxide ($CO_2$; Houghton 2003). Sustainability of this sink capacity under predicted scenarios of elevated $CO_2$ depends at the most fundamental level on plant physiological processes that regulate carbon assimilation, partitioning, and respiration. Despite the crucial contribution of plant carbon metabolism to the global carbon cycle, we know remarkably little about the effects of elevated $CO_2$ on the molecular mechanisms and gene networks that regulate these metabolic pathways (Gonzalez-Meler and Taneva 2005, Hill et al. 2006).

How the molecular regulation of carbon metabolism operates throughout a leaf's lifespan is also still poorly understood (Han et al. 2008) although leaf age can be crucial in the response to elevated $CO_2$. For instance, leaf aging affects the photosynthetic response to elevated $CO_2$ in many species, including tobacco (Backhansen and Scheibe 1999), potato (Katny et al. 2005), and various conifers (Turnbull et al. 1998, Medlyn et al. 1999, Griffin et al. 2000, Luomala et al. 2003, Crous and Ellsworth 2004). However, we do not have a clear understanding of the mechanisms behind this interactive effect between $CO_2$ and leaf age, which can be particularly important in temperate evergreen species

that maintain several cohorts of foliage and photosynthesize throughout most of the year (Pallardy 2008).

Photosynthesis is the primary process sensing and responding to changes in $CO_2$, and thus sets a physiological upper limit for carbon sequestration with increasing atmospheric $CO_2$ levels. In the short-term, elevated $CO_2$ consistently stimulates leaf-level photosynthesis in C3 plants due to a combined effect of increased carboxylation capacity ($V_c$) and decreased oxygenation capacity ($V_o$) of the ribulose-1,5-biphosphate carboxylase/oxygenase (rubisco) protein. However, a continued stimulation of photosynthesis by elevated $CO_2$ in the long-term depends on the leaf physiological status and on an adequate plant sink capacity for the additional photosynthates produced (Stitt 1991, Rogers and Humphries 2000). A reduced sink demand can lead to downregulation of photosynthesis usually accompanied by lower Rubisco content, decreased $V_{c,max}$, and an increase in foliar carbohydrates (Rogers and Humpries, 2000). This suite of traits is thought to be the result of an increased cycling of leaf sugars, which is sensed by proteins such as hexokinase and leads to the repression of rubisco small subunit genes (Krapp et al. 1993, Moore et al. 1998, Moore et al. 1999).

Foliar carbohydrates, in particular sucrose and glucose, are not only important regulators of gene expression and plant physiology (Jang and Sheen 1994, Koch 1996, Rolland et al. 2002, Sheen et al. 2007, Smith and Stitt 2007), but they are also both the products of photosynthesis and the substrates for respiration. It is the balance between $CO_2$ fixation through photosynthesis and $CO_2$ release through respiration that

determines the actual plant carbon storage capacity and the sequestration potential of an ecosystem (Hill 2006).

To fully understand the impact of elevated $CO_2$ on plant carbon metabolism and to strengthen our predictions about the role of terrestrial vegetation in the future, we need a more comprehensive account of the mechanisms operating at the molecular and gene expression level. To improve our understanding of these molecular controls under elevated $CO_2$, we must also address the influence of leaf age on the response of the different metabolic pathways regulating the fate of carbon fixed through photosynthesis. This is particularly important in evergreen species, such as loblolly pine, in which different cohorts of leaves contribute a significant amount of the total carbon sequestered each year.

Using cDNA microarrays, we compared the expression levels of 390 carbon metabolism transcripts (*genes*) in loblolly pine trees growing under ambient and elevated $CO_2$ at the Duke Forest Free-Air-$CO_2$-Enrichment (FACE) site and contrasted the differences in gene expression across two foliage age classes: one-year-old and current-year needles. To interpret our data in light of known leaf-to-canopy level responses of loblolly pine to elevated $CO_2$, we grouped genes into major metabolic groups according to their role in one of the following processes: (1) carbon assimilation, (2) carbon partitioning, (3) carbon oxidation, and (4) energy production (i.e., ATP synthesis). Based on literature reports of leaf-age effects on photosynthetic response to

elevated $CO_2$, we hypothesized that the overall effect of elevated $CO_2$ on gene expression would be more pronounced in current-year needles than in one-year-old needles.

## 4.2 Materials and methods

### *Site description*

The FACTS-I (Forest-Atmosphere Carbon Transfer and Storage I) research site is located in the Blackwood Division of Duke Forest. It uses FACE technology to manipulate $CO_2$ concentrations in the air with minimal disturbance to the ecosystem. In 1996, six circular plots (30-m diameter) where established in a 16-year-old plantation of loblolly pine (*Pinus taeda*, L.). Since then, three of these plots have been maintained as controls at ambient CO2 levels while three treatment plots have been fumigated with air enriched with 200 ppm of CO2 (Hendrey et al. 1999). Elevated CO2 levels were maintained continuously during the first 6 years the experiment, except when the air temperature was below 5°C for more than 1h, or when wind speeds were higher than 6 m s-1. Beginning in 2003, the CO2 treatment was confined to daylight hours. The forest canopy is largely dominated by loblolly pine (98%) but includes sweetgum (*Liquidambar styraciflua*) and tulip poplar (*Liriodendron tulipifera*) trees. Mean annual temperature and precipitation at the site are 15.5°C and 1140mm, respectively (http://face.env.duke.edu).

### *Sampling*

We sampled fascicles of needles from upper-canopy (top 5-10%), sun-lit branches of three pine trees in each of the six replicated plots using platform-lifts (UL48, Upright, Charlotte, NC). Needles were immediately frozen in liquid nitrogen upon removal from each branch and kept in this condition until they could be transferred to a -80°C freezer in the laboratory. Sampling occurred from March through September of 2002 and

included mature needles in two different age classes: one-year-old needles (2001 cohort) and current-year needles (2002 cohort). One-year-old needles were sampled three times during the spring (Day of Year, DOY: 83, 106, 135) and current-year needles were sampled three times in the summer of the same year (DOY: 210, 233, 267; Figure 1). Environmental conditions measured by air temperature, vapor-pressure-deficit, soil moisture, and soil temperature were consistent between ambient and elevated $CO_2$ plots in each sampling date (paired t-test for individual environmental variables, $P > 0.05$).

### *Microarrays experiment*

This study focuses on data generated in the context of a larger-scale analysis which used cDNA microarrays to compare the expression levels of 1784 pine gene transcripts between ambient and elevated $CO_2$ conditions (Chapter 3). The gene transcripts were selected from five pine cDNA libraries at North Carolina State University: NXNV (xylem normal wood vertical), NXCI (xylem compression wood inclined), NXSI (xylem side-wood inclined), ST (shoot-tip), and PC (pollen cone libraries), and subsequently prepared for printing on microarray slides. Microarray slides contained 9216 spots (cDNA probes) that included technical replicates of the 1784 pine transcripts, external control genes, and blanks (a detailed description is available in Chapter 3). Each microarray slide was used for the comparison of two target samples (RNA) prepared from independent biological replicates (defined as pool of needles harvested from trees in an individual experimental plot, either ambient or elevated $CO_2$, at each sampling date). The pair of samples contrasted in each slide was always associated with the same

sampling day and leaf cohort, but a different $CO_2$ concentration, i.e., either ambient (A) or elevated (E).

Ten μg of total RNA from each sample in a pair-wise comparison was labeled with a different fluorescent dye (Cy3 or Cy5) and hybridized to a microarray. Following hybridization, each microarray slide was scanned at two different wavelengths (corresponding to the two different fluorescent dyes) in a ScanArray 5000 (Perkin Elmer, Boston). The relative difference in fluorescence among the two dyes was used as a proxy for the relative difference in expression of each gene across the two $CO_2$ conditions (ambient and elevated). A detailed description of the processes involved in the microarray experiment is included in Chapter 3 of this dissertation.

### *Selection and classification of carbon metabolism genes*

From the complete pool of gene transcripts (1784), we selected those with functional annotations related to central carbon metabolism and energy production. We confirmed the annotation of each transcript sequence against the most updated version of the Pine Gene Index database (DFCI Pine Gene Index Database – release 6.0 available at http://www.danafarber.org/; Quackenbush et al. 2000) and removed from our analysis any transcripts whose annotation had changed to some function outside of the pathways considered for this study. We obtained a final pool of 390 transcripts (29 of which were associated with two metabolic pathways and are therefore represented twice in our dataset). The same gene product (protein or enzyme) is often named differently by individual researchers or in different genomic and protein databases. This redundancy

can be misleading when interpreting results of gene expression, particularly to audiences unfamiliar with these databases and the multiple biochemical synonyms for each protein. For that reason, we compared the annotation of our selected transcripts to protein and enzyme nomenclature databases (UniProt and ENZYME; linked from http://www.expasy.org/), and grouped transcripts putatively coding for the same protein under one common gene annotation used throughout the text. The original annotation for each transcript is available in Appendix B. We assigned genes to specific pathways in this study according to information compiled from the following databases: Kyoto Encyclopedia of Genes and Genomes (KEGG; http://www.genome.jp/kegg/); AraCyc (http://www.arabidopsis.org/), and Mapman mapping files (http://gabi.rzpd.de/projects/MapMan/). Whenever possible, we obtained information about the cellular location (e.g. chloroplastic, nuclear) of the gene product for a more correct assignment to the pathways (e.g., even though glyceraldeyde-3-phosphate dehydrogenase is an enzyme that is involved both in glycolysis and photosynthesis, if the annotation referred specifically to a cytosolic isoform, then the corresponding gene was assigned only to glycolysis). When this specificity was not known, we assigned the transcript to all pathways that share that enzyme. We grouped genes into the following functional categories: Photosynthesis (Light Reactions: Pigments, Light-harvesting-center proteins, Photosystem I, Photosystem II, Photosynthetic Electron Transport; and Carbon fixation reactions: Calvin Cycle, Rubisco, Chaperonins 60), Photorespiration, Sucrose and Starch metabolism (synthesis and degradation pathways), Sugar

transporters, Oxidative Pentose Phosphate pathway (OPPP), Dark Respiration (Glycolysis, Fermentation, Citric Acid Cycle, Mitochondrial transporters, Mitochondrial Oxidative Phosphorylation), and ATP synthesis (Table 1). To better link gene expression data to the ecological and physiological context of carbon exchange, we grouped twenty of these categories into three major metabolic groups: carbon assimilation, carbon partitioning, and carbon oxidation. The ATP synthesis category was defined as a fourth independent group because ATP synthases are involved in a series of pathways that span more than one of these three carbon groups.

### *Statistical analysis*

A two-step mixed linear model (Jin et al. 2001, Wolfinger et al. 2001) was used to determine the significance of the treatment effect and identify transcripts differentially expressed between ambient and elevated $CO_2$ for each sampling date. Details about the model and application to our dataset were described in detail in chapter 3. For each date, genes were grouped into three expression categories according to their response to elevated $CO_2$: unaffected ($P \geq 0.05$), upregulated ($P \leq 0.05$ and $E/A > 1$), or downregulated ($P \leq 0.05$ and $E/A < 1$). We pooled the gene expression data into the two foliage cohorts (one-year-old and current-year needles) and calculated the frequency of each expression type (unaffected, upregulated, and downregulated) in each metabolic group and functional category. Frequencies were reported as a percentage of the total number of counts (genes × sampled times) in each group (Appendix C; Table 2). Differences in the frequency of gene expression types between age classes were

assessed by contingency analysis and Pearson $\chi^2$ tests of independence (JMP 7.0; SAS Institute Inc.). An averaged measure of the magnitude of change between ambient and elevated $CO_2$ conditions was calculated for each foliage age class using the individual relative expression values (E/A) of differentially expressed genes only (Appendix C).

## 4.3 Results

### *Effects of elevated $CO_2$ on the overall gene expression of two needle cohorts*

Elevated $CO_2$ concentration significantly affected the expression of 65% of the 390 transcripts at least once during the sampling period ($P < 0.05$; data not shown). On average, 15% of the total gene pool was differentially expressed between ambient and elevated $CO_2$ when both foliage classes were combined $(P < 0.05)$. The magnitude of the $CO_2$ effect was clearly distinct between the two needle cohorts: while 27% of the total gene pool was differentially expressed between ambient and elevated $CO_2$ conditions in current year needles, only 4% was differentially expressed in one-year-old needles (Table 2; $P < 0.001$). In both cases, more genes were upregulated than were downregulated by elevated $CO_2$ (3.6:1 in current-year needles and 2.:1 in one-year-old needles; Table 2). Although the proportion of differentially expressed genes was much larger in current-year needles, the mean relative change (E/A) in expression of individual genes was only 3% higher in current needles compared to one-year-old (1.16±0.03 vs. 1.13±0.04; Appendix C).

### *Effects of elevated $CO_2$ across four broad metabolic groups*

Overall, ATP synthesis was the metabolic group of genes that showed the highest percentage of differential expression between $CO_2$ conditions (16.2%, n=66; Table 2), Three other metabolic groups showed a similar proportion of differential expression under elevated $CO_2$ (carbon assimilation: 15.5%, n=230; carbon partitioning: 15.4%, n=243; and carbon oxidation: 15.2%, n=630). The same pattern was seen in current-year

needles: ATP had a higher number of differentially expressed genes under elevated $CO_2$ (30.3%) than carbon assimilation (27.4%), carbon partitioning (27.6%) and carbon oxidation (26.0%). In contrast, in one-year-old needles the highest percentage of genes affected by elevated $CO_2$ was associated with the carbon oxidation group (4.3%), followed by carbon assimilation (3.5%), carbon partitioning (3.3%), and ATP synthesis (3.0%). The proportion of genes differentially expressed in each metabolic group was always larger in current-year needles than in one-year-old needles (Table 2).

### *Effects of elevated $CO_2$ within metabolic groups in two needle cohorts*

*1) Carbon assimilation*

In current-year needles, 20% of the gene pool in the carbon assimilation group was upregulated and 7.4% was downregulated by elevated $CO_2$, while in one-year-old needles there was an equal number of genes upregulated and downregulated (each corresponding to 1.7% of the total pool). In both age classes, however, carbon assimilation was the metabolic group with the highest percentage of downregulation (Table 2). This largely reflected a trend of decreased gene expression among photosynthetic light-reactions, in particular within the categories Photosystem I (PSI), Photosystem II (PSII), and Photosynthetic Electron Transport (PET). In all three categories, elevated $CO_2$ was associated with either downregulated genes only (one-year-old needles) or a large proportion of downregulated genes (current-year needles; Figure 2). For example, PET had the highest percentage of downregulated genes (20.8%, n=24; Appendix C) across all twenty-one categories in the metabolic groups of current-

year needles. Similarly, PSI was the category with the highest downregulation percentage among one-year-old needles (8%, n=12; Appendix C). Although pathways of light reactions had a high proportion of downregulated genes overall, the same trend was not observed in the carbon reactions of photosynthesis. In fact, in both cohorts of needles there were more genes being upregulated than downregulated among those coding for enzymes of the Calvin cycle (Figure 2). However, none of the five transcripts coding for ribulose-1,5-carboxylase/oxygenase (rubisco) was differentially expressed between ambient and elevated $CO_2$ in either class of needles (Figure 2).

*2) Carbon partitioning*

There was a distinct pattern of response to elevated $CO_2$ between the two age classes in the carbon partitioning group (Figure 2). In current-year needles, changes under elevated $CO_2$ included both upregulation and downregulation, and all pathways were affected similarly. The main effect of elevated $CO_2$ in one-year-old needles was an increase in expression of genes coding for sugar transporters and for enzymes in sucrose and starch degradation. However, there were no changes in expression among the genes in either sucrose or starch synthesis pathways (Figure 2).

Within this metabolic group, a large proportion of transcripts (9 out of 13) coding for an important regulatory enzyme involved in sucrose degradation and cell wall synthesis – sucrose synthase (Susy) – were upregulated at least once in the current-year cohort of needles. Only two of these transcripts were affected by the $CO_2$ treatment in one-year-old needles. In contrast, the two transcripts coding for hexokinase (another

important enzyme in sucrose degradation) were consistently unaffected by elevated $CO_2$ conditions in both the age classes. Hexokinase is a cytosolic enzyme that phosphorylates hexoses resulting from the breakdown of sucrose, and is implicated as a sensor protein in sugar-mediated repression of rubisco as described in the major model proposed for photosynthetic downregulation under elevated $CO_2$ (Moore et al. 1999, Long et al. 2004). Both suites of hexokinase and rbcS genes in this dataset showed no changes in expression between $CO_2$ conditions.

*3) Carbon oxidation*

The carbon oxidation group showed the smallest difference in $CO_2$ effect across age classes (21.7%), with the largest proportion of differential expression in old needles (4.3%) and the lowest corresponding proportion among current-year needles (26%). Twenty percent of genes were upregulated by elevated $CO_2$ in current-year needles, while only 3.3% were upregulated in old needles. Nevertheless, this was the group with the highest frequency of upregulation within the one-year-old cohort (Table 2). This trend suggests that $CO_2$ consistently increases expression of genes involved in the breakdown of carbohydrates across the needles' lifespan.

In all categories within current-year needles, the percentage of upregulation was higher than percentage of downregulation, and this was particularly evident among genes in the citric acid cycle (TCA) where the percentage of downregulation was particularly low (2%, Figure 2). Glycolysis showed the largest percentage of upregulation (5%) in one-year-old needles in this metabolic group and was matched

only by starch degradation across all categories within this age class (Figure 2). The upregulation of one of the transcripts (transcript NXCI_123_A10) coding for phosphofructokinase (a highly regulated enzyme in the glycolytic pathway), as well as the frequent upregulation among citrate synthase genes (crucial in regulation of the citric acid cycle) in both age classes lends further evidence of increased respiratory carbon breakdown under elevated $CO_2$ regardless of leaf aging.

*4) ATP synthesis*

Leaf age was clearly an important factor in the $CO_2$-induced response of genes involved in ATP synthesis. This was in fact the metabolic group with the largest difference between age classes (10 times more genes were differentially expressed in current needles compared to one-year-old needles; Table 2). Elevated $CO_2$ had little effect on the expression of this suite of genes in one-year-old needles, but upregulated a large percentage of the same genes in current-year-needles (27.3%), the highest percentage of upregulation among the four groups in this foliage class).

## 4.4 Discussion

Elevated $CO_2$ affected the expression level of 15% of the gene pool across time and leaf cohorts ($P < 0.05$, Table 2), although a much larger proportion (65% of the 390 transcripts measured) were sensitive to the $CO_2$ treatment at least once during the sampling period (data not shown). These data provide strong evidence that gene regulation of carbon metabolism is an important component of the response of pine trees to elevated $CO_2$. The magnitude of this response varied considerably between foliage cohorts (4% of genes affected in one-year-old needles compared to 27% in current-year needles; Table 2) supporting the initial hypothesis that the effect of elevated $CO_2$ on carbon-related gene expression is not constant throughout a leaf's lifespan. Leaf age dependent regulation of carbon metabolism under increasing atmospheric $CO_2$ levels may have a significant impact on carbon assimilation and allocation patterns in individual trees. Additionally, it may contribute to differences in forest productivity and the proportion of carbon exported to the soil, a large and long-term carbon storage component of terrestrial ecosystems (Hill et al. 2006). Foliage age should therefore be accounted for in models of the response of vegetation to rising $CO_2$.

### *Carbon assimilation: light and carbon reactions and photosynthetic parameters*

The larger proportion of differential expression among carbon assimilation genes in current-year needles (27.4%) compared to one-year old needles (3.5%; Table 2) is in agreement with reports of leaf-age dependency of the photosynthetic response of plants to elevated $CO_2$ (e.g., Backhansen and Scheibe 1999, Medlyn et al. 1999, Griffin et al.

2000, Katny et al. 2005). The pattern of gene expression in this study also provides mechanistic support to the observed larger stimulation of elevated $CO_2$ on the net photosynthesis of current-year needles (30% higher than one-year-old needles) of pine trees at this site (Crous and Ellsworth, 2004; but see Springer et al. 2004).

Photosynthetic genes evaluated in this study showed a different pattern of response to elevated $CO_2$ according to whether they coded for proteins participating in the light-reactions of photosynthesis or in carbon-fixation (Calvin cycle; Figure 2). Differences between the two components of carbon assimilation are important in the context of biochemical and physiological adjustments of the photosynthetic machinery and have been traditionally described by the relationship among the maximum photosynthetic electron rate ($J_{max}$) and the maximum carboxylation capacity of rubisco ($V_{c,max}$) estimated from leaf-level gas-exchange measurements (Farquhar et al 1980). Although the individual values for each of these parameters vary with species and environmental conditions, the ratio of between the two ($V_{cmax}/J_{max}$) is often fairly constant (Wullschleger 1993), suggesting a tight control of the photosynthetic apparatus and the activity of related enzymes. Our gene expression data suggest, however, that elevated $CO_2$ might affect light and carbon-fixation reactions differently. If the patterns of gene expression were directly scalable to leaf-level photosynthetic rates, one would expect an increase in the $V_{cmax}$ to $J_{max}$ ratio, contradicting the trend emerging from cross-species comparisons of plants exposed to elevated $CO_2$ in the field. In most species analyzed, elevated $CO_2$ caused a large reduction in $V_{cmax}$ and a concomitant small (and often negligible)

reduction in $J_{max}$. However, trees as a whole consistently showed the lowest reduction in $V_{cmax}$ potentially because rubisco is not substrate-saturated at elevated $CO_2$ levels in this plant functional group (Ainsworth and Rogers 2007).

This pattern of decreased expression among genes involved in photosynthetic light reactions was similar in both needle cohorts, although in current-year needles the proportion of upregulated genes was still higher than the propotion of downregulated genes in all light reactions (Figure 2). Although in one-year-old needles three of the light-related categories had a net downregulation response (PET, PSI, and PSII), this was the result of a single transcript measurement in each of the cases and may not reflect a significant biological effect. Crous and Ellsworth (2004) reported signs of downregulation of photosynthesis (reduced values of $V_{c,max}$ and $J_{max}$) under elevated $CO_2$ in one-year-old needles during the first six years of this FACE experiment. However, only $J_{max}$ was significantly different between $CO_2$ conditions and age class across years. These patterns provide a compelling physiological context for the differences in expression between light- and carbon-reaction genes in our dataset (Appendix C).

### *No downregulation of rubisco in either age class*

We found no evidence of $CO_2$ effects on the expression of genes coding for the small subunit of Rubisco (rbcS). In fact, this was a remarkably consistent result as none of the five rbcS transcripts (which encode for at least two different small subunits of the enzyme; Appendix C) showed differential expression between ambient and elevated $CO_2$ on any sampling date for both one-year-old and current-year needles (Figure 2).

Because the amount of rubisco protein is largely regulated bythe transcription of rbcS genes (Buchanan et al. 2000) and the protein is not saturated at the current atmosheric $CO_2$ concentration, these results also argue against a reduction in carboxylation capacity with elevated $CO_2$ (although the total carboxylation capacity depends both on protein content and its activation status). According to our results, sugar-mediated downregulation of photosynthesis (through repression of rbcS) was not likely in either cohort of needles at this point in the experiment. This is consistent with leaf-level gas-exchange data measured at this site during the same year of our sampling. In 2002, there were no differences in $V_{c,max}$ between $CO_2$ treatments (Crous and Ellsworth 2004), nor evidence of a decline in photosynthetic rate stimulation under elevated $CO_2$ compared to measurements made at the beginning of the FACE experiment (Myers et al. 1999, Springer et al. 2004).

### *Carbon partitioning: no changes in synthetic pathways in one-year-old needles*

Carbon partitioning was the metabolic group with the second largest difference between the two needle cohorts; differential gene expression under elevated $CO_2$ was 8.4-times more frequent in current-year needles than in one-year-old needles (Table 2). This result may indicate a crucial point of gene regulation underlying overall differences in the response of different age classes to elevated $CO_2$, and is consistent with extensive research highlighting the importance of foliar carbohydrates, particularly sugars, in regulating gene expression and general plant metabolism (Jang and Sheen 1994, Koch 1996, Rolland et al. 2002, Sheen et al. 2007, Smith and Stitt 2007)

In one-year-old needles, the effect of elevated $CO_2$ on carbon partitioning was primarily to upregulate transcripts in sucrose and starch degradation. This upregulation likely reflects an increased demand for hexoses, which are simultaneously the products of starch and sucrose breakdown and the main substrate for cellular respiration. An increase in cellular respiration in one-year-old needles under elevated $CO_2$ is further corroborated by the relatively large percentage of upregulation among genes in the carbon oxidation group (Table 2) and is consistent with the role of this foliage class as the main source tissue of carbon and energy during the Spring time. One-year-old needles need to provide enough resources for plant growth and for the emergence of the new needle cohort . In current-year needles, the percentage of differentially expressed genes was similar across both synthesis and degradation pathways, suggesting a high proportion of photosynthates allocated to storage (starch) and export (through sucrose). This conclusion is also supported by the upregulation of genes coding for sugar transporters, which promote the flux of hexoses and sucrose across the chloroplast and plasma membranes (Figure 2, Appendix C). The upregulation of genes in these pathways is not surprising given the parallel increase in expression of carbon fixation genes (our data) and in photosynthetic rates in current-year needles under elevated $CO_2$ (Myers et al. 1999, Ellsworth 2000, Crous and Ellsworth 2004), Springer et al. 2004).

### *No accumulation of foliar carbohydrates in current-year needles*

Upregulation of both starch synthesis and degradation genes in the current-year cohort suggests a higher turnover of starch rather than its accumulation in the leaves. Although

this contradicts some other observations of plants exposed to long-term elevated $CO_2$, it is consistent with the patterns observed for trees only (Ainsworth and Long 2005) and is likely explained by the larger sink capacity in this functional group compared to other plants (Rogers and Ainsworth 2006). High sucrose cycling (suggested by increased levels of gene expression in both synthesis and degradation) is expected to increase rates of hexose phosphorylation by hexokinase, which can lead to a feedback mechanism repressing the activity of photosynthetic genes and subsequent downregulation of photosynthesis under elevated $CO_2$ (Moore et al. 1999, Long et al. 2004). In addition to the lack of an effect of elevated $CO_2$ on rbcS genes that we observed, we also saw no evidence of differential expression among the transcripts coding for hexokinase. This enzyme could be responding to higher sucrose levels only at the enzymatic activity level rather than by transcriptional regulation, but the lack of response of photosynthetic genes included in this study that are usually repressed by sucrose (rubisco small subunits, chlorophyll a/b binding genes, and a plastocyanin-family gene (cupredoxin); Appendix C) in combination with no changes in hexokinase gene expression is strong evidence that sucrose is probably not accumulating in these pine needles but instead being utilized or exported at rates comparable to its production. This suggests that there is enough sink demand in these trees (or the soil community adjacent to their roots) for the additional carbon fixed under elevated $CO_2$.

### *Increased cell wall growth underlying increases in canopy leaf-area*

A high rate of sucrose utilization and potential allocation towards cell growth is supported by the frequency of upregulation among genes coding for sucrose synthase (Susy). Sucrose synthase genes are sometimes induced in situations of limited ATP supply and increased sink demand, probably because this enzyme and cellulose synthase participate jointly in a very energy-efficient mechanism of cell wall synthesis (Dennis and Blakely 2000). A higher production and allocation of UDP-glucose (the product of sucrose breakdown by Susy) towards cell wall synthesis under elevated $CO_2$ could lead to increased needle length or thickness in these conditions, and may underlie differences in leaf area values observed at this site (McCarthy et al. 2007). Elevated $CO_2$ enhanced pine leaf area by 16%, on average, compared to ambient trees since canopy closure in 1999 (in 2002, the average increase was 14.5%; McCarthy et al. 2007). Our data provides further evidence that the increase in canopy leaf area is partially due to increased needle growth under elevated $CO_2$ (pers. obs., Rogers and Ellsworth 2002, McCarthy et al. 2007).

### *Increased carbohydrate respiration in both age classes*

The carbon oxidation metabolic group as a whole had the lowest difference in percentage of differentially expressed genes between the two age classes (Table 1). Likewise, the patterns of expression across the different categories were also similar between the two cohorts of needles. The overall predominance of upregulation of genes in the main respiratory pathway (glycolysis, TCA, and oxidative phosphorylation) in

both age classes lends further evidence to an increase in carbohydrate utilization as suggested by the results in the carbon partitioning group described earlier (Table 2). This increase in gene expression among respiration pathways across age classes was not mirrored by transcript levels involved in ATP synthesis. In fact, ATP synthesis showed the largest difference in number of differentially expressed genes across age classes; however this may simply reflect the combination of an average low percentage of differential expression among one-year-old needles and the disparity in sample size between the groups of carbon oxidation and ATP synthesis genes (Table 2).

Photorespiration was included in this group because of its participation in the release of $CO_2$. However, unlike the other pathways, photorespiration does not consume carbohydrates generated by photosynthesis. Photorespiration is a consequence of the oxygenation capacity of rubisco, and competes directly with photosynthesis for the substrate ribulose-biphosphate (RuBP). The general trend of decreased gene expression in this pathway is consistent with the biochemical-based expectations of negative effects of elevated $CO_2$ on the oxygenation capacity of rubisco (e.g., Ehleringer et al. 1991). Theoretical models predict an increase in the efficiency of photosynthesis relative to photorespiration with increasing $CO_2$ concentrations, and our data strongly support such predictions.

In contrast to clear expectations for photorespiration, the effects of elevated $CO_2$ on leaf dark respiration are less clear (Davey et al. 2004, Gonzalez-Meler and Taneva 2005). The high percentage of upregulation among respiratory genes in both cohorts of needles

in our study implies a potential for higher foliar respiration rates under elevated $CO_2$ throughout the needles' lifespan. Leaf respiration rates measured in the third year of the FACE experiment were similar across $CO_2$ concentrations (Hamilton 2001). However, after five years of exposure to elevated $CO_2$, mass-based leaf respiration of one-year-old needles was higher under elevated $CO_2$ compared to ambient $CO_2$ (Davey et al. 2004). No foliar respiration values were reported for current-year needles, but our data suggests that the same trend (of potentially higher magnitude) would be observed in the younger needles. Similarly, transcripts coding for respiratory enzymes were consistently upregulated in both growing and mature leaves of soybean plants exposed to long-term elevated $CO_2$ in the field (Ainsworth et al. 2006).

Overall, a sustained age-independent increase in leaf respiration rates under elevated $CO_2$, accompanied by the increase in canopy leaf area (McCarthy et al. 2007) and reduced photosynthetic rates in one-year-old compared to current-year needles (Crous and Ellsworth 2004), could decrease the carbon sink capacity of this pine forest under higher levels of atmospheric $CO_2$

Table 4.1 – Total number and functional distribution of the carbon metabolism transcripts analyzed. Listed from left to right are the broad carbon metabolism groups specified in this study (1-4), the individual pathways (categories) included in each group, and the genes assigned to each category. The last column indicates the number of gene transcripts analyzed in each hierarchical division.

| Group | Category | Gene annotation | Transcripts (#) |
|---|---|---|---|
| **1 - CARBON ASSIMILATION** | | | **96** |
| | **CALVIN CYCLE** | | **29** |
| | | Aldolase | 2 |
| | | Fructose bisphosphate aldolase | 6 |
| | | Glyceraldehyde-3-phosphate dehydrogenase | 4 |
| | | Phosphoglycerate kinase | 2 |
| | | Ribose 5-phosphate isomerase | 6 |
| | | Ribulose-5-phosphate-3-epimerase | 5 |
| | | Transketolase | 4 |
| | **CHAPERONINS 60** | | **7** |
| | | Chaperonin 60 | 7 |
| | **LIGHT-HARVESTING** | | **8** |
| | | Cab | 4 |
| | | Photosystem II cab | 4 |
| | **PHOTOSYNTHETIC ELECTRON TRANSPORT (PET)** | | **8** |
| | | [QR] Iron/ascorbate family oxidoreductase | 2 |
| | | Cupredoxin | 1 |

| Group | Category | Gene annotation | Transcripts (#) |
|---|---|---|---|
| | | Cytochrome B6-F complex | 1 |
| | | Ferredoxin | 2 |
| | | Quinone oxidoreductase | 1 |
| | | S-adenosylmethionine:2-demethylmenaquinone methyltransferase | 1 |
| | **PIGMENTS** | | **7** |
| | | Aminolevulinate dehydratase | 1 |
| | | Coproporphyrinogen III oxidase | 1 |
| | | Glutamate-1-semialdehyde aminotransferase | 1 |
| | | Glutamyl tRNA reductase | 1 |
| | | Phytoene synthase | 1 |
| | | Prenyl transferase | 1 |
| | | Zeta-carotene desaturase | 1 |
| | **PHOTOSYSTEM I (PS I)** | | **4** |
| | | Photosystem I subunit | 4 |
| | **PHOTOSYSTEM II (PS II)** | | **9** |
| | | Photosystem II subunit | 5 |
| | | PS II OEC | 4 |
| | **RUBISCO** | | **5** |
| | | Rbc, ss | 5 |
| **2 – CARBON PARTITIONING** | | | **81** |

| Group | Category | Gene annotation | Transcripts (#) |
|---|---|---|---|
| | **STARCH DEGRADATION** | | **14** |
| | | Alpha-amylase | 4 |
| | | Beta-amylase | 10 |
| | **STARCH SYNTHESIS** | | **7** |
| | | ADP-glucose pyrophosphorylase | 3 |
| | | Starch synthase | 4 |
| | **SUCROSE DEGRADATION** | | **29** |
| | | Fructokinase | 12 |
| | | Hexokinase | 2 |
| | | Susy | 13 |
| | | UDP-glucose pyrophosphorylase | 2 |
| | **SUCROSE SYNTHESIS** | | **4** |
| | | SPS | 2 |
| | | UDP-glucose pyrophosphorylase | 2 |
| | **SUGAR TRANSPORTERS** | | **27** |
| | | Glucose-6-phosphate/phosphate translocator | 4 |
| | | Hexose transporter | 7 |
| | | Sugar transporter | 16 |
| **3 – CARBON OXIDATION** | | | **191** |

| Group | Category | Gene annotation | Transcripts (#) |
|---|---|---|---|
| | **PHOTORESPIRATION** | | **19** |
| | | Glycine decarboxylase | 3 |
| | | Glycolate oxidase | 1 |
| | | Hydroxymethyltransferase | 12 |
| | | Hydroxypyruvate reductase | 1 |
| | | Phosphoglycerate kinase | 2 |
| | **FERMENTATION** | | **32** |
| | | Alcohol dehydrogenase | 24 |
| | | Lactate dehydrogenase (LDH1) | 1 |
| | | Pyruvate decarboxylase | 7 |
| | **GLYCOLYSIS/GLUCONEOGENESIS** | | **50** |
| | | Aldolase | 2 |
| | | Enolase | 5 |
| | | Fructose 1,6-bisphosphatase | 2 |
| | | Fructose bisphosphate aldolase | 6 |
| | | Glucose-6-phosphate isomerase | 4 |
| | | Glyceraldehyde-3-phosphate dehydrogenase | 8 |
| | | Phosphoenolpyruvate carboxylase | 3 |
| | | Phosphoenolpyruvate carboxylase kinase | 3 |
| | | Phosphofructokinase | 5 |
| | | Phosphoglycerate mutase | 2 |
| | | Pyruvate kinase | 10 |

| Group | Category | Gene annotation | Transcripts (#) |
|---|---|---|---|
| | **OXIDATIVE PENTOSE PHOSPHATE PATHWAY (OPPP)** | | **30** |
| | | 6-phosphogluconate dehydrogenase | 10 |
| | | Glucose-6-phosphate dehydrogenase | 4 |
| | | Ribose 5-phosphate isomerase | 6 |
| | | Ribulose-5-phosphate-3-epimerase | 5 |
| | | Transaldolase | 1 |
| | | Transketolase | 4 |
| | **OXIDATIVE PHOSPHORYLATION** | | **34** |
| | | Cytochrome c | 4 |
| | | Cytochrome C oxidase assembly protein | 12 |
| | | NADH:ubiquinone oxidoreductase | 6 |
| | | Ubiquinol--cytochrome-c reductase | 12 |
| | **MITOCHONDRIAL TRANSPORTERS** | | **9** |
| | | 2-oxoglutarate/malate translocator | 3 |
| | | Phosphate/phosphoenolpyruvate translocator | 6 |
| | **CITRIC ACID CYCLE (TCA)** | | **36** |
| | | 2-oxoglutarate dehydrogenase | 4 |
| | | Citrate synthase | 5 |
| | | Isocitrate dehydrogenase | 4 |
| | | Malate dehydrogenase | 4 |
| | | Pyruvate dehydrogenase | 7 |
| | | Succinate dehydrogenase | 7 |

| Group | Category | Gene annotation | Transcripts (#) |
|---|---|---|---|
| | | Succinyl-CoA-ligase | 5 |
| **4 – ATP SYNTHESIS** | | | **22** |
| | GENERAL | | **8** |
| | | ATP synthase | 2 |
| | | ATP synthase chain 9 | 2 |
| | | ATPase | 1 |
| | | ATP synthase (mitochondrial) | 1 |
| | | Pseudogene ATP synthase C | 2 |
| | MITOCHONDRIAL | | **6** |
| | | Mitochondrial ATP synthase | 2 |
| | | Mitochondrial ATPase | 4 |
| | VACUOLAR | | **8** |
| | | Pseudogene ATP synthase C | 1 |
| | | Vacuolar ATP synthase | 7 |
| **Grand Total** | | | **390** |

Table 4.2 – Number of differential expression counts (upregulated and downregulated) in each foliage age class and both classes combined. Percentages were calculated relative to the total counts in each metabolic group (n=gene transcripts x 3 sampling dates).

| *Metabolic groups* | *Age class (needle cohorts)* | | ***Both classes*** | ***Ratio (Current/Old)*** |
|---|---|---|---|---|
| | ***Current year*** | ***One-year-old*** | | |
| **Group 1: Carbon assimilation** (n=230)[1] | 63 (27.4%) | 8 (3.5%) | 15.5% | 7.9 |
| Upregulation | 46 (20.0%) | 4 (1.7%) | 10.9% | 11.5 |
| Downregulation | 17 (7.4%) | 4 (1.7%) | 4.6% | 4.3 |
| **Group 2: Carbon partitioning** (n=243) | 67 (27.6%) | 8 (3.3%) | 15.4% | 8.4 |
| Upregulation | 57 (23.5%) | 7 (2.9%) | 13.2% | 8.1 |
| Downregulation | 10 (4.1%) | 1 (0.4%) | 2.3% | 10.0 |
| **Group 3: Carbon oxidation** (n=630) | 164 (26.0%) | 27 (4.3%) | 15.2% | 6.1 |
| Upregulation | 124 (19.7%) | 21 (3.3%) | 11.5% | 5.9 |
| Downregulation | 40 (6.3%) | 6 (1.0%) | 3.7% | 6.7 |
| **Group 4: ATP synthesis** (n=66) | 20 (30.3%) | 2 (3.0%) | 16.7% | 10.0 |
| Upregulation | 18 (27.3%) | 1 (1.5%) | 14.4% | 18.0 |
| Downregulation | 2 (3.0%) | 1 (1.5%) | 2.3% | 2.0 |
| **All** (n=1169)[2] | 314 (26.9%) | 45 (3.9%) | 15.4% | 7.0 |
| Upregulation | 245 (21.0%) | 33 (2.8%) | 11.9% | 7.4 |
| Downregulation | 69 (5.9%) | 12 (1.0%) | 3.5% | 5.8 |

[1] In one-year-old needles, group 1 had only 229 counts

[2] Only 1168 available in one-year-old needles. See footnote 1.

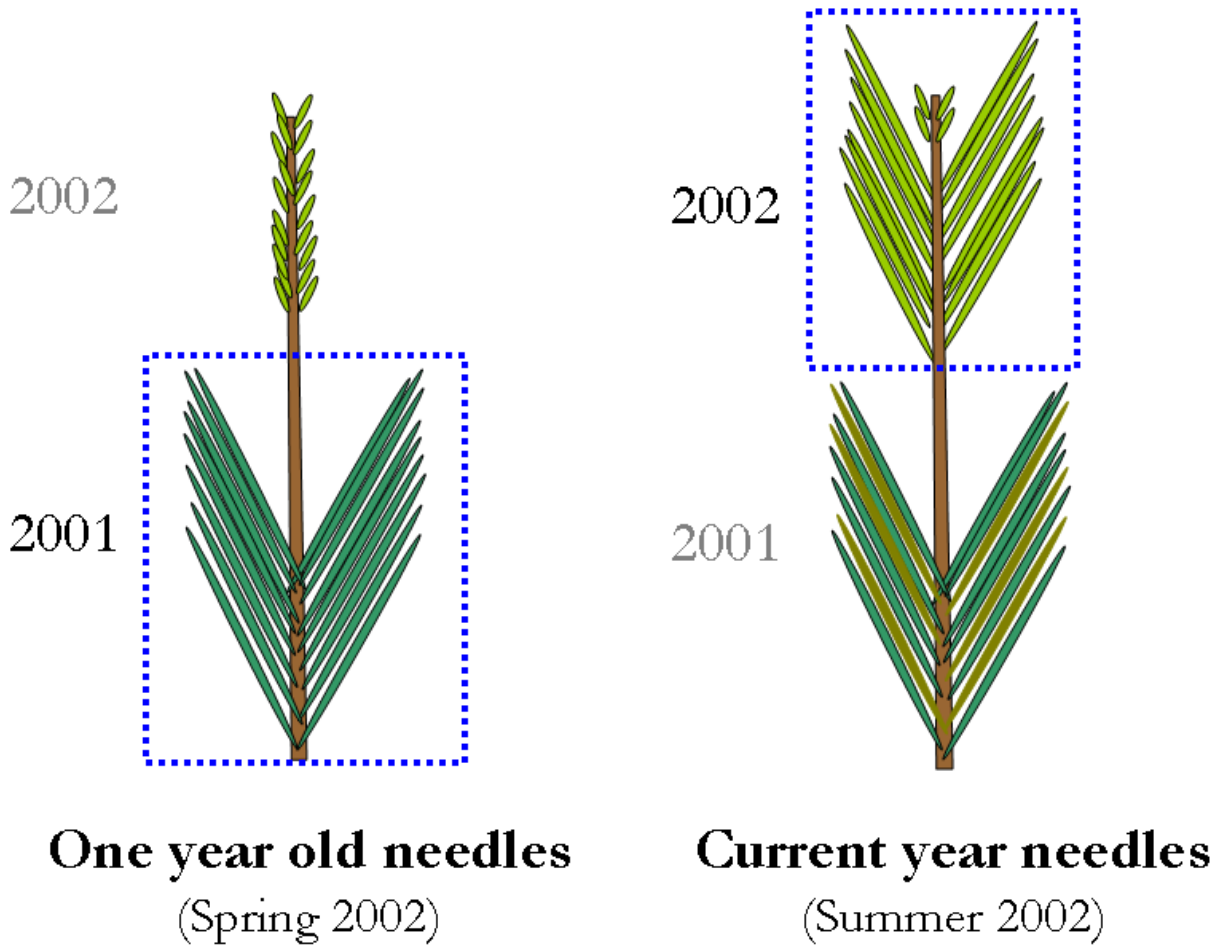


Figure 4.1 – Diagram of sampling scheme indicating the two cohorts of pine needles and their corresponding sampling time.

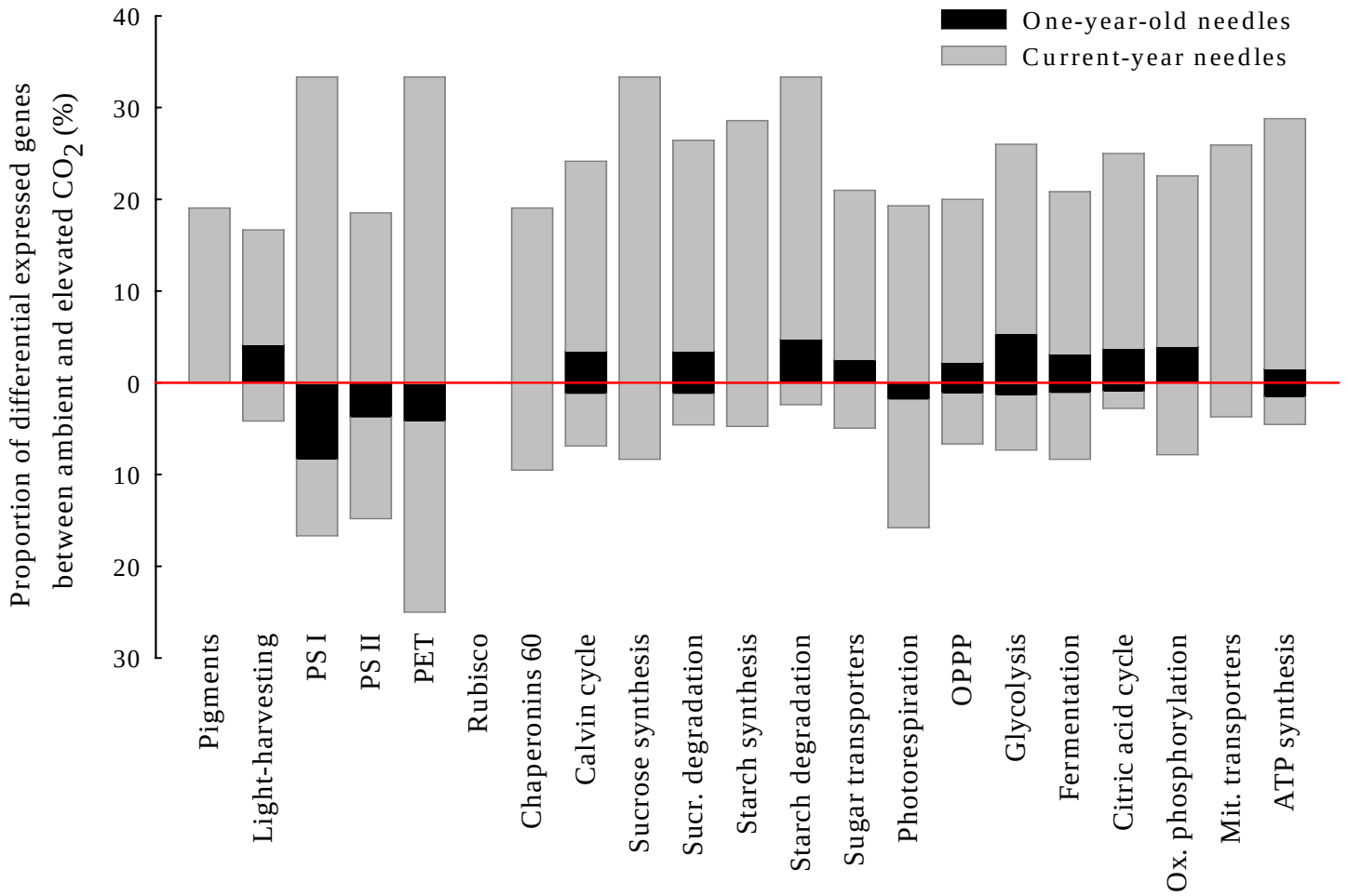


Figure 4.2 – Proportion of genes differentially expressed in two cohorts of pine needles. The proportion of upregulated genes for each category is plotted above the zero-line on the y-axis and the corresponding proportion of downregulated genes is plotted below the zero line of the same axis for direct comparison within categories.

# Chapter 5: Concluding remarks

The work done in the context of this dissertation encompassed multifaceted questions, interdisciplinary methods, and cross-scaling interpretation. Overall it gives a step further in our current understanding of how plants respond, acclimate, and adapt to their environment and contributes towards increasing the predictive power in models of vegetation response to global environmental change.

The results of the cross-comparison analysis in Chapter 2 provide evidence of a trade-off between increased root resistance to cavitation and leaf carbon uptake, suggesting functional coordination of traits at the whole plant-level which may reflect an adaptive response to the environment, in particular to drought conditions. Interestingly, some of the results in this chapter suggest that vulnerability to xylem cavitation in roots might be a fairly plastic trait responding to short-term changes in soil moisture conditions. In Chapter 3, I examine plasticity in plant traits at the molecular level and I identify candidate genes that may be particularly relevant in the response, and potential acclimation, of trees to elevated $CO_2$. In this chapter, I also show that the effects of elevated $CO_2$ on gene expression are clearly influenced by other abiotic factors, such as temperature and soil water availability. I had the opportunity to explore the interaction between a severe drought and elevated $CO_2$ which allowed me to investigate different processes involved in the response of trees to drought. In the short-term, elevated $CO_2$ seems to ameliorate the effects of drought in loblolly pine despite the

relative lack of stomatal response to elevated $CO_2$ in this species. My results suggest that enhanced availability of photoassimilates might allow trees under elevated $CO_2$ to allocate extra metabolic resources towards mechanisms of tolerance to drought, such as the induction of small heat-shock-proteins. An unexpected but extremely exciting finding was the evidence for co-regulation of genes involved in carbon and nitrogen metabolism which is extremely relevant and connected to changes observed in the nitrogen cycle at this FACE site. The results of Chapter 4 provide strong evidence for the role of carbon metabolism in the response of pine trees to elevated $CO_2$ and also suggest that foliage age should be accounted for in models of the response of vegetation to rising $CO_2$, especially in evergreen temperate forests. In this chapter as well, the most important findings are those that provide mechanistic evidence to patterns observed at the leaf to canopy scales – for instance, differences in leaf-level gas exchange between cohorts of needles and the overall increase in canopy leaf area under elevated $CO_2$.

Besides advancing our knowledge about the acclimation potential of pine trees to future scenarios of environmental change, the large data set that was generated by this work should prove useful in inciting new questions and research avenues. Additional exploration of these data through different perspectives is, in my opinion, a possibility that should still reveal important information in the context of plant physiology under elevated $CO_2$. For instance, I believe that exploring natural environmental gradients in other abiotic factors at the FACE site (soil nitrogen and soil moisture) may provide

important clues about fine-scale processes such as the gene expression response to elevated $CO_2$. Moreover, the combination of gene expression evidence with that from other techniques such as QTL analyses, protein and enzymatic essays, measurements of aminoacids and carbohydrates levels, would allow a more robust testing of the some of the mechanisms suggested by these data.

Above all, this dissertation reflects a genuine effort to break communication barriers across fields and to pool together concepts, ideas, and methodologies that can enhance our understanding of the natural world and provide us with the tools to examine it in a comprehensive fashion. I cannot emphasize enough how much we can learn from each other in different fields and how many answers are already out there if only we allow ourselves to bridge the gap.

# Appendices

Appendix B – List of pine cDNA clones and corresponding annotatins grouped by functional category.

| Category | Pine clone name | Annotation |
|---|---|---|
| **CARBON METABOLISM** | 17H3 | putative aldolase |
| | 19F8 | alcohol dehydrogenase-like protein |
| | 1A11 | acyl-CoA oxidase |
| | 20A2 | diacylglycerol pyrophosphate phosphatase, putative |
| | 20B5 | putative beta-amylase |
| | 22D6 | glyceraldehyde-3-phosphate dehydrogenase, putative |
| | 3B2 | UDP-glucose:sterol glucosyltransferase |
| | NXCI_002_F05 | succinyl-CoA ligase beta subunit |
| | NXCI_002_F10 | lipase, putative |
| | NXCI_002_H12 | fructokinase, putative |
| | NXCI_005_H01 | mevalonate diphosphate decarboxylase |
| | NXCI_006_F05 | putative hexose transporter |
| | NXCI_006_H01 | allyl alcohol dehydrogenase, putative |
| | NXCI_008_A07 | putative CDP-diacylglycerol synthetase |
| | NXCI_009_F04 | putative acetyl-CoA acyltransferase |
| | NXCI_009_F11 | pyruvate kinase, plastid isozyme, putative |
| | NXCI_012_A09 | putative malate dehydrogenase |
| | NXCI_018_C02 | acetyl-CoA carboxylase, putative |
| | NXCI_018_D02 | lipase, putative |
| | NXCI_018_D09 | 6-phosphogluconate dehydrogenase |
| | NXCI_019_A12 | delta-8 sphingolipid desaturase |
| | NXCI_020_C07 | 6-phosphogluconate dehydrogenase, putative |
| | NXCI_020_H12 | putative phospholipase C |
| | NXCI_022_C09 | transketolase - like protein |
| | NXCI_022_E12 | 6-phosphogluconate dehydrogenase |
| | NXCI_022_F10 | enoyl CoA hydratase-like protein |

| Category | Pine clone name | Annotation |
|---|---|---|
| | NXCI_022_H06 | allyl alcohol dehydrogenase, putative |
| | NXCI_026_G09 | fructose bisphosphate aldolase - like protein |
| | NXCI_026_H12 | glyceraldehyde-3-phosphate dehydrogenase, putative |
| | NXCI_028_D09 | pyruvate dehydrogenase e1 alpha subunit, putative |
| | NXCI_033_C04 | allyl alcohol dehydrogenase-like protein |
| | NXCI_033_F03 | putative cytochrome P450 |
| | NXCI_033_F08 | fatty acid multifunctional protein (AtMFP2) |
| | NXCI_034_B04 | putative phosphofructokinase beta subunit |
| | NXCI_038_H02 | alcohol dehydrogenase |
| | NXCI_038_H12 | sucrose synthase |
| | NXCI_042_F07 | putative citrate synthase |
| | NXCI_044_D12 | lysophospholipase isolog |
| | NXCI_048_B01 | phospholipase D |
| | NXCI_050_F07 | glucose 6 phosphate/phosphate translocator-like protein |
| | NXCI_054_E03 | ATP citrate-lyase, putative |
| | NXCI_054_E11 | glycosyl hydrolase family 3 |
| | NXCI_056_F06 | enoyl-CoA-hydratase - like protein |
| | NXCI_056_G12 | putative lipase |
| | NXCI_057_H12 | acyltransferase-like protein |
| | NXCI_061_A06 | desaturase/cytochrome b5 protein |
| | NXCI_061_A08 | enoyl-CoA hydratase like protein |
| | NXCI_066_A12 | glucose-6-phosphate isomerase |
| | NXCI_066_G08 | 3-ketoacyl-CoA thiolase |
| | NXCI_066_H04 | acetyl-CoA C-acetyltransferase |
| | NXCI_067_H03 | putative UDP-glucose glucosyltransferase |
| | NXCI_069_F07 | phosphoenolpyruvate carboxylase (PPC) |
| | NXCI_069_H04 | ATP citrate-lyase, putative |

| Category | Pine clone name | Annotation |
|---|---|---|
| | NXCI_071_A06 | acetyl-CoA carboxylase, putative |
| | NXCI_075_E04 | lipase, putative |
| | NXCI_076_D06 | putative lipase |
| | NXCI_076_D08 | ATP citrate-lyase, putative |
| | NXCI_076_F03 | fatty acid hydroxylase (FAH1) |
| | NXCI_083_E07 | NADP-isocitrate dehydrogenase, putative |
| | NXCI_084_G02 | alcohol dehydrogenase |
| | NXCI_084_H02 | fructose bisphosphate aldolase - like protein |
| | NXCI_086_B04 | ATP citrate-lyase, putative |
| | NXCI_093_E06 | putative ribose 5-phosphate isomerase |
| | NXCI_093_F11 | hexose transporter - like protein |
| | NXCI_093_H10 | 6-phosphogluconate dehydrogenase |
| | NXCI_094_G02 | lactoylglutathione lyase, putative |
| | NXCI_094_G12 | phospholipase - like protein |
| | NXCI_095_G01 | putative 3-hydroxyisobutyryl-coenzyme A hydrolase |
| | NXCI_096_D07 | pyruvate dehydrogenase E1 component beta subunit, mitochondrial precursor |
| | NXCI_096_E08 | 3-ketoacyl-CoA thiolase |
| | NXCI_096_G01 | allyl alcohol dehydrogenase-like protein |
| | NXCI_097_D12 | alcohol dehydrogenase (EC 1.1.1.1) class III |
| | NXCI_097_G04 | hexose transporter - like protein |
| | NXCI_098_B08 | biotin carboxyl carrier protein of acetyl-CoA carboxylase precursor (BCCP) (spQ42533) |
| | NXCI_098_D10 | putative cytochrome P450 |
| | NXCI_101_E05 | lipase/hydrolase, putative |
| | NXCI_102_E12 | hexokinase - like protein |
| | NXCI_103_C06 | 6-phosphogluconate dehydrogenase, putative |
| | NXCI_106_A01 | glucose-6-phosphate isomerase |
| | NXCI_106_A03 | putative lipase |

| Category | Pine clone name | Annotation |
|---|---|---|
| | NXCI_106_B08 | 2-oxoglutarate dehydrogenase, E1 subunit - like protein |
| | NXCI_115_A02 | phosphoglycerate kinase, putative |
| | NXCI_121_F10 | NADP-isocitrate dehydrogenase, putative |
| | NXCI_122_A09 | enolase (2-phospho-D-glycerate hydroylase) |
| | NXCI_122_B08 | enoyl-ACP reductase (enr-A) |
| | NXCI_122_H07 | putative lipase |
| | NXCI_123_A10 | putative pyrophosphate-dependent phosphofructokinase alpha subunit |
| | NXCI_123_F01 | alcohol dehydrogenase |
| | NXCI_124_C01 | Diphosphomevalonate decarboxylase - like protein |
| | NXCI_124_F06 | phosphate/phosphoenolpyruvate translocator - like protein |
| | NXCI_128_C06 | sucrose synthase, putative |
| | NXCI_130_D10 | hydroxyacylglutathione hydrolase cytoplasmic (glyoxalase II) (GLX II) |
| | NXCI_133_E10 | S-adenosyl-methionine-sterol-C-methyltransferase, putative |
| | NXCI_141_F06 | lipase, putative |
| | NXCI_144_B08 | chloroplast omega-6 fatty acid desaturase (fad6) |
| | NXCI_144_G08 | hexose transporter, putative |
| | NXCI_150_E08 | pyruvate dehydrogenase E1 alpha subunit |
| | NXCI_150_G05 | sugar transporter - like protein |
| | NXCI_151_C08 | S-adenosyl-methionine-sterol-C-methyltransferase, putative |
| | NXCI_151_G07 | putative UDP-glucose glucosyltransferase |
| | NXCI_153_B03 | ATP citrate-lyase, putative |
| | NXCI_154_B09 | beta-amylase-like |
| | NXCI_154_D09 | lipase, putative |
| | NXCI_155_G06 | phospholipase - like protein |
| | NXCI_156_H12 | putative NADP-dependent glyceraldehyde-3-phosphate dehydrogenase |
| | NXCI_157_A02 | 6-phosphogluconate dehydrogenase, putative |
| | NXCI_162_C01 | putative sugar transporter protein |

| Category | Pine clone name | Annotation |
|---|---|---|
| | NXCI_163_C01 | citrate synthase |
| | NXCI_164_F04 | putative pyruvate kinase |
| | NXCI_165_A01 | glucose-6-phosphate isomerase, cytosolic (GPI) |
| | NXLV_009_E01 | putative pyruvate dehydrogenase E1 beta subunit |
| | NXLV_010_G03 | pyruvate decarboxylase-like protein |
| | NXLV_023_E08 | putative beta-amylase |
| | NXLV_030_C10 | ATP citrate lyase, putative |
| | NXLV_031_E04 | enolase (2-phospho-D-glycerate hydroylase) |
| | NXLV_031_G06 | glyceraldehyde-3-phosphate dehydrogenase, putative |
| | NXLV_032_A05 | phosphoenolpyruvate carboxylase kinase, putative |
| | NXLV_032_E02 | lipase, putative |
| | NXLV_034_A04 | mitochondrial NAD-dependent malate dehydrogenase |
| | NXLV_036_B12 | 3-ketoacyl-acyl carrier protein synthase III (KAS III) |
| | NXLV_036_E06 | putative alpha-amylase |
| | NXLV_036_H12 | putative UDP-glucose glucosyltransferase |
| | NXLV_042_D03 | putative phospholipase D |
| | NXLV_044_D06 | putative lipase |
| | NXLV_045_B12 | pyruvate kinase -like protein |
| | NXLV_046_H01 | phospholipase D alpha, putative |
| | NXLV_048_D06 | phosphoglycerate mutase, putative |
| | NXLV_051_G05 | cytoplasmic aconitate hydratase |
| | NXLV_053_D10 | putative lipoxygenase |
| | NXLV_053_F04 | short chain alcohol dehydrogenase-like |
| | NXLV_053_H11 | cytoplasmatic aconitate hydratase (citrate hydro-lyase)(aconitase)(EC 4.2.1.3) |
| | NXLV_057_B05 | biotin carboxyl carrier protein of acetyl-CoA carboxylase precursor (BCCP) (spQ42533) |
| | NXLV_064_D09 | ATP citrate lyase |
| | NXLV_064_G07 | alcohol dehydrogenase ADH, putative |

| Category | Pine clone name | Annotation |
|---|---|---|
| | NXLV_066_D12 | fructose-bisphosphate aldolase - like protein |
| | NXLV_066_E11 | putative lipase |
| | NXLV_067_B11 | putative pyruvate dehydrogenase kinase |
| | NXLV_068_B03 | putative lysophospholipase |
| | NXLV_068_D05 | allyl alcohol dehydrogenase, putative |
| | NXLV_068_G06 | soluble starch synthase |
| | NXLV_071_C06 | soluble starch synthase |
| | NXLV_071_E08 | putative short chain alcohol dehydrogenase |
| | NXLV085_C09 | putative UDP-glucose glucosyltransferase |
| | NXLV088_H07 | putative phosphate/phosphoenolpyruvate translocator |
| | NXLV090_G07 | phospholipase D1, putative |
| | NXLV102_F08 | sucrose synthase, putative |
| | NXLV103_E01 | putative gibberellin 3 beta-hydroxylase |
| | NXLV105_D05 | glyceraldehyde-3-phosphate dehydrogenase |
| | NXLV105_E08 | delta-8 sphingolipid desaturase |
| | NXLV105_G05 | 3-ketoacyl-acyl carrier protein synthase III (KAS III) |
| | NXLV108_A04 | phosphate/phosphoenolpyruvate translocator - like protein |
| | NXLV109_F08 | citrate synthase |
| | NXLV109_G06 | short chain alcohol dehydrogenase, putative |
| | NXLV109_H12 | enoyl-CoA-hydratase - like protein |
| | NXLV111_F11 | putative glyceraldehyde-3-phosphate dehydrogenase |
| | NXLV112_H04 | putative succinate dehydrogenase flavoprotein subunit |
| | NXLV114_A12 | putative beta-hydroxyacyl-ACP dehydratase |
| | NXLV114_E04 | alcohol dehydrogenase |
| | NXLV119_F11 | putative pyruvate kinase |
| | NXLV120_E09 | putative diacylglycerol kinase |
| | NXLV125_E11 | citrate synthase-like protein |

| Category | Pine clone name | Annotation |
|---|---|---|
| | NXLV126_C04 | stearoyl-ACP desaturase |
| | NXLV127_F02 | alcohol dehydrogenase, putative |
| | NXLV131_G07 | putative phospholipase D |
| | NXLV134_G06 | putative triacylglycerol lipase |
| | NXNV002G12 | putative phospholipase |
| | NXNV003E11 | 2-oxoglutarate/malate translocator precursor -like protein |
| | NXNV004D03 | putative D-ribulose-5-phosphate 3-epimerase |
| | NXNV004D05 | fructose-bisphosphate aldolase |
| | NXNV004F05 | phospholipase A2-like protein |
| | NXNV005B09 | sucrose synthase -like protein |
| | NXNV005C04 | putative phospholipase |
| | NXNV008C04 | phosphoinositide-specific phospholipase - like protein |
| | NXNV010B07 | putative fructose bisphosphate aldolase |
| | NXNV010D07 | phospholipase D |
| | NXNV015H06 | lipase, putative |
| | NXNV027F08 | sucrose synthase -like protein |
| | NXNV028B06 | hexose transporter, putative |
| | NXNV046A09 | putative phosphofructokinase beta subunit |
| | NXNV048A04 | enoyl-CoA hydratase |
| | NXNV060D05 | putative beta-ketoacyl-CoA synthase |
| | NXNV_066_D03 | pyruvate decarboxylase-like protein |
| | NXNV068F10 | stearoyl-acyl carrier protein desaturase |
| | NXNV_074_A06 | putative hydroxymethylglutaryl-CoA lyase |
| | NXNV_074_H11 | pyruvate dehydrogenase e1 alpha subunit, putative |
| | NXNV_075_A12 | putative ribose 5-phosphate isomerase |
| | NXNV_079_G08 | fructokinase, putative |
| | NXNV_081_B12 | putative beta-amylase |

| Category | Pine clone name | Annotation |
|---|---|---|
| | NXNV_086_D06 | putative glyoxysomal malate dehydrogenase precursor |
| | NXNV_100_B03 | alpha-amylase, putative |
| | NXNV_105_B10 | putative UDP-glucose pyrophosphorylase |
| | NXNV_120_A09 | putative trehalose-6-phosphate synthase |
| | NXNV_120_C02 | glycosyl hydrolase family 9 (endo-1,4-beta-glucanase) |
| | NXNV_120_H08 | phosphoenolpyruvate carboxylase kinase, putative |
| | NXNV_123_B01 | putative glyoxysomal malate dehydrogenase precursor |
| | NXNV_123_G08 | acetyl-CoA carboxylase, putative |
| | NXNV_124_D09 | beta-ketoacyl-CoA synthase like protein |
| | NXNV_125_G02 | putative 2,3-bisphosphoglycerate-independent phosphoglycerate mutase |
| | NXNV_126_C11 | alcohol dehydrogenase, putative |
| | NXNV_129_D03 | putative ADP-glucose pyrophosphorylase large subunit |
| | NXNV_131_B12 | family II extracellular lipase 5 (EXL5) |
| | NXNV_132_C06 | ATP citrate lyase |
| | NXNV_132_D12 | phosphoglycerate kinase, putative |
| | NXNV_132_H03 | putative sugar transporter |
| | NXNV_133_C08 | putative acetyl-CoA carboxylase biotin-containing subunit |
| | NXNV_139_B11 | putative beta-amylase |
| | NXNV_143_A08 | putative cytochrome P450 |
| | NXNV_143_C04 | phosphoenolpyruvate carboxykinase (ATP) -like protein |
| | NXNV_143_G05 | cytoplasmic malate dehydrogenase |
| | NXNV_147_F10 | 1-acylcerol-3-phosphate acyltransferase - like protein |
| | NXNV_150_D07 | putative D-3-phosphoglycerate dehydrogenase |
| | NXNV_155_D02 | putative diacylglycerol kinase |
| | NXNV_158_A08 | putative sugar transporter |
| | NXNV_159_E01 | glycosyl hydrolase family 36 |
| | NXNV_162_B11 | glyoxalase I, putative (lactoylglutathione lyase) |

| Category | Pine clone name | Annotation |
|---|---|---|
| | NXNV_164_G09 | putative ribose 5-phosphate isomerase |
| | NXNV_166_G08 | putative ketoacyl-CoA synthase |
| | NXNV_181_E07 | lipase -like protein |
| | NXNV_185_H06 | phosphoinositide-specific phospholipase - like protein |
| | NXNV_186_H12 | beta-amylase, putative |
| | NXNV_98_B06 | putative fatty acid desaturase |
| | NXPV_002_C05 | 6-phosphogluconate dehydrogenase |
| | NXPV_003_C06 | putative CDP-diacylglycerol--glycerol-3-phosphate 3-phosphatidyltransferase |
| | NXPV_003_F06 | terpene cyclase, putative |
| | NXPV_005_C12 | transaldolase - like protein |
| | NXPV_006_B05 | prenyltransferase, putative |
| | NXPV_007_C04 | trehalose-6-phosphate synthase, putative |
| | NXPV_007_G10 | pyruvate decarboxylase-1 (Pdc1) |
| | NXPV_008_B07 | putative pyruvate kinase |
| | NXPV_008_D01 | cytochrome P450, putative |
| | NXPV_008_G07 | terpene synthase-related protein, putative |
| | NXPV_009_E03 | putative fructokinase |
| | NXPV_010_A04 | pyruvate decarboxylase-1 (Pdc1) |
| | NXPV_010_C12 | alcohol dehydrogenase - like protein |
| | NXPV_011_A07 | starch synthase, putative |
| | NXPV_011_H07 | phospholipase D1, putative |
| | NXPV_012_B07 | trehalose-6-phosphate synthase, putative |
| | NXPV_013_H08 | enoyl-ACP reductase (enr-A) |
| | NXPV_014_G06 | ATP citrate-lyase, putative |
| | NXPV_015_C08 | putative glucose-6-phosphate dehydrogenase |
| | NXPV_021_E10 | glucose-6-phosphate/phosphate translocator |
| | NXPV_023_E06 | acetyl-CoA carboxylase, putative |

| Category | Pine clone name | Annotation |
|---|---|---|
| | NXPV_024_E10 | transketolase - like protein |
| | NXPV_026_C06 | lipoxygenase |
| | NXPV_038_C03 | glyceraldehyde-3-phosphate dehydrogenase, putative |
| | NXPV_038_D02 | fructokinase-like protein |
| | NXPV_038_F01 | glucose-6-phosphate/phosphate translocator |
| | NXPV_057_D04 | terpene synthase, putative |
| | NXPV_066_A04 | cytochrome P450-like protein |
| | NXPV_066_E05 | beta-amylase, putative |
| | NXPV_073_A06 | glucose-6-phosphate phosphate-translocator precursor, putative |
| | NXPV_077_E04 | fructokinase - like protein |
| | NXPV_082_G11 | putative zeta-carotene desaturase precursor |
| | NXPV_084_A05 | lipase, putative |
| | NXPV_086_H10 | putative transketolase precursor |
| | NXPV_087_F09 | lipase, putative |
| | NXPV_087_F12 | 2-oxoglutarate dehydrogenase E2 subunit |
| | NXPV_088_H01 | phospholipase D, putative |
| | NXPV_090_F02 | fructokinase, putative |
| | NXPV_090_H12 | putative CDP-diacylglycerol--glycerol-3-phosphate 3-phosphatidyltransferase |
| | NXPV_091_E05 | succinyl-CoA ligase beta subunit |
| | NXPV_094_H12 | putative cytochrome P450 |
| | NXPV_095_A10 | glucose-6-phosphate 1-dehydrogenase |
| | NXPV_095_D08 | pyruvate kinase, plastid isozyme, putative |
| | NXPV_097_H02 | GDSL-motif lipase/hydrolase-like protein |
| | NXPV_104_B11 | putative transketolase precursor |
| | NXPV_112_F02 | isocitrate dehydrogenase - like protein |
| | NXPV_113_A12 | putative fructokinase |
| | NXPV_113_B12 | lactate dehydrogenase (LDH1) |

| Category | Pine clone name | Annotation |
|---|---|---|
| | NXPV_113_E11 | putative cytochrome P450 |
| | NXPV_129_D03 | fructokinase, putative |
| | NXPV_133_B01 | cytochrome P450 - like protein |
| | NXPV_138_E03 | cytochrome P450 - like protein |
| | NXRV_003_F12 | glucose-6-phosphate 1-dehydrogenase |
| | NXRV_003_G10 | putative lipoxygenase |
| | NXRV_004_A09 | ribulose-5-phosphate-3-epimerase |
| | NXRV_004_F05 | putative phospholipase |
| | NXRV_005_G02 | isocitrate dehydrogenase, putative |
| | NXRV_005_H02 | lysophospholipase isolog |
| | NXRV_006_D10 | putative stearoyl-acyl carrier protein desaturase |
| | NXRV_007_D07 | putative enolase |
| | NXRV_008_A02 | succinyl-CoA ligase beta subunit |
| | NXRV_015_D05 | cytochrome P450 |
| | NXRV_016_B06 | putative beta-amylase |
| | NXRV_017_F04 | 6-phosphogluconate dehydrogenase, putative |
| | NXRV_022_H02 | putative sugar transporter |
| | NXRV_025_G02 | pyruvate kinase - like protein |
| | NXRV_026_A11 | lipase, putative |
| | NXRV_031_F07 | putative prenyl transferase (prephytoene pyrophosphatase dehydrogenase) |
| | NXRV_032_E03 | omega-6 fatty acid desaturase, endoplasmic reticulum (FAD2) |
| | NXRV_032_F07 | omega-3 fatty acid desaturase |
| | NXRV_034_D09 | putative pyruvate kinase |
| | NXRV_042_B02 | putative sterol-C5-desaturase |
| | NXRV045_B02 | short-chain alcohol dehydrogenase like protein |
| | NXRV047_F03 | cytochrome P450, putative |
| | NXRV048_G07 | 6-phosphogluconate dehydrogenase |

| Category | Pine clone name | Annotation |
|---|---|---|
| | NXRV053_E08 | acetyl-CoA carboxylase, putative |
| | NXRV055_H02 | fructokinase - like protein |
| | NXRV_057_C11 | sucrose synthase, putative |
| | NXRV058_E09 | fructokinase 1 |
| | NXRV059_A05 | trehalose-phosphatase, putative |
| | NXRV059_G05 | fructokinase-like protein |
| | NXSI_002_E05 | acyl-CoA oxidase ACX3, putative |
| | NXSI_003_B02 | triacylglycerol lipase like protein |
| | NXSI_003_E10 | putative stearoyl-acyl carrier protein desaturase |
| | NXSI_003_F04 | putative lipoxygenase |
| | NXSI_009_D11 | putative phosphoenolpyruvate carboxylase |
| | NXSI_011_E08 | putative cytochrome P450 |
| | NXSI_011_F10 | putative fatty acid desaturase/cytochrome b5 fusion protein |
| | NXSI_012_D10 | succinate dehydrogenase flavoprotein alpha subunit (emb |
| | NXSI_012_H11 | malate synthase -like protein |
| | NXSI_022_H04 | microbody NAD-dependent malate dehydrogenase |
| | NXSI_023_H11 | cytoplasmatic aconitate hydratase (citrate hydro-lyase)(aconitase)(EC 4.2.1.3) |
| | NXSI_025_A07 | ADP-glucose pyrophosphorylase, putative |
| | NXSI_025_H08 | ribulose-5-phosphate-3-epimerase |
| | NXSI_027_C05 | putative alcohol dehydrogenase |
| | NXSI_028_G06 | putative beta-amylase |
| | NXSI_029_D04 | lactoylglutathione lyase, putative |
| | NXSI_030_B09 | succinate dehydrogenase iron-protein subunit, putative |
| | NXSI_031_E04 | putative lipase/acylhydrolase |
| | NXSI_031_H03 | putative glucose acyltransferase |
| | NXSI_038_G11 | putative ribose 5-phosphate isomerase |
| | NXSI_039_D11 | 2-oxoglutarate dehydrogenase, E1 subunit - like protein |

| Category | Pine clone name | Annotation |
|---|---|---|
| | NXSI_040_E10 | lipase - like protein |
| | NXSI_040_H09 | 6-phosphogluconate dehydrogenase, putative |
| | NXSI_042_E10 | putative glucose acyltransferase |
| | NXSI_043_B03 | UDP-glucose pyrophosphorylase |
| | NXSI_043_C06 | lipase-like protein |
| | NXSI_045_E03 | putative phosphomannomutase |
| | NXSI_045_E10 | putative GDSL-motif lipase/hydrolase |
| | NXSI_046_G12 | stearoyl acyl carrier protein desaturase, putative |
| | NXSI_047_E01 | fructose-bisphosphate aldolase -like protein |
| | NXSI_048_B08 | lipase-like protein |
| | NXSI_049_B07 | acetyl-CoA carboxylase, putative |
| | NXSI_049_D11 | lipase, putative |
| | NXSI_049_E10 | putative pyruvate kinase |
| | NXSI_052_C02 | putative sugar transporter |
| | NXSI_052_F09 | putative succinate dehydrogenase flavoprotein subunit |
| | NXSI_054_B07 | cytochrome P450 homolog, putative |
| | NXSI_054_D04 | putative malate dehydrogenase |
| | NXSI_055_B01 | putative sugar transporter |
| | NXSI_055_F12 | fructokinase, putative |
| | NXSI_055_H03 | prenyltransferase, putative |
| | NXSI_056_A07 | alpha-amylase - like protein |
| | NXSI_058_F04 | putative trans-prenyltransferase |
| | NXSI_059_G07 | enoyl CoA hydratase-like protein |
| | NXSI_060_E04 | mitochondrial NAD-dependent malate dehydrogenase |
| | NXSI_066_G12 | enoyl-CoA hydratase like protein |
| | NXSI_067_D02 | putative lipase/acylhydrolase |
| | NXSI_068_G03 | pyruvate decarboxylase |

| Category | Pine clone name | Annotation |
|---|---|---|
| | NXSI_068_G08 | putative lipase |
| | NXSI_068_H06 | phosphate/phosphoenolpyruvate translocator precursor |
| | NXSI_068_H10 | lipase, putative |
| | NXSI_073_F12 | sugar transporter-like protein |
| | NXSI_075_E01 | lysophospholipase -like protein |
| | NXSI_076_C07 | putative phospholipase D-gamma |
| | NXSI_076_D02 | putative fatty acid desaturase/cytochrome b5 fusion protein |
| | NXSI_076_H06 | lipoxygenase AtLOX2 |
| | NXSI_079_A04 | sugar transporter-like protein |
| | NXSI_079_H11 | 3-ketoacyl-ACP synthase, putative |
| | NXSI_082_A04 | putative pyrophosphate-dependent phosphofructokinase alpha subunit |
| | NXSI_085_E06 | ADP-glucose pyrophosphorylase, putative |
| | NXSI_086_G05 | acetyl-CoA carboxylase, putative |
| | NXSI_087_B11 | putative sugar transporter |
| | NXSI_090_F12 | putative acyl-CoA : 1-acylglycerol-3-phosphate acyltransferase |
| | NXSI_091_D05 | fatty acid hydroxylase (FAH1) |
| | NXSI_094_B04 | putative sugar transporter protein |
| | NXSI_097_F06 | short-chain alcohol dehydrogenase like protein |
| | NXSI_098_F07 | pyruvate kinase - like protein |
| | NXSI_098_G04 | glyceraldehyde-3-phosphate dehydrogenase C subunit (GapC) |
| | NXSI_099_A02 | diacylglycerol kinase-like protein |
| | NXSI_099_F09 | sugar transporter-like protein |
| | NXSI_099_H06 | terpene synthase, putative |
| | NXSI_100_E02 | sugar transporter-like protein |
| | NXSI_100_H07 | putative UDP-glucose glucosyltransferase |
| | NXSI_102_G06 | succinate dehydrogenase iron-protein subunit -like |
| | NXSI_104_H08 | pyruvate decarboxylase (gb |

| Category | Pine clone name | Annotation |
|---|---|---|
| | NXSI_105_A10 | putative ribose 5-phosphate isomerase |
| | NXSI_105_C02 | alcohol dehydrogenase ADH, putative |
| | NXSI_105_D02 | 2-oxoglutarate dehydrogenase E2 subunit |
| | NXSI_105_E02 | 3-oxoacyl-[acyl-carrier-protein] synthase I |
| | NXSI_107_B07 | glucose-6-phosphate dehydrogenase |
| | NXSI_110_A02 | omega-6 fatty acid desaturase, endoplasmic reticulum (FAD2) |
| | NXSI_110_B04 | isocitrate dehydrogenase - like protein |
| | NXSI_110_D09 | dihydroxyacid dehydratase, putative |
| | NXSI_110_E09 | lipase, putative |
| | NXSI_112_F08 | lysophospholipase isolog, putative |
| | NXSI_112_F10 | putative GDSL-motif lipase/acylhydrolase |
| | NXSI_114_C01 | lysophospholipase isolog, putative |
| | NXSI_114_G08 | putative GDSL-motif lipase/hydrolase |
| | NXSI_115_D01 | alcohol dehydrogenase-like protein |
| | NXSI_116_A10 | putative CDP-diacylglycerol synthetase |
| | NXSI_116_B12 | 2-oxoglutarate/malate translocator |
| | NXSI_116_C09 | lipase -like protein |
| | NXSI_116_F02 | hexokinase (ATHXK2) |
| | NXSI_116_F10 | putative dTDP-glucose 4-6-dehydratase |
| | NXSI_116_H07 | 3-oxoacyl-[acyl-carrier-protein] synthase I precursor |
| | NXSI_135_F02 | Acyl CoA binding protein, putative |
| | NXSI_136_C07 | glycosyl hydrolase family 3 |
| | NXSI_139_A05 | putative ribose 5-phosphate isomerase |
| | NXSI_139_F06 | putative hexose transporter |
| | NXSI_139_G08 | putative sugar transporter |
| | NXSI_140_F09 | succinate dehydrogenase iron-protein subunit, putative |
| | NXSI_144_E08 | putative lipase |

| Category | Pine clone name | Annotation |
|---|---|---|
| | NXSI_144_F12 | putative lipase |
| | PC03B05 | putative short chain alcohol dehydrogenase |
| | PC06A05 | microbody NAD-dependent malate dehydrogenase |
| | PC06B09 | putative GDSL-motif lipase/acylhydrolase |
| | PC07A09 | GDSL-motif lipase/hydrolase-like protein |
| | PC09E08 | family II extracellular lipase 5 (EXL5) |
| | PC11B12 | alpha-amylase, putative |
| | PC13H06 | enoyl-ACP reductase (enr-A) |
| | PC14E11 | ATP citrate-lyase, putative |
| | PC15D04 | putative lipase |
| | PC18B11 | pyruvate dehydrogenase E1 alpha subunit |
| | PC18H01 | sugar transporter-like protein |
| | PC19C08 | putative phosphate/phosphoenolpyruvate translocator protein |
| | PC22A07 | succinyl-CoA-ligase alpha subunit |
| | PC22A08 | beta-ketoacyl-ACP reductase - like protein |
| | PC22G10 | beta-ketoacyl-CoA synthase like protein |
| | PC23B09 | putative phospholipase C |
| | PC23D10 | beta-ketoacyl-ACP reductase - like protein |
| | ST02B02 | fructose 1,6-bisphosphatase, putative |
| | ST03D04 | putative D-ribulose-5-phosphate 3-epimerase |
| | ST04A02 | oxoglutarate/malate translocator-like protein |
| | ST04D02 | isocitrate dehydrogenase, putative |
| | ST06B11 | putative GDSL-motif lipase/hydrolase |
| | ST07E05 | putative aldolase |
| | ST07G04 | short chain alcohol dehydrogenase-like |
| | ST08B02 | acetyl-CoA carboxylase, putative |
| | ST08F03 | sucrose synthase-like protein |

| Category | Pine clone name | Annotation |
|---|---|---|
| | ST11H08 | fructose 1,6-bisphosphatase, putative |
| | ST13E07 | putative beta-amylase |
| | ST15C09 | pyruvate decarboxylase-like protein |
| | ST16E03 | GDSL-motif lipase/hydrolase-like protein |
| | ST16H01 | putative GDSL-motif lipase/acylhydrolase |
| | ST16H04 | beta-ketoacyl-CoA synthase (FIDDLEHEAD) |
| | ST17E03 | starch synthase, putative |
| | ST18B10 | putative glyceraldehyde-3-phosphate dehydrogenase |
| | ST18G12 | putative NADP-dependent glyceraldehyde-3-phosphate dehydrogenase |
| | ST19F11 | putative lipase/acylhydrolase |
| | ST19H05 | alcohol dehydrogenase like protein |
| | ST20F09 | putative citrate synthase |
| | ST20F10 | ribulose-5-phosphate-3-epimerase |
| | ST20G11 | sucrose synthase |
| | ST21A06 | UDPglucose 4-epimerase - like protein |
| | ST21C06 | putative lipase |
| | ST21E04 | glyceraldehyde-3-phosphate dehydrogenase, putative |
| | ST21H10 | NADP-dependent malate dehydrogenase |
| | ST21H11 | phytoene synthase (gbAAB65697.1) |
| | ST22B11 | ATP citrate-lyase, putative |
| | ST22E12 | putative sugar transporter |
| | ST22H07 | lysophospholipase -like protein |
| | ST22H11 | diacylglycerol kinase (ATDGK1) |
| | ST26C12 | sucrose phosphate synthase 2 udp glucose fructose glucosyltransferase |
| | ST27G04 | putative lipoxygenase |
| | ST28H10 | terpene synthase-related protein |
| | ST29A01 | lipoxygenase AtLOX2 |

| Category | Pine clone name | Annotation |
|---|---|---|
| | ST29F08 | succinyl-CoA-ligase alpha subunit |
| | ST29G06 | lipase |
| | ST29H03 | putative GDSL-motif lipase/hydrolase |
| | ST30C02 | putative phosphoenolpyruvate carboxylase |
| | ST31D08 | putative hexose transporter |
| | ST32A05 | putative pyrophosphate-dependent phosphofructokinase alpha subunit |
| | ST33B07 | putative GDSL-motif lipase hydrolase |
| | ST35H05 | family II extracellular lipase 2 (EXL2) |
| | ST36B03 | putative phosphate/phosphoenolpyruvate translocator protein |
| | ST36G08 | putative enolase (2-phospho-D-glycerate hydroylase) |
| | ST37B12 | glucose-6-phosphate isomerase, cytosolic (GPI) |
| | ST38B04 | enolase (2-phospho-D-glycerate hydroylase) |
| | ST39D06 | succinate dehydrogenase iron-protein subunit -like |
| | ST39E04 | terpene synthase, putative |
| **CELL MEMBRANES** | 18B8 | plasma membrane intrinsic protein 1c, putative |
| | 1D3 | putative phosphatidylinositol/phosphatidylcholine transfer protein |
| | 20H4 | plasma membrane associated protein, putative |
| | 2H7 | amino acid permease-like protein; proline transporter-like protein |
| | NXCI_006_B12 | transport protein particle component Bet3p-like protein |
| | NXCI_006_F05 | putative hexose transporter |
| | NXCI_008_H11 | putative integral membrane protein |
| | NXCI_017_F02 | transport protein subunit - like |
| | NXCI_019_A12 | delta-8 sphingolipid desaturase |
| | NXCI_020_H04 | aquaporin, putative |
| | NXCI_023_B05 | multispanning membrane protein, putative |
| | NXCI_025_G12 | vacuolar H(+)-ATPase subunit-like protein |
| | NXCI_026_E09 | oligopeptide transporter - like protein |

| Category | Pine clone name | Annotation |
|---|---|---|
| | NXCI_026_G07 | putative coated vesicle membrane protein |
| | NXCI_033_H01 | probable plasma membrane intrinsic protein 1c |
| | NXCI_034_B11 | potassium transporter, putative |
| | NXCI_034_E08 | ABC transporter -like protein |
| | NXCI_040_F05 | secretory carrier membrane protein, putative |
| | NXCI_042_G11 | cation-transporting ATPase |
| | NXCI_043_D01 | putative integral membrane protein |
| | NXCI_043_G02 | membrane associated protein |
| | NXCI_047_B08 | leucine-rich repeat transmembrane protein kinase 1, putative |
| | NXCI_047_E11 | ABC transporter, putative |
| | NXCI_050_F07 | glucose 6 phosphate/phosphate translocator-like protein |
| | NXCI_053_A04 | multispanning membrane protein - like |
| | NXCI_053_B07 | membrane import protein, putative |
| | NXCI_053_F10 | integral membrane protein, putative |
| | NXCI_057_C08 | integral membrane protein-like |
| | NXCI_060_G09 | outer envelope membrane protein OEP75 precursor homolog |
| | NXCI_061_E07 | membrane transporter like protein |
| | NXCI_070_H09 | PROTEIN TRANSPORT PROTEIN SEC61 GAMMA SUBUNIT -like |
| | NXCI_081_B12 | putative transmembrane protein |
| | NXCI_093_F11 | hexose transporter - like protein |
| | NXCI_094_B01 | cation-transporting ATPase |
| | NXCI_097_G04 | hexose transporter - like protein |
| | NXCI_098_C12 | aquaporin, putative |
| | NXCI_101_D04 | phosphatidylinositol/phosphatidylcholine transfer protein, putative |
| | NXCI_108_C11 | membrane translocase - like protein |
| | NXCI_114_B08 | integral membrane protein, putative |
| | NXCI_115_E03 | iron-regulated transporter - like protein |

| Category | Pine clone name | Annotation |
|---|---|---|
| | NXCI_120_G03 | putative chloroplast outer membrane protein |
| | NXCI_121_G02 | phosphatidylinositol/phosphatidylcholine transfer protein, putative |
| | NXCI_123_D05 | membrane-bound small GTP-binding - like protein |
| | NXCI_124_E10 | secretory carrier membrane protein, putative |
| | NXCI_124_F06 | phosphate/phosphoenolpyruvate translocator - like protein |
| | NXCI_125_E08 | sulfate transporter |
| | NXCI_130_B12 | membrane-associated salt-inducible-like protein |
| | NXCI_132_G01 | putative integral membrane protein |
| | NXCI_133_B11 | vacuolar H+-ATPase subunit B, putative |
| | NXCI_144_G08 | hexose transporter, putative |
| | NXCI_150_G05 | sugar transporter - like protein |
| | NXCI_153_E05 | putative L-ascorbate oxidase |
| | NXCI_162_C01 | putative sugar transporter protein |
| | NXCI_165_D03 | ABC transporter, ATP-binding protein-like |
| | NXCI_165_F02 | transmembrane protein, putative |
| | NXLV_003_E01 | PROTEIN TRANSPORT PROTEIN SEC61 GAMMA SUBUNIT -like |
| | NXLV_011_H08 | putative phosphatidylinositol/phosphatidylcholine transfer protein |
| | NXLV_013_B06 | cleft lip and palate associated transmembrane protein-like |
| | NXLV_018_C06 | putative leucine-rich repeat transmembrane protein kinase |
| | NXLV_020_H09 | ABC transporter homolog PnATH - like |
| | NXLV_037_E01 | 3-phosphoinositide-dependent protein kinase-1 PDK1 |
| | NXLV_037_F06 | phosphatidylinositol synthase (PIS1) |
| | NXLV_042_E09 | putative membrane-associated salt-inducible protein |
| | NXLV_044_G12 | calcium-transporting ATPase |
| | NXLV_053_G05 | membrane protein common family |
| | NXLV_053_H10 | ABC transporter -like protein |
| | NXLV_054_C04 | integral membrane protein, putative |

| Category | Pine clone name | Annotation |
|---|---|---|
| | NXLV_064_B06 | Ca2+-dependent membrane-binding protein annexin |
| | NXLV_068_B02 | putative non-green plastid inner envelope membrane protein |
| | NXLV_068_E03 | nitrate transporter NTL1, putative |
| | NXLV_068_H07 | putative nitrate transporter |
| | NXLV_072_G07 | aquaporin-like protein |
| | NXLV_076_A03 | putative leucine-rich repeat transmembrane protein kinase |
| | NXLV_078_H01 | ABC transporter protein 1-like |
| | NXLV_079_G07 | leucine-rich repeat transmembrane protein kinase 1, putative |
| | NXLV087_C01 | transporter -like protein |
| | NXLV088_H07 | putative phosphate/phosphoenolpyruvate translocator |
| | NXLV091_C07 | ABC transporter homolog PnATH - like |
| | NXLV103_G07 | putative membrane-associated salt-inducible protein (AL021637) |
| | NXLV105_E08 | delta-8 sphingolipid desaturase |
| | NXLV108_A04 | phosphate/phosphoenolpyruvate translocator - like protein |
| | NXLV108_F07 | ABC transporter, ATP-binding protein-like |
| | NXLV111_C06 | putative membrane protein |
| | NXLV112_B02 | leucine-rich repeat transmembrane protein kinase, putative |
| | NXLV126_C09 | putative coated vesicle membrane protein |
| | NXNV001H04 | transporter-like protein |
| | NXNV002C02 | 3-phosphoinositide-dependent protein kinase-1 PDK1 |
| | NXNV003D06 | plasma membrane associated protein –like |
| | NXNV003E11 | 2-oxoglutarate/malate translocator precursor -like protein |
| | NXNV005E02 | plasma membrane intrinsic protein (SIMIP) |
| | NXNV005E03 | mipC protein - like (aquaporin) |
| | NXNV005E05 | integral membrane protein, putative |
| | NXNV015H10 | putative secretory carrier-associated membrane protein |
| | NXNV018F05 | putative integral membrane protein |

| Category | Pine clone name | Annotation |
|---|---|---|
| | NXNV019D05 | putative aquaporin (plasma membrane intrinsic protein) |
| | NXNV028B06 | hexose transporter, putative |
| | NXNV047E01 | copper transport protein – like |
| | NXNV_065_B11 | nuclear envelope membrane protein – like |
| | NXNV_065_H07 | potassium transporter, putative |
| | NXNV_066_D05 | type 1 membrane protein, putative |
| | NXNV_066_E02 | type 1 membrane protein, putative |
| | NXNV067C04 | putative plasma membrane intrinsic protein |
| | NXNV_071_H07 | plasma membrane associated protein, putative |
| | NXNV_075_H09 | secretory carrier membrane protein |
| | NXNV_081_C08 | membrane channel protein-like; aquaporin (tonoplast intrinsic protein)-like |
| | NXNV_083_E11 | H+-transporting ATPase - like protein |
| | NXNV_088_A03 | ABC transporter-like protein |
| | NXNV_096_E02 | putative WD repeat membrane protein |
| | NXNV_096_E12 | chloroplast membrane protein (ALBINO3)(OXA1p) |
| | NXNV_120_G07 | secretory carrier membrane protein |
| | NXNV_123_B10 | voltage-dependent anion-selective channel protein hsr2 |
| | NXNV_129_F09 | H+-transporting ATPase chain E, vacuolar |
| | NXNV_130_D10 | ABC transporter-like protein |
| | NXNV_132_H03 | putative sugar transporter |
| | NXNV_133_B05 | ABC transporter, putative |
| | NXNV_144_G04 | Ca2+-transporting ATPase - like protein |
| | NXNV_145_C08 | putative phosphatidylinositol/phosphatidylcholine transfer protein |
| | NXNV_145_D01 | integral membrane protein, putative |
| | NXNV_147_D04 | putative membrane channel protein |
| | NXNV_149_C04 | putative inner mitochondrial membrane protein |
| | NXNV_151_E03 | putative zinc transporter ZIP2 – like |

| Category | Pine clone name | Annotation |
|---|---|---|
| | NXNV_158_A08 | putative sugar transporter |
| | NXNV_158_C06 | putative membrane-associated salt-inducible protein |
| | NXNV_159_G04 | amino acid transporter |
| | NXNV_164_D07 | H+-transporting ATPase 16K chain P2, vacuolar |
| | NXNV_173_F01 | integral membrane protein, putative |
| | NXNV_173_G07 | L-ascorbate oxidase precursor, putative |
| | NXNV_186_D07 | phosphatidylinositol 4-kinase, putative |
| | NXNV_98_D06 | protein transport protein subunit – like |
| | NXPV_001_E10 | membrane associated protein |
| | NXPV_003_C01 | ABC transporter-like protein |
| | NXPV_004_A03 | putative transmembrane protein |
| | NXPV_004_F10 | putative plasma membrane intrinsic protein, almost identical to aquaporin PIP3 (GB:U78297) |
| | NXPV_006_D11 | putative cation transport protein |
| | NXPV_006_D12 | potassium transporter - like protein |
| | NXPV_007_C08 | putative aquaporin (tonoplast intrinsic protein gamma) |
| | NXPV_007_E09 | putative cell wall-plasma membrane disconnecting CLCT protein (AIR1A) |
| | NXPV_008_F04 | putative membrane-associated salt-inducible protein (AL021637); |
| | NXPV_008_G08 | aquaporin (plasma membrane intrinsic protein 2B) |
| | NXPV_011_D04 | sulfate transporter, putative |
| | NXPV_013_A12 | aquaporin/MIP - like protein |
| | NXPV_013_D04 | K+ transporter, AKT1 |
| | NXPV_013_F07 | putative 3-phosphoinositide-dependent protein kinase-1 |
| | NXPV_014_A11 | outer membrane lipoprotein - like |
| | NXPV_015_D01 | putative sulfate transporter |
| | NXPV_015_D06 | putative phosphatidylinositol phophatidylcholine transfer protein |
| | NXPV_016_F02 | putative multispanning membrane protein |
| | NXPV_019_B02 | membrane transporter like protein |

| Category | Pine clone name | Annotation |
|---|---|---|
| | NXPV_019_B07 | cadmium-transporting ATPase-like protein |
| | NXPV_020_B01 | ABC transporter protein, putative |
| | NXPV_021_B10 | proline transporter 2 |
| | NXPV_021_E10 | glucose-6-phosphate/phosphate translocator |
| | NXPV_022_A03 | phosphatidylinositol-4-phosphate 5-kinase, putative |
| | NXPV_027_A11 | ABC transporter, ATP-binding protein-like |
| | NXPV_027_D07 | putative membrane protein |
| | NXPV_038_F01 | glucose-6-phosphate/phosphate translocator |
| | NXPV_038_G10 | integral membrane protein, putative |
| | NXPV_057_A02 | aquaporin-like protein |
| | NXPV_066_B01 | plasma membrane intrinsic protein 1c, putative |
| | NXPV_066_D10 | putative membrane protein |
| | NXPV_073_A06 | glucose-6-phosphate phosphate-translocator precursor, putative |
| | NXPV_076_A01 | putative integral membrane protein nodulin |
| | NXPV_077_C06 | cadmium-transporting ATPase-like protein |
| | NXPV_077_G05 | putative transmembrane protein G5p |
| | NXPV_077_H07 | phosphatidylinositol-4-phosphate 5-kinase-like protein |
| | NXPV_078_B04 | chromaffin granule ATPase II homolog, putative |
| | NXPV_081_A05 | cation-transporting ATPase |
| | NXPV_090_A02 | ABC transporter - like protein |
| | NXPV_090_D12 | plasma membrane intrinsic protein 1a |
| | NXPV_096_D01 | transmembrane protein FT27/PFT27-like |
| | NXPV_097_G04 | high affinity K+ transporter (AtKUP1/AtKT1p) |
| | NXPV_098_E01 | vacuolar H+-ATPase subunit B, putative |
| | NXPV_104_E07 | putative inner mitochondrial membrane protein |
| | NXPV_108_C06 | endomembrane protein EMP70 precusor isolog |
| | NXPV_112_B04 | putative peptide/amino acid transporter |

| Category | Pine clone name | Annotation |
|---|---|---|
| | NXPV_123_D08 | putative potassium transporter |
| | NXRV_006_E04 | putative membrane channel protein |
| | NXRV_011_H07 | membrane-bound small GTP-binding - like protein |
| | NXRV_016_G04 | membrane protein PTM1 precursor isolog |
| | NXRV_018_A05 | putative 3-phosphoinositide-dependent protein kinase-1 |
| | NXRV_019_F12 | integral membrane protein, putative |
| | NXRV_021_D08 | potential calcium-transporting ATPase11, plasma membrane-type ($Ca^{2+}$-ATPase, isoform 11) |
| | NXRV_022_H02 | putative sugar transporter |
| | NXRV_025_B04 | putative vesicle-associated membrane protein, synaptobrevin 7B |
| | NXRV_027_A12 | H+-transporting ATPase 16K chain P2, vacuolar |
| | NXRV_029_G07 | membrane protein common family |
| | NXRV_030_D06 | copper transport protein - like |
| | NXRV_032_E09 | putative aquaporin (tonoplast intrinsic protein) |
| | NXRV_036_H05 | nitrate transporter NTL1, putative |
| | NXRV045_E06 | nuclear envelope membrane protein - like |
| | NXRV045_G09 | membrane protein, putative |
| | NXRV047_F11 | putative phosphatidylinositol/phophatidylcholine transfer protein |
| | NXRV050_F06 | putative peroxisomal membrane carrier protein |
| | NXRV051_D05 | ABC transporter-like protein |
| | NXRV055_E01 | choline kinase (GmCK2p), putative |
| | NXRV056_D12 | aquaporin (plasma membrane intrinsic protein 1B) |
| | NXRV058_B02 | calcium-binding transporter-like protein |
| | NXSI_008_F03 | putative chloroplast outer membrane protein |
| | NXSI_011_B12 | membrane related protein-like |
| | NXSI_011_D08 | high affinity K+ transporter (AtKUP1 AtKT1p) |
| | NXSI_023_G05 | [ZD] Ca2+-binding protein (centrin/caltractin) EF-Hand superfamily ,Magpie No BQ701203 |

| Category | Pine clone name | Annotation |
|---|---|---|
| | NXSI_029_H03 | phosphatidylinositol phosphatidylcholine transfer protein, No BF517756 |
| | NXSI_031_H03 | putative glucose acyltransferase |
| | NXSI_036_E05 | aquaporin (plasma membrane intrinsic protein 1B) |
| | NXSI_036_G09 | transporter-like protein |
| | NXSI_038_A10 | amino acid permease-like protein; proline transporter-like protein |
| | NXSI_039_A10 | metal ion transporter |
| | NXSI_039_C08 | putative nitrate transporter |
| | NXSI_042_E10 | putative glucose acyltransferase |
| | NXSI_043_E08 | H+-transporting ATPase chain E, vacuolar |
| | NXSI_048_C09 | plasma membrane intrinsic protein (SIMIP) |
| | NXSI_049_C10 | plasma membrane intrinsic protein 1a |
| | NXSI_052_C02 | putative sugar transporter |
| | NXSI_052_D03 | leucine-rich repeat transmembrane protein kinase, putative |
| | NXSI_053_A06 | inner mitochondrial membrane protein |
| | NXSI_054_H10 | ABC transporter -like protein |
| | NXSI_055_B01 | putative sugar transporter |
| | NXSI_056_A02 | vacuolar H+-transporting ATPase 16K chain |
| | NXSI_057_H09 | potential calcium-transporting ATPase 10, plasma membrane-type (Ca2+-ATPase, isoform 10) |
| | NXSI_060_A09 | aquaporin, putative |
| | NXSI_064_B04 | EMB:Q9XG70 Q9XG70 AQUAGLYCEROPORIN |
| | NXSI_068_H06 | phosphate/phosphoenolpyruvate translocator precursor |
| | NXSI_069_B01 | aquaporin/MIP - like protein |
| | NXSI_070_A10 | VAMP (vesicle-associated membrane protein)-associated protein-like |
| | NXSI_070_C12 | probable H+-transporting ATPase |
| | NXSI_071_C11 | putative phosphatidylinositol-4-phosphate 5-kinase |
| | NXSI_073_F12 | sugar transporter-like protein |
| | NXSI_073_G01 | L-ascorbate oxidase precursor, putative |

| Category | Pine clone name | Annotation |
|---|---|---|
| | NXSI_076_H01 | putative proline transporter |
| | NXSI_079_A04 | sugar transporter-like protein |
| | NXSI_079_E01 | ABC transporter protein, putative |
| | NXSI_079_H06 | probable plasma membrane intrinsic protein 1c |
| | NXSI_085_F02 | plasma membrane associated protein -like |
| | NXSI_085_G08 | amino acid transporter AAP4 |
| | NXSI_087_B11 | putative sugar transporter |
| | NXSI_088_F04 | sulfate transporter |
| | NXSI_091_G10 | ABC transporter, putative |
| | NXSI_092_H07 | transmembrane protein, putative |
| | NXSI_094_B04 | putative sugar transporter protein |
| | NXSI_095_C07 | Membrane integral protein (MIP) -like |
| | NXSI_095_F07 | aquaporin/MIP - like protein |
| | NXSI_097_E04 | protein transport protein subunit - like |
| | NXSI_097_F11 | plasma membrane intrinsic protein 2a |
| | NXSI_098_E08 | transmembrane protein FT27/PFT27-like |
| | NXSI_099_F09 | sugar transporter-like protein |
| | NXSI_100_E02 | sugar transporter-like protein |
| | NXSI_101_E08 | putative membrane associated protein |
| | NXSI_102_A08 | putative cell wall-plasma membrane disconnecting CLCT protein (AIR1A) |
| | NXSI_104_D07 | membrane channel protein-like; aquaporin (tonoplast intrinsic protein)-like |
| | NXSI_106_C01 | aquaporin MIP - like protein |
| | NXSI_106_H07 | putative chloroplast membrane protein, ALBINO3 |
| | NXSI_107_E08 | peptide transporter - like protein |
| | NXSI_107_G12 | putative aquaporin (plasma membrane intrinsic protein) |
| | NXSI_107_H06 | sulfate transporter ATST1 |
| | NXSI_109_D12 | vacuolar H+-transporting ATPase 16K chain |

| Category | Pine clone name | Annotation |
|---|---|---|
| | NXSI_110_C07 | multispanning membrane protein - like |
| | NXSI_110_E02 | calcium-binding transporter-like protein |
| | NXSI_110_F06 | Membrane integral protein (MIP) -like |
| | NXSI_115_A04 | peptide transporter - like protein |
| | NXSI_116_B12 | 2-oxoglutarate/malate translocator |
| | NXSI_116_C07 | aquaporin (plasma membrane intrinsic protein 1B) |
| | NXSI_138_F07 | putative plasma membrane intrinsic protein |
| | NXSI_139_E04 | ABC transporter, putative |
| | NXSI_139_F06 | putative hexose transporter |
| | NXSI_139_G08 | putative sugar transporter |
| | NXSI_142_B01 | proline transporter 1 |
| | NXSI_142_B02 | aquaporin (plasma membrane intrinsic protein 2B) |
| | NXSI_145_D07 | H+-transporting ATPase type 2, plasma membrane |
| | NXSI_145_E06 | transmembrane transport protein-like |
| | NXSI_149_E09 | putative Na+-dependent inorganic phosphate cotransporter |
| | PC04B10 | K+ transporter, AKT1 |
| | PC04H09 | putative proline transporter |
| | PC06C10 | putative amino acid transport protein |
| | PC18H01 | sugar transporter-like protein |
| | PC19C08 | putative phosphate/phosphoenolpyruvate translocator protein |
| | PC20C12 | integral membrane protein, putative |
| | ST04A02 | oxoglutarate/malate translocator-like protein |
| | ST07A03 | aquaporin |
| | ST07G03 | putative Golgi-associated membrane trafficking protein |
| | ST09A10 | vacuolar H+-ATPase proteolipid (16 kDa) subunit |
| | ST12G04 | membrane-associated salt-inducible protein isolog |
| | ST14C11 | transporter -like protein |

| Category | Pine clone name | Annotation |
|---|---|---|
| | ST16C09 | Oxygen evolving enhancer protein 2 chloroplast precursor OEE2 23 kDa subunit system |
| | | photosystem II oec 23 23 thylakoid membrane complex 23 ,Magpie No AW011066 |
| | ST16G08 | putative metal ion transporter (NRAMP) |
| | ST17B03 | leucine-rich repeat transmembrane protein kinase, putative |
| | ST18G02 | integral membrane protein, putative |
| | ST19B09 | proline transporter 2 |
| | ST22C04 | multispanning membrane protein, putative |
| | ST22E12 | putative sugar transporter |
| | ST22H08 | high affinity nitrate transporter protein – like |
| | ST23C09 | putative plasma membrane intrinsic protein, almost identical to aquaporin PIP3 (GB:U78297) |
| | ST23E03 | putative sulfate transporter |
| | ST24G11 | choline kinase, putative |
| | ST27F02 | endomembrane protein, putative |
| | ST29F02 | VAMP (vesicle-associated membrane protein)-associated protein-like |
| | ST31D08 | putative hexose transporter |
| | ST33G03 | Ca2+-transporting ATPase - like protein |
| | ST36B03 | putative phosphate/phosphoenolpyruvate translocator protein |
| | ST36D05 | phosphatidylinositol 3-kinase, putative |
| | ST38A08 | putative integral membrane protein |
| | ST38F05 | vacuolar H(+)-ATPase subunit-like protein |
| | ST39B08 | putative ABC transporter |
| | ST39C06 | membrane translocase - like protein |
| | ST39H11 | ABC transporter-like protein |
| **CELL STRUCTURE AND DIFFERENTIATION** | NXCI_044_E01 | putative nucleotide-binding protein |
| | NXNV_187_B04 | Cyclin-dependent kinase B1;1 |
| | NXPV_007_E09 | putative cell wall-plasma membrane disconnecting CLCT protein (AIR1A) |

| Category | Pine clone name | Annotation |
|---|---|---|
| | NXSI_001_F11 | putative nucleotide-binding protein |
| | NXSI_009_E01 | putative nucleotide-binding protein |
| | NXSI_030_C07 | nucleotide-binding protein |
| | NXSI_030_E06 | nucleotide-binding protein |
| | NXSI_083_G05 | guanine nucleotide-binding protein, putative |
| | NXSI_102_A08 | putative cell wall-plasma membrane disconnecting CLCT protein (AIR1A) |
| | ST02H06 | guanine nucleotide-binding protein, putative |
| | ST25B04 | actin 11 (ACT11) |
| | ST37A10 | Putative S-phase-specific ribosomal protein |
| **CELL WALL RELATED** | NXCI_020_E05 | putative GDP-mannose pyrophosphorylase |
| | NXCI_022_B06 | UDP-glucose glucosyltransferase, putative |
| | NXCI_025_D02 | sucrose-phosphate synthase, putative |
| | NXCI_033_G05 | UDP-glucose glucosyltransferase, putative |
| | NXCI_038_H12 | sucrose synthase |
| | NXCI_054_F12 | UDP-glucose glucosyltransferase, putative |
| | NXCI_067_H03 | putative UDP-glucose glucosyltransferase |
| | NXCI_081_H03 | UDP-glucose glucosyltransferase, putative |
| | NXCI_094_F10 | UDP-glucose glucosyltransferase, putative |
| | NXCI_101_A06 | pectinesterase (pectin methylesterase), putative |
| | NXCI_128_C06 | sucrose synthase, putative |
| | NXCI_129_A02 | putative xyloglucan endotransglycosylase |
| | NXCI_132_E11 | putative xyloglucan endotransglycosylase |
| | NXCI_147_E01 | UDP-glucose glucosyltransferase, putative |
| | NXCI_151_G07 | putative UDP-glucose glucosyltransferase |
| | NXCI_165_A01 | glucose-6-phosphate isomerase, cytosolic (GPI) |
| | NXLV_036_H12 | putative UDP-glucose glucosyltransferase |
| | NXLV085_C09 | putative UDP-glucose glucosyltransferase |

| Category | Pine clone name | Annotation |
|---|---|---|
| | NXLV102_F08 | sucrose synthase, putative |
| | NXNV005B09 | sucrose synthase -like protein |
| | NXNV007F05 | UDP-glucose glucosyltransferase, putative |
| | NXNV027F08 | sucrose synthase -like protein |
| | NXNV055D06 | ankyrin repeat-containing protein 2 |
| | NXNV_066_A07 | xyloglucan endotransglycosylase (EXGT-A4) |
| | NXNV_082_H01 | phosphomannose isomerase, putative |
| | NXNV_105_B10 | putative UDP-glucose pyrophosphorylase |
| | NXNV_120_A09 | putative trehalose-6-phosphate synthase |
| | NXNV_127_E04 | pinoresinol-lariciresinol reductase TH2 |
| | NXNV_132_G06 | xyloglucan endotransglycosylase, putative |
| | NXNV_132_G09 | UDP-glucose dehydrogenase, putative |
| | NXNV_139_B12 | putative xyloglucan endotransglycosylase type 1 |
| | NXNV_159_E06 | UDP-glucose glucosyltransferase, putative |
| | NXNV_164_H08 | xyloglucan endotransglycosylase, putative |
| | NXNV_187_F06 | xyloglucan endotransglycosylase XTR9 |
| | NXPV_007_C04 | trehalose-6-phosphate synthase, putative |
| | NXPV_007_E09 | putative cell wall-plasma membrane disconnecting CLCT protein (AIR1A) |
| | NXPV_012_B07 | trehalose-6-phosphate synthase, putative |
| | NXPV_133_H02 | phosphomannose isomerase, putative |
| | NXRV_032_G10 | putative arabinogalactan protein |
| | NXRV056_D08 | putative arabinogalactan/proline-rich protein |
| | NXRV_057_C11 | sucrose synthase, putative |
| | NXRV059_A05 | trehalose-phosphatase, putative |
| | NXSI_043_B03 | UDP-glucose pyrophosphorylase |
| | NXSI_058_B08 | UDP-glucose glucosyltransferase, putative |
| | NXSI_069_D06 | UDP-glucose glucosyltransferase, putative |

| Category | Pine clone name | Annotation |
|---|---|---|
| | NXSI_100_H07 | putative UDP-glucose glucosyltransferase |
| | NXSI_102_A08 | putative cell wall-plasma membrane disconnecting CLCT protein (AIR1A) |
| | NXSI_135_A11 | arabinogalactan like protein ,Magpie No BQ702988 |
| | ST08F03 | sucrose synthase-like protein |
| | ST16D12 | proline rich protein putative ,Magpie No AW011080 |
| | ST20G11 | sucrose synthase |
| | ST21H02 | expansin, putative |
| | ST26C12 | sucrose phosphate synthase 2 udp glucose fructose glucosyltransferase |
| | ST37B12 | glucose-6-phosphate isomerase, cytosolic (GPI) |
| **CHLOROPLAST ASSOCIATED** | NXCI_022_D04 | putative rubisco subunit binding-protein alpha subunit |
| | NXCI_026_A11 | Putative glutaredoxin ,Magpie No BE582191 |
| | NXCI_044_F11 | putative ATPase |
| | NXCI_050_F02 | monodehydroascorbate reductase (NADH) - like protein |
| | NXCI_053_G09 | H+-transporting ATP synthase chain 9 - like protein |
| | NXCI_070_A03 | photosystem II polypeptide, putative |
| | NXCI_075_F10 | putative thioredoxin |
| | NXCI_076_A10 | H+-transporting ATP synthase chain 9 - like protein |
| | NXCI_120_D06 | GSH-dependent dehydroascorbate reductase 1, putative |
| | NXCI_133_F08 | photosystem I subunit X precursor |
| | NXCI_144_D10 | putative ATP synthase |
| | NXCI_153_E05 | putative L-ascorbate oxidase |
| | NXLV_013_D10 | photosystem II type I chlorophyll a b binding protein |
| | NXLV_054_B06 | L-ascorbate peroxidase |
| | NXLV_054_B12 | L-ascorbate peroxidase |
| | NXLV_058_C10 | putative thioredoxin-m |
| | NXLV085_B07 | putative coproporphyrinogen III oxidase |
| | NXLV090_C10 | thioredoxin f2 |

| Category | Pine clone name | Annotation |
|---|---|---|
| | NXLV090_H04 | S-adenosylmethionine:2-demethylmenaquinone methyltransferase-like |
| | NXLV105_B09 | vacuolar ATP synthase, putative |
| | NXLV107_D11 | superoxide dismutase (EC 1.15.1.1) (Fe)(fragment) |
| | NXLV111_C05 | photosystem I subunit V precursor, putative |
| | NXLV130_G08 | ATP synthase delta chain, mitochondrial precursor (sp |
| | NXLV131_E01 | ATP synthase delta chain, mitochondrial precursor (sp |
| | NXLV133_G11 | putative monodehydroascorbate reductase (NADH) |
| | NXNV002G06 | Rubisco subunit binding-protein beta subunit |
| | NXNV_007_B09 | putative ferredoxin-thioredoxin reductase |
| | NXNV031A04 | ATP synthase gamma-subunit, putative |
| | NXNV046C04 | thylakoid lumenal L-ascorbate peroxidase chloroplast precursor, putative |
| | NXNV055E12 | Glutaredoxin |
| | NXNV_070_E05 | chaperonin 60 beta, putative |
| | NXNV_081_G02 | putative thioredoxin-m |
| | NXNV_120_A05 | putative rubisco subunit binding-protein alpha subunit |
| | NXNV_120_H01 | pseudogene, vacuolar ATP synthase subunit B |
| | NXNV_123_C03 | vacuolar ATP synthase subunit B |
| | NXNV_131_G01 | putative monodehydroascorbate reductase |
| | NXNV_147_H08 | putative aminolevulinate dehydratase |
| | NXNV_154_C07 | putative ATP synthase |
| | NXNV_162_D12 | putative M-type thioredoxin |
| | NXNV_162_H07 | Thioredoxin-like ,Magpie No BE187354 |
| | NXNV_183_G11 | vacuolar ATP synthase, putative |
| | NXPV_003_G08 | glutamate-1-semialdehyde 2,1-aminomutase 1 precursor (GSA 1) |
| | NXPV_082_G11 | putative zeta-carotene desaturase precursor |
| | NXPV_092_D11 | L-ascorbate peroxidase - like protein |
| | NXRV_015_H05 | putative vacuolar ATP synthase subunit E |

| Category | Pine clone name | Annotation |
|---|---|---|
| | NXRV_016_D02 | thylakoid-bound ascorbate peroxidase |
| | NXRV_016_G05 | putative vacuolar ATP synthase proteolipid subunit |
| | NXRV_031_F07 | putative prenyl transferase (prephytoene pyrophosphatase dehydrogenase) |
| | NXRV046_E10 | light harvesting pigment - like protein |
| | NXRV046_F06 | putative vacuolar ATP synthase subunit E |
| | NXRV047_G07 | putative ferredoxin-thioredoxin reductase |
| | NXRV049_H10 | pseudogene, ATP synthase C subunit |
| | NXRV056_C07 | light harvesting pigment - like protein |
| | NXSI_001_C03 | light-harvesting complex protein |
| | NXSI_001_C04 | putative photosystem II type I chlorophyll a b binding protein. |
| | NXSI_007_D08 | photosystem II reaction center 6.1KD protein |
| | NXSI_023_E09 | stromal ascorbate peroxidase, putative (sAPX) |
| | NXSI_040_A09 | putative glutamyl tRNA reductase |
| | NXSI_047_C03 | putative photosystem II type I chlorophyll a b binding protein. |
| | NXSI_049_H07 | mitochondrial F1-ATPase, gamma subunit (ATP3_ARATH) |
| | NXSI_052_B04 | GSH-dependent dehydroascorbate reductase 1, putative |
| | NXSI_071_D07 | putative M-type thioredoxin |
| | NXSI_083_C02 | vacuolar ATP synthase subunit C, putative |
| | NXSI_083_C04 | photosystem II type I chlorophyll a/b binding protein |
| | NXSI_096_C09 | chaperonin precursor, putative |
| | NXSI_102_A02 | iron superoxide dismutase 3 (gb |
| | NXSI_107_H09 | L-ascorbate peroxidase - like protein |
| | NXSI_116_C10 | oxygen-evolving complex 25.6 kD protein, chloroplast precursor, putative |
| | NXSI_135_D07 | Cupredoxins ,Magpie No BQ703010 |
| | PC04C10 | pseudogene, ATP synthase C subunit |
| | PC09A10 | epsilon subunit of mitochondrial F1-ATPase |
| | PC15C08 | GSH-dependent dehydroascorbate reductase 1-like |

| Category | Pine clone name | Annotation |
|---|---|---|
| | ST05D04 | ribulose-bisphosphate carboxylase small unit, putative |
| | ST07C06 | Quinone oxidoreductase like protein ,Magpie No AW010478 |
| | ST08A10 | putative component of cytochrome B6-F complex |
| | ST12D01 | photosystem I subunit X precursor |
| | ST14H03 | 4FE4S ferredoxin ,Magpie No AW010851 |
| | ST16D01 | photosystem II oxygen-evolving complex 23 (OEC23) |
| | ST17C05 | delta subunit of mitochondrial F1-ATPase |
| | ST19A09 | photosystem II protein W – like |
| | ST19D03 | RuBisCO small subunit ,Magpie No AW011316 |
| | ST19E02 | thioredoxin m4 |
| | ST20F08 | photosystem I reaction center subunit PSI-N precursor (PSI-N) |
| | ST20G04 | [QR] Iron/ascorbate family oxidoreductases ,Magpie No AW011436 |
| | ST21G10 | [QR] Iron/ascorbate family oxidoreductases ,Magpie No AW011521 |
| | ST21H11 | phytoene synthase (gbAAB65697.1) |
| | ST28F02 | photosystem II oxygen-evolving complex 23 (OEC23) |
| | ST30C03 | RuBisCO subunit binding-protein beta subunit precursor; chaperonin, 60 kDa |
| | ST31H04 | photosystem II reaction center 6.1KD protein |
| | ST32B06 | ribulose-bisphosphate carboxylase small unit, putative |
| | ST32C01 | photosystem II protein W – like |
| | ST34C01 | ribulose bisphosphate carboxylase small chain 3b precursor (RuBisCO small subunit 3b) |
| | ST36A10 | light-harvesting complex protein |
| | ST37E03 | delta subunit of mitochondrial F1-ATPase |
| | ST39B12 | putative rubisco subunit binding-protein alpha subunit |
| | ST39F03 | ferredoxin precusor isolog |
| **ENVIRONMENT** | 1F7 | putative superoxide-generating NADPH oxidase flavocytochrome |
| | 1G7 | putative heat-shock protein |
| | 20B2 | pseudogene, putative clpB heat shock protein |

| Category | Pine clone name | Annotation |
|---|---|---|
| | 22D11 | putative glutathione S-transferase |
| | NXCI_001_A09 | protein-methionine-S-oxide reductase |
| | NXCI_002_C10 | EMB:Q9XEL3 Q9XEL3 PUTATIVE DEHYDRIN. >GEN:4704603 AF109916 |
| | NXCI_002_F03 | putative glutathione S-transferase TSI-1 |
| | NXCI_020_B03 | dnaK-type molecular chaperone hsc70.1 |
| | NXCI_020_H04 | aquaporin, putative |
| | NXCI_021_C02 | putative heat shock protein |
| | NXCI_022_G01 | SWP:HS7M_SOLTU Q08276 HEAT SHOCK 70 KDA PROTEIN, MITOCHONDRIAL |
| | NXCI_023_H02 | putative glutathione S-transferase |
| | NXCI_032_F07 | putative heat-shock protein |
| | NXCI_048_D06 | N-hydroxycinnamoyl/benzoyltransferase |
| | NXCI_050_F02 | monodehydroascorbate reductase (NADH) - like protein |
| | NXCI_055_A01 | cysteine synthase - like |
| | NXCI_069_G10 | putative heat-shock protein |
| | NXCI_070_B12 | cysteine synthase AtcysC1 |
| | NXCI_075_D08 | heat shock protein 70 |
| | NXCI_075_F10 | putative thioredoxin |
| | NXCI_075_F11 | thioredoxin, putative |
| | NXCI_085_H12 | glutathione transferase, putative |
| | NXCI_094_G02 | lactoylglutathione lyase, putative |
| | NXCI_095_F09 | S-adenosyl-L-methionine:salicylic acid carboxyl methyltransferase-like protein |
| | NXCI_098_C12 | aquaporin, putative |
| | NXCI_102_D01 | EMB:Q9LKW3 Q9LKW3 DEHYDRATION-INDUCED PROTEIN ERD15 |
| | NXCI_107_G02 | 70kDa heat shock protein ,Magpie No BE997207 |
| | NXCI_118_A05 | heat shock protein 70 (gb |
| | NXCI_118_D07 | Pathogenesis related protein PR 1 precursor gene 1 ,Magpie No BF060621 |
| | NXCI_120_D06 | GSH-dependent dehydroascorbate reductase 1, putative |

| Category | Pine clone name | Annotation |
|---|---|---|
| | NXCI_127_C04 | DRE binding protein (DREB2B) |
| | NXCI_130_B12 | membrane-associated salt-inducible-like protein |
| | NXCI_130_D10 | hydroxyacylglutathione hydrolase cytoplasmic (glyoxalase II) (GLX II) |
| | NXCI_132_H04 | PIR:T09832 T09832 water-stress-inducible protein LP3 |
| | NXCI_135_C12 | S-adenosyl-L-methionine:salicylic acid carboxyl methyltransferase-like protein |
| | NXCI_135_H12 | PIR:T09832 T09832 water-stress-inducible protein LP3 |
| | NXCI_141_C06 | mitochondria-localized low molecular weight heat shock protein 23.5 |
| | NXCI_149_C10 | N-hydroxycinnamoyl/benzoyltransferase - like protein |
| | NXCI_153_E05 | putative L-ascorbate oxidase |
| | NXCI_162_C03 | putative heat-shock protein |
| | NXCI_164_H03 | immunophilin (FKBP15-1) |
| | NXLV_010_G04 | glutathione transferase, putative |
| | NXLV_013_F09 | putative anthranilate N-hydroxycinnamoyl/benzoyltransferase |
| | NXLV_018_F02 | putative glutathione peroxidase |
| | NXLV_027_C09 | putative glutathione peroxidase |
| | NXLV_032_D05 | pseudogene, putative clpB heat shock protein |
| | NXLV_037_G03 | 70kD heat shock protein |
| | NXLV_039_H11 | ascorbate peroxidase, putative (APX) |
| | NXLV_042_E09 | putative membrane-associated salt-inducible protein |
| | NXLV_048_B03 | heat-shock protein, putative |
| | NXLV_049_G11 | low-molecular-weight heat shock protein - like |
| | NXLV_053_H05 | glutathione S-transferase, putative |
| | NXLV_054_B06 | L-ascorbate peroxidase |
| | NXLV_054_B12 | L-ascorbate peroxidase |
| | NXLV_058_C10 | putative thioredoxin-m |
| | NXLV_059_A11 | dnaK-type molecular chaperone hsc70.1 |
| | NXLV_064_F10 | N-hydroxycinnamoyl benzoyltransferase - like protein |

| Category | Pine clone name | Annotation |
|---|---|---|
| | NXLV_066_B09 | glutathione-s-transferase, putative |
| | NXLV_066_C03 | mitochondrial heat shock 22 kd protein-like |
| | NXLV_069_F03 | cysteine synthase |
| | NXLV_072_G07 | aquaporin-like protein |
| | NXLV_073_C11 | heat-shock protein - like |
| | NXLV_075_A12 | heat shock protein 101 (HSP101) |
| | NXLV082_A10 | glutathione transferase, putative |
| | NXLV083_H09 | Defense-related protein containing scp domain ,Magpie No BQ106965 |
| | NXLV089_C09 | glutathione S-transferase, putative |
| | NXLV090_C10 | thioredoxin f2 (gb |
| | NXLV103_G07 | putative membrane-associated salt-inducible protein (AL021637) |
| | NXLV107_D11 | superoxide dismutase (EC 1.15.1.1) (Fe)(fragment) |
| | NXLV108_A02 | low-molecular-weight heat shock protein - like |
| | NXLV114_D08 | putative glutathione S-transferase |
| | NXLV118_D02 | similar to late embryogenesis abundant proteins |
| | NXLV119_B12 | putative copper/zinc superoxide dismutase |
| | NXLV123_E04 | putative small heat shock protein |
| | NXLV129_F06 | glutathione S-transferase-like protein |
| | NXLV133_G11 | putative monodehydroascorbate reductase (NADH) |
| | NXNV005E03 | mipC protein - like (aquaporin) |
| | NXNV005E04 | cold acclimation protein homolog |
| | NXNV_007_B09 | putative ferredoxin-thioredoxin reductase |
| | NXNV008F04 | heat shock protein 101 (HSP101),putative |
| | NXNV012H04 | cysteine synthase |
| | NXNV017G11 | glutathione synthetase gsh2 |
| | NXNV019D05 | putative aquaporin (plasma membrane intrinsic protein) |
| | NXNV025B05 | heat shock protein-like protein |

| Category | Pine clone name | Annotation |
|---|---|---|
| | NXNV046C04 | thylakoid lumenal L-ascorbate peroxidase chloroplast precursor, putative |
| | NXNV046E03 | dehydrin Xero2 |
| | NXNV047B02 | heat shock protein 70 (Hsc70-5) |
| | NXNV_063_C10 | dehydration-induced protein (ERD15) |
| | NXNV_066_E07 | heat-shock protein |
| | NXNV067B01 | catalase 1 |
| | NXNV_070_B04 | chloroplast-localized small heat shock protein, putative |
| | NXNV_070_C09 | putative thioredoxin |
| | NXNV_070_C10 | putative thioredoxin |
| | NXNV_073_E01 | cysteine synthase (cpACS1) |
| | NXNV_081_C08 | membrane channel protein-like; aquaporin (tonoplast intrinsic protein)-like |
| | NXNV_081_G02 | putative thioredoxin-m |
| | NXNV_119_D12 | putative heat shock protein |
| | NXNV_120_F09 | FKBP-type peptidyl-prolyl cis-trans isomerase |
| | NXNV_123_C02 | heat shock protein 17.6-II |
| | NXNV_123_C06 | heat shock protein 70 like protein |
| | NXNV_123_E04 | Cu/Zn superoxide dismutase-like protein |
| | NXNV_123_E11 | drought-induced protein |
| | NXNV_123_H12 | ascorbate peroxidase (APX) |
| | NXNV_124_C05 | cysteine synthase |
| | NXNV_126_G05 | putative cold acclimation protein |
| | NXNV_128_D04 | putative heat-shock protein |
| | NXNV_131_G01 | putative monodehydroascorbate reductase |
| | NXNV_132_H12 | similar to TIR-class disease resistance proteins |
| | NXNV_133_D07 | glutathione S-transferase |
| | NXNV_143_H07 | heat shock cognate protein |
| | NXNV_146_C11 | heat shock protein 40-like |

| Category | Pine clone name | Annotation |
|---|---|---|
| | NXNV_149_E10 | EMB:Q9M555 Q9M555 PUTATIVE HEAT-SHOCK PROTEIN 90 (FRAGMENT). |
| | NXNV_158_C06 | putative membrane-associated salt-inducible protein |
| | NXNV_160_F07 | ascorbate peroxidase, putative (APX) |
| | NXNV_162_B11 | glyoxalase I, putative (lactoylglutathione lyase) |
| | NXNV_162_D12 | putative M-type thioredoxin |
| | NXNV_164_D12 | cysteine synthase |
| | NXNV_173_A04 | heat shock protein DnaJ, putative |
| | NXNV_173_G07 | L-ascorbate oxidase precursor, putative |
| | NXNV_187_E01 | putative thioredoxin reductase |
| | NXPV_002_F09 | glutathione reductase, cytosolic |
| | NXPV_004_F10 | putative plasma membrane intrinsic protein, almost identical to aquaporin PIP3 (GB:U78297) |
| | NXPV_005_H07 | heat shock protein 70 (gbAAF27639.1) |
| | NXPV_007_C08 | putative aquaporin (tonoplast intrinsic protein gamma) |
| | NXPV_007_E07 | pseudogene, N-hydroxycinnamoyl/benzoyltransferase |
| | NXPV_008_F04 | putative membrane-associated salt-inducible protein (AL021637) |
| | NXPV_008_G08 | aquaporin (plasma membrane intrinsic protein 2B) |
| | NXPV_010_F04 | glutathione peroxidase - like protein |
| | NXPV_013_A12 | aquaporin/MIP - like protein |
| | NXPV_019_C12 | DNAJ-like heatshock protein |
| | NXPV_023_F12 | glutathione peroxidase - like protein |
| | NXPV_038_E07 | pseudogene, N-hydroxycinnamoyl/benzoyltransferase |
| | NXPV_057_A02 | aquaporin-like protein |
| | NXPV_073_A12 | DRE binding protein (DREB1B) |
| | NXPV_073_H03 | DRE binding protein (DREB2A) |
| | NXPV_077_E08 | heat shock protein, putative |
| | NXPV_080_A02 | disease resistance protein tir nbs lrr class putative ,Magpie No BG832789 |
| | NXPV_083_B10 | DRE binding protein (DREB1C) |

| Category | Pine clone name | Annotation |
|---|---|---|
| | NXPV_084_C06 | putative [Mn] superoxide dismutase |
| | NXPV_085_A06 | DREB-like AP2 domain transcription factor |
| | NXPV_088_C02 | putative heat shock protein |
| | NXPV_092_D11 | L-ascorbate peroxidase - like protein |
| | NXPV_103_H07 | catalase 3 |
| | NXPV_127_D07 | DRE binding protein (DREB1A) |
| | NXRV_003_F06 | hypothetical protein, contains DnaJ motif: prokaryotic heat shock protein motif |
| | NXRV_003_H02 | putative thioredoxin |
| | NXRV_006_A02 | catalase 2 |
| | NXRV_012_C04 | FKBP-type peptidyl-prolyl cis-trans isomerase, putative |
| | NXRV_012_E07 | catalase 3 |
| | NXRV_013_H08 | putative glutathione transferase |
| | NXRV_016_D02 | thylakoid-bound ascorbate peroxidase |
| | NXRV_016_G12 | heat shock protein 70 like protein |
| | NXRV_022_C02 | hypothetical protein, contains DnaJ motif: prokaryotic heat shock protein motif |
| | NXRV_022_F07 | heat shock protein (emb |
| | NXRV_030_D05 | putative heat shock protein |
| | NXRV_032_E09 | putative aquaporin (tonoplast intrinsic protein) |
| | NXRV047_G07 | putative ferredoxin-thioredoxin reductase |
| | NXRV048_A07 | putative heat shock protein |
| | NXRV049_G10 | putative cold-regulated protein |
| | NXRV056_A06 | type 2 peroxiredoxin, putative |
| | NXRV056_D12 | aquaporin (plasma membrane intrinsic protein 1B) |
| | NXRV059_A10 | heat shock protein 17.6-II |
| | NXRV059_C10 | heat shock protein (emb |
| | NXSI_001_E02 | heat shock protein – like |
| | NXSI_002_D03 | drought-induced protein |

| Category | Pine clone name | Annotation |
|---|---|---|
| | NXSI_002_E10 | ascorbate oxidase-like protein |
| | NXSI_002_G10 | alpha-galactosidase |
| | NXSI_002_H07 | putative thioredoxin reductase |
| | NXSI_011_D04 | 17.6 kDa heat shock protein (AA 1-156) |
| | NXSI_011_G01 | heat shock protein 90 |
| | NXSI_012_B12 | putative heat-shock protein |
| | NXSI_013_H11 | putative glutathione transferase |
| | NXSI_021_A06 | heat-shock protein, putative |
| | NXSI_021_B01 | DREB-like AP2 domain transcription factor |
| | NXSI_021_E03 | cysteine synthase (cpACS1) |
| | NXSI_021_F01 | DRE binding protein (DREB2B) |
| | NXSI_021_G01 | ascorbate oxidase promoter-binding protein, putative |
| | NXSI_023_E09 | stromal ascorbate peroxidase, putative (sAPX) |
| | NXSI_027_B11 | heat shock protein-like protein |
| | NXSI_029_D04 | lactoylglutathione lyase, putative |
| | NXSI_030_H08 | putative small heat shock protein |
| | NXSI_031_C12 | putative heat shock protein |
| | NXSI_036_E05 | aquaporin (plasma membrane intrinsic protein 1B) |
| | NXSI_040_C11 | putative heat shock protein |
| | NXSI_041_C09 | heat shock protein 17 |
| | NXSI_041_E09 | HEAT SHOCK PROTEIN 81-2 (HSP81-2) (spP55737) |
| | NXSI_045_A12 | glutathione transferase AtGST 10 (emb |
| | NXSI_050_G02 | putative heat shock protein |
| | NXSI_052_B04 | GSH-dependent dehydroascorbate reductase 1, putative |
| | NXSI_057_A09 | cysteine synthase AtcysC1 |
| | NXSI_059_F07 | dehydrin Xero2 |
| | NXSI_059_G01 | putative heat shock protein |

| Category | Pine clone name | Annotation |
|---|---|---|
| | NXSI_060_A09 | aquaporin, putative |
| | NXSI_064_B04 | EMB:Q9XG70 Q9XG70 AQUAGLYCEROPORIN. >GEN:4584429 AJ237751 |
| | NXSI_067_H12 | Arabidopsis mitochondrion-localized small heat shock protein (AtHSP23.6-mito) |
| | NXSI_069_B01 | aquaporin/MIP - like protein |
| | NXSI_070_C02 | defensin ,Magpie No BF777583 |
| | NXSI_070_G12 | ascorbate oxidase-like protein |
| | NXSI_071_D07 | putative M-type thioredoxin |
| | NXSI_073_G01 | L-ascorbate oxidase precursor, putative |
| | NXSI_079_E04 | cysteine synthase - like |
| | NXSI_081_D09 | glutathione-s-transferase, putative |
| | NXSI_082_C06 | 17.6 kDa heat shock protein (AA 1-156) |
| | NXSI_085_G06 | cysteine synthase (cpACS1) |
| | NXSI_095_F07 | aquaporin/MIP - like protein |
| | NXSI_097_F02 | heat shock transcription factor-like protein |
| | NXSI_102_A02 | iron superoxide dismutase 3 (gb |
| | NXSI_104_C10 | ascorbate oxidase promoter-binding protein, putative |
| | NXSI_104_D04 | Arabidopsis mitochondrion-localized small heat shock protein (AtHSP23.6-mito) |
| | NXSI_104_D07 | membrane channel protein-like; aquaporin (tonoplast intrinsic protein)-like |
| | NXSI_106_C01 | aquaporin MIP - like protein |
| | NXSI_106_E07 | putative heat-shock protein |
| | NXSI_106_H09 | heat shock protein 90 |
| | NXSI_107_A01 | DRE binding protein (DREB1C) |
| | NXSI_107_E09 | heat shock protein 21 |
| | NXSI_107_G12 | putative aquaporin (plasma membrane intrinsic protein) |
| | NXSI_107_H09 | L-ascorbate peroxidase - like protein |
| | NXSI_110_D11 | N-hydroxycinnamoyl/benzoyltransferase-like protein |
| | NXSI_110_F03 | similar to late embryogenesis abundant proteins |

| Category | Pine clone name | Annotation |
|---|---|---|
| | NXSI_110_F05 | putative ascorbate peroxidase |
| | NXSI_112_H01 | small heat shock protein –like |
| | NXSI_116_B04 | SWP:HS82_ORYSA P33126 HEAT SHOCK PROTEIN 82. >PIR:S25541 |
| | NXSI_116_C04 | heat shock protein hsp70, putative |
| | NXSI_116_C07 | aquaporin (plasma membrane intrinsic protein 1B) |
| | NXSI_138_G09 | heat shock protein 101 (HSP101),putative |
| | NXSI_139_C05 | small heat-shock protein of cytosolic class I |
| | NXSI_140_G08 | putative [Mn] superoxide dismutase |
| | NXSI_142_B02 | aquaporin (plasma membrane intrinsic protein 2B) |
| | NXSI_142_E03 | putative glutathione transferase |
| | NXSI_145_A11 | CuZn superoxide dismutase |
| | NXSI_148_C11 | putative late embryogenesis abundant protein |
| | PC02A11 | similar to late embryogenesis abundant proteins |
| | PC03F07 | putative cold-regulated protein |
| | PC04A07 | glutathione S-transferase-like protein |
| | PC04D07 | heat shock protein 40-like |
| | PC07D03 | glutathione peroxidase -like protein |
| | PC08D03 | late embryogenesis abundant protein-like |
| | PC11A02 | putative anthranilate N-hydroxycinnamoyl/benzoyltransferase |
| | PC11H05 | similar to late embryogenesis abundant proteins |
| | PC12E10 | late-embryogenesis abundant protein, putative |
| | PC14C08 | late embryogenesis-abundant protein, putative |
| | PC15B10 | putative ascorbate peroxidase |
| | PC15C08 | GSH-dependent dehydroascorbate reductase 1-like |
| | PC18A04 | late embryogenesis abundant protein (AtECP63) |
| | PC18E09 | putative cold acclimation protein |
| | PC22B06 | glutathione transferase-like |

| Category | Pine clone name | Annotation |
|---|---|---|
| | PC23A09 | similar to late embryogenesis abundant proteins |
| | PC23F04 | glutathione transferase-like |
| | ST01B10 | metallothionein-like protein |
| | ST03F06 | putative glutathione S-transferase TSI-1 |
| | ST03G04 | "ascorbate peroxidase, putative (APX) " |
| | ST06H02 | metallothinein like protein |
| | ST07A03 | Aquaporin |
| | ST07D03 | 2,4-D inducible glutathione S-transferase, putative |
| | ST08H06 | metallothionein-like protein EMB30 |
| | ST12D10 | FKBP-type peptidyl-prolyl cis-trans isomerase, putative |
| | ST12G04 | membrane-associated salt-inducible protein isolog |
| | ST12G08 | heat shock protein 70 |
| | ST13H05 | putative heat shock protein |
| | ST14D07 | putative dehydrine |
| | ST16F12 | heat shock protein 80 |
| | ST16H07 | glutathione reductase, cytosolic |
| | ST17D07 | heat-shock protein (At-hsc70-3) |
| | ST19E02 | thioredoxin m4 |
| | ST21H08 | putative ascorbate peroxidase |
| | ST22B08 | putative heat-shock protein |
| | ST23A08 | water stress inducable proteinLp3 |
| | ST23C09 | putative plasma membrane intrinsic protein, almost identical to aquaporin PIP3 (GB:U78297) |
| | ST29D05 | putative ascorbate peroxidase |
| | ST29D06 | putative cold-regulated protein |
| | ST31D06 | putative glutathione transferase |
| | ST32A06 | heat shock protein 101 (HSP101) |
| | ST32C09 | putative late embryogenesis abundant protein |

| Category | Pine clone name | Annotation |
|---|---|---|
| | ST33E05 | FKBP-type peptidyl-prolyl cis-trans isomerase, putative |
| | ST34H09 | water stress inducable protein LP3-3 |
| | ST35A01 | metallothionine like protein |
| | ST35A07 | pseudogene, putative heat shock protein |
| | ST39A03 | heat shock protein DnaJ, putative |
| | ST39E09 | glutathione S-transferase |
| | ST40D12 | putative glutathione S-transferase |
| | ST40F04 | heat shock protein 17 |
| | ST40G02 | similar to cold acclimation protein WCOR413 [Triticum aestivum] |
| **GENE EXPRESSION** | 1G7 | putative heat-shock protein |
| | 20B2 | pseudogene, putative clpB heat shock protein |
| | NXCI_018_D01 | Zea mays acidic ribosomal protein P2a-4 |
| | NXCI_020_A02 | PIR:T09264 T09264 embryonic abundant protein EMB32 - white spruc... 84 7e-16 |
| | NXCI_020_B03 | dnaK-type molecular chaperone hsc70.1 |
| | NXCI_021_C02 | putative heat shock protein |
| | NXCI_021_G04 | PIR:T09288 T09288 late embryonic abundant protein EMB7 - white s... 184 5e-46 |
| | NXCI_022_G01 | SWP:HS7M_SOLTU Q08276 HEAT SHOCK 70 KDA PROTEIN, MITOCHONDRIAL |
| | NXCI_032_F07 | putative heat-shock protein |
| | NXCI_047_E01 | thioredoxin, putative |
| | NXCI_049_A10 | glycine-rich RNA binding protein 7 |
| | NXCI_064_H03 | thioredoxin h, putative |
| | NXCI_069_G10 | putative heat-shock protein |
| | NXCI_075_D08 | heat shock protein 70 (gb |
| | NXCI_075_F10 | putative thioredoxin |
| | NXCI_075_F11 | thioredoxin, putative |
| | NXCI_083_D04 | peptidyl-prolyl cis-trans isomerase - like protein |
| | NXCI_085_B12 | 10 kDa chaperonin (CPN10) |

| Category | Pine clone name | Annotation |
|---|---|---|
| | NXCI_118_A05 | heat shock protein 70 (gb |
| | NXCI_153_E04 | putative thioredoxin |
| | NXCI_162_C03 | putative heat-shock protein |
| | NXCI_164_H03 | immunophilin (FKBP15-1) |
| | NXLV_014_B05 | thioredoxin h |
| | NXLV_032_D05 | pseudogene, putative clpB heat shock protein |
| | NXLV_032_E03 | thioredoxin-like protein |
| | NXLV_037_G03 | 70kD heat shock protein |
| | NXLV_048_B03 | heat-shock protein, putative |
| | NXLV_049_G11 | low-molecular-weight heat shock protein - like |
| | NXLV_058_C10 | putative thioredoxin-m |
| | NXLV_059_A11 | dnaK-type molecular chaperone hsc70.1 |
| | NXLV_066_C03 | mitochondrial heat shock 22 kd protein-like |
| | NXLV_073_C11 | heat-shock protein - like |
| | NXLV_075_A12 | heat shock protein 101 (HSP101) |
| | NXLV090_C10 | thioredoxin f2 (gb |
| | NXLV103_G03 | thioredoxin, putative |
| | NXLV108_A02 | low-molecular-weight heat shock protein - like |
| | NXLV123_E04 | putative small heat shock protein |
| | NXNV_007_B09 | putative ferredoxin-thioredoxin reductase |
| | NXNV008F04 | heat shock protein 101 (HSP101),putative |
| | NXNV025B05 | heat shock protein-like protein |
| | NXNV047B02 | heat shock protein 70 (Hsc70-5) |
| | NXNV_066_E07 | heat-shock protein |
| | NXNV_070_B04 | chloroplast-localized small heat shock protein, putative |
| | NXNV_070_C09 | putative thioredoxin |
| | NXNV_070_C10 | putative thioredoxin |

| Category | Pine clone name | Annotation |
|---|---|---|
| | NXNV_081_G02 | putative thioredoxin-m |
| | NXNV_119_D12 | putative heat shock protein |
| | NXNV_120_F09 | FKBP-type peptidyl-prolyl cis-trans isomerase |
| | NXNV_123_C02 | heat shock protein 17.6-II |
| | NXNV_123_C06 | heat shock protein 70 like protein |
| | NXNV_127_F09 | peptidylprolyl isomerase ROC4 |
| | NXNV_128_D04 | putative heat-shock protein |
| | NXNV_132_E06 | EMB:Q9ZWK3 Q9ZWK3 DNAJ HOMOLOG. >GEN:4008159 AB015601 |
| | NXNV_143_H07 | heat shock cognate protein |
| | NXNV_146_C11 | heat shock protein 40-like |
| | NXNV_147_G04 | RNA-binding protein AKIP1 |
| | NXNV_149_E10 | EMB:Q9M555 Q9M555 PUTATIVE HEAT-SHOCK PROTEIN 90 (FRAGMENT) |
| | NXNV_157_G10 | putative TCP1-chaperonin cofactor A protein |
| | NXNV_160_B12 | phi-1-like protein |
| | NXNV_162_D12 | putative M-type thioredoxin |
| | NXNV_162_F01 | Thioredoxin |
| | NXNV_173_A04 | heat shock protein DnaJ, putative |
| | NXNV_187_E01 | putative thioredoxin reductase |
| | NXPV_005_H07 | heat shock protein 70 (gbAAF27639.1) |
| | NXPV_019_C12 | DNAJ-like heatshock protein |
| | NXPV_077_E08 | heat shock protein, putative |
| | NXPV_088_C02 | putative heat shock protein |
| | NXPV_102_A11 | putative peptidyl-prolyl cis-trans isomerase |
| | NXPV_102_A12 | putative peptidyl-prolyl cis-trans isomerase |
| | NXRV_003_F06 | hypothetical protein, contains DnaJ motif: prokaryotic heat shock protein motif |
| | NXRV_003_H02 | putative thioredoxin |
| | NXRV_012_C04 | FKBP-type peptidyl-prolyl cis-trans isomerase, putative |

| Category | Pine clone name | Annotation |
|---|---|---|
| | NXRV_016_G12 | heat shock protein 70 like protein |
| | NXRV_022_C02 | hypothetical protein, contains DnaJ motif: prokaryotic heat shock protein motif |
| | NXRV_022_F07 | heat shock protein (emb |
| | NXRV_027_H10 | putative thioredoxin |
| | NXRV_028_H09 | thioredoxin, putative |
| | NXRV_030_D05 | putative heat shock protein |
| | NXRV047_G07 | putative ferredoxin-thioredoxin reductase |
| | NXRV048_A07 | putative heat shock protein |
| | NXRV048_C10 | thioredoxin-like 3 |
| | NXRV059_A10 | heat shock protein 17.6-II |
| | NXRV059_C10 | heat shock protein (emb |
| | NXSI_001_E02 | heat shock protein – like |
| | NXSI_002_A04 | putative eukaryotic translation initiation factor 2 alpha subunit, eIF2 |
| | NXSI_002_H07 | putative thioredoxin reductase |
| | NXSI_011_D04 | 17.6 kDa heat shock protein (AA 1-156) |
| | NXSI_011_G01 | heat shock protein 90 |
| | NXSI_012_B12 | putative heat-shock protein |
| | NXSI_021_A06 | heat-shock protein, putative |
| | NXSI_027_B11 | heat shock protein-like protein |
| | NXSI_030_H08 | putative small heat shock protein |
| | NXSI_031_C12 | putative heat shock protein |
| | NXSI_040_C11 | putative heat shock protein |
| | NXSI_041_A02 | elongation factor 1-alpha (EF-1-alpha) |
| | NXSI_041_C09 | heat shock protein 17 |
| | NXSI_041_E09 | HEAT SHOCK PROTEIN 81-2 (HSP81-2) (spP55737) |
| | NXSI_050_G02 | putative heat shock protein |
| | NXSI_054_A01 | PIR:T09146 T09146 late-embryogenesis protein EMB11 |

| Category | Pine clone name | Annotation |
|---|---|---|
| | NXSI_059_G01 | putative heat shock protein |
| | NXSI_067_H12 | Arabidopsis mitochondrion-localized small heat shock protein (AtHSP23.6-mito) |
| | NXSI_071_D07 | putative M-type thioredoxin |
| | NXSI_082_C06 | 17.6 kDa heat shock protein (AA 1-156) |
| | NXSI_097_F02 | heat shock transcription factor-like protein |
| | NXSI_104_D04 | Arabidopsis mitochondrion-localized small heat shock protein (AtHSP23.6-mito) |
| | NXSI_106_E07 | putative heat-shock protein |
| | NXSI_106_H09 | heat shock protein 90 |
| | NXSI_107_E09 | heat shock protein 21 |
| | NXSI_112_H01 | small heat shock protein -like |
| | NXSI_116_B04 | SWP:HS82_ORYSA P33126 HEAT SHOCK PROTEIN 82 |
| | NXSI_116_C04 | heat shock protein hsp70, putative |
| | NXSI_117_C08 | PIR:T45471 T45471 dnaK-type molecular chaperone hsc70 |
| | NXSI_117_F12 | putative peptidyl-prolyl cis-trans isomerase |
| | NXSI_138_G09 | heat shock protein 101 (HSP101),putative |
| | NXSI_139_C05 | small heat-shock protein of cytosolic class I |
| | PC04D07 | heat shock protein 40-like |
| | PC08E04 | LEA76 homologue type2 |
| | PC14G04 | LEA76 homologue type2 |
| | PC23D04 | LEA76 homologue type2 |
| | ST07D12 | cytosolic ribosomal protein S11 |
| | ST07E01 | peptidylprolyl isomerase ROC1 |
| | ST08G12 | flower pigmentation protein ATAN11 |
| | ST12D10 | FKBP-type peptidyl-prolyl cis-trans isomerase, putative |
| | ST12G08 | heat shock protein 70 |
| | ST12H08 | thioredoxin, putative |
| | ST13C12 | putative peptidyl-prolyl cis-trans isomerase |

| Category | Pine clone name | Annotation |
|---|---|---|
| | ST13H05 | putative heat shock protein |
| | ST14F05 | thioredoxin, putative |
| | ST16F12 | heat shock protein 80 |
| | ST17D07 | heat-shock protein (At-hsc70-3) |
| | ST18B09 | peptidylprolyl isomerase (cyclophilin) |
| | ST19E02 | thioredoxin m4 |
| | ST20H07 | putative peptidyl-prolyl cis-trans isomerase |
| | ST21A12 | splicing factor SRZ_22 |
| | ST21E10 | thioredoxin, putative |
| | ST21F02 | eukaryotic translation initiation factor 4A (eIF4A), putative |
| | ST21F11 | elongation factor 1-alpha (EF-1-alpha) |
| | ST21G02 | thioredoxin -like protein |
| | ST22B08 | putative heat-shock protein |
| | ST25B09 | 60S ribosomal protein L27A |
| | ST25E06 | cyclophilin (CYP2) |
| | ST32A06 | heat shock protein 101 (HSP101) |
| | ST33E05 | FKBP-type peptidyl-prolyl cis-trans isomerase, putative |
| | ST35A07 | pseudogene, putative heat shock protein |
| | ST37A10 | Putative S-phase-specific ribosomal protein |
| | ST37B02 | putative thioredoxin |
| | ST37C01 | thioredoxin-like protein |
| | ST37H09 | cyclophilin (CYP2) |
| | ST38A10 | metallothionine-like prot EMB 30 |
| | ST38H03 | peptidyl proline isomerase |
| | ST39A03 | heat shock protein DnaJ, putative |
| | ST39A04 | thioredoxin -like protein |
| | ST39D09 | putative peptidyl-prolyl cis-trans isomerase |

| Category | Pine clone name | Annotation |
|---|---|---|
| | ST39H08 | peptidyl prolyl CIS-TRANS isomerase |
| | ST40F04 | heat shock protein 17 |
| **METALS** | NXCI_115_E03 | iron-regulated transporter - like protein |
| | NXNV047E01 | copper transport protein - like |
| | NXNV_151_E03 | putative zinc transporter ZIP2 - like |
| | NXPV_019_B07 | cadmium-transporting ATPase-like protein |
| | NXPV_077_C06 | cadmium-transporting ATPase-like protein |
| | NXPV_078_B04 | chromaffin granule ATPase II homolog, putative |
| | NXRV_030_D06 | copper transport protein - like |
| | NXSI_039_A10 | metal ion transporter |
| | ST16G06 | Mn2+ and Fe2+ transporters the nramp family ,Magpie No AW011104 |
| | ST16G08 | putative metal ion transporter (NRAMP) |
| **MITOCHONDRION** | 18F4 | NADH:ubiquinone oxidoreductase, putative |
| | 1F7 | putative superoxide-generating NADPH oxidase flavocytochrome |
| | 23C11 | ubiquinol-cytochrome C reductase complex ubiquinone-binding protein (QP-C)-like protein |
| | NXCI_008_D02 | ubiquinol-cytochrome C reductase complex ubiquinone-binding protein (QP-C)-like protein |
| | NXCI_026_C06 | cytochrome b5, putative |
| | NXCI_064_H09 | NADH-ubiquinone oxidoreductase |
| | NXCI_070_C02 | putative ubiquinol-cytochrome C reductase complex ubiquinone-binding protein (QP-C) |
| | NXCI_081_F07 | NADH-ubiquinone oxidoreductase |
| | NXCI_108_B12 | cytochrome c |
| | NXCI_129_D09 | cytochrome b245 beta chain homolog RbohAp108, putative |
| | NXLV_049_A02 | ubiquinol--cytochrome-c reductase - like protein |
| | NXLV_057_E12 | ubiquinol--cytochrome-c reductase - like protein |
| | NXLV109_A08 | putative cytochrome c oxidase Vc subunit |

| Category | Pine clone name | Annotation |
|---|---|---|
| | NXLV111_G05 | cytochrome C oxidase assembly protein, putative |
| | NXLV115_G05 | cytochrome c |
| | NXLV120_G12 | putative cytochrome oxidase biogenesis protein |
| | NXLV129_H09 | putative ubiquinol--cytochrome-c reductase |
| | NXNV027G09 | cytochrome c oxidase subunit - like |
| | NXNV046A05 | putative cytochrome b5 |
| | NXNV_132_B09 | cytochrome c oxidase subunit, putative |
| | NXNV_147_B12 | cytochrome-b5 reductase - like protein |
| | NXPV_008_G04 | cytochrome c oxidoreductase like protein |
| | NXRV_004_C07 | cytochrome c oxidoreductase like protein |
| | NXRV_008_E10 | NADH:ubiquinone oxidoreductase, putative |
| | NXRV_026_H12 | putative cytochrome c oxidase subunit Vb |
| | NXRV045_A10 | cytochrome c oxidase subunit, putative |
| | NXRV049_G03 | ubiquinol--cytochrome-c reductase-like protein |
| | NXRV_057_D08 | cytochrome b5 |
| | NXSI_011_F10 | putative fatty acid desaturase/cytochrome b5 fusion protein |
| | NXSI_042_A08 | putative cytochrome c oxidase subunit Vb |
| | NXSI_049_H07 | mitochondrial F1-ATPase, gamma subunit (ATP3_ARATH) |
| | NXSI_067_E07 | cytochrome b5 (dbj |
| | NXSI_076_D02 | putative fatty acid desaturase/cytochrome b5 fusion protein |
| | NXSI_079_G09 | cytochrome b5, putative |
| | NXSI_102_H10 | ubiquinol--cytochrome-c reductase-like protein |
| | NXSI_105_C11 | putative cytochrome c oxidase Vc subunit |
| | NXSI_108_C10 | ubiquinol-cytochrome c reductase - like protein |
| | NXSI_115_G09 | NADH:ubiquinone oxidoreductase - like protein |
| | NXSI_116_E10 | cytochrome c1 precursor |
| | PC09A10 | epsilon subunit of mitochondrial F1-ATPase |

| Category | Pine clone name | Annotation |
|---|---|---|
| | PC09E04 | cytochrome b5 (dbj |
| | PC11D12 | putative ubiquinol-cytochrome C reductase complex ubiquinone-binding protein (QP-C) |
| | PC15B05 | cytochrome c oxidase subunit - like |
| | PC22C10 | putative ubiquinol--cytochrome-c reductase |
| | ST12H04 | cytochrome c1 precursor |
| | ST17C05 | delta subunit of mitochondrial F1-ATPase |
| | ST18E03 | NADH:ubiquinone oxidoreductase - like protein |
| | ST22C06 | NADH-cytochrome b5 reductase |
| | ST23C02 | ubiquinol-cytochrome c reductase - like protein |
| | ST31D11 | NADH-cytochrome b5 reductase |
| **NITROGEN AND SULFUR METABOLISM** | 1C11 | putative s-adenosylmethionine synthetase |
| | 2H7 | amino acid permease-like protein; proline transporter-like protein |
| | 3G3 | putative phosphoserine aminotransferase |
| | NXCI_005_B05 | chorismate mutase/prephenate dehydratase-like protein |
| | NXCI_006_D07 | glutamine synthetase, putative |
| | NXCI_007_F10 | pyrroline-5-carboxylate reductase |
| | NXCI_016_F11 | putative chloroplast prephenate dehydratase |
| | NXCI_017_E03 | putative s-adenosylmethionine synthetase |
| | NXCI_022_A07 | s-adenosylmethionine synthetase |
| | NXCI_022_C01 | homocysteine S-methyltransferase AtHMT-2 |
| | NXCI_026_B11 | Putative NADP-dependent oxidoreductases ,Magpie No BE582198 |
| | NXCI_026_F05 | putative glycine dehydrogenase |
| | NXCI_026_F11 | glutamine synthetase, putative |
| | NXCI_034_E01 | 2-dehydro-3-deoxyphosphoheptonate aldolase |
| | NXCI_044_B11 | pseudogene, phospho-2-dehydro-3-deoxyheptonate aldolase |
| | NXCI_044_F12 | arginine decarboxylase |
| | NXCI_047_C05 | 2-dehydro-3-deoxyphosphoheptonate aldolase |

| Category | Pine clone name | Annotation |
|---|---|---|
| | NXCI_047_H05 | polyamine oxidase |
| | NXCI_049_B04 | aspartate aminotransferase |
| | NXCI_050_B05 | pyrroline-5-carboxylate reductase |
| | NXCI_053_F05 | 2-dehydro-3-deoxyphosphoheptonate aldolase |
| | NXCI_055_A01 | cysteine synthase - like |
| | NXCI_055_C02 | putative aspartate aminotransferase |
| | NXCI_058_H04 | delta-1-pyrroline 5-carboxylase synthetase (P5C1) |
| | NXCI_062_B10 | PIR:T14866 T14866 probable gamma-thionin precursor SPI1 |
| | NXCI_068_G02 | 2-dehydro-3-deoxyphosphoheptonate aldolase |
| | NXCI_069_F04 | asparagine synthetase ASN3 |
| | NXCI_070_B12 | cysteine synthase AtcysC1 |
| | NXCI_085_B09 | Predicted NAD-dependent oxidoreductase ,Magpie No BF010518 |
| | NXCI_086_H02 | 2-dehydro-3-deoxyphosphoheptonate aldolase |
| | NXCI_095_E03 | nitrate reductase, putative |
| | NXCI_097_C12 | ADC-O arginine decarboxylase (spe2) gene |
| | NXCI_101_C01 | 5-enolpyruvylshikimate-3-phosphate (EPSP) synthase, putative |
| | NXCI_101_H05 | putative chorismate mutase/prephenate dehydratase |
| | NXCI_123_G08 | chorismate mutase |
| | NXCI_124_H09 | aspartate aminotransferase (Asp3) |
| | NXCI_125_A09 | 5-methyltetrahydropteroyltriglutamate-homocysteine S-methyltransferase - like protein |
| | NXCI_125_E08 | sulfate transporter |
| | NXCI_127_G06 | arginine decarboxylase |
| | NXCI_156_F04 | S-adenosylmethionine decarboxylase, putative |
| | NXLV_024_B06 | spermidine synthase |
| | NXLV_040_G04 | arginine decarboxylase |
| | NXLV_047_F12 | aminotransferase, putative |
| | NXLV_051_G05 | cytoplasmic aconitate hydratase |

| Category | Pine clone name | Annotation |
|---|---|---|
| | NXLV_052_B09 | tetrahydrofolylpolyglutamate synthase-like protein |
| | NXLV_053_H11 | cytoplasmatic aconitate hydratase (citrate hydro-lyase)(aconitase)(EC 4.2.1.3) |
| | NXLV_068_E03 | nitrate transporter NTL1, putative |
| | NXLV_068_H07 | putative nitrate transporter |
| | NXLV_069_F03 | cysteine synthase |
| | NXLV_073_C01 | aminotransferase, putative |
| | NXLV_080_H04 | tRNA-glutamine synthetase, putative |
| | NXLV082_B07 | Alanine aminotransferase |
| | NXLV085_F06 | Thioredoxin reductase ,Magpie No BQ107019 |
| | NXLV099_D04 | phosphoribosylanthranilate transferase, putative |
| | NXLV107_A05 | putative methionine synthase |
| | NXLV109_E07 | putative methionine synthase |
| | NXNV001E03 | Phosphoribosylanthranilate transferase |
| | NXNV002B01 | 5-methyltetrahydropteroyltriglutamate--homocysteine S-methyltransferase |
| | NXNV012H04 | cysteine synthase |
| | NXNV015B07 | arginine decarboxylase SPE2 |
| | NXNV025D09 | putative phosphoribosylanthranilate transferase |
| | NXNV060H10 | 5-enolpyruvylshikimate-3-phosphate (EPSP) synthase |
| | NXNV_071_E12 | 2-dehydro-3-deoxyphosphoheptonate aldolase |
| | NXNV_073_E01 | cysteine synthase (cpACS1) |
| | NXNV_075_H05 | lysine decarboxylase-like protein |
| | NXNV_077_H04 | putative sulfite oxidase |
| | NXNV_085_D12 | 3-isopropylmalate dehydratase, small subunit |
| | NXNV_085_E08 | chorismate mutase CM2 |
| | NXNV_089_B07 | alanine aminotransferase, putative |
| | NXNV_096_E04 | ADC-O arginine decarboxylase (spe2) gene |
| | NXNV_105_G04 | aspartate aminotransferase Asp2 |

| Category | Pine clone name | Annotation |
|---|---|---|
| | NXNV_123_C11 | branched-chain amino acid aminotransferase, putative |
| | NXNV_124_C05 | cysteine synthase |
| | NXNV_125_E12 | aspartate aminotransferase (AAT1) |
| | NXNV_132_F03 | aspartate aminotransferase |
| | NXNV_134_E07 | pseudogene, phospho-2-dehydro-3-deoxyheptonate aldolase |
| | NXNV_135_A05 | Phosphoribosylanthranilate transferase |
| | NXNV_136_C09 | 3 hydroxyisobutyryl coenzyme A hydrolase ,Magpie No AW985423 |
| | NXNV_136_H03 | aspartate aminotransferase |
| | NXNV_136_H04 | aspartate aminotransferase |
| | NXNV_143_G05 | cytoplasmic malate dehydrogenase |
| | NXNV_150_B07 | lysine decarboxylase-like protein |
| | NXNV_159_G04 | amino acid transporter |
| | NXNV_162_F11 | malate dehydrogenase - like protein |
| | NXNV_164_D12 | cysteine synthase |
| | NXNV_164_G08 | 3-deoxy-D-arabino-heptulosonate 7-phosphate, putative |
| | NXNV_166_C11 | Thioredoxin |
| | NXPV_002_D09 | polyamine oxidase, putative |
| | NXPV_002_F03 | glutamine-dependent asparagine synthetase |
| | NXPV_003_G08 | glutamate-1-semialdehyde 2,1-aminomutase 1 precursor (GSA 1) |
| | NXPV_004_F05 | tyrosine aminotransferase |
| | NXPV_005_D11 | arginine decarboxylase |
| | NXPV_010_C07 | serine acetyltransferase (Sat-1) |
| | NXPV_010_G03 | glutamine synthetase, putative |
| | NXPV_011_D04 | sulfate transporter, putative |
| | NXPV_012_C02 | putative P-protein: chorismate mutase, prephenate dehydratase |
| | NXPV_015_A06 | 5-methyltetrahydropteroyltriglutamate-homocysteine S-methyltransferase - like protein |
| | NXPV_015_D01 | putative sulfate transporter |

| Category | Pine clone name | Annotation |
|---|---|---|
| | NXPV_021_B10 | proline transporter 2 |
| | NXPV_023_F09 | branched-chain amino acid aminotransferase |
| | NXPV_027_C02 | putative phosphoribosylanthranilate transferase |
| | NXPV_086_E04 | chorismate synthase, putative |
| | NXPV_098_A06 | putative shikimate kinase precursor |
| | NXPV_112_B04 | putative peptide/amino acid transporter |
| | NXRV_015_A04 | putative aminotransferase |
| | NXRV_029_H05 | phosphoribosylanthranilate transferase, putative |
| | NXRV_036_H05 | nitrate transporter NTL1, putative |
| | NXRV_040_C06 | 3-isopropylmalate dehydratase, small subunit |
| | NXRV047_G01 | 2-isopropylmalate synthase, putative |
| | NXRV054_C09 | S-adenosylmethionine synthase 2 |
| | NXRV054_F05 | S-adenosylmethionine synthase 2 |
| | NXSI_003_C01 | alanine aminotransferase, putative |
| | NXSI_007_H09 | asparagine synthetase (gb |
| | NXSI_011_B02 | asparagine synthetase ASN3 |
| | NXSI_013_A11 | aspartate aminotransferase (Asp3) |
| | NXSI_021_E03 | cysteine synthase (cpACS1) |
| | NXSI_023_H11 | cytoplasmatic aconitate hydratase (citrate hydro-lyase)(aconitase)(EC 4.2.1.3) |
| | NXSI_037_A11 | putative aspartate aminotransferase |
| | NXSI_038_A10 | amino acid permease-like protein; proline transporter-like protein |
| | NXSI_039_C08 | putative nitrate transporter |
| | NXSI_040_F12 | malate dehydrogenase - like protein |
| | NXSI_043_D06 | putative alanine aminotransferase |
| | NXSI_045_E07 | branched-chain amino acid aminotransferase, putative |
| | NXSI_048_D06 | cytosolic malate dehydrogenase |
| | NXSI_052_A04 | putative phosphoribosylanthranilate transferase |

| Category | Pine clone name | Annotation |
|---|---|---|
| | NXSI_053_D05 | NADH-dependent glutamate synthase |
| | NXSI_057_A09 | cysteine synthase AtcysC1 |
| | NXSI_071_A05 | putative phosphoribosylanthranilate transferase |
| | NXSI_076_H01 | putative proline transporter |
| | NXSI_079_E04 | cysteine synthase – like |
| | NXSI_083_D07 | cystathionine gamma-synthase, putative |
| | NXSI_085_G06 | cysteine synthase (cpACS1) |
| | NXSI_085_G08 | amino acid transporter AAP4 (pir |
| | NXSI_088_F04 | sulfate transporter |
| | NXSI_088_H01 | chorismate mutase |
| | NXSI_089_E03 | phosphoserine aminotransferase |
| | NXSI_091_F07 | phosphoribosylanthranilate transferase-like protein |
| | NXSI_093_D07 | chorismate mutase/prephenate dehydratase-like protein |
| | NXSI_099_F06 | aspartate aminotransferase |
| | NXSI_099_F10 | S-adenosylmethionine decarboxylase |
| | NXSI_104_B08 | cytosolic malate dehydrogenase |
| | NXSI_104_E11 | ornithine aminotransferase |
| | NXSI_106_G06 | putative sulfite oxidase |
| | NXSI_107_H06 | sulfate transporter ATST1 |
| | NXSI_110_C01 | s-adenosylmethionine synthetase |
| | NXSI_110_D09 | dihydroxyacid dehydratase, putative |
| | NXSI_114_F08 | putative cystathionine gamma-synthase |
| | NXSI_138_A06 | tryptophan synthase beta chain |
| | NXSI_139_B10 | putative shikimate kinase precursor |
| | NXSI_142_B01 | proline transporter 1 |
| | PC04H09 | putative proline transporter |
| | PC06C10 | putative amino acid transport protein |

| Category | Pine clone name | Annotation |
|---|---|---|
| | ST04E04 | serine acetyltransferase |
| | ST04G02 | putative phosphoribosylanthranilate transferase |
| | ST14E11 | aspartate aminotransferase (AAT1) |
| | ST15A11 | glutamine synthetase, putative |
| | ST17E04 | putative phosphoserine aminotransferase |
| | ST19B09 | proline transporter 2 |
| | ST20D09 | methionine/cystathionine gamma lyase, putative |
| | ST21H03 | putative s-adenosylmethionine synthetase |
| | ST22D05 | similar to UP\|Q93XV7, Hydroxypyruvate reductase |
| | ST22H02 | putative phosphoribosylanthranilate transferase |
| | ST22H08 | high affinity nitrate transporter protein – like |
| | ST23E03 | putative sulfate transporter |
| | ST27B01 | cytosolic malate dehydrogenase |
| | ST28D11 | chorismate mutase CM2 |
| | ST30F10 | putative phosphoribosylanthranilate transferase |
| | ST31A11 | ornithine aminotransferase |
| | ST32H12 | 2-dehydro-3-deoxyphosphoheptonate aldolase |
| | ST39C04 | glycosylasparaginase - like protein |
| **NUCLEUS** | NXNV_132_E02 | histone H2A.F |
| | NXNV_135_C04 | putative DNA-binding protein |
| | NXNV_159_D07 | Putative retroelement |
| | ST37B11 | Histon H3 |
| **OSMOLYTES** | 2H7 | amino acid permease-like protein; proline transporter-like protein |
| | NXCI_007_F10 | pyrroline-5-carboxylate reductase |
| | NXCI_050_B05 | pyrroline-5-carboxylate reductase |
| | NXCI_058_H04 | delta-1-pyrroline 5-carboxylase synthetase (P5C1) |
| | NXCI_101_D04 | phosphatidylinositol/phosphatidylcholine transfer protein, putative |

| Category | Pine clone name | Annotation |
|---|---|---|
| | NXCI_115_G03 | putative choline kinase |
| | NXCI_121_G02 | phosphatidylinositol/phosphatidylcholine transfer protein, putative |
| | NXPV_021_B10 | proline transporter 2 |
| | NXSI_038_A10 | amino acid permease-like protein; proline transporter-like protein |
| | NXSI_076_H01 | putative proline transporter |
| | NXSI_085_E07 | betaine aldehyde dehydrogenase, putative |
| | NXSI_114_E07 | betaine aldehyde dehydrogenase, putative |
| | NXSI_142_B01 | proline transporter 1 |
| | PC04H09 | putative proline transporter |
| | ST19B09 | proline transporter 2 |
| **PHENYLPROPANOID PATHWAY** | 20F6 | putative cytochrome P450 |
| | NXCI_005_B05 | chorismate mutase/prephenate dehydratase-like protein |
| | NXCI_005_C10 | putative laccase (diphenol oxidase) |
| | NXCI_005_E02 | laccase, putative |
| | NXCI_006_E08 | laccase - like protein |
| | NXCI_028_G01 | laccase-like protein |
| | NXCI_045_E06 | phenylalanine ammonia lyase (PAL1) |
| | NXCI_048_D06 | N-hydroxycinnamoyl/benzoyltransferase |
| | NXCI_048_H09 | cytochrome P450-like protein |
| | NXCI_054_E03 | ATP citrate-lyase, putative |
| | NXCI_056_E08 | 4-coumarate:CoA ligase 3 |
| | NXCI_068_D11 | putative laccase (diphenol oxidase) |
| | NXCI_069_H04 | ATP citrate-lyase, putative |
| | NXCI_070_F06 | cytochrome p450 like protein |
| | NXCI_075_B08 | 4-coumarate:CoA ligase 3 |
| | NXCI_075_H12 | flavanone 3-hydroxylase, putative |
| | NXCI_076_D08 | ATP citrate-lyase, putative |

| Category | Pine clone name | Annotation |
|---|---|---|
| | NXCI_081_F08 | putative phenylalanine ammonia-lyase |
| | NXCI_084_G04 | phenylalanine ammonia-lyase PAL3 |
| | NXCI_086_B04 | ATP citrate-lyase, putative |
| | NXCI_086_C09 | 4-coumarate--CoA ligase -like protein |
| | NXCI_095_F09 | S-adenosyl-L-methionine:salicylic acid carboxyl methyltransferase-like protein |
| | NXCI_098_F08 | cytochrome P450 |
| | NXCI_098_F10 | chalcone isomerase |
| | NXCI_101_H05 | putative chorismate mutase/prephenate dehydratase |
| | NXCI_115_C07 | cytochrome P450, putative |
| | NXCI_117_C04 | putative cytochrome P450 |
| | NXCI_122_H06 | laccase (diphenol oxidase), putative |
| | NXCI_123_G08 | chorismate mutase |
| | NXCI_135_C12 | S-adenosyl-L-methionine:salicylic acid carboxyl methyltransferase-like protein |
| | NXCI_136_E11 | 4-coumarate:CoA ligase 1 |
| | NXCI_147_A06 | putative 4-coumarate:CoA ligase 2 |
| | NXCI_149_C10 | N-hydroxycinnamoyl/benzoyltransferase - like protein |
| | NXCI_150_H07 | laccase (diphenol oxidase), putative |
| | NXCI_153_B03 | ATP citrate-lyase, putative |
| | NXCI_155_E08 | phenylalanine ammonia-lyase |
| | NXCI_156_F01 | cytochrome P450-like protein |
| | NXCI_157_B03 | phenylalanine ammonia-lyase |
| | NXLV_013_D11 | 4-coumarate:coenzyme A ligase, putative |
| | NXLV_013_F09 | putative anthranilate N-hydroxycinnamoyl/benzoyltransferase |
| | NXLV_030_C10 | ATP citrate lyase, putative |
| | NXLV_034_H02 | pseudogene, cytochrome P450 (fragment) |
| | NXLV_064_D09 | ATP citrate lyase |
| | NXLV_064_F10 | N-hydroxycinnamoyl benzoyltransferase - like protein |

| Category | Pine clone name | Annotation |
|---|---|---|
| | NXLV_070_E09 | cytochrome P450, putative |
| | NXLV_077_H10 | cytochrome P450-like protein |
| | NXLV083_C05 | cytochrome P450-like |
| | NXLV103_E01 | putative gibberellin 3 beta-hydroxylase |
| | NXLV103_F06 | 4-coumarate:CoA ligase 1 |
| | NXLV107_D10 | cytochrome p450 like protein |
| | NXLV134_H07 | chalcone synthase (naringenin-chalcone synthase) (testa 4 protein) |
| | NXNV006D11 | putative cytochrome P450 |
| | NXNV006G04 | putative chalcone synthase |
| | NXNV009G04 | cytochrome P450-like |
| | NXNV046B12 | chalcone synthase - like protein |
| | NXNV052F10 | cinnamoyl CoA reductase, putative |
| | NXNV_066_B07 | putative laccase |
| | NXNV_066_E09 | isoflavone reductase, putative |
| | NXNV_085_E08 | chorismate mutase CM2 |
| | NXNV_123_A03 | chalcone isomerase |
| | NXNV_124_A07 | ferulate-5-hydroxylase (FAH1) |
| | NXNV_126_H07 | cytochrome P450 - like protein |
| | NXNV_127_E04 | pinoresinol-lariciresinol reductase TH2 |
| | NXNV_129_F04 | CYTOCHROME P450 - like protein |
| | NXNV_132_C06 | ATP citrate lyase |
| | NXNV_132_E10 | 4-coumarate--CoA ligase - like protein |
| | NXNV_133_B02 | hyoscyamine 6-dioxygenase hydroxylase, putative |
| | NXNV_162_G05 | laccase precursor - like |
| | NXNV_181_B12 | cytochrome P450, putative |
| | NXNV_98_G10 | cytochrome P450-like protein |
| | NXPV_003_G07 | putative flavanone 3-beta-hydroxylase |

| Category | Pine clone name | Annotation |
|---|---|---|
| | NXPV_005_H12 | putative S-adenosyl-L-methionine:trans-caffeoyl-Coenzyme A 3-O-methyltransferase |
| | NXPV_006_D09 | putative S-adenosyl-L-methionine:trans-caffeoyl-Coenzyme A 3-O-methyltransferase |
| | NXPV_007_E07 | pseudogene, N-hydroxycinnamoyl/benzoyltransferase |
| | NXPV_012_C02 | putative P-protein: chorismate mutase, prephenate dehydratase |
| | NXPV_014_G06 | ATP citrate-lyase, putative |
| | NXPV_016_E02 | cytochrome P450 - like protein |
| | NXPV_038_E07 | pseudogene, N-hydroxycinnamoyl/benzoyltransferase |
| | NXPV_066_G08 | cytochrome P450, putative |
| | NXPV_072_H05 | putative flavanone 3-beta-hydroxylase |
| | NXPV_086_E04 | chorismate synthase, putative |
| | NXPV_091_A10 | cytochrome P450 |
| | NXPV_094_D03 | flavanone 3-hydroxylase, putative |
| | NXPV_094_H06 | flavanone 3-hydroxylase, putative |
| | NXPV_095_D09 | 4-coumarate-CoA ligase-like protein |
| | NXPV_113_E05 | cytochrome P450 - like protein |
| | NXRV_003_A06 | cytochrome P450, putative |
| | NXRV_033_A06 | cinnamoyl CoA reductase, puitative |
| | NXSI_008_D09 | putative phenylalanine ammonia-lyase |
| | NXSI_012_F04 | cinnamate-4-hydroxylase |
| | NXSI_036_B01 | putative cinnamoyl CoA reductase |
| | NXSI_041_B05 | cytochrome P450, putative |
| | NXSI_050_D04 | cinnamate-4-hydroxylase |
| | NXSI_051_D09 | phenylalanine ammonia-lyase PAL3 |
| | NXSI_056_H05 | cytochrome P450 - like protein |
| | NXSI_057_D07 | flavanone 3-hydroxylase-like protein |
| | NXSI_058_B12 | putative cytochrome P450 |

| Category | Pine clone name | Annotation |
|---|---|---|
| | NXSI_059_F06 | CYTOCHROME P450-like protein |
| | NXSI_070_A12 | cytochrome P450 monooxygenase, putative |
| | NXSI_088_H01 | chorismate mutase |
| | NXSI_090_D08 | cytochrome P450, putative |
| | NXSI_092_E06 | putative cytochrome P450 |
| | NXSI_093_D07 | chorismate mutase/prephenate dehydratase-like protein |
| | NXSI_097_A09 | flavanone 3-hydroxylase (FH3) |
| | NXSI_097_A11 | chalcone synthase (naringenin-chalcone synthase) (testa 4 protein) (sp |
| | NXSI_101_F05 | flavanone 3-hydroxylase, putative |
| | NXSI_106_D11 | putative cytochrome P450 |
| | NXSI_106_F02 | putative cytochrome P450 |
| | NXSI_107_A08 | 4-coumarate:coenzyme A ligase, putative |
| | NXSI_110_D11 | N-hydroxycinnamoyl/benzoyltransferase-like protein |
| | NXSI_139_E05 | cytochrome P450 GA3 |
| | NXSI_142_A01 | cytochrome P450 monooxygenase, putative |
| | NXSI_144_B02 | CYTOCHROME P450-like protein |
| | NXSI_145_G07 | chalcone synthase - like protein |
| | NXSI_147_E12 | flavonoid 3,5-hydroxylase like protein |
| | PC04G01 | cinnamoyl-CoA reductase - like protein |
| | PC05D10 | cinnamoyl CoA reductase, puitative |
| | PC05H11 | probable cytochrome P450 |
| | PC07B01 | 4-coumarate-CoA ligase - like |
| | PC11A02 | putative anthranilate N-hydroxycinnamoyl/benzoyltransferase |
| | PC14B06 | hyoscyamine 6-dioxygenase hydroxylase, putative |
| | PC14E11 | ATP citrate-lyase, putative |
| | PC20C06 | cinnamoyl CoA reductase, putative |
| | ST08G12 | flower pigmentation protein ATAN11 |

| Category | Pine clone name | Annotation |
|---|---|---|
| | ST12C06 | putative cytochrome P450 |
| | ST17E09 | cytochrome P450, putative |
| | ST17G12 | putative cytochrome P450 monooxygenase |
| | ST18B12 | putative cytochrome P450 |
| | ST22B11 | ATP citrate-lyase, putative |
| | ST23A11 | Chalcone isomerase ,Magpie No AW042662 |
| | ST26H07 | Flavonol reductase/cinnamoyl-CoA reductase ,Magpie No AW042907 |
| | ST28D11 | chorismate mutase CM2 |
| | ST29E05 | flavanone 3-hydroxylase (FH3) |
| | ST30E11 | cytochrome P450 - like protein |
| | ST32B07 | cytochrome P450 GA3 |
| **PHOSPHATE ASSOCIATED** | NXCI_057_A12 | mitochondrial phosphate transporter |
| | NXLV_040_B09 | putative phosphate transporter |
| | NXNV_105_H10 | putative phosphate transporter |
| | NXSI_050_A01 | mitochondrial phosphate transporter |
| | NXSI_149_E09 | putative Na+-dependent inorganic phosphate cotransporter |
| | ST13A07 | putative phosphate transporter |
| | ST33E11 | phosphate transporter (AtPT2) |
| **PHOTORESPIRATION** | 11C11 | putative hydroxymethyltransferase |
| | NXCI_115_A02 | phosphoglycerate kinase, putative |
| | NXNV001A10 | glycine hydroxymethyltransferase - like protein |
| | NXNV003E11 | 2-oxoglutarate/malate translocator precursor -like protein |
| | NXNV_132_D12 | phosphoglycerate kinase, putative |
| | NXPV_001_H08 | glycine hydroxymethyltransferase like protein |
| | NXRV_029_C09 | glycine hydroxymethyltransferase - like protein |
| | NXRV045_D07 | glycine hydroxymethyltransferase like protein |
| | NXRV046_H03 | glycine hydroxymethyltransferase, putative |

| Category | Pine clone name | Annotation |
|---|---|---|
| | NXRV050_D09 | hydroxymethyltransferase |
| | NXRV055_D02 | hydroxymethyltransferase |
| | NXRV055_E12 | putative hydroxymethyltransferase |
| | NXRV056_B11 | glycine decarboxylase complex H-protein |
| | NXRV058_B08 | glycine decarboxylase complex H-protein |
| | NXSI_008_D06 | glycine hydroxymethyltransferase (EC 2.1.2.1) - like protein |
| | NXSI_059_F04 | glycine hydroxymethyltransferase - like protein |
| | NXSI_110_D05 | glycine hydroxymethyltransferase - like protein |
| | NXSI_115_A03 | glycine decarboxylase complex H-protein |
| | NXSI_116_B12 | 2-oxoglutarate/malate translocator |
| | ST04A02 | oxoglutarate/malate translocator-like protein |
| | ST22D05 | similar to UP\|Q93XV7, Hydroxypyruvate reductase |
| | ST36G06 | glycolate oxidase - like protein |
| **PLANT GROWTH REGULATION** | 1C11 | putative s-adenosylmethionine synthetase |
| | NXCI_002_C10 | EMB:Q9XEL3 Q9XEL3 PUTATIVE DEHYDRIN. >GEN:4704603 AF109916 |
| | NXCI_002_D03 | MADS-box protein |
| | NXCI_006_H04 | PIR:T09264 T09264 embryonic abundant protein EMB32 |
| | NXCI_008_G01 | NAM (no apical meristem)-like protein |
| | NXCI_017_B04 | ACC oxidase, putative |
| | NXCI_017_E03 | putative s-adenosylmethionine synthetase |
| | NXCI_020_A02 | PIR:T09264 T09264 embryonic abundant protein EMB32 |
| | NXCI_020_B09 | auxin response factor, putative |
| | NXCI_021_G04 | PIR:T09288 T09288 late embryonic abundant protein EMB7 |
| | NXCI_022_A07 | s-adenosylmethionine synthetase |
| | NXCI_026_B08 | auxin response transcription factor |
| | NXCI_047_E01 | thioredoxin, putative |
| | NXCI_054_F11 | homeotic protein AGL30 |

| Category | Pine clone name | Annotation |
|---|---|---|
| | NXCI_064_H03 | thioredoxin h, putative |
| | NXCI_075_H04 | ACC oxidase, putative |
| | NXCI_082_E07 | putative 1-aminocyclopropane-1-carboxylate |
| | NXCI_095_D03 | ethylene responsive element binding factor 3 (AtERF3) |
| | NXCI_124_G09 | auxin response transcription factor |
| | NXCI_133_G11 | putative MADS-box protein |
| | NXCI_151_A10 | MADS-box protein |
| | NXCI_153_E04 | putative thioredoxin |
| | NXLV_014_B05 | thioredoxin h |
| | NXLV_017_H01 | MADS-box protein (AGL20) |
| | NXLV_020_G04 | putative indole-3-glycerol phosphate synthase |
| | NXLV_032_E03 | thioredoxin-like protein |
| | NXLV_049_F01 | homeotic protein, putative |
| | NXLV_053_D10 | putative lipoxygenase |
| | NXLV_072_D02 | indole-3-glycerol phosphate synthase |
| | NXLV091_G10 | auxin response transcription factor |
| | NXLV103_E01 | putative gibberellin 3 beta-hydroxylase |
| | NXLV108_G07 | auxin response transcription factor (ARF7) |
| | NXLV114_G01 | homeotic protein (ATK1) |
| | NXLV114_G02 | homeotic protein (ATK1) |
| | NXLV118_D02 | similar to late embryogenesis abundant proteins |
| | NXLV122_B08 | homeotic protein (ATK1) |
| | NXNV_002_B06 | putative amino-cyclopropane-carboxylic acid oxidase (ACC oxidase) |
| | NXNV008B07 | auxin response factor 1, putative |
| | NXNV012G01 | UDP-glucose:indole-3-acetate beta-D-glucosyltransferase, putative |
| | NXNV019E08 | UDP-glucose:indole-3-acetate beta-D-glucosyltransferase, putative |
| | NXNV027D05 | 12-oxophytodienoate reductase (OPR2) |

| Category | Pine clone name | Annotation |
|---|---|---|
| | NXNV046E03 | dehydrin Xero2 |
| | NXNV_065_B12 | NAM(no apical meristem) protein, putative |
| | NXNV_120_E06 | root hair defective, putative |
| | NXNV_124_G04 | auxin response factor, putative |
| | NXNV_126_F05 | NAM(no apical meristem) protein, putative |
| | NXNV_134_E05 | similar to auxin-regulated protein |
| | NXNV_134_G01 | MADS-box protein (AGL20) |
| | NXNV_156_B02 | auxin response factor, putative |
| | NXNV_162_F01 | thioredoxin |
| | NXNV_164_D05 | IAA-amino acid hydrolase (ILR1) |
| | NXNV_165_C07 | putative amino-cyclopropane-carboxylic acid oxidase (ACC oxidase) |
| | NXNV_76_C05 | putative MADS box protein |
| | NXPV_002_C11 | auxin response factor-like protein |
| | NXPV_003_B06 | auxin response transcription factor (ARF9) |
| | NXPV_013_D07 | putative MADS-box protein |
| | NXPV_015_B02 | gibberellin 3 beta-hydroxylase, putative |
| | NXPV_020_D12 | floral homeotic protein agamous (AGAMOUS) |
| | NXPV_021_A10 | floral homeotic protein AGL15 (sp |
| | NXPV_026_C06 | lipoxygenase |
| | NXPV_038_B10 | NAM(no apical meristem) protein, putative |
| | NXPV_066_C06 | putative MADS-box protein |
| | NXPV_073_B11 | NAM-like protein (no apical meristem) |
| | NXPV_080_A07 | NAM (no apical meristem)-like protein |
| | NXPV_086_B02 | NAM (no apical meristem)-like protein |
| | NXPV_091_A12 | EREBP - like protein |
| | NXPV_098_A03 | 12-oxophytodienoate reductase (OPR1) |
| | NXPV_101_E03 | NAM (no apical meristem)-like protein |

| Category | Pine clone name | Annotation |
|---|---|---|
| | NXPV_103_H06 | NAM (no apical meristem)-like protein |
| | NXPV_113_F01 | auxin response transcription factor(ARF6) |
| | NXPV_129_D08 | NAM (no apical meristem)-like protein |
| | NXPV_129_D09 | NAM (no apical meristem)-like protein |
| | NXRV_003_G10 | putative lipoxygenase |
| | NXRV_015_D05 | cytochrome P450 |
| | NXRV_021_C01 | ethylene-responsive element binding factor 12(AtERF12) |
| | NXRV_027_H10 | putative thioredoxin |
| | NXRV_028_H09 | thioredoxin, putative |
| | NXRV_032_H04 | LFY floral meristem identity control protein |
| | NXRV048_C10 | thioredoxin-like 3 |
| | NXRV049_A09 | putative indole-3-glycerol phosphate synthase |
| | NXRV050_D03 | putative MADS box protein |
| | NXRV056_E10 | auxin response transcription factor |
| | NXRV_057_A06 | auxin response transcription factor |
| | NXSI_001_F05 | auxin response transcription factor |
| | NXSI_003_F04 | putative lipoxygenase |
| | NXSI_008_C03 | MADS-box protein |
| | NXSI_024_C02 | homeotic protein (ATK1) |
| | NXSI_025_G11 | gibberellin 3 beta-hydroxylase - like protein |
| | NXSI_026_D05 | homeotic protein AGL30 |
| | NXSI_029_A12 | NAM (no apical meristem)-like protein |
| | NXSI_036_D07 | auxin response transcription factor |
| | NXSI_036_F03 | NAM (no apical meristem)-like protein, putative |
| | NXSI_041_B07 | homeotic protein (ATK1) |
| | NXSI_047_G05 | MADS-box protein |
| | NXSI_048_C11 | 12-oxophytodienoate reductase (OPR2) |

| Category | Pine clone name | Annotation |
|---|---|---|
| | NXSI_053_B04 | auxin response transcription factor(ARF6) |
| | NXSI_054_A01 | PIR:T09146 T09146 late-embryogenesis protein EMB11 |
| | NXSI_054_B07 | cytochrome P450 homolog, putative |
| | NXSI_059_E09 | DNA-binding homeotic protein Athb-2 |
| | NXSI_059_F07 | dehydrin Xero2 |
| | NXSI_070_C11 | putative MADS-box protein |
| | NXSI_071_E03 | MADS-box protein |
| | NXSI_076_H06 | lipoxygenase AtLOX2 |
| | NXSI_077_C08 | putative MADS-box protein |
| | NXSI_080_G02 | homeotic protein, putative |
| | NXSI_082_G07 | floral homeotic protein agamous (AGAMOUS) |
| | NXSI_083_F09 | MADS-box protein |
| | NXSI_087_C11 | NAM (no apical meristem)-like protein |
| | NXSI_089_C07 | UDP-glucose:indole-3-acetate beta-D-glucosyltransferase, putative |
| | NXSI_099_F04 | floral homeotic protein agamous (AGAMOUS) |
| | NXSI_106_C09 | floral homeotic protein agamous (AGAMOUS) |
| | NXSI_106_H12 | ethylene responsive element binding factor 4 (AtERF4) |
| | NXSI_107_B10 | ethylene-responsive element binding factor(AtERF6) |
| | NXSI_108_H08 | EREBP - like protein |
| | NXSI_110_C01 | s-adenosylmethionine synthetase |
| | NXSI_110_F03 | similar to late embryogenesis abundant proteins |
| | NXSI_116_D12 | homeotic protein, putative |
| | NXSI_138_A11 | UDP-glucose:indole-3-acetate beta-D-glucosyltransferase, putative |
| | NXSI_139_B03 | floral homeotic protein apetala2-like |
| | NXSI_145_D03 | NAM (no apical meristem)-like protein |
| | NXSI_148_C11 | putative late embryogenesis abundant protein |
| | PC02A11 | similar to late embryogenesis abundant proteins |

| Category | Pine clone name | Annotation |
|---|---|---|
| | PC04G10 | MADS box transcription factor-like protein |
| | PC08D03 | late embryogenesis abundant protein-like |
| | PC11H05 | similar to late embryogenesis abundant proteins |
| | PC12E10 | late-embryogenesis abundant protein, putative |
| | PC14C08 | late embryogenesis-abundant protein, putative |
| | PC18A04 | late embryogenesis abundant protein (AtECP63) |
| | PC18B10 | putative NAM (no apical meristem)-like protein |
| | PC19G08 | putative MADS-box protein |
| | PC23A09 | similar to late embryogenesis abundant proteins |
| | ST06D02 | putative MADS-box protein |
| | ST12H08 | thioredoxin, putative |
| | ST14D07 | putative dehydrine |
| | ST14F05 | thioredoxin, putative |
| | ST14G02 | putative MADS-box protein |
| | ST17H08 | ethylene responsive element binding factor 3 (AtERF3) |
| | ST21E10 | thioredoxin, putative |
| | ST21G02 | thioredoxin -like protein |
| | ST21H03 | putative s-adenosylmethionine synthetase |
| | ST22D10 | homeotic gene regulator - like protein |
| | ST23D08 | auxin response factor 1, putative |
| | ST27G04 | putative lipoxygenase |
| | ST29A01 | lipoxygenase AtLOX2 |
| | ST30E11 | cytochrome P450 - like protein |
| | ST32B07 | cytochrome P450 GA3 |
| | ST32C09 | putative late embryogenesis abundant protein |
| | ST35G05 | NAM-like protein (No Apical Meristem) |
| | ST36D01 | ACC synthase (AtACS-6) |

| Category | Pine clone name | Annotation |
|---|---|---|
| | ST37B02 | putative thioredoxin |
| | ST37C01 | thioredoxin-like protein |
| | ST39A04 | thioredoxin -like protein |
| **PROTEASES** | NXCI_047_H01 | cysteine proteinase RD21A |
| | NXNV_120_F02 | 26S proteasome subunit 4 |
| | NXNV_132_E09 | E2 ubiquitin-conjugating-like enzyme, Ahus5 |
| | NXNV_153_D05 | 26S proteasome ATPase subunit, putative |
| | NXNV_164_D02 | E2, ubiquitin-conjugating enzyme, putative |
| | NXNV_187_D12 | E2, ubiquitin-conjugating enzyme, putative |
| | ST21F01 | 26S proteasome AAA-ATPase subunit RPT3 |
| | ST37A12 | E2, ubiquitin-conjugating enzyme, putative |
| **SIGNAL TRANSDUCTION** | 1D3 | putative phosphatidylinositol/phosphatidylcholine transfer protein |
| | 20A2 | diacylglycerol pyrophosphate phosphatase, putative |
| | NXCI_002_E11 | transcription factor DREB1A, putative |
| | NXCI_002_F10 | lipase, putative |
| | NXCI_008_A07 | putative CDP-diacylglycerol synthetase |
| | NXCI_018_D02 | lipase, putative |
| | NXCI_020_G05 | HD-Zip transcription factor, Athb-14 |
| | NXCI_020_H12 | putative phospholipase C |
| | NXCI_025_C02 | G-protein beta-subunit (transducin) family |
| | NXCI_028_B03 | MYB family transcription factor (Atmyb3), putative |
| | NXCI_028_B08 | HD-Zip transcription factor |
| | NXCI_040_G11 | putative SNF2 subfamily transcription regulator |
| | NXCI_044_D12 | lysophospholipase isolog |
| | NXCI_047_B08 | leucine-rich repeat transmembrane protein kinase 1, putative |
| | NXCI_048_B01 | phospholipase D |
| | NXCI_048_C09 | mitogen activated protein kinase kinase (nMAPKK) |
| | NXCI_054_C06 | Ras-related GTP-binding protein (RAB11D) |

| Category | Pine clone name | Annotation |
|---|---|---|
| | NXCI_056_G12 | putative lipase |
| | NXCI_061_A03 | protein kinase C-receptor |
| | NXCI_061_C04 | HD-Zip transcription factor |
| | NXCI_064_G02 | transcription factor TFIIB |
| | NXCI_069_B09 | mitogen-activated protein kinase-like protein |
| | NXCI_075_E04 | lipase, putative |
| | NXCI_076_D06 | putative lipase |
| | NXCI_082_G01 | calcium-binding protein (pollen allergen) |
| | NXCI_094_G12 | phospholipase - like protein |
| | NXCI_095_D03 | ethylene responsive element binding factor 3 (AtERF3) |
| | NXCI_101_D04 | phosphatidylinositol/phosphatidylcholine transfer protein, putative |
| | NXCI_101_E05 | lipase/hydrolase, putative |
| | NXCI_103_C02 | HD-Zip transcription factor, Athb-14 |
| | NXCI_106_A03 | putative lipase |
| | NXCI_111_F10 | bZIP family transcription factor |
| | NXCI_121_G02 | phosphatidylinositol/phosphatidylcholine transfer protein, putative |
| | NXCI_122_H07 | putative lipase |
| | NXCI_127_C04 | DRE binding protein (DREB2B) |
| | NXCI_141_F06 | lipase, putative |
| | NXCI_147_F07 | putative SNF2 subfamily transcription regulator |
| | NXCI_149_B01 | G-box binding bZIP transcription factor |
| | NXCI_154_D09 | lipase, putative |
| | NXCI_155_G06 | phospholipase - like protein |
| | NXCI_163_E01 | putative transcription factor BTF3 (RNA polymerase B transcription factor 3) |
| | NXLV_011_H08 | putative phosphatidylinositol/phosphatidylcholine transfer protein |
| | NXLV_014_G03 | bZIP transcription factor family protein |
| | NXLV_018_C06 | putative leucine-rich repeat transmembrane protein kinase |

| Category | Pine clone name | Annotation |
|---|---|---|
| | NXLV_032_E02 | lipase, putative |
| | NXLV_037_E01 | 3-phosphoinositide-dependent protein kinase-1 PDK1 |
| | NXLV_037_F06 | phosphatidylinositol synthase (PIS1) |
| | NXLV_038_F09 | HD-Zip transcription factor, Athb-8 |
| | NXLV_042_D03 | putative phospholipase D |
| | NXLV_044_D06 | putative lipase |
| | NXLV_044_G12 | calcium-transporting ATPase |
| | NXLV_046_H01 | phospholipase D alpha, putative |
| | NXLV_047_D10 | protein kinase C-receptor |
| | NXLV_064_B06 | Ca2+-dependent membrane-binding protein annexin |
| | NXLV_066_E11 | putative lipase |
| | NXLV_068_B03 | putative lysophospholipase |
| | NXLV_076_A03 | putative leucine-rich repeat transmembrane protein kinase |
| | NXLV_079_G07 | leucine-rich repeat transmembrane protein kinase 1, putative |
| | NXLV090_G07 | phospholipase D1, putative |
| | NXLV103_A12 | mitogen activated protein kinase kinase, putative |
| | NXLV112_B02 | leucine-rich repeat transmembrane protein kinase, putative |
| | NXLV114_H07 | mitogen activated protein kinase – like |
| | NXLV120_E09 | putative diacylglycerol kinase |
| | NXLV124_H06 | bZIP protein, putative |
| | NXLV131_G07 | putative phospholipase D |
| | NXLV134_G06 | putative triacylglycerol lipase |
| | NXNV002C02 | 3-phosphoinositide-dependent protein kinase-1 PDK1 |
| | NXNV002G12 | putative phospholipase |
| | NXNV003B07 | WRKY family transcription factor |
| | NXNV004F05 | phospholipase A2-like protein |
| | NXNV005C04 | putative phospholipase |

| Category | Pine clone name | Annotation |
|---|---|---|
| | NXNV008C04 | phosphoinositide-specific phospholipase - like protein |
| | NXNV009G09 | bZIP family transcription factor |
| | NXNV010D07 | phospholipase D |
| | NXNV015H06 | lipase, putative |
| | NXNV055D06 | ankyrin repeat-containing protein 2 |
| | NXNV_071_G09 | protein kinase C-receptor |
| | NXNV_079_D09 | HD-Zip transcription factor, Athb-14 |
| | NXNV_081_F06 | transcription factor TINY, putative |
| | NXNV_093_H08 | G-protein beta-subunit (transducin) family |
| | NXNV_105_G09 | Dof zinc finger protein |
| | NXNV_128_A07 | histidine kinase - like protein |
| | NXNV_131_B12 | family II extracellular lipase 5 (EXL5) |
| | NXNV_139_C09 | putative CCAAT-binding transcription factor subunit |
| | NXNV_144_G04 | Ca2+-transporting ATPase - like protein |
| | NXNV_144_G07 | WRKY family transcription factor |
| | NXNV_145_C08 | putative phosphatidylinositol/phosphatidylcholine transfer protein |
| | NXNV_147_G05 | mitogen activated protein kinase kinase (nMAPKK) |
| | NXNV_155_D02 | putative diacylglycerol kinase |
| | NXNV_181_E07 | lipase -like protein |
| | NXNV_185_H06 | phosphoinositide-specific phospholipase - like protein |
| | NXNV_186_D07 | phosphatidylinositol 4-kinase, putative |
| | NXNV_187_B04 | Cyclin-dependent kinase B1;1 |
| | NXPV_003_C06 | putative CDP-diacylglycerol--glycerol-3-phosphate 3-phosphatidyltransferase |
| | NXPV_003_E09 | putative mitogen-activated protein kinase |
| | NXPV_011_H07 | phospholipase D1, putative |
| | NXPV_013_F07 | putative 3-phosphoinositide-dependent protein kinase-1 |
| | NXPV_015_D06 | putative phosphatidylinositol phophatidylcholine transfer protein |

| Category | Pine clone name | Annotation |
|---|---|---|
| | NXPV_022_A03 | phosphatidylinositol-4-phosphate 5-kinase, putative |
| | NXPV_022_C01 | bZIP protein |
| | NXPV_027_C05 | myb DNA-binding protein(Atmyb103) |
| | NXPV_073_A12 | DRE binding protein (DREB1B) |
| | NXPV_073_H03 | DRE binding protein (DREB2A) |
| | NXPV_077_H07 | phosphatidylinositol-4-phosphate 5-kinase-like protein |
| | NXPV_078_C08 | transcription factor DREB1A, putative |
| | NXPV_083_B10 | DRE binding protein (DREB1C) |
| | NXPV_084_A05 | lipase, putative |
| | NXPV_084_G10 | bZIP transcription factor (POSF21) |
| | NXPV_085_A06 | DREB-like AP2 domain transcription factor |
| | NXPV_086_E11 | transcription factor TINY, putative |
| | NXPV_087_F09 | lipase, putative |
| | NXPV_088_H01 | phospholipase D, putative |
| | NXPV_089_G10 | HD-Zip transcription factor, Athb-9 |
| | NXPV_090_H12 | putative CDP-diacylglycerol--glycerol-3-phosphate 3-phosphatidyltransferase |
| | NXPV_091_A12 | EREBP - like protein |
| | NXPV_097_H02 | GDSL-motif lipase/hydrolase-like protein |
| | NXPV_104_B12 | bZIP family transcription factor |
| | NXPV_123_B02 | Dof zinc finger protein |
| | NXPV_127_D07 | DRE binding protein (DREB1A) |
| | NXRV_001_D11 | HD-Zip transcription factor, Athb-14 |
| | NXRV_004_F05 | putative phospholipase |
| | NXRV_005_H02 | lysophospholipase isolog |
| | NXRV_012_A06 | bZIP transcription factor, OBF5 |
| | NXRV_018_A05 | putative 3-phosphoinositide-dependent protein kinase-1 |
| | NXRV_021_C01 | ethylene-responsive element binding factor 12(AtERF12) |

| Category | Pine clone name | Annotation |
|---|---|---|
| | NXRV_021_D08 | potential calcium-transporting ATPase11, plasma membrane-type ($Ca^{2+}$-ATPase, isoform 11) |
| | NXRV_026_A11 | lipase, putative |
| | NXRV047_F11 | putative phosphatidylinositol/phophatidylcholine transfer protein |
| | NXRV054_D07 | myb family transcription factor(AtMYB84) |
| | NXRV058_B02 | calcium-binding transporter-like protein |
| | NXSI_003_B02 | triacylglycerol lipase like protein |
| | NXSI_013_H09 | putative sensory transduction histidine kinase |
| | NXSI_021_B01 | DREB-like AP2 domain transcription factor |
| | NXSI_021_F01 | DRE binding protein (DREB2B) |
| | NXSI_021_G01 | ascorbate oxidase promoter-binding protein, putative |
| | NXSI_021_H06 | homeobox-leucine zipper protein HAT5 (HD-ZIP protein 5) (HD-ZIP protein ATHB-1) |
| | NXSI_023_G01 | myb DNA-binding protein (AtMYB73) |
| | NXSI_023_G05 | [ZD] Ca2+-binding protein (centrin/caltractin) EF-Hand superfamily ,Magpie No BQ701203 |
| | NXSI_031_E04 | putative lipase/acylhydrolase |
| | NXSI_040_E10 | lipase - like protein |
| | NXSI_043_C06 | lipase-like protein |
| | NXSI_045_E10 | putative GDSL-motif lipase/hydrolase |
| | NXSI_048_B08 | lipase-like protein |
| | NXSI_049_D11 | lipase, putative |
| | NXSI_050_B12 | HD-Zip transcription factor, Athb-9 |
| | NXSI_052_D03 | leucine-rich repeat transmembrane protein kinase, putative |
| | NXSI_053_C11 | myb DNA-binding protein(Atmyb103) |
| | NXSI_057_H09 | potential calcium-transporting ATPase 10, plasma membrane-type (Ca2+-ATPase, isoform 10) |
| | NXSI_067_D02 | putative lipase/acylhydrolase |

| Category | Pine clone name | Annotation |
|---|---|---|
| | NXSI_068_G08 | putative lipase |
| | NXSI_068_H10 | lipase, putative |
| | NXSI_071_C11 | putative phosphatidylinositol-4-phosphate 5-kinase |
| | NXSI_075_E01 | lysophospholipase -like protein |
| | NXSI_076_C07 | putative phospholipase D-gamma |
| | NXSI_077_G11 | Nicotiana EREBP-3 like |
| | NXSI_088_C07 | bZIP family transcription factor |
| | NXSI_099_A02 | diacylglycerol kinase-like protein |
| | NXSI_104_C10 | ascorbate oxidase promoter-binding protein, putative |
| | NXSI_106_H12 | ethylene responsive element binding factor 4 (AtERF4) |
| | NXSI_107_A01 | DRE binding protein (DREB1C) |
| | NXSI_107_B10 | ethylene-responsive element binding factor(AtERF6) |
| | NXSI_108_H08 | EREBP - like protein |
| | NXSI_110_E02 | calcium-binding transporter-like protein |
| | NXSI_110_E09 | lipase, putative |
| | NXSI_112_F08 | lysophospholipase isolog, putative |
| | NXSI_112_F10 | putative GDSL-motif lipase/acylhydrolase |
| | NXSI_113_C10 | mitogen-activated protein kinase, putative |
| | NXSI_114_C01 | lysophospholipase isolog, putative |
| | NXSI_114_G08 | putative GDSL-motif lipase/hydrolase |
| | NXSI_116_A10 | putative CDP-diacylglycerol synthetase |
| | NXSI_116_C09 | lipase -like protein |
| | NXSI_135_C08 | putative acid phosphatase ,Magpie No BQ703000 |
| | NXSI_136_E08 | transcription factor, putative |
| | NXSI_144_E08 | putative lipase |
| | NXSI_144_F12 | putative lipase |
| | PC06B09 | putative GDSL-motif lipase/acylhydrolase |

| Category | Pine clone name | Annotation |
|---|---|---|
| | PC07A09 | GDSL-motif lipase/hydrolase-like protein |
| | PC08G06 | homeobox-leucine zipper protein ATHB-5 (HD-zip protein ATHB-5) |
| | PC09E08 | family II extracellular lipase 5 (EXL5) |
| | PC10A01 | WRKY family transcription factor |
| | PC13G09 | HD-Zip transcription factor |
| | PC15D04 | putative lipase |
| | PC23B09 | putative phospholipase C |
| | ST03A09 | calmodulin (cam2) |
| | ST06B11 | putative GDSL-motif lipase/hydrolase |
| | ST08G12 | flower pigmentation protein ATAN11 |
| | ST16E03 | GDSL-motif lipase/hydrolase-like protein |
| | ST16H01 | putative GDSL-motif lipase/acylhydrolase |
| | ST17B03 | leucine-rich repeat transmembrane protein kinase, putative |
| | ST17H08 | ethylene responsive element binding factor 3 (AtERF3) |
| | ST18F02 | myb family transcription factor (ATMYB3) |
| | ST19F11 | putative lipase/acylhydrolase |
| | ST21C06 | putative lipase |
| | ST22A06 | HD-Zip transcription factor, Athb-13 |
| | ST22H07 | lysophospholipase -like protein |
| | ST22H11 | diacylglycerol kinase (ATDGK1) |
| | ST24A11 | Nicotiana EREBP-3 like |
| | ST24H11 | bZIP protein |
| | ST29G06 | lipase |
| | ST29H03 | putative GDSL-motif lipase/hydrolase |
| | ST33A06 | putative transcription factor BTF3 (RNA polymerase B transcription factor 3) |
| | ST33B04 | G-protein beta family |
| | ST33B07 | putative GDSL-motif lipase hydrolase |

| Category | Pine clone name | Annotation |
|---|---|---|
| | ST33F02 | mitogen-activated protein kinase, putative |
| | ST33G03 | Ca2+-transporting ATPase - like protein |
| | ST33H05 | myb family transcription factor (ATMYB3) |
| | ST35B09 | transcriptional coactivator - like protein |
| | ST35G10 | "putative WD-40 repeat protein, MSI4 " |
| | ST35H05 | family II extracellular lipase 2 (EXL2) |
| | ST36D05 | phosphatidylinositol 3-kinase, putative |
| | ST36G01 | mitogen activated protein kinase - like |
| | ST39H05 | MYB family transcription factor (Atmyb3), putative |
| **TRAFFICKING** | NXCI_026_G07 | putative coated vesicle membrane protein |
| | NXCI_040_F05 | secretory carrier membrane protein, putative |
| | NXCI_123_D05 | membrane-bound small GTP-binding - like protein |
| | NXCI_124_E10 | secretory carrier membrane protein, putative |
| | NXLV_046_G01 | putative component of vesicle-mediated transport |
| | NXLV126_C09 | putative coated vesicle membrane protein |
| | NXNV015H10 | putative secretory carrier-associated membrane protein |
| | NXNV_075_H09 | secretory carrier membrane protein |
| | NXNV_120_G07 | secretory carrier membrane protein |
| | NXNV_144_F04 | spot 3 protein and vacuolar sorting receptor homolog, putative |
| | NXNV_162_C02 | secretory peroxidase |
| | NXPV_108_C06 | endomembrane protein EMP70 precusor isolog |
| | NXRV_011_H07 | membrane-bound small GTP-binding - like protein |
| | NXRV_025_B04 | putative vesicle-associated membrane protein, synaptobrevin 7B |
| | NXRV056_C11 | putative coatomer protein |
| | NXSI_070_A10 | VAMP (vesicle-associated membrane protein)-associated protein-like |
| | ST07G03 | putative Golgi-associated membrane trafficking protein |
| | ST27F02 | endomembrane protein, putative |

| Category | Pine clone name | Annotation |
|---|---|---|
| | ST29F02 | VAMP (vesicle-associated membrane protein)-associated protein-like |
| | ST35G03 | putative ADP-ribosylation factor |
| **UNASSIGNED/NO HITS** | 10D12 | Not Available |
| | 11G5 | Not Available |
| | 17B10 | Not Available |
| | 17H9 | Not Available |
| | 18E5 | putative laccase (diphenol oxidase) |
| | 19D4 | Not Available |
| | 20C12 | Not Available |
| | 20G4 | Not Available |
| | 22C1 | Not Available |
| | 22E3 | Not Available |
| | 22F5 | Not Available |
| | 23D3 | Not Available |
| | 23E12 | peptidyl-prolyl cis-trans isomerase - like protein |
| | 2B1 | Not Available |
| | 2E9 | Not Available |
| | 2F11 | Not Available |
| | 3A3 | Not Available |
| | 3C4 | Not Available |
| | Missing | Not Available |
| | NXCI_006_F12 | putative anthocyanin 5-aromatic acyltransferase |
| | NXCI_007_G09 | Not Available |
| | NXCI_018_G04 | Not Available |
| | NXCI_049_H10 | Not Available |
| | NXCI_053_A10 | Not Available |
| | NXCI_104_C12 | Not Available |

| Category | Pine clone name | Annotation |
|---|---|---|
| | NXCI_106_G05 | cinnamyl alcohol dehydrogenase, putative |
| | NXCI_109_G01 | Not Available |
| | NXCI_148_D05 | Not Available |
| | NXCI_148_D07 | cytochrome P-450, putative |
| | NXCI_148_G08 | Not Available |
| | NXCI_164_A11 | Not Available |
| | NXLV_002_C02 | prolyl 4-hydroxylase, putative |
| | NXLV_071_F08 | Not Available |
| | NXLV107_B07 | Not Available |
| | NXNV_065_F04 | Not Available |
| | NXNV_071_F05 | Not Available |
| | NXNV_071_G06 | Not Available |
| | NXNV_079_C05 | prolyl 4-hydroxylase, alpha subunit-like protein |
| | NXNV_083_A10 | Not Available |
| | NXNV_120_E10 | Not Available |
| | NXNV_122_A01 | Not Available |
| | NXNV_122_H05 | Not Available |
| | NXNV_126_C09 | Not Available |
| | NXNV_127_A03 | Not Available |
| | NXNV_139_H09 | Hydroxyindole-O-methyltransferase; related SAM-dependent methyltransferase |
| | NXNV_139_H09 | Hydroxyindole-O-methyltransferase and related SAM-dependent methyltransferases |
| | NXNV_144_C06 | Not Available |
| | NXNV_147_D05 | Not Available |
| | NXNV_147_D12 | Not Available |
| | NXNV_153_E12 | cinnamyl-alcohol dehydrogenase ELI3-1 |
| | NXNV_158_B01 | Not Available |
| | NXNV_162_B03 | cinnamyl alcohol dehydrogenase |

| Category | Pine clone name | Annotation |
|---|---|---|
| | NXNV_162_F07 | cinnamyl-alcohol dehydrogenase ELI3-2 |
| | NXNV_166_B02 | Not Available |
| | NXNV_76_C09 | Not Available |
| | NXNV_76_F01 | Not Available |
| | NXNV019C01 | Not Available |
| | NXNV055B06 | Not Available |
| | NXPV_008_D06 | Not Available |
| | NXPV_017_E08 | putative anthocyanin 5-aromatic acyltransferase |
| | NXPV_026_B01 | cinnamyl-alcohol dehydrogenase - like protein |
| | NXPV_038_D11 | Not Available |
| | NXPV_083_B11 | Not Available |
| | NXPV_086_C03 | Not Available |
| | NXPV_091_C09 | cinnamyl alcohol dehydrogenase |
| | NXPV_093_A11 | Not Available |
| | NXPV_101_F04 | Not Available |
| | NXPV_103_D04 | Not Available |
| | NXPV_126_F10 | cinnamyl alcohol dehydrogenase -like protein, LCADa |
| | NXPV_129_F03 | Not Available |
| | NXRV_008_B03 | cinnamyl alcohol dehydrogenase - like protein |
| | NXRV_050_B09 | Not Available |
| | NXRV053_A09 | Not Available |
| | NXRV055_D08 | putative phosphocholine cytidylyltransferase |
| | NXRV055_D09 | putative phosphocholine cytidylyltransferase |
| | NXRV057_F05 | Not Available |
| | NXSI_002_A02 | Not Available |
| | NXSI_004_E02 | cinnamyl-alcohol dehydrogenase ELI3-2 |
| | NXSI_021_A09 | Not Available |

| Category | Pine clone name | Annotation |
|---|---|---|
| | NXSI_022_E03 | putative cinnamyl alcohol dehydrogenase |
| | NXSI_029_F11 | Not Available |
| | NXSI_036_H10 | Not Available |
| | NXSI_047_B07 | Not Available |
| | NXSI_050_F04 | prolyl 4-hydroxylase, alpha subunit-like protein |
| | NXSI_059_D01 | prolyl 4-hydroxylase, putative |
| | NXSI_070_B04 | Not Available |
| | NXSI_077_A11 | Not Available |
| | NXSI_077_G09 | anaphylatoxin 1 ,Magpie No BF778157 |
| | NXSI_077_G09 | anaphylatoxin 1 ,Magpie No BF778157 |
| | NXSI_080_G04 | cinnamyl alcohol dehydrogenase - like protein |
| | NXSI_083_E10 | Not Available |
| | NXSI_083_G03 | Not Available |
| | NXSI_092_E12 | Not Available |
| | NXSI_092_H05 | Not Available |
| | NXSI_096_H09 | Not Available |
| | NXSI_097_H07 | Not Available |
| | NXSI_105_G03 | cinnamyl-alcohol dehydrogenase CAD1 |
| | NXSI_112_E02 | Not Available |
| | NXSI_114_B03 | Not Available |
| | NXSI_116_C06 | cinnamyl-alcohol dehydrogenase CAD1 |
| | NXSI_116_H03 | Not Available |
| | NXSI_136_A01 | Not Available |
| | NXSI_138_C04 | cinnamyl alcohol dehydrogenase |
| | PC03H02 | cinnamyl alcohol dehydrogenase, putative |
| | PC04E04 | Not Available |
| | PC18d03 | Not Available |

| Category | Pine clone name | Annotation |
|---|---|---|
| | PC19F10 | Not Available |
| | PC23D07 | cinnamyl-alcohol dehydrogenase - like protein |
| | ST02B03 | cinnamyl-alcohol dehydrogenase ELI3-1 |
| | ST17D08 | Not Available |
| | ST19D02 | Not Available |
| | ST19D09 | Not Available |
| | ST21E01 | Not Available |
| | ST22A10 | Not Available |
| | ST22E6 | Not Available |
| | ST23B03 | putative phosphocholine cytidylyltransferase |
| | ST25A05 | Not Available |
| | ST34F04 | cinnamyl alcohol dehydrogenase, putative |
| | ST35C08 | Not Available |
| | ST37A06 | Not Available |
| | ST38E01 | Not Available |
| | ST7B06 | Not Available |

Appendix C – Percentage of upregulated and downregulated genes in each functional category and metabolic group in two cohorts of pine needles. Percentages were calculated relatively to the total pool of gene measurements, i.e., number of genes in each group times three sampling times. The magnitude of the effect of elevated $CO_2$ is given as the mean relative expression value calculated from the differentially expressed genes (both up- and down-regulated) in each category and foliage cohort.

| Group | Cohort | Category | Total | Up (%) | Down (%) | Diff. expressed (Up + Down; %) | Relative expression (E/A) | | |
|---|---|---|---|---|---|---|---|---|---|
| **Group 1: CARBON ASSIMILATION** | | | **459** | **10.9%** | **4.6%** | **15.5%** | **(Mean)** | **(N)** | **(SE)** |
| | **ONE-YEAR-OLD** | | **229** | **1.7%** | **1.7%** | **3.5%** | **0.95** | **5** | **0.09** |
| | | Pigments | 21 | 0.0% | 0.0% | 0.0% | | 0 | |
| | | Light-harvesting | 24 | 4.2% | 0.0% | 4.2% | 1.22 | 1 | |
| | | PS I | 12 | 0.0% | 8.3% | 8.3% | 0.77 | 1 | |
| | | PS II | 27 | 0.0% | 3.7% | 3.7% | 0.82 | 1 | |
| | | PET | 24 | 0.0% | 4.2% | 4.2% | 0.85 | 1 | |
| | | Rubisco | 13 | 0.0% | 0.0% | 0.0% | | 0 | |
| | | Chaperonins 60 | 21 | 0.0% | 0.0% | 0.0% | | 0 | |
| | | Calvin cycle | 87 | 3.4% | 1.1% | 4.6% | 1.09 | 4 | 0.08 |
| | | Light reactions | 108 | 0.9% | 2.8% | 3.7% | 0.92 | 4 | 0.10 |
| | | Carbon reactions | 121 | 2.5% | 0.8% | 3.3% | 1.09 | 1 | |
| | **CURRENT-YEAR** | | **230** | **20.0%** | **7.4%** | **27.4%** | **1.13** | **7** | **0.03** |
| | | Pigments | 21 | 19.0% | 0.0% | 19.0% | 1.20 | 4 | 0.06 |
| | | Light-harvesting | 24 | 12.5% | 4.2% | 16.7% | 1.26 | 4 | 0.27 |
| | | PS I | 12 | 33.3% | 8.3% | 41.7% | 1.15 | 5 | 0.09 |
| | | PS II | 27 | 18.5% | 11.1% | 29.6% | 1.04 | 8 | 0.07 |
| | | PET | 24 | 33.3% | 20.8% | 54.2% | 1.06 | 13 | 0.05 |
| | | Rubisco | 14 | 0.0% | 0.0% | 0.0% | | 0 | |
| | | Chaperonins 60 | 21 | 19.0% | 9.5% | 28.6% | 1.07 | 6 | 0.05 |

| Group | Cohort | Category | Total | Up (%) | Down (%) | Diff. expressed (Up + Down; %) | Relative expression (E/A) | | |
|---|---|---|---|---|---|---|---|---|---|
| | | Calvin cycle | 87 | 20.7% | 5.7% | 26.4% | 1.13 | 23 | 0.05 |
| | | Light reactions | 108 | 22.2% | 9.3% | 31.5% | 1.14 | 5 | 0.04 |
| | | Carbon reactions | 122 | 18.0% | 5.7% | 23.8% | 1.10 | 2 | 0.03 |
| **GROUP 2: CARBON PARTITIONING** | | | **486** | **13.2%** | **2.3%** | **15.4%** | **1.21** | | |
| | **ONE-YEAR-OLD** | | **243** | **2.9%** | **0.4%** | **3.3%** | **1.25** | **3** | **0.04** |
| | | Sucrose synthesis | 12 | 0.0% | 0.0% | 0.0% | | 0 | |
| | | Sucrose degradation | 87 | 3.4% | 1.1% | 4.6% | 1.32 | 4 | 0.24 |
| | | Starch synthesis | 21 | 0.0% | 0.0% | 0.0% | | 0 | |
| | | Starch degradation | 42 | 4.8% | 0.0% | 4.8% | 1.22 | 2 | 0.05 |
| | | Sugar transporters | 81 | 2.5% | 0.0% | 2.5% | 1.22 | 2 | 0.02 |
| | **CURRENT-YEAR** | | **243** | **23.5%** | **4.1%** | **27.6%** | **1.16** | **5** | **0.04** |
| | | Sucrose synthesis | 12 | 33.3% | 8.3% | 41.7% | 1.11 | 5 | 0.06 |
| | | Sucrose degradation | 87 | 23.0% | 3.4% | 26.4% | 1.12 | 23 | 0.04 |
| | | Starch synthesis | 21 | 28.6% | 4.8% | 33.3% | 1.13 | 7 | 0.05 |
| | | Starch degradation | 42 | 28.6% | 2.4% | 31.0% | 1.31 | 13 | 0.12 |
| | | Sugar transporters | 81 | 18.5% | 4.9% | 23.5% | 1.13 | 19 | 0.06 |
| **GROUP 3: CARBON OXIDATION** | | | **1260** | **11.5%** | **3.7%** | **15.2%** | **1.12** | | |
| | **ONE-YEAR-OLD** | | **630** | **3.3%** | **1.0%** | **4.3%** | **1.05** | **6** | **0.05** |
| | | Photorespiration | 57 | 0.0% | 1.8% | 1.8% | 0.87 | 1 | |
| | | OPPP | 90 | 2.2% | 1.1% | 3.3% | 0.93 | 3 | 0.24 |
| | | Glycolysis | 150 | 5.3% | 1.3% | 6.7% | 1.11 | 10 | 0.04 |
| | | Fermentation | 96 | 3.1% | 1.0% | 4.2% | 1.07 | 4 | 0.10 |

| Group | Cohort | Category | Total | Up (%) | Down (%) | Diff. expressed (Up + Down; %) | Relative expression (E/A) | | |
|---|---|---|---|---|---|---|---|---|---|
| | | Citric acid cycle | 108 | 3.7% | 0.9% | 4.6% | 1.12 | 5 | 0.06 |
| | | Oxidative Phosphorylation | 102 | 3.9% | 0.0% | 3.9% | 1.21 | 4 | 0.01 |
| | | Mitochondrial transporters | 27 | 0.0% | 0.0% | 0.0% | | | |
| | **CURRENT-YEAR** | | **630** | **19.7%** | **6.3%** | **26.0%** | **1.18** | **8** | **0.04** |
| | | Photorespiration | 57 | 19.3% | 14.0% | 33.3% | 1.05 | 19 | 0.14 |
| | | OPPP | 90 | 17.8% | 5.6% | 23.3% | 1.43 | 21 | 0.23 |
| | | Glycolysis | 150 | 20.7% | 6.0% | 26.7% | 1.10 | 40 | 0.04 |
| | | Fermentation | 96 | 17.7% | 7.3% | 25.0% | 1.09 | 24 | 0.06 |
| | | Citric acid cycle | 108 | 21.3% | 1.9% | 23.1% | 1.28 | 25 | 0.12 |
| | | Oxidative Phosphorylation | 102 | 18.6% | 7.8% | 26.5% | 1.17 | 27 | 0.14 |
| | | Oxoglutarate transporters | 9 | 33.3% | 0.0% | 33.3% | 1.22 | 3 | 0.07 |
| | | PEP/Pi transporters | 18 | 22.2% | 5.6% | 27.8% | 1.12 | 5 | 0.12 |
| | | Mitochondrial transporters | 27 | 25.9% | 3.7% | 29.6% | 1.17 | 2 | 0.05 |
| **GROUP 4: ATP SYNTHESIS** | | | **132** | **14.4%** | **2.3%** | **16.7%** | **1.38** | | |
| | **ONE-YEAR-OLD** | | **66** | **1.5%** | **1.5%** | **3.0%** | **1.51** | **1** | |
| | | General | 24 | 0.0% | 0.0% | 0.0% | | 0 | |
| | | Mitochondrial | 18 | 0.0% | 0.0% | 0.0% | | 0 | |
| | | Vacuolar | 24 | 4.2% | 4.2% | 8.3% | 1.51 | 2 | 0.75 |
| | | ATP synthesis | 66 | 1.5% | 1.5% | 3.0% | 1.51 | 1 | |
| | **CURRENT-YEAR** | | **66** | **27.3%** | **3.0%** | **30.3%** | **1.25** | **3** | **0.10** |
| | | General | 24 | 37.5% | 8.3% | 45.8% | 1.13 | 11 | 0.05 |
| | | Mitochondrial | 18 | 27.8% | 0.0% | 27.8% | 1.17 | 5 | 0.02 |
| | | Vacuolar | 24 | 16.7% | 0.0% | 16.7% | 1.46 | 4 | 0.32 |

| Group | Cohort | Category | Total | Up (%) | Down (%) | Diff. expressed (Up + Down; %) | Relative expression (E/A) | | |
|---|---|---|---|---|---|---|---|---|---|
| | | ATP synthesis | 66 | 27.3% | 3.0% | 30.3% | 1.25 | 3 | 0.10 |
| **ALL** | | | **2337** | **11.9%** | **3.5%** | **15.4%** | **1.14** | | |
| | **ONE-YEAR-OLD** | | | | | | | | |
| | | All | 1168 | 2.8% | 1.0% | 3.9% | 1.13 | 45 | 0.04 |
| | **CURRENT-YEAR** | | | | | | | | |
| | | All | 1169 | 21.0% | 5.9% | 26.9% | 1.16 | 314 | 0.03 |

## References


Ackerly D.D. (2000) Taxon sampling, correlated evolution, and independent contrasts. *Evolution* 54, 1480-1492.

Ackerly D.D. (2004) Functional strategies of chaparral shrubs in relation to seasonal water deficit and disturbance. *Ecological Monographs* 74, 25-44.

Ackerly D.D. and Reich P.B. (1999) Convergence and correlations among leaf size and function in seed plants: a comparative test using independent contrasts. *American Journal of Botany* 86, 1272-1281.

Ainsworth E.A. and Long S.P. (2005) What have we learned from 15 years of free-air CO2 enrichment (FACE)? A meta-analytic review of the responses of photosynthesis, canopy. *New Phytologist*, 165, 351-371.

Ainsworth E.A. and Rogers A. (2007) The response of photosynthesis and stomatal conductance to rising [CO2]: mechanisms and environmental interactions. *Plant Cell and Environment*, 30, 258-270.

Ainsworth E.A., Rogers A., Vodkin L.O., Walter A. and Schurr U. (2006) The effects of elevated CO2 concentration on soybean gene expression. An analysis of growing and mature leaves. *Plant Physiology*, 142, 135-147.

Alder N.N, Pockman W.T., Sperry J.S., and Nuismer S. (1997) Use of centrifugal force in the study of xylem cavitation. *Journal of Experimental Botany* 48, 665-674.

Amthor J.S. (1995) Terrestrial Higher-Plant Response to Increasing Atmospheric [$CO_2$] in Relation to the Global Carbon-Cycle. *Global Change Biology*, 1, 243-274.

Backhausen J.E., and Scheibe R. 1999. Adaptation of tobacco plants to elevated CO2: influence of leaf age on changes in physiology, redox states and NADP-malate dehydrogenase activity. Journal Of Experimental Botany, **50**, 665-675.

Benjamini Y. and Hochberg Y. (1995) Controlling the false discovery rate: a practical and powerful approach to multiple testing. . *Journal of the Royal Statistical Society. Series B (Methodological)*, 57, 289-300.

Boyce C.K., Zwieniecki M.A., Cody G.D., Jacobsen C., Wirick S., Knoll A.H. and Holbrook N.M. (2004) Evolution of xylem lignification and hydrogel transport regulation. *Proceedings of the National Academy of Sciences of the U.S.A.* 101, 17555-17558.

Brodribb T.J., Holbrook N.M. and Gutiérrez M.V. (2002) Hydraulic and photosynthetic

co-ordination in seasonally dry tropical forest trees. *Plant Cell and Environment* 25, 1435-1444.

Brodribb T.J., Holbrook N.M., Edwards E.J. and Gutiérrez M.V. (2003) Relations between stomatal closure, leaf turgor and xylem vulnerability in eight tropical dry forest trees. *Plant, Cell and Environment* 26, 443-450.

Buchanan B., Gruissem W. and Jones R., eds (2000) *Biochemistry and Molecular Biology of Plants*. American Society of Plant Physiologists, Rockville, Maryland.

Chang S., J. P. and J. C. (1993) A simple and efficient method for isolating RNA from pine trees. *Plant Molecular Biology Reporter*, 113-116.

Cochard H., Cruiziat P. and Tyree M.T. (1992) Use of positive pressures to establish vulnerability curves. *Plant Physiology* 100, 205-209.

Comstock J.P. and Sperry J.S. (2000) Some theoretical considerations of optimal conduit length for water transport in plants. *New Phytologist* 148, 195-218.

Crous K.Y. and Ellsworth D.S. (2004) Canopy position affects photosynthetic adjustments to long-term elevated CO2 concentration (FACE) in aging needles in a mature Pinus taeda forest. *Tree Physiology*, 24, 961-970.

Davey P.A., Hunt S., Hymus G.J., DeLucia E.H., Drake B.G., Karnosky D.F. and Long S.P. (2004) Respiratory oxygen uptake is not decreased by an instantaneous elevation of [CO2], but is increased with long-term growth in the field at elevated [Co-2](1). *Plant Physiology*, 134, 520-527.

Davis S.D., Ewers F.W., Sperry J.S., Portwood K.A., Crocker M.C. and Adams G.C. 2002. Shoot dieback during prolonged drought in *Ceanothus* (Rhamnaceae) chaparral of California: a possible case of hydraulic failure. *American Journal of Botany* 89, 820-828

Dennis D.T. and Blakely S.D. (2000) Carbohydrate Metabolism. In: *Biochemistry and Molecular Biology of Plants* (eds B. Buchanan, W. Gruissem, and R. Jones). American Society of Plant Physiologists, Rockville, Maryland.

Eamus D. and Jarvis P.G. (1989) The Direct Effects of Increase in the Global Atmospheric $CO_2$ Concentration on Natural and Commercial Temperate Trees and Forests. *Advances in Ecological Research*, 19, 1-55.

Ehleringer J.R., Sage R.F., Flanagan L.B. and Pearcy R.W. (1991) Climate Change and the Evolution of C4 Photosynthesis. *Trends in Ecology and Evolution*, 6, 95-99.

Ellsworth D.S. (1999) CO2 enrichment in a maturing pine forest: are CO2 exchange and water status in the canopy affected? Plant *Cell And Environment*, 22, 461-472.

Ellsworth D.S. (2000) Seasonal CO2 assimilation and stomatal limitations in a Pinus taeda canopy. *Tree Physiology*, 20, 435-445.

Farquhar G.D., Ehleringer J.R. and Hubick K.T. (1989) Carbon isotope discrimination and photosynthesis. *Annual Review of Plant Physiology and Plant Molecular Biology* 40, 503-537.

Farquhar, G.D., S. von Caemmerer and J.A. Berry (1980) A biochemical model of photosynthetic $CO_2$ assimilation in leaves of C3 species. *Planta* 149, 78–90.

Felsenstein J. (1985) Phylogenies and the comparative method. *American Naturalist* 125, 1-15.

Garland T. and Ives A.R. (2000) Using the past to predict the present: Confidence intervals for regression equations in phylogenetic comparative methods. *American Naturalist* 155, 346-364.

Garland T., Harvey P.H. and Ives A.R. (1992) Procedures for the analysis of comparative data using phylogenetically independent contrasts. *Systematic Biology* 41, 18-32.

Garland T., Midford P.E. and Ives A.R. (1999) An introduction to phylogenetically based statistical methods, with a new method for confidence intervals on ancestral states. *American Zoologist* 39, 374-388.

Gonzalez-Meler M. and Taneva L. (2005) Integrated Effects of Atmospheric $CO_2$ concentration on Pland and Ecosystem Repiration. In: *Advances in Photosynthesis and Respiration: Plant Respiration: From Cell to Ecosystem* (eds H. Lambers and M. RibasCarbo).

Griffin K.L., Tissue D.T., Turnbull M.H. & Whitehead D. (2000) The onset of photosynthetic acclimation to elevated CO2 partial pressure in field-grown Pinus radiata D. Don. after 4 years. *Plant Cell And Environment*, **23**, 1089-1098.

Gupta P., Duplessis S., White H., Karnosky D.F., Martin F. and Podila G.K. (2005) Gene expression patterns of trembling aspen trees following long-term exposure to interacting elevated CO2 and tropospheric O-3. *New Phytologist*, 167, 129-142.

Hacke U.G., Sperry J.S. and Pittermann J. (2000) Drought experience and cavitation resistance in six shrubs from the Great Basin, Utah. *Basic and Applied Ecology* 1, 31-41.

Hacke U.G., Sperry J.S., Pockman W.T., Davis S.D. and McCulloch K.A. (2001a) Trends in wood density and structure are linked to prevention of xylem implosion by negative pressure. *Oecologia* 126, 457-461.

Hacke U.G., Stiller V., Sperry, J.S. Pittermann J. and McCulloh K. (2001b) Cavitation fatigue: embolism and refilling cycles can weaken the cavitation resistance of xylem. *Plant Physiology* 125, 779-786.

Harvey P.H. and Pagel M. (1991) The comparative method in evolutionary biology. Oxford University Press, Oxford, UK.

Hendrey G.R., Ellsworth D.S., Lewin K.F. and Nagy J. (1999) A free-air enrichment system for exposing tall forest vegetation to elevated atmospheric CO2. *Global Change Biology*, 5, 293-309.

Hill P.W., Farrar J.F., Boddy E.L., Gray A.M. and Jones D.L. (2006) Carbon Partitioning and Respiration-Their Control and Role in Plants at High $CO_2$. In: *Managed Ecosystems and CO2: Case Studies, Processes, and Perspectives* (eds J. Nösberger, S.P. Long, R.J. Norby, M. Stitt, G.R. Hendrey, and H. Blum), pp. 459. Springer Verlag.

Hofmockel K., Schlesinger W. and Jackson R. (2007) Effects of elevated atmospheric CO2 on amino acid and NH4+-N cycling in a temperate pine ecosystem. *Global Change Biology*, 13, 1950-1959.

Houghton R.A. (2003) The Contemporary Carbon Cycle. In: *Biogeochemistry* (ed W.H. Schlesinger), pp. 473-513. Elsevier - Pergamon, Oxford.

Hubbard R.M., Ryan M.G., Stiller V. and Sperry J.S. (2001) Stomatal conductance and photosynthesis vary linearly with plant hydraulic conductance in ponderosa pine. *Plant, Cell and Environment* 24, 113-121.

IPCC (2007) *Climate Change 2007: The Physical Science Basis. Contribution of Working Group I to the Fourth Assessment* Cambridge University Press, Cambridge, United Kingdom and New York, NY, USA.

Jackson R.B., Linder C.R., Lynch M., Purugganan M., Somerville S. and Thayer S.S. (2002) Linking molecular insight and ecological research. Trends *in Ecology and Evolution*, 17, 409-414.

Jackson R.B., Sperry J.S. and Dawson T.E. (2000) Root water uptake and transport: using physiological processes in global predictions. *Trends in Plant Science* 5, 482-488.

Jang J.C. and Sheen J. (1994) Sugar sensing in higher plants. *Plant Cell*, 6, 1665–1679.

Jarbeau J.A., Ewers F.W. and Davis S.D. (1995) The mechanism of water stress induced embolism in two species of chaparral shrubs. *Plant, Cell and Environment* 18, 189-196.

Jin W., Riley R.M., Wolfinger R.D., White K.P., Passador-Gurgel G. and Gibson G. (2001) The contributions of sex, genotype and age to transcriptional variance in Drosophila melanogaster. *Nature Genetics*, 29, 389-395.

Katny M.A.C., Hoffmann-Thoma G., Schrier A.A., Fangmeier A., Jager H.J., and van Bel A.J.E. 2005. Increase of photosynthesis and starch in potato under elevated CO2 is dependent on leaf age. *Journal of Plant Physiology*, **162**, 429-438.

Kavanagh K.L., Bond B.J., Aitken S.N., Gartner B.L. and Knowe S. (1999) Shoot and root vunerability to xylem cavitation in four populations of Douglas-fir seedlings. *Tree Physiology* 19, 31-38

Koch K.E. (1996) Carbohydrate-modulated gene expression in plants, pp. 509 - 540.

Körner C. (2006) Plant CO2 responses: an issue of definition, time and resource supply. *New Phytologist*, 172, 393-411.

Krapp A., Hofmann B., Schafer C. and Stitt M. (1993). Regulation of the Expression of Rbcs and Other Photosynthetic Genes by Carbohydrates - a Mechanism for the Sink Regulation of Photosynthesis. Plant Journal, **3**, 817-828.

Lev-Yadun S. and Sederoff R. (2000) Pines as model gymnosperms to study evolution, wood formation, and perennial growth. *Journal Of Plant Growth Regulation*, 19, 290-305.

Lewis A.M. and Boose E.R. (1995) Estimating volume flow rates through xylem conduits. *American Journal of Botany* 82, 1112-1116.

Lewis J.D., Tissue D.T. and Strain B.R. (1996) Seasonal response of photosynthesis to elevated CO2 in loblolly pine (Pinus taeda L) over two growing seasons. *Global Change Biology*, 2, 103-114.

Long S.P., Ainsworth E.A., Rogers A. and Ort D.R. (2004) Rising atmospheric carbon dioxide: Plants face the future. *Annual Review of Plant Biology*, 55, 591-628.

Luomala E.M., Laitinen K., Kellomaki S. and Vapaavuori E. (2003) Variable photosynthetic acclimation in consecutive cohorts of Scots pine needles during 3 years of growth at elevated CO2 and elevated temperature. *Plant Cell and Environment*, 26, 645-660.

Maddison W.P. and Maddison D.R. (2004) Mesquite: a modular system for evolutionary analysis. Version 1.02 http://mesquiteproject.org

Maherali H., Pockman W.T. and Jackson R.B. (2004) Adaptive variation in the vulnerability of woody plants to xylem cavitation. *Ecology* 85, 2184-2199.

Martínez-Vilalta J., Prat E., Oliveras I. and Pinol J. (2002) Xylem hydraulic properties of roots and stems of nine Mediterranean woody species. *Oecologia* 133, 19-29.

Martínez-Vilalta J., Sala A. and Pinol J. (2004) The hydraulic architecture of Pinaceae – a review. *Plant Ecology* 171, 3-13.

McCarthy H.R., Oren R., Finzi A.C., Ellsworth D.S., Kim H.S., Johnsen K.H. & Millar B. (2007) Temporal dynamics and spatial variability in the enhancement of canopy leaf area under elevated atmospheric CO2. *Global Change Biology*, **13**, 2479-2497.

McCarthy H.R., Oren R., Kim H.S., Johnsen K.H., Maier C., Pritchard S.G. and Davis M.A. (2006) Interaction of ice storms and management practices on current carbon sequestration in forests with potential mitigation under future CO2 atmosphere. *Journal of Geophysical Research-Atmospheres*, 111.

McElrone A.J., Pockman W.T., Martínez-Vilalta J. and Jackson R.B. (2004) Variation in xylem structure and function in stems and roots of trees to 20 m depth. *New Phytologist* 163, 507-517.

Medlyn B.E., Badeck F.W., De Pury D.G.G., Barton C.V.M., Broadmeadow M., Ceulemans R., De Angelis P., Forstreuter M., Jach M.E., Kellomaki S., Laitat E., Marek M., Philippot S., Rey A., Strassemeyer J., Laitinen K., Liozon R., Portier B., Roberntz P., Wang K. and Jarvis P.G. (1999) Effects of elevated [CO2] on photosynthesis in European forest species: a meta-analysis of model parameters. *Plant Cell and Environment*, 22, 1475-1495.

Meinzer F.C. (2002) Coordination of vapour and liquid phase water transport properties in plants. *Plant, Cell and Environment* 25, 265-274.

Miglietta F., Peressotti A., Vaccari F.P., Zaldei A., deAngelis P. and Scarascia-Mugnozza G. (2001) Free-air CO2 enrichment (FACE) of a poplar plantation: the POPFACE fumigation system. *New Phytologist*, 150, 465-476.

Miyazaki S., Fredricksen M., Hollis K.C., Poroyko V., Shepley D., Galbraith D.W., Long S.P. and Bohnert H.J. (2004) Transcript expression profiles of Arabidopsis thaliana grown under controlled conditions and open-air elevated concentrations of CO2 and

of O-3. *Field Crops Research*, 90, 47-59.

Moore B.D., Cheng S.H., Rice J. and Seemann J.R. (1998). Sucrose cycling, Rubisco expression, and prediction of photosynthetic acclimation to elevated atmospheric CO2. *Plant Cell And Environment*, 21, 905-915.

Moore B.D., Cheng S.H., Sims D. and Seemann J.R. (1999) The biochemical and molecular basis for photosynthetic acclimation to elevated atmospheric CO2. *Plant Cell and Environment*, 22, 567-582.

Myers D.A., Thomas R.B. and Delucia E.H. (1999a) Photosynthetic capacity of loblolly pine (Pinus taeda L.) trees during the first year of carbon dioxide enrichment in a forest ecosystem. *Plant Cell and Environment*, 22, 473-481.

Myers, D. A., R. B. Thomas, and E. H. DeLucia. (1999b). Photosynthetic responses of loblolly pine (Pinus taeda) needles to experimental reduction in sink demand. *Tree Physiology* 19:235-242.

Nardini A. and Salleo S. (2000) Limitation of stomatal conductance by hydraulic traits: sensing or preventing xylem cavitation? *Trees* 15, 14-24.

Norby R.J., DeLucia E.H., Gielen B., Calfapietra C., Giardina C.P., King J.S., Ledford J., McCarthy H.R., Moore D.J.P., Ceulemans R., De Angelis P., Finzi A.C., Karnosky D.F., Kubiske M.E., Lukac M., Pregitzer K.S., Scarascia-Mugnozza G.E., Schlesinger W.H. and Oren R. (2005) Forest response to elevated CO2 is conserved across a broad range of productivity. *Proceedings of the National Academy of Sciences of the United States of America*, 102, 18052-18056.

Norby R.J., Wullschleger S.D., Gunderson C.A., Johnson D.W. and Ceulemans R. (1999) Tree responses to rising CO2 in field experiments: implications for the future forest. *Plant Cell and Environment*, 22, 683-714.

Nösberger J. and Long S.P. (2006) Introduction. In: *Managed Ecosystems and CO2: Case Studies, Processes, and Perspectives* (ed J.L. Nösberger, S.P.; Norby, R.J.; Stitt, M.; Hendrey, G.R.; Blum, H), pp. 3-13. Springer Verlag.

Oren R., Sperry J.S., Katul G.G., Pataki D.E., Ewers B.E., Phillips N. and Schafer K.V.R. (1999) Survey and synthesis of intra- and interspecific variation in stomatal sensitivity to vapour pressure deficit. *Plant, Cell and Environment* 22, 1515-1526.

Pagel M.D. (1993) Seeking the evolutionary regression coefficient: an analysis of what comparative methods measure. *Journal of Theoretical Biology* 164, 191-205.

Palenchar P., Kouranov A., Lejay L. and Coruzzi G. (2004) Genome-wide patterns of carbon and nitrogen regulation of gene expression validate the combined carbon and nitrogen (CN)-signaling hypothesis in plants, *Genome Biology*, 5, pp. R91.

Pallardy S.G. (2008) *Physiology of Woody Plans*. Academic Press, San Diego, CA, USA.

Palumbi S.R. (2001) Humans as the World's Greatest Evolutionary Force. *Science*, 293, 1786-1790.

Pammenter N.W. and Van Der Willigen, C. (1998) A mathematical and statistical analysis of the curves illustrating vulnerability of xylem to cavitation. *Tree Physiology* 18, 589-593

Pockman W.T. and Sperry J.S. (2000) Vulnerability to xylem cavitation and the distribution of sonoran desert vegetation. *American Journal of Botany* 87, 1287-1299.

Pockman W.T., Sperry J.S. and O'Leary J.W. (1995) Sustained and significant negative water pressure in xylem. *Nature* 378, 715-716.

Quackenbush J., Liang F., Holt I., Pertea G. and Upton J. (2000) The TIGR Gene Indices: reconstruction and representation of expressed gene sequences. *Nucleic Acids Research*, 28, 141-145.

Rogers A. and Ainsworth E.A. (2006) The response of foliar carbohydrates to elevated [CO2]. In: *Ecological Studies*, pp. 293-308.

Rogers A. and Ellsworth D.S. (2002) Photosynthetic acclimation of Pinus taeda (loblolly pine) to long-term growth in elevated pCO(2) (FACE). *Plant Cell and Environment*, 25, 851-858.

Rogers A. and Humphries S.W. (2000) A mechanistic evaluation of photosynthetic acclimation at elevated CO2. *Global Change Biology*, 6, 1005-1011.

Rolland F., Baena-Gonzalez E. & Sheen J. (2006) Sugar sensing and signaling in plants: Conserved and Novel Mechanisms, pp. 675-709.

Rolland F., Moore B. and Sheen J. (2002) Sugar sensing and signaling in plants, pp. S185 - S205.

Sack L., Cowan P.D., Jaikumar N. and Holbrook N.M. (2003) The “hydrology” of leaves: co-ordination of structure and function in temperate woody species. *Plant, Cell and Environment* 26, 1343-1356.

Saxe H., Ellsworth D.S. and Heath J. (1998) Tree and forest functioning in an enriched

CO2 atmosphere. *New Phytologist*, 139, 395-436.

Schena M., Shalon D., Davis R.W. and Brown P.O. (1995) Quantitative Monitoring Of Gene-Expression Patterns With A Complementary-DNA Microarray. Science, 270, 467-470.

Schlesinger W.H. (1997) Biogeochemistry: An Analysis of Global Change. (2nd ed.). Academic Press, San Diego.

Schwilk D.W. and Ackerly D.D. (2001) Flammability and serotiny as strategies: correlated evolution in pines. *Oikos* 94, 326-336.

Smith A.M. and Stitt M. (2007) Coordination of carbon supply and plant growth. *Plant, Cell and Environment*, 30, 1126-1149.

Somerville C. and Somerville S. (1999) Plant functional genomics. *Science*, 285, 380-383.

Sparks J.P. and Black R.A. (1999) Regulation of water loss in populations of Populus trichocarpa: the role of stomatal control in preventing xylem cavitation. *Tree Physiology* 19, 453-459.

Sperry J.S. and Hacke U.G. (2004) Analysis of circular bordered pit function. I. Angiosperm vessels with homogenous pit membranes. *American Journal of Botany* 91, 369-385.

Sperry J.S. and Pockman W. T. (1993) Limitation of transpiration by hydraulic conductance and xylem cavitation in *Betula occidentalis*. *Plant, Cell and Environment* 16, 279-287.

Sperry J.S. and Saliendra N. Z. (1994) Intra-and inter-plant variation in xylem cavitation in *Betula occidentalis. Plant, Cell and Environment* 17, 1233-1241.

Sperry J.S., Donnelly J.R. and Tyree M.T. (1988) A method for measuring hydraulic conductivity and embolism in xylem. *Plant, Cell and Environment* 11, 35-40.

Sperry J.S., Hacke U.G., Oren R. and Comstock J.P. (2002) Water deficits and hydraulic limits to leaf water supply. *Plant, Cell and Environment* 25, 251-263.

Sperry J.S., Hacke UG and Wheeler J.K. (2005) Comparative analysis of end wall resistance in xylem conduits. *Plant, Cell and Environment* 28, 456-465.

Springer C.J., DeLucia E.H. & Thomas R.B. (2005) Relationships between net photosynthesis and foliar nitrogen concentrations in a loblolly pine forest ecosystem

grown in elevated atmospheric carbon dioxide. *Tree Physiology*, 25, 385-394.

Stasolla C., van Zyl L., Egertsdotter U., Craig D., Liu W.B. and Sederoff R.R. (2003) The effects of polyethylene glycol on gene expression of developing white spruce somatic embryos. *Plant Physiology*, 131, 49-60.

Stitt M. (1991) Rising $CO_2$ levels and their potential significance for carbon flow in photosynthetic cells, *Plant Cell and Environment*, pp. 741-762.

Stitt M. and Krapp A. (1999) The interaction between elevated carbon dioxide and nitrogen nutrition: the physiological and molecular background. *Plant Cell and Environment*, 22, 583-621..

Taylor G., Street N.R., Tricker P.J., Sjodin A., Graham L., Skogstrom O., Calfapietra C., Scarascia-Mugnozza G. and Jansson S. (2005) The transcriptome of Populus in elevated CO2. *New Phytologist*, 167, 143-154.

Thimm O, Blaesing O, Gibon Y, Nagel A, Meyer S, Krüger P, Selbig J, Müller LA, Rhee SY and Stitt M. (2004) MAPMAN: a user-driven tool to display genomics data sets onto diagrams of metabolic pathways and other biological processes. *Plant Journal*, 37, 914-39.

Tissue D.T., Thomas R.B. and Strain B.R. (1996) Growth and photosynthesis of loblolly pine (Pinus taeda) after exposure to elevated CO2 for 19 months in the field. *Tree Physiology*, 16, 49-59.

Tissue D.T., Thomas R.B. and Strain B.R. (1997) Atmospheric CO2 enrichment increases growth and photosynthesis of Pinus taeda: a 4 year experiment in the field. *Plant Cell and Environment*, 20, 1123-1134.

Turnbull M.H., Tissue D.T., Griffin K.L., Rogers G.N.D. & Whitehead D. (1998) Photosynthetic acclimation to long-term exposure to elevated CO2 concentration in Pinus radiata D. Don. is related to age of needles. *Plant Cell And Environment*, 21, 1019-1028.

Tyree M. T. and Sperry J. S. (1989) Vulnerability of xylem to cavitation and embolism. *Annual Review of Plant Physiology and Plant Molecular Biology* 40, 19-38.

Tyree M.T. and Ewers F.W. (1991) The hydraulic architecture of trees and other woody plants. *New Phytologist* 119, 345-360.

Vitousek P.M., Mooney H.A., Lubchenco J. and Melillo J.M. (1997) Human Domination

of Earth's Ecosystems. *Science*, 277, 494-499.

Ward J.K. and Kelly J.K. (2004) Scaling up evolutionary responses to elevated CO2: lessons from Arabidopsis. *Ecology Letters*, 7, 427-440.

Ward J.K. and Strain B.R. (1999) Elevated CO2 studies: past, present and future. *Tree Physiology*, 19, 211-220.

Watkinson J.I., Sioson A.A., Vasquez-Robinet C., Shukla M., Kumar D., Ellis M., Heath L.S., Ramakrishnan N., Chevone B., Watson L.T., van Zyl L., Egertsdotter U., Sederoff R.R. and Grene R. (2003) Photosynthetic acclimation is reflected in specific patterns of gene expression in drought-stressed loblolly pine. *Plant Physiology*, 133, 1702-1716.

Westoby M., Falster D.S., Moles A.T., Vesk P.A. and Wright I.J. (2002) Plant ecological strategies: some leading dimensions of variation between species. *Annual Review of Ecology and Systematics* 33, 125-159.

Wolfinger R.D., Gibson G., Wolfinger E.D., Bennett L., Hamadeh H., Bushel P., Afshari C. and Paules R.S. (2001) Assessing gene significance from cDNA microarray expression data via mixed models. *Journal of Computational Biology*, 8, 625-637.

Wong S.C., Cowan I.R. and Farquhar G.D. (1979) Stomatal conductance correlates with photosynthetic capacity. *Nature* 282, 424–426.

Woodward F.I., Thompson G.B. and McKee I.F. (1991) The Effects of Elevated Concentrations of Carbon-Dioxide on Individual Plants, Populations, Communities and Ecosystems. *Annals of Botany*, 67, 23-38.

Wu S.H., Ramonell K., Gollub J. and Somerville S. (2001) Plant gene expression profiling with DNA microarrays. *Plant Physiology and Biochemistry*, 39, 917-926.

Wullschleger S.D. (1993) Biochemical Limitations to Carbon Assimilation in C(3) Plants - a Retrospective Analysis of the a/Ci Curves from 109 Species. *Journal of Experimental Botany*, 44, 907-920.

Zimmermann M.H. (1983) Xylem structure and the ascent of sap. Springer, New York, USA.

Zwieniecki M.A., Melcher P.J. and Holbrook N.M. (2001) Hydrogel control of hydraulic resistance in plants. *Science* 291, 1059-1062.

## Biography

Catarina Fernandes Moura was born in Coimbra, Portugal on September 3rd, 1977. Daughter of two university students at the time, her father a future Engineer and her mother a future Doctor, Catarina early on acquired her love for books and for the university world. Family stories tell that at age three, after carefully examining one of her *O Grande Livro de Perguntas e Respostas de Charlie Brown*[1] books about the functioning of earth and space, she said assertively "I want to be a scientist!". Though the world turned many times around, and her interests spread widely, when the time came (after concluding 9th grade) she chose indeed the field of "Sciences" at the Highschool Avelar Brotero in Coimbra. In her senior year, through the remarkable and unforgettable pedagogic skills of her Biology teacher (Dr. Júlia Jaleco), Catarina discovered her inner passion for the *living things* and her curiosity about the mechanisms operating in Nature. She continued on to study Life Sciences (Biology – Research Path) at the University of Coimbra and chose to develop her final year's research thesis in the sub-field of Plant Physiological Ecology under the supervision of Professor Helena Freitas at the Department of Botany. Catarina graduated in 1999 with High Honors ("Very Good with Distinction") already with a strong conviction of pursuing a doctoral degree overseas. Under guidance and encouragement of Professor Helena Freitas as well as the

[1] Portuguese version of the series *Charlie Brown's Super Book of Questions and Answers*

sponsorship of Professor Robert Jackson, Catarina applied both for a doctoral fellowship from the Portuguese Foundation for Science and Technology, and to attend Graduate School at Duke University. Together, the acceptance by Duke and the award of the fellowship resulted in a long journey that started by crossing the Atlantic ocean and is culminating in the doctoral dissertation here presented. Main milestones achieved by Catarina since obtaining her B.Sc. degree are summarized below.

## *Milestones*

### *Fellowships*

2004-05 Doctoral Fellowship from the Foundation Calouste Gulbenkian, Portugal

2000-03 Doctoral Fellowship PRAXIS XXI, Science and Technology Foundation-Ministry for Science and Technology (FCT), Portugal

1999 Short-term scholarship to visit a US institution, Luso-American Foundation (FLAD), Portugal

### *Grants and Awards*

2007 Scholarship to cover partial expenses during the Stable Isotope Ecology Summer courses (Biology 7473 and 7475) at SIRFER lab, University of Utah

2005 Billings Award Honorable Mention, Physiological Ecology Section of the Ecological Society of America

2005 International Travel Award, Duke University Graduate School

2004 Best Poster Honorable Mention, Physiological Ecology Section of the Ecological Society of America

2004 Duke University Graduate School Conference Travel Award

2004 Duke Biology Departmental Grant-in-Aid

2004 Tuition scholarship, Summer Institute of Statistical Genetics, North Carolina State University

2003 Duke University Graduate School Conference Travel Awards

2002 Best Poster Honorable Mention, Physiological Ecology Section of the Ecological Society of America (87$^{th}$ annual meeting: Tucson, AZ, August 4-9$^{th}$)

2002 Lawrence Giles Research Award, Department of Biology, Duke University

2001 Catherine Keever and L. Giles Research Awards, Department of Biology, Duke University

1999 Graduation with High Honors ("Very good with Distinction"), University of Coimbra, Portugal

### *Publications*

Maherali H.*, **Moura C.F.***, Caldeira M.C., Willson C.J. and Jackson R.B. 2005. Functional coordination between leaf gas exchange and vulnerability to xylem cavitation in temperate forest trees. *Plant Cell and Environment*, 29: 571-583 (* these authors contributed equally to this work)

**Moura C.F.**, Watkinson J., Grene R., McElrone A. and Jackson R.B. Effects of elevated $CO_2$ on the gene expression of field-grown, mature loblolly pine trees. *To be submitted.*

### *Invited presentations*

2006 From the atmosphere to the transcriptome: loblolly pine trees FACE a rise in $CO_2$. University Program in Ecology seminar series. 10th November, Duke University

2004 Gene expression trends for a *Pinus taeda* forest. Duke Forest Field Trip (Poster)- Forum in Landscapes, Genomics and Transgenic Conifer Forests. 17-19th November, Nicholas School of the Environment and Earth Sciences, Duke University

2004 Effects of elevated $CO_2$ on the gene expression of field-grown loblolly pine. Global Change Mini-Symposium: Annual Meeting of the American Society of Plant Biologists, 24-28th July, Lake Buena Vista, Florida

### *Professional societies*

AAAS (American Association for the Advancement of Science), ASPB (American Association of Plant Biologists), ESA (Ecological Society of America), Sigma-Xi, SPECO (Portuguese Society of Ecology)